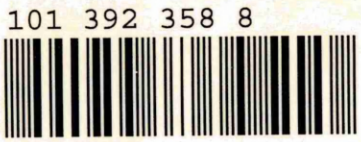

# Mathematical Modelling of Pulsatility in Neuroendocrine Systems

David Bryan Barrass

A thesis submitted in partial fulfilment of the requirements of Sheffield Hallam University for the degree of Doctor of Philosophy

April 1993

In collaboration with:

AFRC Institute of Animal Physiology and Genetics Research
Babraham

ABSTRACT

MODELLING OF PULSATILITY IN NEUROENDOCRINE SYSTEMS

BY D B BARRASS

A thesis submitted in partial fulfilment of the requirements for the award of PhD.

The work described in this thesis concerns the mathematical description of the characteristic oscillatory electrical behaviour of certain neurosecretory cells found in the hypothalamus of the mammalian brain. This study concentrates on those cells which secrete the hormone oxytocin. A model first described by Hodgkin and Huxley is used as a starting point for the derivation of a description comprising a system of coupled non-linear partial differential equations. The equations have been based wherever possible on experimental data relevant to the system being studied. Where this has not been possible, alternative models based on data from other, related systems have been used.

The thesis starts with a discussion of the physiology of the system under study and presents some background material. The second chapter discusses the process of mathematical modelling of neurones and presents some of the relevant work in the area. The model due to Hodgkin and Huxley is significant and is discussed in detail. The research methodology is then outlined. Experimental procedures for recording the electrical behaviour of nerve cells and methods of recording selected ionic currents are the subject of chapter three. Chapter four presents a discussion of oscillatory behaviour in nerve cells at a general level and outlines the features necessary for a nerve cell to exhibit oscillation. The next three chapters discuss the characteristics of the different ionic currents involved and describe the author's derivation of models of these currents. Chapter Five presents the author's model of the sodium current, Chapter Six, the potassium currents and Chapter Seven, the calcium current. The experimental work undertaken and the results obtained are then presented and discussed.

During the course of this study a number of computer programs were written and tested by the author. The program listings appear in the appendix.

The thesis is significant and contributes to the body of knowledge in that no other mathematical model of the unique bursting behaviour of oxytocin-secreting cells exists as far as the author is aware.

# CONTENTS

ACKNOWLEDGEMENTS

I would like to thank the following people:

Dr I. Basarab for suggesting the project and for constant encouragement.

Dr G Leng for his help with the physiological aspects of the project and for providing data for the project.

Dr W A Barraclough for his quiet efficiency and for numerous helpful suggestions and discussions. Especially for his help with ACSL.

Thanks to Sue Willingham for constant support and encouragement.

Thanks to Mr D Smith for his help and advice on the wordprocessing package.

# INTRODUCTION

The work described in this report concerns the derivation of a mathematical model to describe the electrical activity characteristsic of certain nerve cells in a specific part of the mammalian brain. The nerve cells that are the subject of this study are found in the hypothalamus and are neurosecretory. This means that they are nerve cells that have evolved for the production of hormones. The two types of cell of interest to this study secrete either oxytocin or vasopressin. These hormones control the contraction of smooth muscle and blood osmolarity respectively. A model that describes the unusual electrical behaviour of the oxytocin-secreting cells is being sought. Electrical activity in the cell body is transmitted along the nerve axons to trigger the release of hormone into the blood supply. When the electrical activity of these nerve cells is recorded in lactating rats, unusual patterns are noted. Prior to ejection of milk from the mammary gland, a very high frequency burst of action potentials is recorded. The cells that show this behaviour normally fire action potentials only sporadically.

Dehydration causes the vasopressin-secreting cells to produce action potentials in a pattern that comprises a burst of oscillation followed by a period of silence followed by another burst.

Probably the best known mathematical model of the electrical behaviour of nerve cells is the one derived by Hodgkin and Huxley. Their model successfully described the generation and propagation of a nerve impulse in the giant

axon of the squid. Although this model was first published in 1952, it is still widely acknowledged to be a good starting point on which to base models of more complicated electrical activity. This model is discussed in Chapter Two of this thesis. The model-building procedure used by Hodgkin and Huxley has been used in this project in order to formulate a mathematical description of the bursting behaviour observed in oxytocin-secreting cells.

Building on the current body of knowledge about the mechanisms responsible for generating electrical impulses in nerve cells and using experimental results obtained from the specific cell types under consideration, a mathematical representation of the electrical behaviour has been postulated. This involved a literature survey to establish the current state of modelling neural electrical activity and to become familiar with the techniques involved. Once this step had been completed, a strategy for building a model of the cell was formulated. This entailed obtaining experimental data from the collaborating establishment and the literature for the ionic currents known to be present in the cell, writing sets of equations to describe these currents individually and performing computer simulations of the resulting systems of equations. Several computer programs were written and tested by the author. Besides the modelling programs which involved numerical integration of the differential equations derived, a curve-fitting program was written and used to derive the model parameters from the available experimental data.

This thesis explains the background to the study,

discusses the process of building mathematical models, discusses important work in this field and describes the derivation of the model in detail. The results generated by the model are presented, discussed and compared with practice.

CHAPTER ONE

# PROJECT BACKGROUND

Neurosecretion , the process of releasing hormones into the systemic circulation by neurones, is an important regulatory mechanism in all animals. Vasopressin (Arginine Vasopressin) (AVP) and oxytocin (OXT) are two such neurosecretory hormones. These hormones are produced in the supraoptic and paraventricular nuclei (SON & PVN) of the mammalian hypothalamus (see Figure 1.1). Oxytocin-secreting and vasopressin-secreting neurones are found in both nuclei (Poulain & Wakerley 1982; Lincoln & Wakerley 1974; Renaud, Bourque, Day, Ferguson & Randle 1985).

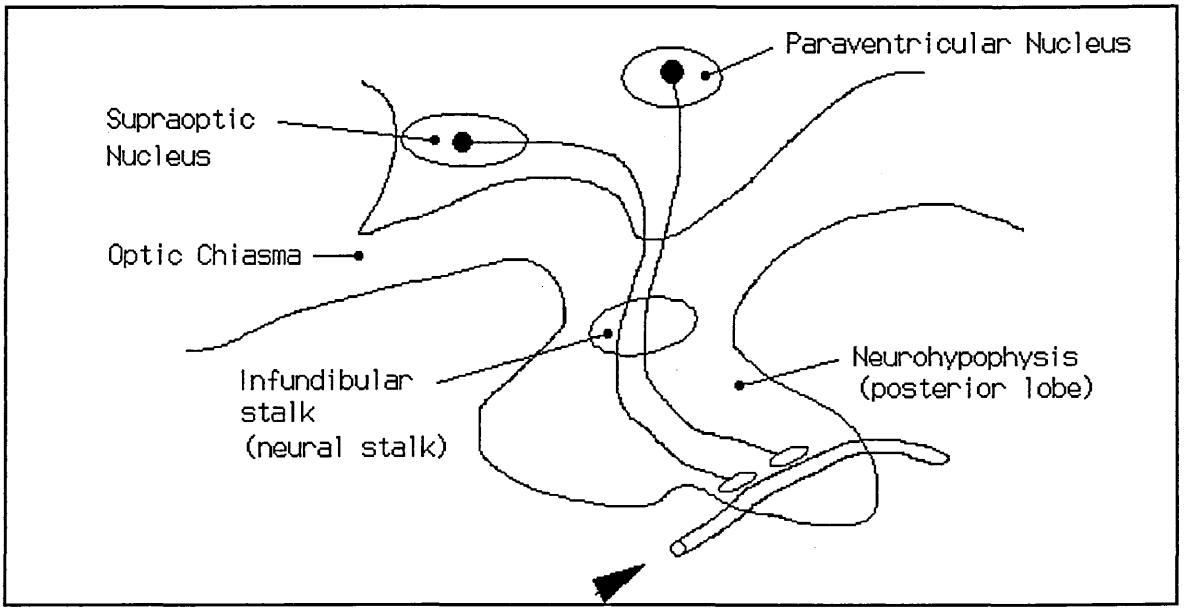


**Figure 1.1**

Diagram showing the location of the Paraventricular and Supraoptic Nuclei.

The cell bodies are spherical or ovoid in shape with diameters from 10μm to 40μm (Renaud, Bourque, Day, Ferguson & Randle 1985; Andrew & Dudek 1984; Legendre, Cooke & Vincent 1982; Erickson, Ronnekleiv & Kelly 1990; Mason 1983; Cobbett, Legendre & Mason 1989). Each cell has a few short, thick dendrites and one long, thin axon (Mason 1983; Leng & Dyball 1983; Mason, Cobbett, Inenaga & Legendre 1988).

Cell resting membrane potentials are in the region of -60mV (-45mV to -80mv) (Bourque & Renaud 1985; Bourque, Randle & Renaud 1986; Abe & Ogata 1982; Poulain & Wakerley 1982; Legendre, Cooke & Vincent 1982; Cobbett & Mason 1987; Mason 1983; Mason, Cobbett, Inenaga & Legendre 1988). Cell input resistances range from 50M Ohm to 1G Ohm (Trifaro & Poisner 1985; Erickson, Ronnekleiv & Kelly 1990; Bourque & Renaud 1985; Renaud 1987; Abe & Ogata 1982; Andrew & Dudek 1984; Legendre, Cooke & Vincent 1982; Cobbett & Mason 1987; Mason 1983). Cell time constants range from 9 to 15 ms (Erickson, Ronnekleiv & Kelly 1990; Renaud 1987; Bourque, Randle & Renaud 1986; Mason 1983). From the cell input resistance and time constant the whole cell capacitance may be calculated from the equation

$$\tau = RC \quad \ldots\ldots\ldots\ldots\ldots\ldots\ldots\ldots \quad (1.1)$$

where R is the input resistance, C is the cell capacitance and $\tau$ is the time constant. Using the values above a range of 45pF to 300pF is obtained. These values may be compared with values calculated from the standard value of membrane

capacitance of 1μF/sq. cm assuming spherical geometry and cell diameters as given above. This calculation yields capacitance values between 3 and 50 pF. Calculations of this kind can be a little misleading since some cell types have extensive infoldings which dramatically increases the cell surface area. A low value is to be expected from calculations involving the cell geometry which involve only the calculation of the surface area of a sphere since such a calculation does not include any dendritic or axonic processes.

Action potential amplitudes are in the range 40 to 106 mV (Dudek, Hatton & MacVicar 1980; Bourque, Randle & Renaud 1986; Poulain & Wakerley 1982; Andrew & Dudek 1984; Mason 1983; Mason, Cobbett, Inenaga & Legendre 1988). Spike durations range from 1 to 5 ms. (Bourque & Renaud 1985; Andrew & Dudek 1984; Legendre, Cooke & Vincent 1982; Hatton, Ho & Mason 1983; Cobbett & Mason 1987; Mason 1983; Mason & Leng 1984).

The axons from the neurones in the paraventricular and supraoptic nuclei collect together to form the infundibular stalk (neural stalk) and then branch out to form the neurohypophysis (posterior lobe).

The neurohypophysis is a richly vascularized region that provides an exception to the normal separation of the brain and the blood (the blood-brain barrier). For this reason, the neurohypophysis is known as a neurohaemal organ. (Maddrell & Nordmann 1979).

Oxytocin and vasopressin are synthesized in the cell bodies (somata) of magnocellular neurosecretory cells (MNC's)

and packed into neurosecretory granules along with peptides known as neurophysins that bind to them (Maddrell & Nordmann 1979; Smythies, Beaton, Bradley & Morin 1976). These neurosecretory granules are moved by the process of axonal transport to the neurohypophysis where they may be released by the usual mechanism of exocytosis. (This is where vesicles packed with hormone fuse with the membrane and in doing so, the contents become exposed to the exterior.) The process of exocytosis is triggered by action potentials at the axon end terminals and it is the unusual pattern of action potentials that this study is concerned with.

Vasopressin, otherwise known as the antidiuretic hormone (ADH) is, as its name suggests, involved with maintaining the water balance in the body by promoting water reabsorption in the kidney. This process is known as osmoregulation and there is evidence that the vasopressin-secreting cells themselves act as osmoreceptors. (Mason 1980; Leng, Mason & Dyer 1982; Dyball & Leng 1984; Abe & Ogata 1981)

Oxytocin acts on smooth muscle cells and causes contraction of uterine muscles (myometrium) during parturition. It also acts on the myoepithelial cells in mammary glands causing contraction and therefore milk ejection (Renaud 1987; Lincoln & Wakerley 1974; Poulain & Wakerley 1982).

Both types of MNC show very characteristic electrical behaviour. During periods of hypovolemic or osmotic stimuli (ie. reduction in the volume of blood or dehydration), vasopressin-secreting neurones fire action potentials in a

phasic burst (see Figure 1.2). Phasic firing does not start immediately after the application of the stimulus but follows a period of continuous firing (Brimble & Dyball 1977; Maddrell & Nordmann 1979). Phasic firing displays a very characteristic pattern consisting of periods of action potential discharge lasting about 7 - 30s at frequencies of between 4 - 12 spikes per second followed by silent periods of 15 - 40s (Leng 1981; Leng & Bicknell 1984; Brimble & Dyball 1977; Dutton & Dyball 1979). This pattern of firing has been shown to be optimal for the release of hormone (Dutton & Dyball 1979; Leng & Bicknell 1984; Renaud, Bourque, Day, Ferguson & Randle 1985; Ingram, Bicknell, Brown & Leng 1982; Dyball, Barnes & Shaw 1985).

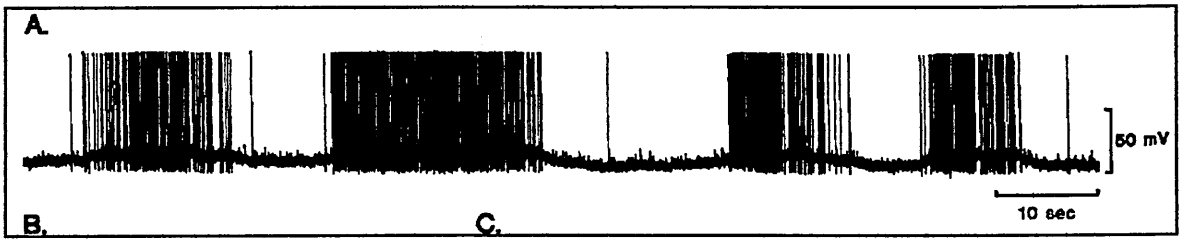


**Figure 1.2**

Recording of phasic firing. Reproduced courtesy Dr. G. Leng

Oxytocin-secreting neurones may be distinguished from vasopressin-secreting cells on the basis of their electrical behaviour as well as their response to osmotic stimuli since they very rarely display phasic activity (Brimble & Dyball 1977). However, they do fire spontaneous action potentials at

a low background rate until stimulated to fire an intense burst (Lincoln & Wakerley 1974; Poulain & Wakerley 1982; Leng & Dyball 1983). This short, intense burst of action potentials causes the release of a bolus of oxytocin that then acts on the myoepithelial cells of the mammary gland producing an ejection of milk. The milk ejection reflex occurs only during lactation and the characteristic burst of action potentials is not observed in males or in virgin females. It is essential that the release of oxytocin occurs as a bolus since it has been shown that the same amount of hormone injected over a longer period of time does not cause contraction of the myoepithelial cells (Leng 1981 , Leng & Bicknell 1984). A typical burst of action potentials that precedes a milk ejection consists of a rapid acceleration in firing rate up to a maximum of around 80 spikes/second (Leng & Bicknell 1984 , Cobbett, Legendre & Mason 1989). A recording from a neurone in the SON displaying such a burst is shown in Figure 1.3. The general pattern of activity is a slow irregular or continuous background firing (slow; less than 3 spikes/second-Bicknell 1988; Poulain & Wakerly 1982; fast continuous; more than 3 spikes/second-Bicknell 1988; Poulain & Wakerly 1982) which is interrupted every few ( 4 to 8 - Robinson & Dyer 1988) minutes by a short (1-2s) burst of high frequency discharge (50-80 spikes/s Renaud, Bourque, Day, Ferguson & Randle 1985). There may be up to 100 spikes in a single burst (Richard, Moos & Freund-Mercier 1988).

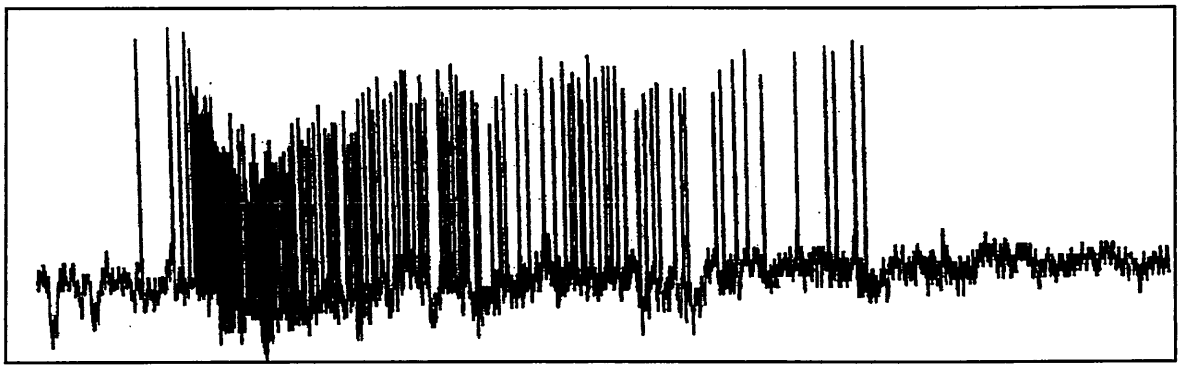

**Figure 1.3**

Recording of a milk ejection burst. Reproduced courtesy Dr. G. Leng

In order to release the maximum amount of hormone in a brief burst, the oxytocin-secreting cells in the SON fire synchronously (Poulain & Wakerley 1982). It is of interest to discover how this synchronization is effected. There are several possibilities:-

1. The oxytocin-secreting cells in the SON and PVN are all driven by a common synaptic input.
2. Positive feedback is provided by mutual synaptic coupling from oxytocin-containing synapses.
3. Coupling between cells is provided by interneurones.
4. Electrotonic coupling between cells.
5. Electric field effects cause depolarization of surrounding neurones.
6. Changes in the potassium concentration in the extracellular space cause depolarization of the cell population.

Various pieces of evidence are available to support some of these hypotheses. Dye coupling between cells suggests the existence of electrotonic coupling between cells (Bourque, Randle & Renaud 1985; Dyball & Leng 1986; Cooke & Stuenkel 1985; Taylor & Dudek 1982; Dudek, Andrew, MacVicar, Snow & Taylor 1983). The electric field and changes in potassium concentration hypotheses need to explain why vasopressin cells are not so affected since both the SON and PVN contain a fairly heterogenous mixture of oxytocin and vasopressin-secreting cells (Dyball & Leng 1986). Electric field effects are discussed by Taylor & Dudek (Taylor & Dudek 1984 a & b). A model is proposed by Sperelakis & Mann (Sperelakis & Mann 1977). Changes in concentration of extracellular potassium ions have been investigated (Leng, Shibuki & Way 1987; Leng, Shibuki & Way 1988). Dyball and Leng discuss some of these possibilities and offer evidence that there is no local positive feedback mechanism linking oxytocin-secreting cells during reflex milk ejection since, in their experiments, stimulation of the neural stalk failed to trigger bursts (Dyball & Leng 1986). In the same paper they suggest that local release of oxytocin may influence reflex milk ejection in the SON. The actions of oxytocin and vasopressin as neuromodulators are also dicussed by these authors in an earlier paper (Leng & Dyball 1983) and also by Richard, Moos & Freund-Mercier (Leng 1988).

During lactation there appears to be a retraction of the glial cells that separate neurons and a closer connection

between cells that may facilitate ephaptic communication (ie. direct cell-to-cell communication) (Poulain & Wakerley 1982; Theodosis, Poulain & Vincent 1981; Dyball & Leng 1986; Leng 1988).

Evidence for the interneurone hypothesis is also given in the above-mentioned paper (Dyball & Leng 1986). The evidence is that supraoptic neurons have projections that extend into areas immediately outside the SON and that neurons in these areas have projections that reach into the SON. In another paper (Leng & Dyball 1983) the subject of communication between cells in the supraoptic nucleus is discussed and several of the ideas mentioned above are analyzed. In the 1983 paper they note the existence of 'stellate' cells that may act as interneurones.

The details of the bursting behaviour of oxytocin-secreting cells during the milk ejection reflex raises some interesting questions which should be addressed by a model that seeks to elucidate the mechanisms behind these oscillations. Besides the question of synchronization of the population of oxytocin-secreting cells there is the question as to the origin of the burst. Here there are two possibilities, (1) the burst is caused by the cells being driven by an external input or (2), an endogenous mechanism. In either case a model should explain how the cells are able to sustain the high rate of firing that has been observed. Suckling is the stimulus that initiates the burst, so a neural pathway from touch receptors in the nipple to synapses on the oxytocin-secreting cells must exist. However the question is whether the burst is driven by

a patterned afferent synaptic input or whether the input merely triggers an endogenous burst. Leng and Bicknell state that the burst duration is between 2 and 4 seconds and the maximum firing rate is between 40 and 80 spikes/second (Leng & Bicknell 1984; Dyball & Leng 1986; Lincoln & Wakerley 1974). Such a high frequency of firing is not usually observed in such cells although high frequency firing is observed in other systems, for example the squid giant axon.

If the interspike interval histograms obtained from recordings of oxytocin-secreting cells are examined it can be seen that the modal interspike interval is 47.1 +/- 3.1 ms for action potentials occurring between milk ejection bursts. This is similar to the situation in male rats. Less than 1.4% of the interspike intervals are less than 20ms in duration. However, during a milk ejection burst 40% of the interspike intervals are between 8 and 20 ms (Dyball & Leng 1986).

A feature of action potentials generated by oxytocin-secreting neurones is a calcium component to the inward current (Mason, Cobbett, Inenaga & Legendre 1988; Renaud 1987; Mason & Leng 1984). In the action potentials recorded from squid giant axons the inward current that causes depolarization of the membrane and the upstroke of the spike is carried by sodium ions only (Hodgkin & Huxley 1952 d). The calcium current produces a 'shoulder' on the action potential and is responsible for a depolarizing after potential (Mason & Leng 1984; Cobbett & Mason 1987; Renaud 1987; Renaud, Bourque, Day, Ferguson & Randle 1985). Calcium also appears to be implicated

in the activity-dependent increase of spike duration during a burst (spike broadening). Spike durations of 1.74 +/- 0.03ms are observed during relatively quiet periods (less than 0.5 spikes/s), but during periods of more rapid firing (greater than 10 spikes/s) this increases to 2.68 +/- 0.05ms (Bourque & Renaud 1985; Renaud 1987; Mason & Leng 1984). These features should also be explained by a model.

The aim of this project is therefore to construct a mathematical model that goes some way to answering some of the questions that are raised by considerations of the unusual repetitive firing behaviour of oxytocin-secreting neurones.

# CHAPTER TWO

## THE HODGKIN - HUXLEY AND RELATED CELL MODELS

A mathematical model of a system or process should fulfil several criteria in order to be useful. The behaviour of the model should closely match the observed behaviour of the system. It should be capable of predicting the behaviour of the system in unusual or abnormal situations or circumstances that are difficult to create experimentally and of generating predictions that are unexpected. It should provide insight into, and understanding of, the workings of the system.

Leng (Leng 1988) defines two types of approach to modelling; the *mechanistic* approach which seeks to elucidate mechanisms responsible for the observed behaviour and the *analytical* approach which seeks understanding in terms of a purely mathematical model. Of these he favours the analytical approach as being the more fundamental. The models discussed here are generally mechanistic in nature but with several notable exceptions.

The model proposed by Hodgkin and Huxley to describe the generation and propagation of nerve impulses in the squid giant axon fulfils the above criteria and represents a milestone in biophysical modelling as evidenced by its very widespread use (Hodgkin & Huxley 1952d). Although further work has cast doubt over details of the model, the approach they used remains valuable and many current models are based on their model (see Hille 1984; Meves 1984; Plant & Kim 1976 Smith 1978; Hencek & Zachar 1977; Ramón, Anderson, Joyner & Moore 1976; Sherman, Rinzel & Keizer 1988; Sanchez & Stefani

1983).

The basic premise of the model is that the action potential is caused by inorganic ions (sodium and potassium) crossing the nerve membrane through separate ion-specific channels. This hypothesis, although not originally propounded by Hodgkin & Huxley, has been validated by the discovery of ionic channels and the isolation and purification of membrane proteins that form them (see Page 26). The step that Hodgkin and Huxley made was to electrically record separate currents and fit mathematical curves to those currents. They pursued this line of work and went on to propose a kinetic model of the currents using coupled non-linear differential equations based on chemical rate equations. Since a substantial amount of subsequent work has been based on Hodgkin and Huxley's work, the model they proposed (the Hodgkin-Huxley model, H-H model) will be discussed in some detail (see Noble 1962; Frankenhaeuser & Huxley 1964; Smith 1978).

By making changes to the bathing solutions in which the squid giant axon was maintained, Hodgkin and Huxley were able to separate and record, using the voltage clamp method (for a space-clamped axon), the individual ionic currents that made up the action potential response of an electrically stimulated axon. (The terms voltage-clamp and space-clamp are explained in Chapter 3). The data from the conductance curves were manipulated mathematically to yield rate "constants" that are functions of voltage. By fitting mathematical functions to these curves Hodgkin and Huxley were able to reconstruct action potentials by numerically integrating (using a hand calculator) the resulting system of equations.

The results they obtained fitted well with the experimental results and predicted several phenomena that have been subsequently confirmed (see Meves 1984).

## THE HODGKIN-HUXLEY MODEL

$$C_m \frac{dV}{dt} = I_i + I_m \quad \ldots\ldots\ldots\ldots\ldots\ldots\ldots\ldots\ldots\ldots (2.1)$$

$$I_i = \bar{g}_{Na}\, m^3 h (V-V_{Na}) + \bar{g}_K n^4 (V-V_K) + \bar{g}_L (V-V_L) \quad \ldots\ldots\ldots (2.2)$$

$$\frac{dm}{dt} = \alpha_m(V)(1-m) - \beta_m(V)m \quad \ldots\ldots\ldots\ldots\ldots\ldots\ldots (2.3)$$

$$\frac{dh}{dt} = \alpha_h(V)(1-h) - \beta_h(V)h \quad \ldots\ldots\ldots\ldots\ldots\ldots\ldots (2.4)$$

$$\frac{dn}{dt} = \alpha_n(V)(1-n) - \beta_n(V)n \quad \ldots\ldots\ldots\ldots\ldots\ldots\ldots (2.5)$$

Where $I_i$ is the total ionic current given by Equation (2.2) , $I_m$ is the membrane current. For calculating a membrane potential the capacity current is equated to the ionic current ($I_i = I_c$). The functions $\alpha_j(V)$ and $\beta_j(V)$ are :-

$$\alpha_m(V) = \frac{0.1(25-V)}{[\exp\{0.1(25-V)\} - 1]} \quad \ldots\ldots\ldots\ldots\ldots\ldots (2.6)$$

$$\beta_m(V) = 4 \exp\{-V/18\} \quad \ldots\ldots\ldots\ldots\ldots\ldots\ldots (2.7)$$

$$\alpha_h(V) = 0.07 \exp\{-V/20\} \quad \ldots\ldots\ldots\ldots\ldots\ldots\ldots (2.8)$$

$$\beta_h(V) = \frac{1}{[\exp\{0.1(30-V)\} + 1]} \quad \ldots\ldots\ldots\ldots\ldots\ldots (2.9)$$

$$\alpha_n(V) = \frac{0.01(10-V)}{[\exp\{0.1(10-V)\} - 1]} \quad \ldots\ldots\ldots\ldots\ldots\ldots (2.10)$$

$$\beta_n(V) = 0.125 \exp\{-V/80\} \quad \ldots\ldots\ldots\ldots\ldots\ldots (2.11)$$

$$\tau_j = \frac{1}{\alpha_j + \beta_j} \quad \ldots\ldots\ldots\ldots\ldots\ldots\ldots\ldots (2.12)$$

$$j_\infty = \alpha_j \tau_j \quad \ldots\ldots\ldots\ldots\ldots\ldots\ldots\ldots (2.13)$$

j = m,h,n

This model has an equivalent electrical circuit representation that is shown below.

EQUIVALENT CIRCUIT

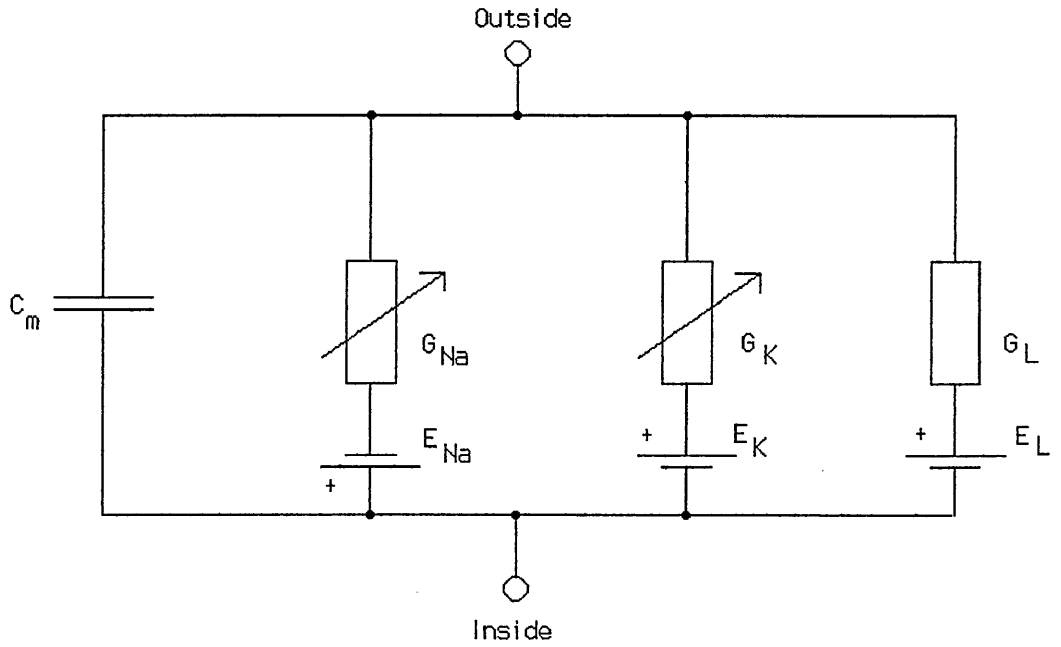


**Figure 2.1**

Circuit diagram representation of the H-H model

The above equations and circuit diagram embody current physiological conventions for the direction of current flow and polarity of membrane voltage. The convention is that membrane voltage is measured with the external bathing solution as the zero volt reference, with the interior of the membrane having a negative resting potential. Positive current flow is taken to be outward. Depolarization of the membrane is regarded as a shift in the positive direction (FitzHugh 1969; Plant & Kim 1976). The equations as

originally formulated by Hodgkin and Huxley reverse this convention such that inward current is positive and the functions for $\alpha_j(V)$ and $\beta_j(V)$ were written with the signs of voltage V being positive. The circuit diagram clarifies the origin of the capacity current. Since the neural membrane is a lipid bilayer surrounded on both sides by conducting fluids it possesses the property of electrical capacitance. A change of voltage across the capacitance is caused by a current flow in or out of the capacitor. The non-linear time- and voltage-dependent conductances are due to the properties of ion-selective channels in the membrane. Although they did not propose any detailed mechanism for the behaviour of what we now know as ionic channels they suggested a model in which flow of current across the membrane was controlled by charged components in the membrane. Movement of these "gating charges" gives rise to gating currents which have subsequently been recorded (see page 32). Detailed consideration of the gating currents has shown that the H-H model is incorrect in detail but this possibility was acknowledged by the authors who admitted that the functions used were a reasonable empirical fit to their data but were not intended to have any physiological significance. Another aspect of the model that we need to be aware of is that the equations were normalized, such that the membrane resting potential was taken to be zero Volts and voltage changes were measured as displacements from resting potential. The H-H equations have been rewritten by other workers to take account of the resting potential being around -62mV (Meves 1984).

TABLE 2.1

UNITS AND MODEL PARAMETERS USED BY HODGKIN AND HUXLEY

| | |
|---|---|
| $C_m$ (membrane capacitance) $1\mu F/cm^2$ | |
| $g_{Na} = 120mS/cm^2$ | $g_K = 36mS/cm^2$ |
| $g_L = 0.3mS/cm^2$ | $V_{Na} = 115mV$ |
| $V_K = -12mV$ | $V_L = 10.613mV$ |
| I $\mu A/cm^2$ | |
| t ms | |
| $\tau_j$ ms | |

Conductance changes are represented by "activation" and "inactivation" variables m,h and n that describe what fraction of the maximum available conductance ($g_X$ where X represents $Na^+$ or $K^+$) is carrying current at any particular instant. The activation variables m and n and inactivation variable h vary between 0 and 1. As shown above, the changes in activation and inactivation variables are governed by first order linear differential equations. The activation and inactivation variables are necessary to describe the rise and subsequent fall of sodium conductance with maintained stimulation whereas only one activation variable, n, is needed to describe changes in potassium conductance. Here again, Hodgkin and Huxley acknowledge a simplification in that the potassium conductance, for example, is described by a variable that follows a first order differential equation, but in order to adequately describe the sigmoidal shape of the rise in potassium conductance, the variable is raised to the fourth power. This simplifies the mathematics

considerably since higher order differential equations are more difficult to solve, but has implications for the type of model that the equations describe. Implicit in these equations is the fact that the activation and inactivation variables are independent. A class of models known as "coupled models" have been explored subsequently by various workers and these show a better fit to the experimental data (see later and also Chapter 5). Graphs showing steady-state activation and inactivation as a function of membrane voltage are shown in Figures 2.2 to 2.4. Also shown are the activation and inactivation time constants as a function of voltage in Figures 2.5 and 2.6. The alpha and beta functions are shown in Figures 2.7, 2.8 and 2.9.

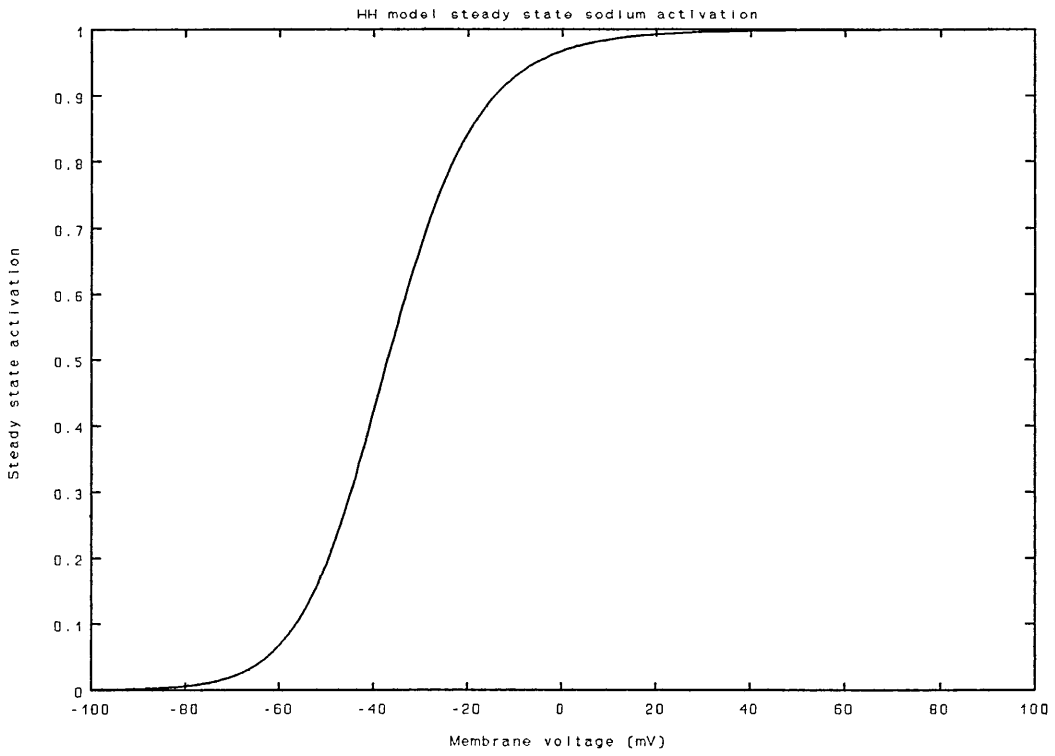


**Figure 2.2**
Graph showing the variation of steady-state sodium activation with voltage.

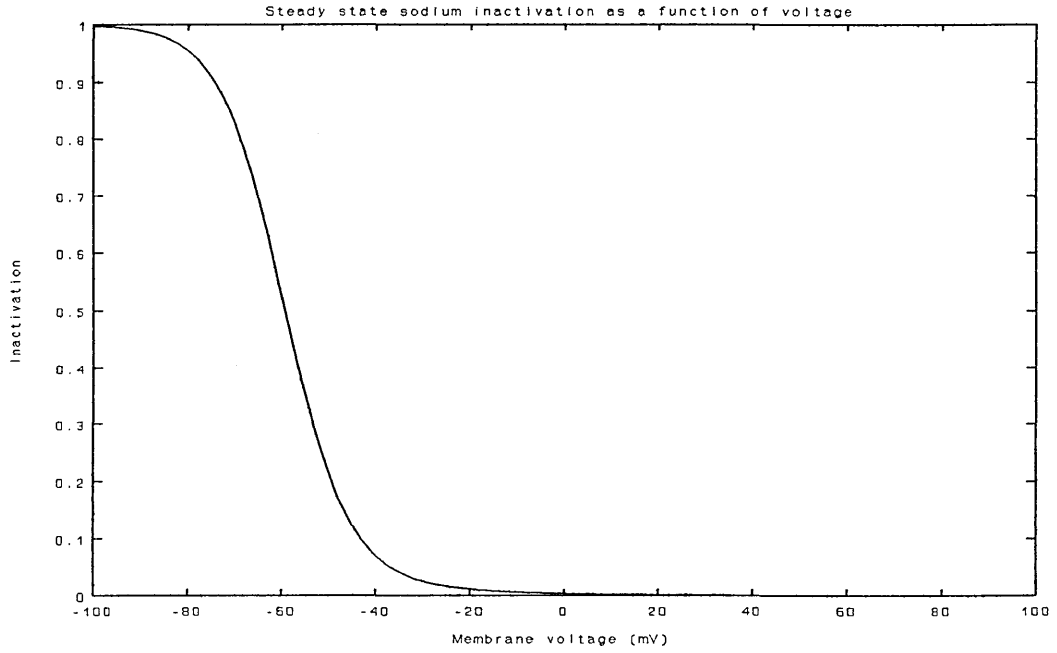


**Figure 2.3**
Graph showing the variation of steady-state sodium inactivation with voltage.

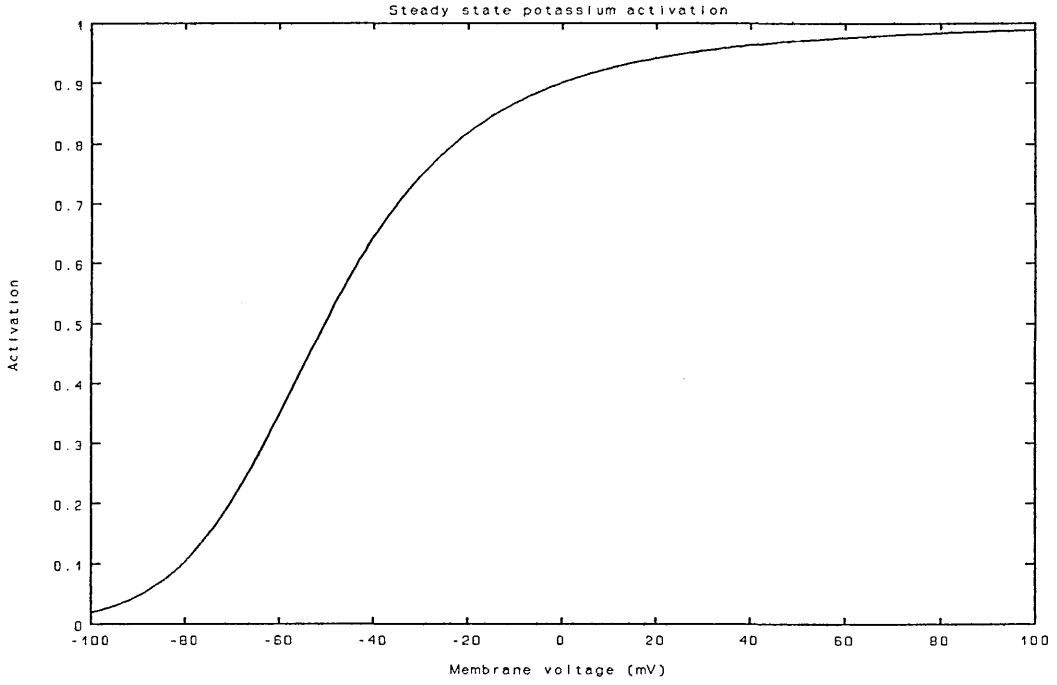


**Figure 2.4**
Graph showing the variation of steady-state potassium activation with voltage.

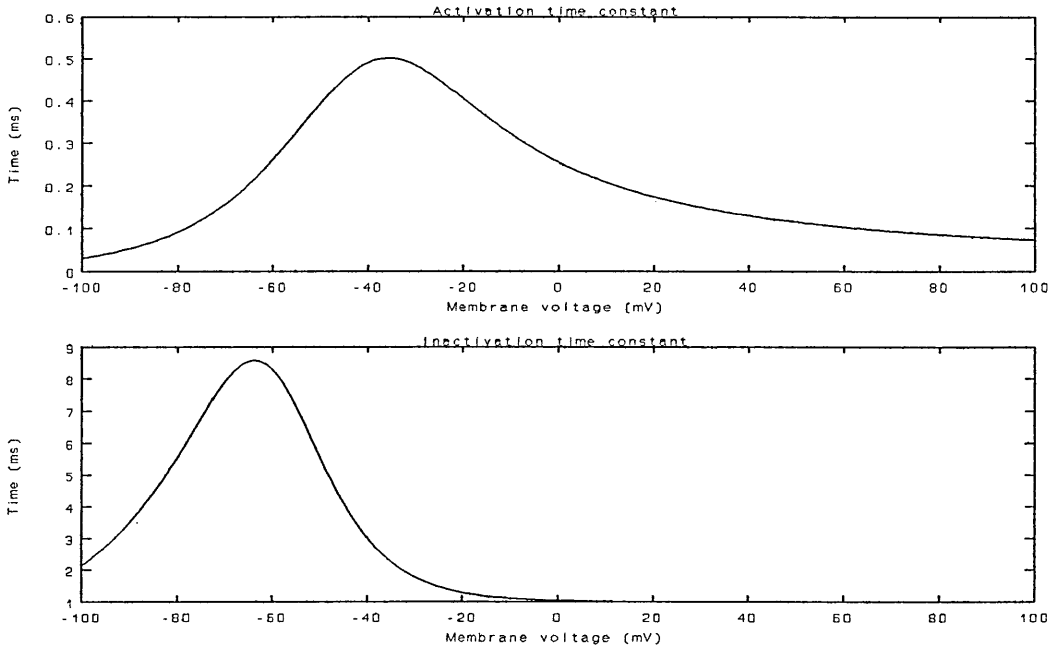


**Figure 2.5**
Graph showing the sodium activation and inactivation time constants as a function of voltage.

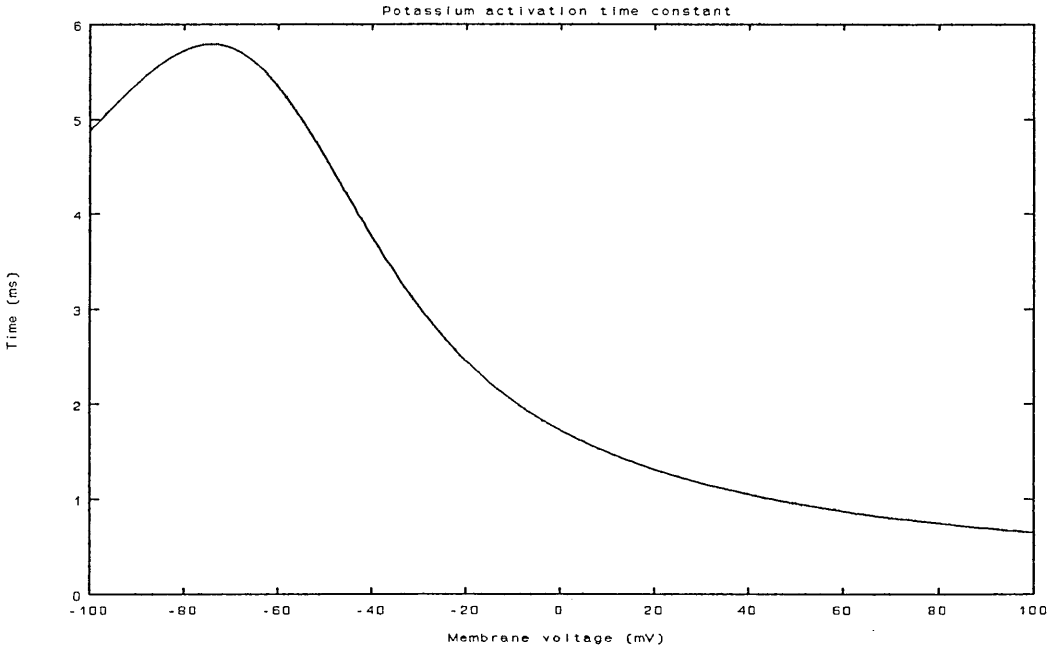


**Figure 2.6**
Graph showing the potassium activation time constant as a function of voltage.

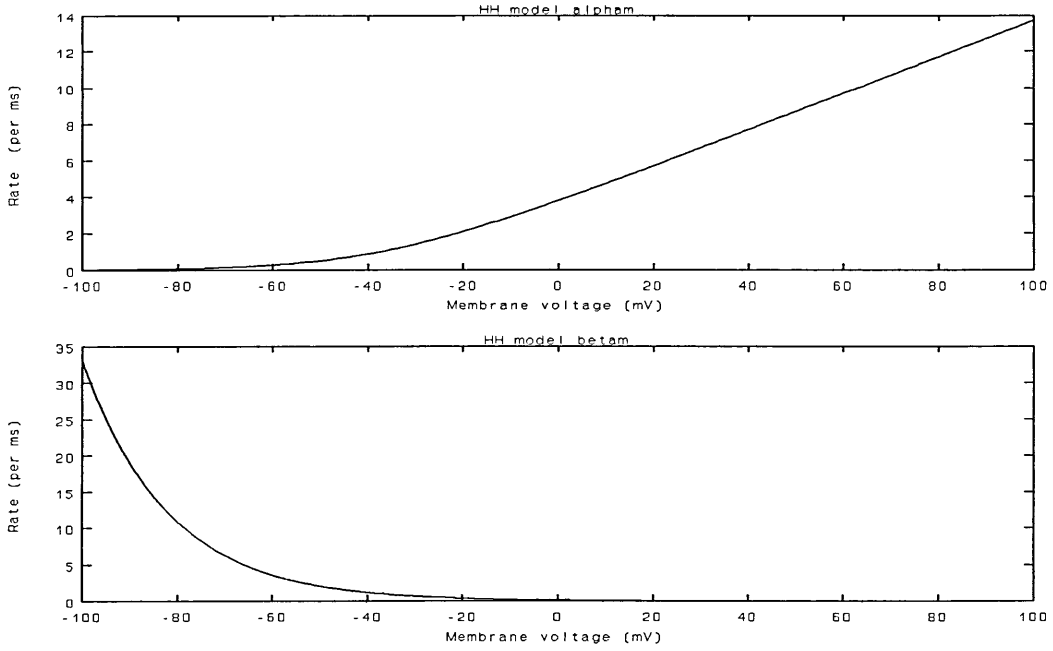


**Figure 2.7**
Graph showing sodium activation rate "constants" as functions of voltage.

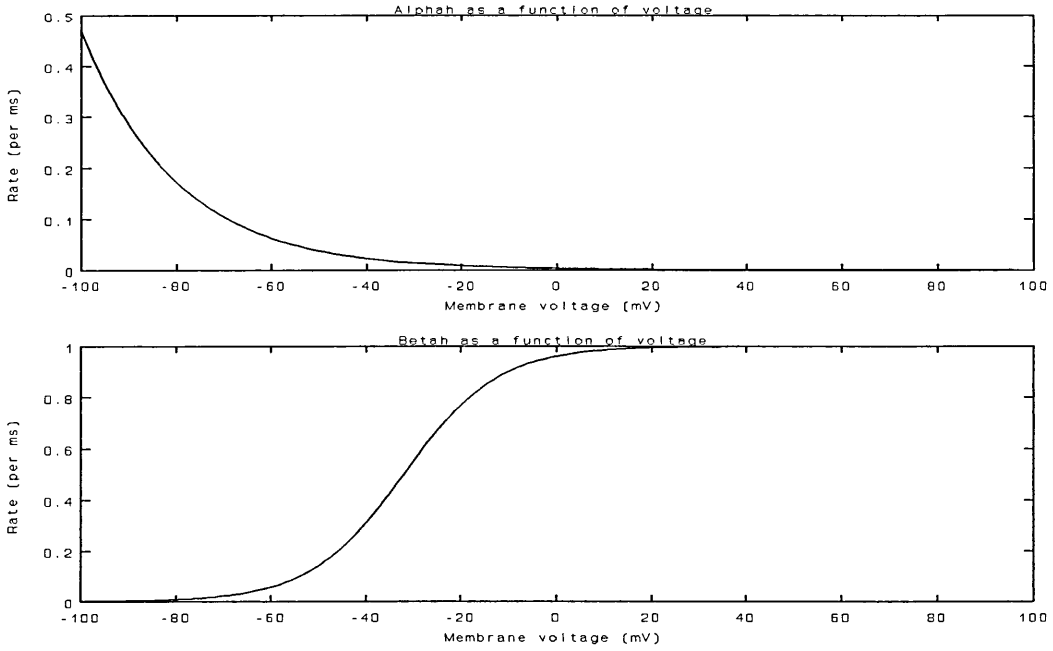


**Figure 2.8**
Graph showing sodium inactivation rate "constants" as functions of voltage.

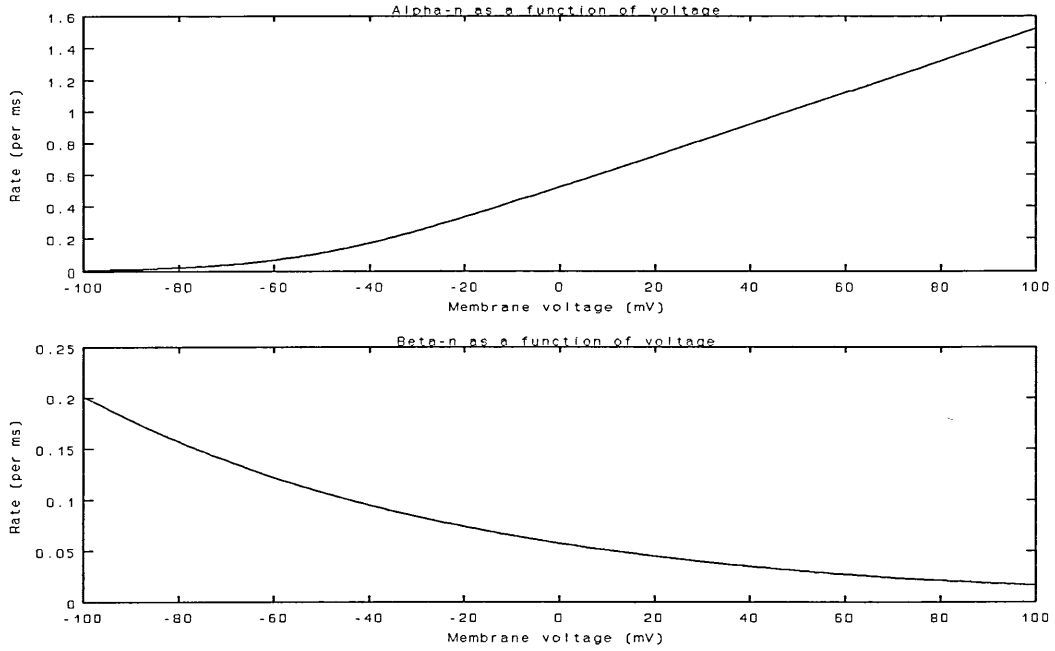


**Figure 2.9**
Graph showing potassium activation rate "constants" as functions of voltage.

Hodgkin and Huxley reconstructed two types of action potential: the membrane potential mentioned above , and the propagated action potential. The total membrane current is composed of a contribution due to ionic fluxes through the membrane and the capacity current as described above. When the ionic current is set equal to the capacity current a membrane potential results. If the membrane current is allowed to propagate along the axon, exciting subsequent patches of membrane, then the result is a propagated action potential which is calculated using cable theory. This study is primarily concerned with membrane potentials.

The activation and inactivation variables that have been mentioned previously merit further explanation. The recorded potassium conductance shows a marked delay and inflection following a depolarizing stimulus. In order to describe this

mathematically, Hodgkin and Huxley multiplied the value of conductance by a dimensionless first order variable n, raised to the fourth power. This variable was given the name "activation". The rate of change of potassium activation is a time and voltage-dependent process and may be derived by assuming that a charged entity governs the opening and closing of a "gate" in the potassium-selective channel such that in one particular conformation the gate is closed and in another conformation, the gate is open, allowing potassium ions to flow through the channel. The particle moves between these two conformations according to a first-order differential equation. The Boltzmann distribution is a probability distribution that describes the probability of a finding a given number of particles in a particular energy state. The concepts involved may be used here since movement of a charged particle through an electric field involves a change of energy level. If the probability of n particles being in the open conformation is given by n, then 1-n gives the probability of the gate being in the closed state (since the sum of all probabilities should equal unity).

$$1 - n \underset{\beta_n}{\overset{\alpha_n}{\rightleftharpoons}} n \qquad \ldots\ldots\ldots\ldots\ldots\ldots\ldots\ldots\ldots\ldots \quad (2.14)$$

The rate of change of state is given by the differential equation (2.5). Solving this differential equation yields an exponential expression with time constant

$$\tau_n = \frac{1}{(\alpha_n + \beta_n)} \quad \ldots\ldots\ldots\ldots\ldots\ldots \quad (2.15)$$

and steady-state value of activation given by

$$n_\infty = \frac{\alpha_n}{(\alpha_n + \beta_n)} \quad \ldots\ldots\ldots\ldots\ldots\ldots \quad (2.16)$$

To fit the sigmoidal rise in potassium current, the activation variable is raised to the fourth power as mentioned before.

$$g_K = \bar{g}_K \, n^4 \quad \ldots\ldots\ldots\ldots\ldots\ldots \quad (2.17)$$

This is interpreted as meaning that, for the gate to be open four such "gating particles" must simultaneously be in the open configuration.

Thus, the solution of Equation (2.5) is

$$n_\infty = n_\infty - (n_\infty - n_0) \exp\{-\tau/\tau_n\} \quad \ldots\ldots\ldots\ldots \quad (2.18)$$

where $n_0$ is the initial state of the activation variable.

The sodium activation and inactivation follow the same derivation. The activation is deduced to be controlled by three particles and the inactivation by one. For a sodium

channel to be open, all three activation and the inactivation particles have to be in the correct configuration.

Hodgkin and Huxley's model yields good results for the velocity of the propagated action potential and its shape. It also demonstrates a threshold for excitation and latency between action potentials. The all-or-nothing response to stimulation is another feature that the model successfully reproduces. Given a maintained suprathreshold stimulus, the H-H model fires an infinite train of action potentials (Cooley & Dodge 1966; Cole,Antosiewicz & Rabinowitz 1955), which is not observed experimentally. In this respect, the model lacks an adaptation variable (FitzHugh 1969) (see discussion of FitzHugh's model Page 37). Bathing the squid axon in a medium containing a low concentration of calcium or magnesium does produce repetitive firing (Huxley 1959; Meves 1984). The model also predicts a strength-duration curve that is a reasonable fit to experimental results (Cooley & Dodge 1966).

Ionic channels have been mentioned previously and it is appropriate at this point to discuss their nature.

Bernstein (Bernstein 1902) first proposed the theory that there are channels or pores in nerve membrane , but it has only been fairly recently that the existence of such channels has been confirmed. It is now possible to record the current through a single ionic channel (see single-channel recording in Chapter 3). It is also possible to extract, purify and reconstitute ionic channels experimentally (Hille 1984; Latorre, Alvarez, Cecchi & Vergara 1985; Ehrenstein, Lecar & Nossal 1970). Ionic channels are formed by large transmembrane proteins which may be inserted into artificially-created lipid bilayers to form pores with the same characteristics as are observed naturally. Alamethicin and gramicidin A are two such pore-forming molecules that have been studied (Hille 1984; Neher & Stevens 1977).

A major piece of evidence that transport of ions across the nerve membrane is due to flow through ion-specific channels is that the observed rate of ionic flux is too high to be explained by a carrier model whereby ions bind to a membrane protein which then undergoes a conformational change of one sort or another to move the ion from one side of the membrane to the other (Hille 1984). However, calculations of ionic fluxes on the basis that transport across the membrane is by flow of ions through a water-filled pore do yield results that are consistent with the observed rates. ( more than $10^6$ ions/s Hille 1984). This is not to say that carriers do not exist, merely that the currents which are observed to be responsible for generating the action poten-

tial are not due to that method of transport. Pore diameters are assumed to be such that ions have to shed some of their water of hydration in order to fit through the channel. The gramicidin A pore has a diameter of 4 Å (Hille 1984) which is in accordance with these calculations.

Single channel recording as described in Chapter 3 also provides evidence for the existence of ionic channels. In fact the existence of ionic channels is now regarded as beyond all reasonable doubt (Hille 1984). Single ionic channels are either open or closed (though there is evidence for the existence of so-called conductance substates) and the current recorded from them appears as rectangular pulses. The channels open and close stochastically with the mean open time and shut time being functions of membrane potential. This gives rise to interesting questions about single channel currents and macroscopic currents which are smooth functions of time and voltage. Because the macroscopic currents are smooth it is apparent that what is being observed is the overall behaviour of a very large number of channels and the contribution of an individual channel is very small compared with the total current. As an indication of the scale of these currents, Hodgkin and Huxley recorded currents with magnitudes of hundreds of microampères per square centimetre, whereas single channel currents are of the order of a few picoampères to a few nanoampères. Comparison of macroscopic currents and single channel currents also allow the estimation of the channel density in a membrane. Because of the large numbers of channels carrying such small currents, which is a feature of nerve membranes, some of the

ideas from statistical mechanics may be applied. Specifically, the Boltzmann equation, mentioned earlier, which relates the number of particles in two different energy states to the energy difference between the states, often appears in descriptions of channels.

As stated previously, the aim of this study is to provide a satisfactory explanation of the unique bursting behaviour of the oxytocin-secreting neurone and to achieve this a model is being sought. The model is a model of the macroscopic currents. As various authors report, much work is being done on elucidating the properties of the ionic channels that underlie action potentials. Modelling the electrical behaviour of nerve membrane at this molecular level using fundamental physical and chemical properties of ions in solution, the lipid bilayer and the pore-forming membrane proteins, is considered to be too complex at this stage and will not be attempted. Work towards this end is in progress, see for example Gillespie (1976a,b). It is however acknowledged that one aim of research in this area is to be able to provide a satisfactory explanation of all the observed features of ionic conduction through nerve membranes using such a fundamental model.

Hille (1984) gives a detailed background of the theory behind ion transport in pores and reviews research in the area. Other related articles not explicitly referenced in the text, but which contain much useful background are Latorre & Alvarez 1981; Latorre, Alvarez, Cecchi & Vergara 1985; Laüger 1984; Neher & Stevens 1977. The precise conformational changes that the membrane proteins undergo have not yet been

fully elucidated and this is an area of active research. Hille (1984) discusses various proposed structures and models and the reader is referred to this volume for further detail.

## MECHANISTIC IMPLICATIONS OF THE H-H MODEL

The Hodgkin-Huxley model carries with it implications about the mechanisms involved in controlling the flow of ions through channels. The activation and inactivation variables invoked by Hodgkin and Huxley are merely convenient empirical descriptions of the number of ionic channels open at any instant. The observed macroscopic current flow is the sum of ion flow through open channels. The opening and closing of ionic channels is governed by processes known as gating. The observed macroscopic currents are a manifestation of the underlying opening and closing behaviour of ionic channels on a microscopic level. French and Horn (1983) show how adding together the responses of many individual channels reproduces the observed sodium current. Using the sodium current as an example, the implications that the H-H model has for the underlying gating of the sodium channel, will be briefly investigated.

The variations in sodium current with time and voltage are reasonably well fitted using the $m^3h$ description. This model supposes that the conductance state of the channels is governed by three "activating" particles and one "inactivating" particle. Chemical rate kinetics are then used to describe the movement of these particles, giving the linear, first order differential equations as derived above. (see Equations 2.3,2.4 & 2.5). Hodgkin and Huxley assumed that the

processes of activation and inactivation were independent. In fact, detailed studies have since shown that there is some interaction between the processes of activation and inactivation. (French & Horn 1983; Bezanilla & Armstrong 1977 (I); Armstrong 1981) However, activation and inactivation are separate processes since treatment of nerve membrane using pronase has been shown to remove inactivation of the sodium current without affecting activation (Hille 1976; Bezanilla & Armstrong 1977(I); Armstrong 1981; French & Horn 1983).

A useful discussion of the H-H model of sodium conductance variation is provided by French & Horn (French & Horn 1983) alongside a coupled model. A cyclic kinetic scheme for describing sodium conductance, having three coupled states is discussed by Jakobsson (Jakobsson 1976). The reader is referred to these, and the other references cited, for further details of the various kinetic schemes that have been proposed. Tests for these models may be provided by the predictions of mean channel open times that are measurable experimentally using single channel recording methods.

The model proposed by this study is concerned with the macroscopic behaviour of the ionic currents present in the oxytocin-secreting cell membrane and so the underlying kinetic behaviour of channel gating will not be discussed further.

Ionic channels are normally considered to have just two conductance states, open and closed. In going from the open conformation to the closed conformation and vice versa, the channel will pass through several different conformations each with a different energy state. Consideration of these states and transitions between them in pictorial form leads to a state diagram. A state diagram for the sodium current of the H-H model may be derived by considering their hypothetical gating particles. Activation is governed by three m particles giving rise to the $m^3$ description. Inactivation is governed by a single gating particle h. There are thus two inactivation states, "inactivated" and "non-inactivated". There are four activation states, "activated", one "active" particle, two "active" particles and "non-activated". This gives a total of eight conformational states for the channel. Such a verbal description is very clumsy and French and Horn (French & Horn 1983) give a diagrammatic description of these states that conveys the information much more efficiently and elegantly. Such a state diagram is shown in Fig. 2.10. State diagrams are widely used in attempting to prove or disprove various kinetic schemes. The H-H scheme as given above does not give predictions of gating current that are seen in practice.

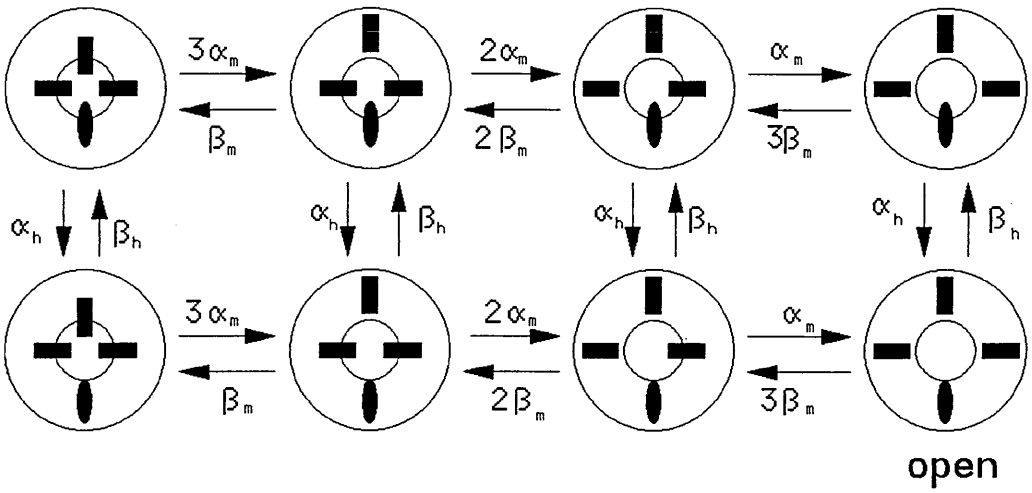


**Figure 2.10**
State diagram for H-H sodium channel.

## GATING CURRENTS

Hodgkin and Huxley predicted the existence of gating currents as a consequence of their model of the squid axon in 1952. Stated simply, gating current is simply the element of membrane current that arises from the movement of the gating "particles" or charges in the membrane. However, due to the small size of the current, it was not until 1973 that the sodium gating current was first observed by Armstrong and Bezanilla, using special pulse protocols and signal averaging techniques (Armstrong & Bezanilla 1973). Gating currents arise due to asymmetrical charge movement within the membrane and are a necessary consequence of the voltage sensitivity of the ionic channels. It appears that the opening and closing of the channels are controlled by molecules having an overall charge, giving them a polar nature and hence, a dipole moment. It is this property that endows the gate with its voltage sensitivity. Since the gating current is an asymmetrical charge movement it may be distinguished from the

linear capacitive component of the membrane current by using equal and opposite stimulating pulses. A more complicated "P/4" procedure is favoured by Armstrong and Bezanilla (Armstrong & Bezanilla 1977) for separating gating current from capacitive current. Details of the experimental protocols are to be found in Armstrong & Bezanilla 1974. As this study is concerned with descriptions of the macroscopic currents only, no further discussion will be given. Gating currents are very small as stated above and so can be safely neglected when modelling the macroscopic currents. It should be noted, however that the study of gating currents provides evidence to support or refute the various proposed channel gating mechanisms. As far as the author is aware there has been no published work on gating currents in oxytocin-secreting cells to date. A model that included gating currents could not be tested by currently available means since although it is possible to reject models that produce incorrect results, it is not possible to distinguish between two models yielding similar results. Useful discussions of gating currents are to be found in Bezanilla & Armstrong 1974; Adams & Gage 1975; Armstrong 1975; Horn 1984; Meves 1984; Ulbricht 1977; Lundström & Stenberg 1977.

Hodgkin and Huxley's model of the squid giant axon is essentially empirical in that mathematical equations were chosen to fit the experimental data without specific reference to any underlying physical model. The criterion for fitting was that the chosen equations should provide a close fit to the data over the range of interest. Another modelling approach is to work from fundamental principles and build up a model from a theoretical framework. As mentioned above, this approach will not be used here since this would involve a very complicated and cumbersome model that would probably not be useful in providing insights into the physical processes involved. (See Gillespie 1976a; Gillespie 1976b; Goulden 1976 Attwell & Jack 1978 for discussions of various theoretical approaches.) A further possiblity for building up a mathematical model is from knowledge of the behaviour of systems of differential equations. This approach is taken by Hindmarsh and Rose (Hindmarsh & Rose 1982; Hindmarsh & Rose 1984). The first of these two papers describes a model that reproduces continual firing. The second paper extends the model to show the generation of bursts of action potentials using a third differential equation. The observed behaviour of the oxytocin secreting cell is oscillatory with the additional complication that the spike train does not repeat indefinitely but rather appears to be gated on and off. In this respect the model of Hindmarsh and Rose, using three coupled first order differential equations, adequately represents the observed activity. This model was investigated

by the author but initial results were not encouraging. A slightly different, but allied approach is taken by Zeeman (Zeeman 1972) who uses the catastrophe theory of René Thom to derive a model for the heartbeat and nerve impulse. Leng (Leng 1988) also explains the use of catastrophe theory in modelling biological systems. FitzHugh (FitzHugh 1969) also provides a good example of this approach to modelling and the models of Hindmarsh and Rose are based on a generalization of equations derived by FitzHugh. However, there is a drawback here since most models of this type are reduced order, simplified models. Such models do not show the details of observed behaviour due to the simplifications involved. There are several aspects of the bursting behaviour that are of interest, such as the shoulder on the repolarizing phase of the action potential waveform, spike broadening and the changes in firing rate during the burst that may not be reproduced by such a simplified model. The advantage in using reduced order models is that techniques such as the phase plane are applicable and this enhances the understanding of the system behaviour. Rinzel uses this approach and introduces the idea of a model that exhibits bistable behaviour and that movement between the two types of activity is driven by an additional model variable (Rinzel "Bistable behavior of bursting cells" pre-publication communication). This approach may be used since there are fast and slow variables in the model with widely differing time constants. This enables variables to be treated as parameters for the purposes of analysis.

FitzHugh (FitzHugh 1969) discusses several models and

provides a useful classification of the types of model variable that are used in describing membrane behaviour. These variables are ; 1) Membrane potential, 2) Excitation variables (m in H-H model), 3) Recovery variables (h,n in H-H model) and 4) Adaptation variables. The subject of this study is the bursting behaviour of the oxytocin-secreting neurone which requires all four of these types of variable. A single action potential or an infinite train of impulses may be simulated using a computer model based on the H-H model which does not contain any adaptation variables. (See Colding-Jφrgensen (1976) for discussion of adaptation.) Refinements to the H-H model to include the phenomenon of adaptation usually invoke the concentration of calcium ions at the inside of the membrane acting on calcium-gated potassium channels to provide feedback and burst termination. (Smith 1978; Rinzel ; Maddrell & Nordmann 1979; Gorman & Thomas 1978). This mechanism is explored in the present study since calcium channels and calcium-gated potassium channels are known to exist in the oxytocin-secreting cell (Bourque, Randle & Renaud 1985; Cobbett, Legendre & Mason 1989; Mason & Leng 1985; Bourque & Renaud 1985). Inclusion of calcium channels and calcium-gated potassium channels further complicate the H-H model but are necessary since these channels are known to exist and play an important rôle in governing the electrical properties of the oxytocin-secreting cell.

The generalised set of equations given by FitzHugh are reproduced here.

$$\frac{dV}{dt} = \frac{1}{C}[\ I - I_i(V,W_1,\ldots,W_\mu)] \quad \ldots\ldots\ldots\ldots \quad (2.19)$$

$$\frac{dW_j}{dt} = F_j(V,W_1,\ldots,W_\mu) \quad j=1,\ldots,\mu \quad \ldots\ldots\ldots \quad (2.20)$$

These equations represent a set of coupled first order differential equations where V is the membrane potential and $W_1,\ldots,W_\mu$ are state variables. The Hodgkin-Huxley model belongs to this general class as do other models that represent the membrane by its capacitance in parallel with variables controlling the flow of current through the membrane. The electrical equivalent circuit described by these equations follows the form given in Fig. 2.1 above.

There is a class of models introduced by FitzHugh based on extensions to the Van der Pol oscillator equation. They are the Bonhoeffer-van der Pol (BVP) models. The van der Pol equation is a well-known equation used to model non-linear relaxation oscillators.

A further approach to modelling involves the construction of an analogous system. Analogue computers use electronic circuits to solve sets of differential equations. Rather than use a general purpose analogue computer a common approach is to construct a Neuromime (MacGregor & Lewis 1977; Patton 1980): an electronic circuit designed to mimic the electrical behaviour of nerve cells. As with other approaches to modelling, only certain aspects of the system are simulated and other features are neglected in order to produce a simplified model. An example of an early neuromime is due to Nagumo, Arimoto & Yoshizawa (Nagumo, Arimoto &

Yoshizawa 1962). Here, tunnel diodes were used as the active elements in an active transmission line used to simulate various properties of an axon. The model was based on FitzHugh's BVP model after acknowledging the complexities of the H-H equations. The equations used were :-

NAGUMO'S MODEL

$$\frac{dV}{d\tau} = \frac{1}{C}\{j + i + f(e)\} \quad . . . . . \quad (2.21)$$

$$\frac{di}{dt} = \frac{1}{L}\{ -Ri - V \} \quad . . . . . \quad (2.22)$$

McKean (McKean 1970) discusses the mathematics of the model. That such an approach is still relevant is evidenced by the recent implementation of a FitzHugh-Nagumo neurone model using integrated circuit fabrication techniques (Linares-Barranco, Sánchez-Sinencio, Rodriguéz-Vázquez & Huertas 1991). This approach has not been used in this study and the use of analogue computing and neuromimes will not be discussed further.

Derivation of the BVP cubic equations is given in FitzHugh (FitzHugh 1969) and will not be reproduced here. The actual equations are of interest and are given here.

$$\frac{dV}{dt} = V - \frac{V^3}{3} - W + I \quad \ldots\ldots\ldots\ldots\ldots\ldots \quad (2.23)$$

$$\frac{dW}{dt} = \phi(V + a - bW) \quad \ldots\ldots\ldots\ldots\ldots\ldots \quad (2.24)$$

where a,b and $\phi$ are positive constants.

Since these equations are derived from a second order differential equation, the phase plane method of analysis of second order systems may be used. This technique is graphical and is useful for identifying the qualitative behaviour of the system in terms of stability, identification of limit cycles and other oscillatory phenomena. The original H-H model is of too high order to be amenable to this technique. FitzHugh (FitzHugh 1969) uses the phase plane to demonstrate the behaviour of the cubic BVP model and shows various possible trajectories. The model shows either single impulse responses or an infinite train of impulses in response to various stimuli, indicative of the absence of the adaptation variable from this model.

Rinzel ("Bistable behaviour of bursting cells" pre-publication communication) discusses the behaviour of a model based on the H-H model, the Chay-Keizer model, of the pancreatic ß cell. He analyzes the model to reveal a negative resistance region in the model`s I-V characteristic, essential for maintaining repetitive activity (Wilson & Wachtel 1974), and an underlying bistability. The slow variable is the intracellular free calcium concentration which drives the model between two stable states. The upper state is characterised by continuous firing and the lower state by silence. In this model the calcium concentration is controlled by influx of calcium through channels whose conductance is an instantaneous function of the membrane voltage. This simplification means that the conductance follows changes in voltage without the delays inherent in the activation and inactivation variables normally used to characterise channel kinetics. Also included in the model is a variable representing the external concentration of potassium ions, which is treated as an unchanging parameter. The model equations are reproduced here.

$$C_m \frac{dV}{dt} = -I_{Ca}(Ca) - [g_K n^4 + g_{K\text{-}Ca}\{Ca/(1+Ca)\}](V-V_K) - g_L(V-V_L) \quad (2.25)$$

$$\frac{dn}{dt} = \Gamma_n[n_\infty(V) - n]/\tau_n(V) \quad . . . . . \quad (2.26)$$

$$\frac{dCa}{dt} = f\,[-\alpha I_{Ca}(V) - k_{Ca}Ca] \quad . . . . . \quad (2.27)$$

$$I_{Ca}(V) = g_{Ca} m_\infty^3(V) h_\infty\,(V-V_{Ca}) \quad . . . . . \quad (2.28)$$

Numerical integration of the model equations results in characteristic bursting behaviour and a representative voltage-time graph is shown in his paper. The model equations and parameter values are given in the appendix and allow reconstruction of the model.

A related model is that due to Sherman, Rinzel & Keizer (Sherman, Rinzel & Keizer 1988). This model describes bursting in pancreatic beta cells. The model equations are reproduced here.

As part of this study, the model of the ß-cell as given by Rinzel et al. was translated into a FORTRAN-77 and subsequently an ACSL program. The model demonstrated characteristic bursting behaviour. The results are not included here for reasons of space.

$$C_m \frac{dm}{dt} = -\bar{g}_K n(V-V_K) - \bar{g}_{Ca} m_\infty(V) h(V)(V-V_{Ca}) - \bar{g}_{K\text{-}Ca}(Ca_i)(V-V_K) \quad (2.29)$$

$$\frac{dn}{dt} = \lambda[n_\infty(V) - n/\tau_n(V)] \quad (2.30)$$

$$\frac{dCa_i}{dt} = f(-\alpha I_{Ca} - k_{Ca} Ca_i) \quad (2.31)$$

$$g_{K\text{-}Ca}(Ca_i) = \bar{g}_{K\text{-}Ca}\left(\frac{Ca_i}{[k_d + Ca_i]}\right) \quad (2.32)$$

$$m_\infty(V) = \frac{1}{1+\exp[(V_m - V)/S_m]} \quad (2.33)$$

$$h_\infty(V) = \frac{1}{1+\exp[(V-V_h)/S_h]} \quad (2.34)$$

$$n_\infty(V) = \frac{1}{1+\exp[(V_n - V)/S_n]} \quad (2.35)$$

$$\tau_n(V) = \frac{C}{\exp[(V-\bar{V})]/a]} + \exp[-(V-\bar{V})/b] \quad (2.36)$$

$$\alpha = \frac{1}{2V_{cell}F} \quad (2.37)$$

TABLE 2.2

MODEL PARAMETERS

| | |
|---|---|
| Cell radius r = 6μm | $C_m$ = 5310fF |
| $V_{cell}$ = 1150$\mu m^3$ | F = 96.487 C/Mol |
| $V_m$ = 4mV | $S_m$ = 14mV |
| $V_n$ = -15mV | $S_n$ = 5.6mV |
| a = 65mV | b = 20mV |
| c = 60mV | $\bar{V}$ = -75mV |
| $V_h$ = -10mV | $S_h$ = 10mV |
| $\hat{g}_K$ = 2500pS | $\hat{g}_{Ca}$ = 1400pS |
| $V_K$ = -75mV | $V_{Ca}$ = 110mV |
| λ = 1.7 | $K_d$ = 100μM |
| $\hat{g}_{K\text{-}Ca}$ = 30000pS | f = 0.001 |
| $k_{Ca}$ = 0.03$ms^{-1}$ | |

Another example of a bursting model based on the H-H model is given by Smith (Smith 1978). Here, the bursting behaviour of the mollusc *Tritonia diomedia* is modelled using eight ionic currents as well as a variable representing the intracellular free calcium concentration. The characteristics of the currents were obtained from voltage clamp experiments and fitted by empirical curves in much the same way as Hodgkin and Huxley did for the squid giant axon. Numerical integration of the resulting system of coupled differential equations, including solving the partial differential equation used to represent diffusion of calcium within the cell, yielded bursting which showed good agreement with experimentally observed behaviour.

Noble (Noble 1962; 1966) also derives a model based upon the H-H model. In this case, the system under study is the heart and the model describes action and pacemaker potentials in Purkinje fibres. The latter paper is a review paper which discusses the H-H model and its applicability to other electrically excitable tissues.

A further model of interest is that due to Plant & Kim (Plant & Kim 1976). The bursting pacemaker neurone known as R15 in *Aplysia* was modelled using a modification of the H-H equations to include a cyclical variation in the potassium conductance. A later paper by one of the authors (Plant 1978) refines the model to include the effects of calcium ions. The earlier paper concludes that the model successfully represents many of the features of the bursting neurone. Phase portraits are included for a reduced order system in order to derive parameter values that ensure limit cycle behaviour.

$$\frac{dV}{dt} = \frac{1}{C}[(g_I X_I^3 Y_I + g_T)(V_I - V) + (g_K X_K^4 + g_A X_A Y_A + g_p X_p)(V_K - V) + I_{ep} + I_{ext}] \quad (2.29)$$

$$\frac{dX_I}{dt} = \frac{1}{\tau_{XI}(V)}[S_I(V) - X_I] \quad (2.30)$$

$$\frac{dY_I}{dt} = \frac{1}{\tau_{XI}(V)}[Z_I(V) - Y_I] \quad (2.31)$$

$$\frac{dX_K}{dt} = \frac{1}{\tau_{XK}(V)}[s_K(V) - X_K] \quad (2.32)$$

$$\frac{dX_p}{dt} = \frac{1}{\tau_{XP}(V)}[S_p(V) - X_p] \quad (2.33)$$

TABLE 2.2

Model Parameters and functions

$g_I = 4.0mS \qquad g_K = 0.3mS \qquad g_L = 0.003mS$

$V_I = 30mV \qquad V_K = -75mV \qquad V_L = -40mV$

$C = 1\mu F$

$$S_I(V) = \alpha_m/(\alpha_m + \beta_m)$$

$$Z_I(V) = \alpha_h/(\alpha_h + \beta_h)$$

$$S_K(V) = \alpha_n/(\alpha_n + \beta_n)$$

$$\tau_{XI} = 12.5/(\alpha_m + \beta_m)$$

$$\tau_{YI} = 12.5/(\alpha_h + \beta_h)$$

$$\tau_{XK} = 12.5/(\alpha_n + \beta_n)$$

$$\alpha_m(V) = (0.1[-26-1.2V])/\{\exp([26-V]/10)-1\}$$

$$\beta_m(V) = 4\exp([51-1.2V]/18)$$

$$\alpha_h(V) = (0.07\{\exp(-51-1.21V)\}/20)$$

$$\beta_h(V) = 1/\{\exp([21-1.3V]/10) + 1\}$$

$$\alpha_n(V) = (0.01[-21-1.21V])/\{\exp([-21-1.21V]/10) -1\}$$

$$\beta_n(V) = 0.125\exp([-31-V]/80)$$

Mathematical models usually start off as fairly minimal structures that are subsequently refined to include more detail. Many small effects are often ignored in the early stages and later included when the basic model has been discovered to be fundamentally sound. In this respect, the model derived later ignores several aspects of the actual behaviour of nerve membranes. One such aspect is the voltage dependence of the electrical capacitance of the membrane (Adrian & Almers 1976; Takashima & Yantorno). Although the effects of changing membrane capacitance are not included in the proposed model, a brief investigation of changing capacitance was performed by the author and the results are shown in Chapter 8. This yielded the expected result that, for a given membrane current, a smaller membrane capacitance would charge and discharge more rapidly than a larger value capacitance. This also shows up in the amplitude of the resulting action potential. Since the effect is fairly small and the estimates of the total capacitance of the cell can vary significantly it was felt that such voltage dependence is a second order effect and as such is not essential in determining the overall behaviour of the system. For these reasons it was decided that the omission of the effect from the model was justified.

From this brief review it can be seen that the H-H model is a very useful starting point for modelling the electrical behaviour of nerve cells and that calcium appears to play a vital rôle in controlling bursting activity. This area of research has yielded much important work but time and space limitations preclude a detailed discussion of more than a few

papers. However, in the course of background reading many more research papers and articles have been studied and a list of those not cited already, is now given.

Fleisher, Studer & Moschytz 1984; Fleisher 1984. These two papers propose a mathematical model for a propagated action potential referred to as a synthetic Gaussian model.

George & Johnson 1961 discuss the H-H model with parameters adjusted so as to represent the experimental conditions of potassium-rich bathing solution in one case, and the presence of the potassium channel blocker TEA (Tetraethylammonium ions) in the other.

Real axons often have many branches and the effects of axon branching are examined in a paper by Joyner, Westerfield, Moore & Stockbridge 1978.

Another mathematical model of the action potential is proposed by Strandberg (Strandberg 1976). The author aims to create a model based on theoretical considerations rather than follow the empirical approach of Hodgkin and Huxley.

Action potentials in smooth muscles are modelled using a modification of the H-H model by Ramón, Anderson, Joyner & Moore in their 1976 paper.

Electrical stimulation of myelinated nerve by a particular electrode configuration is considered by McNeal (McNeal 1976).

The H-H and the FitzHugh-Nagumo model are considered by Rinzel in "Models in Neurobiology" published by Plenum 1981. Hastings (Hastings 1975) also briefly considers the H-H model and gives a detailed mathematical analysis of a simplified model based on FitzHugh's and Nagumo's work.

# CHAPTER THREE

## EXPERIMENTAL METHODS

Hodgkin and Huxley derived their model of the action potential in squid giant axon by arranging the experimental conditions such that they could record the individual contributions of the major ions to the overall ionic current. They then proceeded to describe the sodium and potassium currents using mathematical equations. The resulting system of equations (the Hodgkin-Huxley model) is a mathematical description of the electrical behaviour of the axon. The final step in model building is validation of the model. In the case of the H-H model this involves numerical integration of the system of differential equations and comparison of the results with the experimentally recorded action potentials. This approach to model building (ie. the derivation of equations from experimental data and solution of those equations) contrasts with the approach where a model is derived from considerations of the fundamental physical principles that govern the system being studied. In control engineering terminology, a process of system identification is undertaken. It is therefore useful to look at the methods by which the data are obtained and analyzed. This chapter describes some of the experimental methods used in obtaining the data and briefly mentions some methods of analyzing the data.

The model being sought is a mathematical description of all the macroscopic membrane currents known to be present in the oxytocin-secreting cell. Such currents are modelled by

their amplitude, duration and gating properties. Mathematical reconstructions of the time courses of the various currents are therefore required. It is known that the macroscopic currents arise from the current contributions of individual ionic channels, so knowledge of the kinetic and gating behaviour of single channels may enable a model of the macroscopic currents to be constructed. Individual ionic channels are characterised by their open and shut times and by their conductance.

One of the major steps forward in the study of nerves was the creation of an experimental method for recording the electrical signals produced by nerve cells under varying experimental conditions. George Marmont (Marmont 1949) describes a method whereby an axon may be held in position and measurements of the various currents made using an electronic "voltage clamp". Curtis and Cole (1942) and Hodgkin and Huxley (1945) had previously managed to insert electrodes into the giant axon of the squid and make electrical measurements on it. The so-called voltage clamp procedure is still used today to make electrical measurements on cells, usually using specially prepared glass microelectrodes. The purpose of the voltage clamp is to maintain a fixed voltage across the nerve membrane using feedback amplifiers so that measurements of the various currents flowing through the membrane may be made. Using pharmacological or other methods, currents due to various ions may be prevented from flowing, thus allowing the separation of currents and the characterisation of each current in turn. In this way, a mathematical model of the

electrical behaviour of the nerve membrane may be built up. A block diagram of such a voltage clamp arrangement is shown in Figure 3.1. In Chapter 2 the term "space-clamp" was used. This is a reference to the use of electrodes large enough to maintain the section of membrane under study at the same voltage. If the voltage clamp applies only to a small part of the membrane then local circuit currents will flow, disturbing the recording.

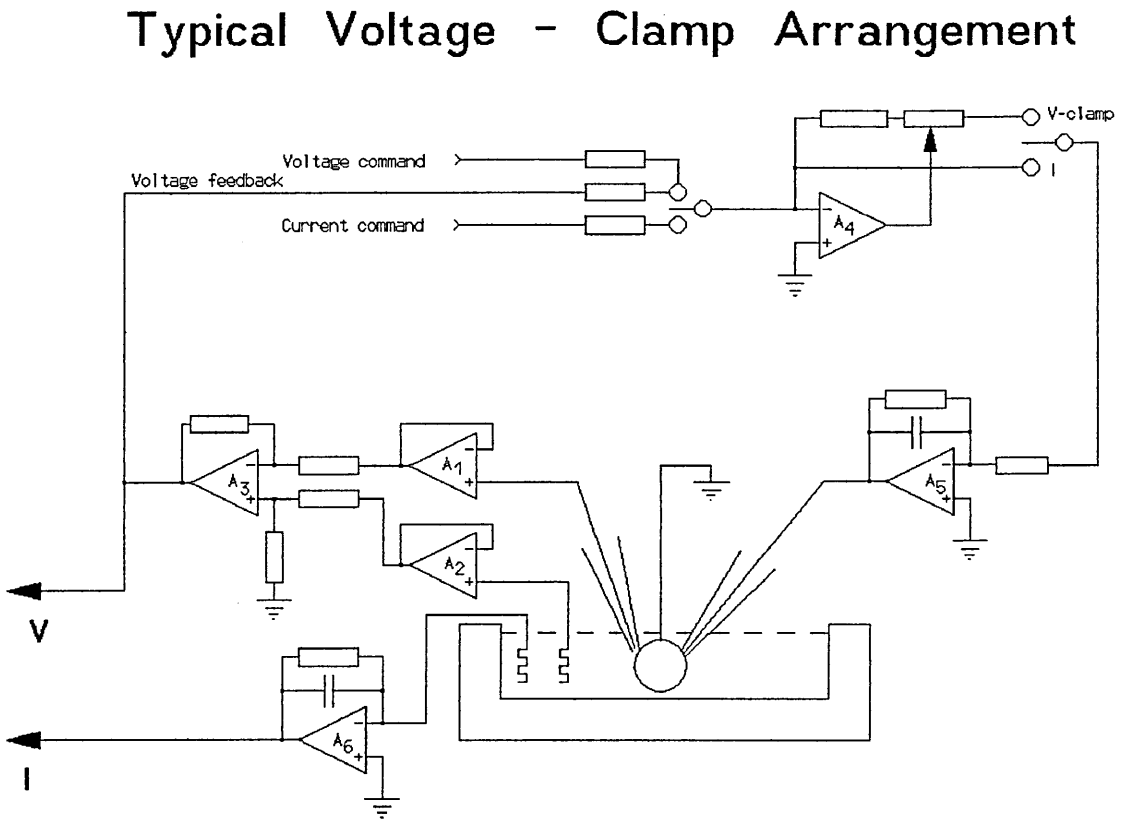


**Figure 3.1**
Circuit diagram of voltage-clamp arrangement.

A major step forward in the techniques of making electrical recordings from various cell preparations was the so called patch clamp method described by Sakmann, Neher et al (Hamill, Marty, Neher, Sakmann & Neher 1981; Sakmann & Neher 1984). The essence of the method revolves around applying

gentle suction to a specially prepared glass micropipette in contact with the cleaned surface of the cell being studied. (Enzymes are usually employed to ensure that the membrane surface is clean.) The suction causes an Ω shaped patch of membrane to enter the pipette and form a tight seal to the walls. The seal has the desirable properties of good mechanical stability and extremely high resistance. This latter feature gives rise to the name gigaohm seal since the measured resistance can be of the order of 100 gigaohms. The tight seal also isolates the attached patch of membrane chemically so that the solution in the pipette may be different to the normal bathing solution. One method of determining whether a gigaseal has been formed, since the seal forms in an all or nothing manner, is to observe the dramatic reduction in electrical noise that occurs on seal formation. This reduction in noise gives this method a significant advantage over conventional recording techniques and allows the resolution of picoampère currents. Thus, the current flowing through a single ionic channel may be observed. This mode of current recording is known as single channel recording. There are other configurations of the pipette and membrane patch that are worth discussing briefly. These are: i) Cell attached recording ii) Whole cell recording iii) outside-out patch and iv) inside-out patch.

Cell attached recording simply refers to recording the membrane currents from a small patch under conditions of a gigaohm seal.

Once the seal has been established, further suction causes the patch of membrane inside the pipette to rupture

allowing exchange of cell and pipette contents. Because the seal has a high resistance it is possible to voltage clamp an entire cell provided that it is relatively small (10μm dia.). This configuration is known as whole cell recording.

Due to the mechanical stability of the seal it is possible to pull the membrane patch completely free of the rest of the cell. This gives rise to the possibility of creating an inside-out or an outside-out patch of membrane. If after rupturing the membrane by suction, the pipette is pulled away from the cell, the attached patch of membrane and some of the remaining surrounding membrane may reseal, forming a hemisphere. The outer surface of the membrane is still in contact with the external bathing solution, meaning that the patch has its outer surface on the outside, hence the name. If the pipette is pulled away from the cell without previously rupturing the membrane then it is possible to yield a patch of membrane whose external surface formed the internal surface of the cell. This is achieved either by using a bathing solution having a low concentration of calcium ions or by air exposure of the vesicle that forms by pulling the patch in normal solution.

These techniques are fully explained in a book edited by Sakmann and Neher entitled "Single Channel Recording" (see bibliography) and also mentioned in a review paper by the same two authors (Sakmann & Neher 1984). It is worthwhile to note that these two workers have recently been awarded the Nobel prize for their work on developing the technique. Diagrams of these recording methods are shown in Fig. 3.2.

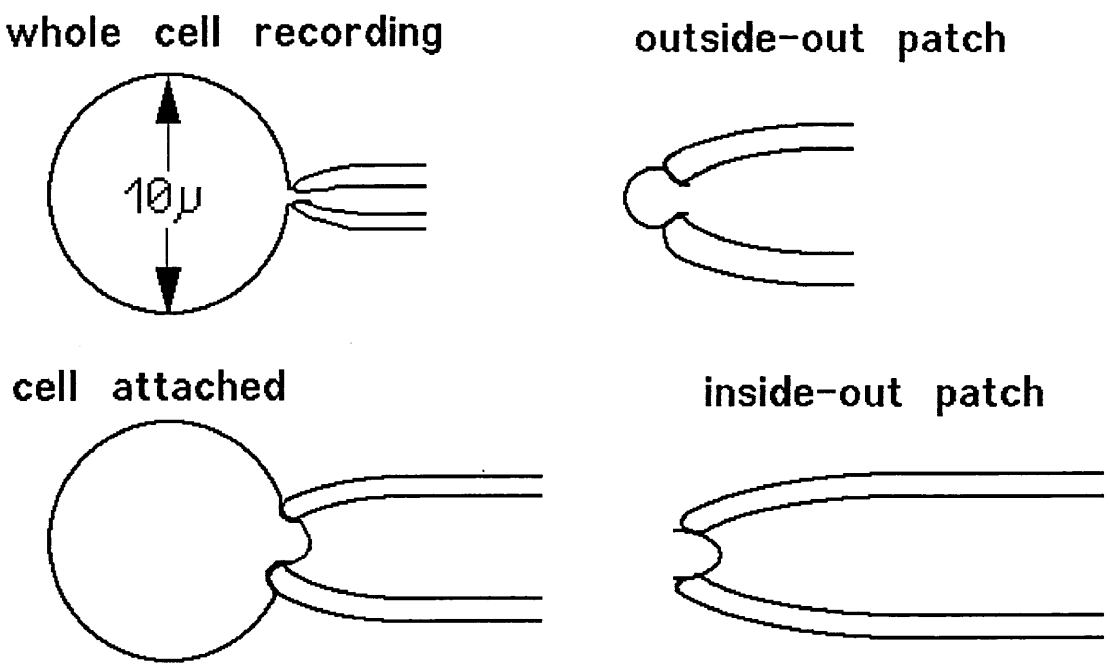


**Figure 3.2**
Diagram showing the various cell patch recording techniques.

## FLUCTUATION (NOISE) ANALYSIS

The macroscopic current observed during depolarizations of excitable tissue is made up from contributions of ion flux through individual channels. This means that due to the stochastic nature of channel openings any steady current will have a certain amount of fluctuation or electrical noise associated with it. Provided that the instrumentation used to monitor the current contributes a negligible amount of noise itself, analysis of the frequency spectrum and the statistical properties of the noise can yield information on fundamental channel properties such as single channel conductance and mean open lifetime (Neher & Stevens 1977).

A simple ionic channel with two conductance states (open and closed) yields a spectral density function which is a simple Lorenzian curve (Kolb 1984, Hille 1984). This result is based on a model where the transitions between the two

states are random events. In some real ionic channels the analysis is further complicated by the existence of conductance substates (Sachs Ch.17 Sakmann & Neher 1983). This means that the results obtained contain a sum of exponentials.

There are two type of fluctuation analysis used, stationary fluctuations and non-stationary fluctuations. Stationary fluctuations refer to the fact that current records are measured after the transients due to experimentally induced perturbations have died away. Non-stationary fluctuations are recorded during transients. Both methods involve perturbing a membrane away from its equilibrium state by applying a voltage step or an agonist. Current records are then taken. Signal processing is performed by computer so the records need to be digitized and stored. With stationary fluctuations the transients are allowed to die away and current recordings of the random fluctuations around the new equilibrium point are measured at high gain. The mean current is extracted from the current recording and is used in the analysis. The variance of the current is then measured and by using the probability of channel opening, the single channel current may be estimated. By performing a Fourier transform of the data, the mean open lifetime may also be estimated. Non-stationary fluctuation analysis involves recording the current during the transient part of the response and repeating the experiment many times. From the collection of current records obtained, the ensemble average is calculated and subtracted from each of the individual current records. The variance is then calculated on a point by point basis

using all the current records (Sigworth 1980).

The important point to note is that the kinetic data obtained from fluctuation analysis is the same as that obtained from macroscopic observations.

For the purposes of this project, it is the modelling of the behaviour of the macroscopic currents that is important.

## NUMERICAL SOLUTION OF THE MODEL EQUATIONS

The models described in this thesis are generally in the form of systems of coupled non-linear differential equations. Part of the modelling process therefore involves the solution of these equations. Analytical solution is not possible due to the non-linearity and complexity of the equations so numerical methods are used. During the initial phase of the project, computer programs were written using the language FORTRAN 77 and run on an IBM mainframe computer. These programs implemented an algorithm for the solution of differential equations known as the Runge-Kutta method (or more specifically, a fourth order Runge-Kutta method). Other methods, notably that due to Bulirsch and Stoer, were also investigated. However, it was decided that the fourth order Runge-Kutta method yielded sufficiently accurate results and would remain the preferred method of solution. A problem that was discovered when using a variable step length algorithm was that the step length would oscillate due to the oscillatory nature of the solution. The algorithm spent much of its time adjusting the integration step length. This problem has also been noted by Plant and Kim (Plant & Kim 1976) who decided that a fixed step size Runge-Kutta routine was adequate for solving a very similar problem. The Runge-Kutta method is a very popular algorithm for solving differential equations but is not well suited to "stiff systems". Stiff systems are those systems having responses containing components of the total response with widely varying timescales. Another way of explaining this is to say that the system eigenvalues may take on widely differing

values. Although the bursting behaviour does show periodic activity on the scale of seconds and milliseconds this has not proved to be a major problem in solving the equations.

In order to produce results in a more accessible form than a series of numbers, several programs were also written to convert the output of the numerical integration routine into graphical format and to provide "hardcopy" of the results. After pursuing this route for some time it was suggested that the modelling package ACSL (Advanced Continuous Simulation Language) might be more suitable, since all the necessary interactive graphics and program management are provided. This has proved to be the case and ACSL has been an extremely useful and powerful tool for investigating the behaviour of various proposed models. One very useful feature of ACSL is the ability to very simply change the numerical integration routine used. This is especially useful when dealing with stiff systems, since one of the available algorithms is one due to Gear which has proved useful in solving stiff sets of equations (Gerald & Wheatley 1989). However, this option has not been used and the normal fourth order Runge-Kutta method remains the preferred algorithm.

One problem with numerical integration is the amount of data produced. In order to preserve the accuracy and stability of the integration, small time steps are often needed. Such small steps are not required for the presentation of the results graphically. The way in which ACSL deals with this dilemma is to only store the data points at selected intervals that are larger than the actual integration time steps. These larger intervals are known as communication

intervals and may be specified by the user.

## DIMENSIONS AND SCALING

Hodgkin and Huxley (Hodgkin & Huxley 1952d) rescaled their equations and data to give the membrane resting potential a value of zero. All voltages are measured as displacements from this value. The Nernst potentials for the active ions are adjusted to take account of this fact. For instance, instead of using the sodium equilibrium potential $E_{Na}$ to calculate the sodium current, the difference between $E_{Na}$ and the resting potential $E_r$ is used.

$$V = E - E_r \quad . . . . . (3.1)$$

$$V_{Na} = E_{Na} - E_r \quad . . . . . (3.2)$$

Establishing the resting potential as the baseline voltage has the effect of shifting all functions of voltage along the voltage axis by an amount equal to the resting potential. Graphs showing this are given here in Figures 3.3 and 3.4. The amplitude of simulated action potentials is simply the maximum value observed. In comparing the results of Hodgkin and Huxley with other work and in reproducing their work, this must be taken into consideration.

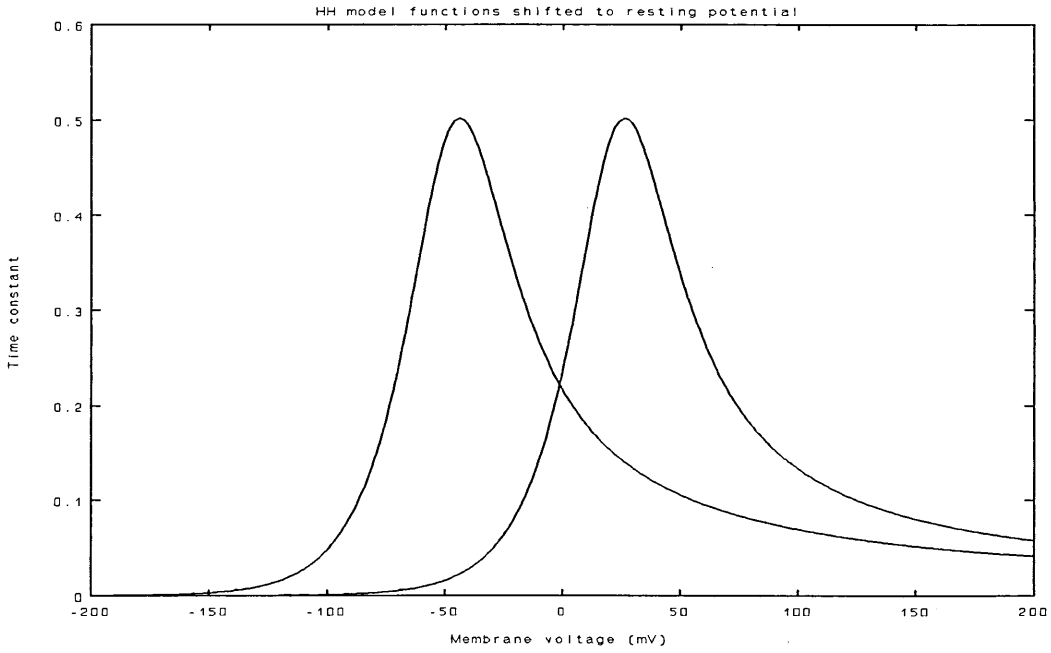


**Figure 3.3**
Graph showing the effect of applying a constant offset voltage to the H-H activation variable time constant.

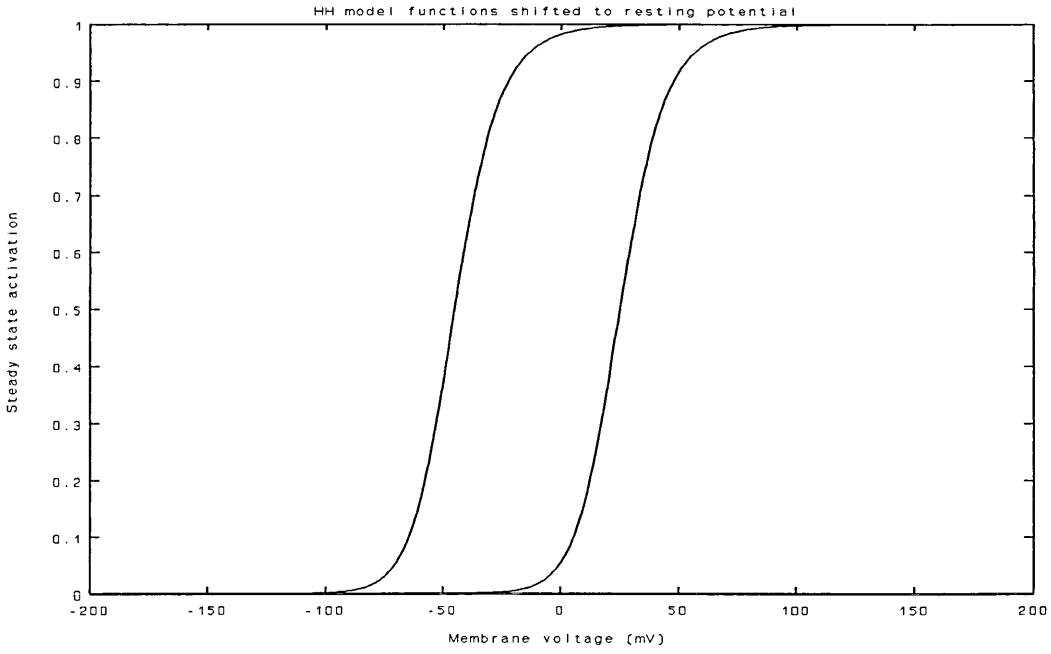


**Figure 3.4**
Graph showing the effect of applying a constant voltage offset to the H-H model sodium activation variable.

Scaling of variables and model parameters is also an important point to be considered when running simulations. Hodgkin and Huxley measured voltages using the millivolt as the base unit. The unit of time they used was the millisecond, currents were measured as $\mu A/cm^{-2}$ and conductances were measured in units of $mS/cm^{-2}$. Much work in this project has been performed using standard SI units. Care must be taken in translating between the two systems of units in order to maintain compatibility. There are several implicit dimensioned constants in the Hodgkin-Huxley model equations, for example in equation 23 (Hodgkin & Huxley 1952d) the rate "constant" is given as

$$\alpha_h = 0.07\exp(V/20) \quad . \; . \; . \; . \; . \; . \; . \; (3.3)$$

The constant "20" has units of mV to ensure the exponent is dimensionless and since the overall expression must have units of $ms^{-1}$, the constant "0.07" has units of $ms^{-1}$.

As part of the study, the H-H equations were converted to SI units and the functions shifted along the voltage axis by an amount equal to the resting potential. The model that resulted was called HODGHABS to indicate that the voltages were expressed in terms of absolute voltage (ie referred to the bathing solution being the zero volt reference) rather than referred to a resting potential of zero.

It has been noted in Chapter 2 that the H-H model is complex and requires significant computing power to be able to solve the equations and that reduced order models are popular for studying repetitive activity. The phase plane technique has been mentioned in this context so some elucidation of the method is appropriate.

Strictly speaking the phase plane applies only to second order systems and contains trajectories of a state variable plotted against its time derivative. As such it is a graphical technique and therefore gives a readily understandable interpretation of the behaviour of the system. Its usefulness is such that the technique has been extended and the term phase portrait is more loosely used to describe plots of one system variable against another (see for example, FitzHugh 1969). Shown here in Figures 3.5 and 3.6 are the results of the simulation of a simple second order non-linear oscillator. The equation is the van der Pol equation mentioned in Chapter 2 and the outputs are the two state variables. The two Figures show the state variables plotted as functions of time. The second Figure shows the phase portrait of the system.

The logical extension of the phase plane to higher dimensions results in trajectories in phase space. The variables that are plotted are the state variables and their derivatives. A phase portrait for a third order system cannot easily be represented on a two dimensional page and the simple graphical appeal of the technique is lost. However higher order systems can be analyzed using computers.

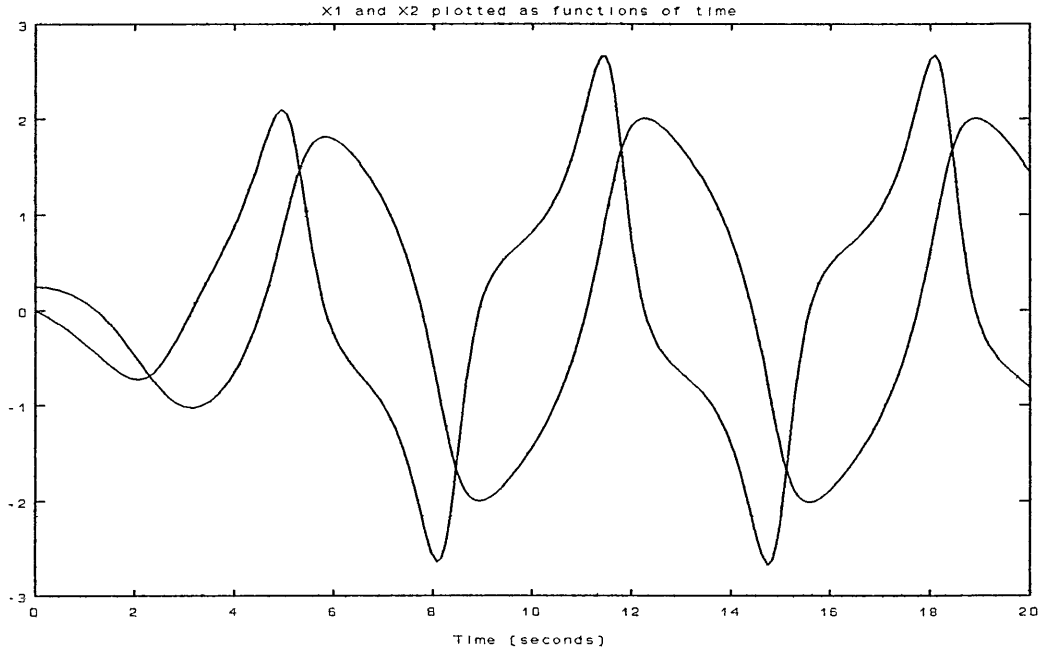


**Figure 3.5**
Graph showing the variation with time of the two state variables in a simple van der Pol oscillator.

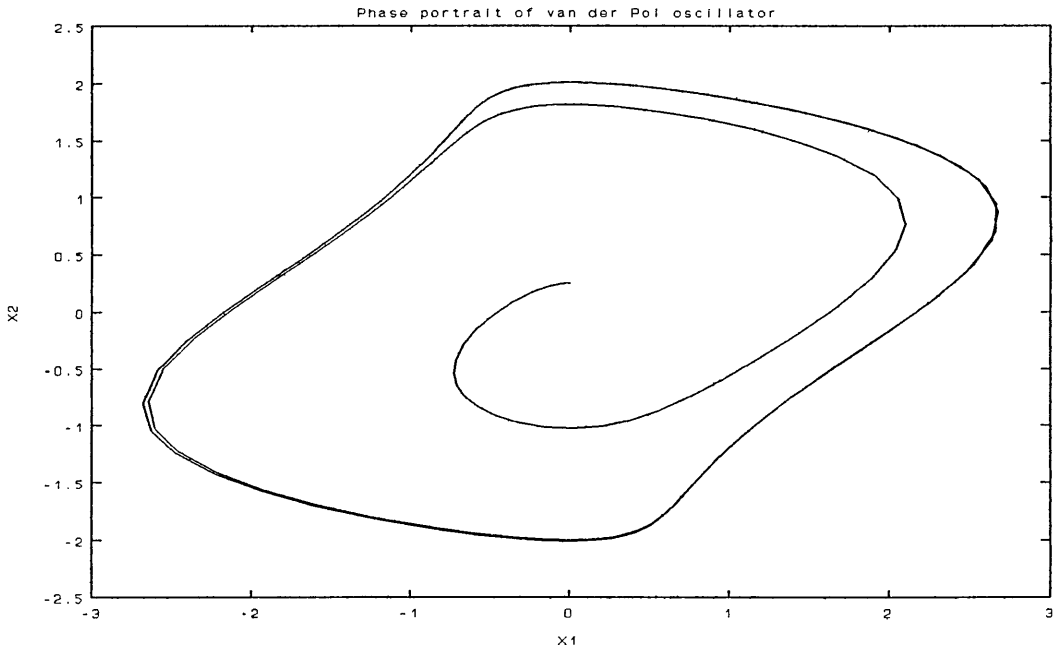


**Figure 3.6**
Graph showing the same state variables shown in Figure 3.5, plotted here in the form of a phase portrait.

It is a common situation in scientific work that a curve of one form or another be fitted to a set of experimental results and various parameters obtained. Hodgkin and Huxley obtained their model parameters by fitting empirically derived curves to their data. Various methods are now available that automate the process of finding the "best fit" of a given curve to a set of data. What is also usually provided is a measure of the "goodness of fit." The Least Squares method is a way of finding the minimum distance between a set of data points and a curve. If the least squares is adopted as a measure of the closeness of a point to a line then the problem of fitting a curve to a set of data points is one of constrained optimization or more precisely, of minimization where the objective function to be minimized is the sum of the squares. The parameters of the curve are adjusted to find the minimum. In the simple case of fitting a straight line through a set of data, the calculations are straightforward. In this case the procedure is commonly known as linear regression. What is needed for this project is a means of finding the parameters of a function that give the best fit to a given set of data points. The functions that are to be fitted to the data in this instance are non-linear and there are several variables (the function parameters) involved which presents additional complications. The problem of minimization is a multivariable minimization. This may be expressed mathematically as follows:-

$$S \triangleq \sum_{i=1}^{N} e_i^2 \quad \ldots\ldots\ldots\ldots\ldots\ldots\ldots\ldots\ldots\ldots \quad (3.1)$$

Where $e_i$ is given by :-

$$e_i = y_i - f(x_i;\underline{a}) \quad \ldots\ldots\ldots\ldots\ldots\ldots\ldots\ldots\ldots\ldots \quad (3.2)$$

S is the sum of the squared errors over all N data points, **a** is the vector of parameters. At the minimum of the objective function the partial derivatives of S with respect to the fitting parameters should be zero.

$$\frac{\partial S}{\partial a_k} = 0 \quad \ldots\ldots\ldots\ldots\ldots\ldots\ldots\ldots\ldots\ldots \quad (3.3)$$

for all of the parameters. S is the objective function to be minimized. Writing this out explicitly for one of the parameters gives :-

$$\frac{\partial S}{\partial a_k} = -2\sum_{i=1}^{N} [y_i - f(x_i;a_k)] \frac{\partial f(x_i;a)}{\partial a_k} = 0 \quad \ldots\ldots\ldots\ldots \quad (3.4)$$

Generalising to all parameters this may be written in matrix notation as :-

$$\frac{\partial S}{\partial \mathbf{a}} = -2[J_{\mathbf{a}}\, \mathbf{f}(\mathbf{x};\mathbf{a})]^T (\mathbf{y}-\mathbf{f}(\mathbf{X};\mathbf{a})) = \mathbf{0} \quad \ldots\ldots\ldots\ldots \quad (3.5)$$

where $J_{\mathbf{a}}\, \mathbf{f}(\mathbf{x};\mathbf{a})$ is the Jacobian matrix whose (i,j) element

is $\frac{\partial \mathbf{f}_i}{\partial \mathbf{a}_j}$ . There are several methods of minimizing such a

function, the method of steepest descent being the preferred one in this case. However, if we write the function to be minimized as $\mathbf{f}(\mathbf{x})$ then we can approximate the function at a point using a Taylor series expansion.

$$\mathbf{f}(\mathbf{x}) = \mathbf{f}(\mathbf{P}) + \sum_i \frac{\partial \mathbf{f}}{\partial x_i} x_i + \frac{1}{2} \sum_{i,j} \frac{\partial \mathbf{f}}{\partial x_i, x_j} x_i x_j + \cdots \quad \ldots\ldots (3.6)$$

which may be approximated by a matrix equation in quadratic form :-

$$\mathbf{f}(\mathbf{x}) \approx c - J\mathbf{x} + \frac{1}{2}\mathbf{x}^T H\mathbf{x} \quad \ldots\ldots\ldots\ldots\ldots (3.7)$$

Where J is the Jacobian and H is the Hessian matrix. This system of equations may be solved to find the minimum as follows :-

$$\mathbf{a}_{min} = \mathbf{a}_k + H^{-1}[-J(\mathbf{a}_k)] \quad \ldots\ldots\ldots\ldots\ldots (3.8)$$

where $a_k$ is the current estimate of the parameters.

No package to perform this task was available therefore a suitable algorithm was chosen and implemented using FORTRAN 77 on a desktop computer. The actual program written differs slightly from the preceding explanation in that rather than using a straightforward least squares estimate of the

"goodness of fit" , the program uses a "Chi-squared" estimate. The algorithm chosen was one due to Levenberg and Marquardt (Levenberg 1944, Marquardt 1963). This method was taken from the text on numerical methods by Press, Flannery,Teukolsky and Vetterling. (Press, Flannery, Teukolsky and Vetterling 1986). (See also Fidler and Nightingale (1978) Chapter 7, Norton (1986) and Scales (1985).) The method uses two methods of finding the minimum. Initially, the method of steepest descent is used, but as the minimum is approached the normal equations are solved by Gauss-Jordan elimination. (The second partial derivatives are not actually used since they are computationally expensive to evaluate and tend to have a destabilising effect on the algorithm.) The second method relies on the matrix equations being in quadratic form close to the minimum. The contribution due to Levenberg and Marquardt was to find a method of switching between these two methods. They used a factor $\lambda$ to determine the method of obtaining the next iterated estimate. The program starts off with a small value for lambda and adjusts it as the iteration towards the minimum proceeds. With a large value for lambda, the method steps towards the minimum in a steepest descent manner and does this until it gets close to the minimum whereupon lambda is decreased.

The model equation to be fitted to the data is written into the program as a subroutine. The program also uses a set of function derivatives in the form of a matrix. The elements of this matrix are also returned by the subroutine that calculates the function values. In the case of the functions used, it was relatively straightforward to find analytical

derivatives of the fitting function with respect to each of the parameters. If this was not the case, it is also possible to use numerical techniques to estimate these derivatives. To start the algorithm off, a set of initial parameter estimates are also given. The program returns the best fit parameters and an estimate of the likeliehood that they are the "true" parameters given the data set. Since the measurement uncertainties are not entered but assumed to be equal, this estimate is not particularly meaningful. As a final check on the fit of the given equation to the data set, a graph may be drawn, showing the individual data points and the estimated best fit curve passing through them. In this way, expressions for the rate "constants" used in the overall mathematical model may be derived. Colquhoun and Sigworth give a good description of the process of fitting a model to a data set in "Single Channel Recording" edited by Sakmann and Neher (Sakmann & Neher 1983).

The program was used in finding the parameters for the rate functions for the potassium currents and a typical curve is shown in Figure 6.1 on page 124. The fitting functions chosen to fit the data were of the same form as those used by Hodgkin and Huxley. A listing of the program is given in the Appendix on page A47. To run the program, the subroutines are compiled separately and then linked to form a program with the name of the main routine. This name is simply typed in at the DOS command line, which causes the program to be loaded and run. When the iteration process has stopped, the parameters displayed on the monitor screen are those which give the best fit. Since only a few curves were to be fitted

to data points it was not thought that the additional programming effort involved in making the program more general and prompting the user to enter the initial parameter values was worthwhile.

# CHAPTER FOUR

## REPETITIVE ACTIVITY IN NEURONES

Oscillation is an important phenomenon in many biological systems, the mammalian heart, for example, is a very important biological oscillator (Noble 1979). It has already been noted (Chapter 1, Page 5) that the secretion of the hormones oxytocin and vasopressin is enhanced by patterns of action potential discharge characterised by periods of activity interspersed with periods of electrical silence. This type of behaviour is not unique to these particular cells and bursting behaviour has been observed in other systems , for example, the bursting neurone R15 in *Aplysia* (Smith 1978) and pancreatic ß-cells (Rinzel 1988; Matthews & O'Connor 1979). One important question that arises from the study of such systems is whether the oscillations occur due to intrinsic mechanisms or are the result of an external input. An endogenous mechanism is responsible for bursting in the R15 cell (Adams 1985; Adams & Benson 1985; Gorman & Herman 1982; Pinsker 1977), and it appears that in the oxytocin-secreting cell the milk ejection burst is the result of the properties of the cell membrane and the internal and external environment rather than a synaptic input. The evidence for an endogenous mechanism in R15 comes from the lack of periodic synaptic input and from experiments involving isolating cells from the ganglion and recording the bursting behaviour that still occurs (Adams & Benson 1985). It also appears that bursting in oxytocin-secreting neurones is due to an endogenous mechanism although Richard,Moos &

Freund-Mercier advance an argument for the importance of afferent input in controlling a burst (Richard, Moos & Freund-Mercier 1988). One piece of evidence for this is that suckling is a constant stimulus which makes it likely that the synaptic input to the cells is constant during suckling whereas bursting is periodic (Leng 1988). If this is indeed the case then it would be reasonable to assume that the synaptic input serves only as a trigger. It is significant that bursting in oxytocin-secreting cells has not been recorded *in vitro* (Leng 1988; Richard,Moos & Freund-Mercier 1988). The very long time period between bursts is an unusual feature of oxytocin-secreting neurones and would seem to argue against an endogenous mechanism since the underlying "slow wave" would have an extremely long time constant (Richard,Moos & Freund-Mercier 1988).

It has been noted that oxytocin itself increases the excitability of oxytocin-secreting cells and it may be that the presence of oxytocin in the extracellular space acts as a neuromodulator (Richard,Moos & Freund-Mercier 1988).

Once it has been established that synaptic input is not responsible for the bursting behaviour of neurones and that the mechanism is to be found in the cell itself, the question of what the mechanism is, arises. One possibility is oscillations due to metabolic processes as these are well known, eg. glycolytic oscillations, (Carnevale & Wachtel 1980; Mironov 1983). The Belousov-Zhabotinskii reaction is a well known example of a chemical oscillator (Rinzel & Troy 1983). In order to produce bursting behaviour the metabolic oscillations would have to modulate the membrane voltage

either through ion pumps or through the ionic conductances (Adams & Benson 1985; Mironov 1983). Such a mechanism has been ruled out for the R15 cell since no underlying oscillations of membrane current are observed when a bursting neurone is voltage-clamped (Carnevale & Wachtel 1980). However, a link between calcium conductance and the level of intracellular cyclic AMP in molluscan neurones has been noted by Mironov and others (Mironov 1983; Gillette 1988).

## MATHEMATICAL MODELS FOR OSCILLATION AND BURSTING

One of the aims of this project is to devise a model for the stereotyped bursting behaviour in oxytocin-secreting cells. A good place to start this process is to investigate models proposed for other similar systems. It has been found (Cole, Antosiewicz & Rabinwitz 1955; Connor 1985; Cooley & Dodge 1966; Guttman & Barnhill 1970; Hassard 1978; Noble 1966) that the Hodgkin-Huxley model can sustain a train of action potentials when given a sufficient stimulus. The frequency of firing is dependent upon temperature and the magnitude of the stimulus (Guttman & Barnhill 1970; Noble 1966). The Hodgkin-Huxley model is rather complicated and it is common practice to use simpler models to study bursting behaviour (FitzHugh 1969; Jack, Noble & Tsien 1985).

One such model is that proposed by Hindmarsh and Rose (Hindmarsh & Rose 1984) which is an extension of their previous, simpler model of the nerve impulse which shows repetitive firing (Hindmarsh & Rose 1982). The models discussed in these two papers are of an analytic nature since

they are based upon the behaviour of coupled differential equations rather than derived from consideration of a physical or biological system (see Chapter 2). The models were however inspired by a biological system and use data taken from voltage clamp experiments on pond snails. As with most models of this type there are nonlinearities present in the equations which make analysis difficult and numerical integration is required to solve the equations. As part of this investigation, the model by Hindmarsh and Rose (Hindmarsh & Rose 1982) was simulated using the ACSL language. The simulation did not reproduce the behaviour shown in the paper and closer examination of the equations given and the data revealed some discrepancies. For this reason it was decided not to pursue this particular line of work any further.

Another class of mathematical model is also used as a simpler basis for the investigation of bursting behaviour. This is the Bonhoeffer van der Pol system of equations as mentioned in Chapter 2.

## THE IMPORTANCE OF NEGATIVE RESISTANCE

One feature of oscillation in electrical systems is the presence of a region of negative resistance in the overall current-voltage characteristic of the system. Negative resistance is not an essential precondition for oscillation since a simple circuit comprising an inductor and capacitor will oscillate if given a suitable input. However, the oscillations will die away with an exponential envelope

unless the energy dissipated by the inevitable resistance is replenished. In constructing electronic oscillators an active device is used for this purpose. As mentioned in Chapter 2, Nagumo's model (Nagumo, Arimoto & Yoshizawa 1962) uses a tunnel diode. This is a two-terminal active device that possesses a region of negative slope resistance in its current-voltage characteristic. The device is not capable of supplying energy, it requires a bias voltage to establish an operating point in the negative resistance region and it is the power supply that provides the energy. The negative resistance of the diode cancels some of the dissipative resistance in the circuit and ensures that the energy is supplied in phase so as to maintain the oscillation. In the context of neurones showing repetitive and/or bursting behaviour a region of negative conductance in the overall current-voltage relation is required for maintaining a train of action potentials. This requirement is met in the case of the proposed model as can be seen in Fig. 4.1 which shows the I-V characteristic plotted during an action potential. Bourque (Bourque 1987) and Renaud (Renaud 1987) note that the depolarizing after potential recorded in magnocellular neurosecretory cells in the supraoptic nucleus gives these cells a region of negative resistance. Wilson and Wachtel (Wilson & Wachtel 1974) and Carnevale and Wachtel (Carnevale & Wachtel 1980) emphasize this requirement for the mollusc *Aplysia californica* and demonstrate that cooling, which stops bursting behaviour, abolishes the negative resistance region. The existence of negative resistance in artificial lipid membranes treated with excitability-inducing material was

demonstrated by Ehrenstein, Lecar and Nossal (Ehrenstein, Lecar & Nossal 1970).

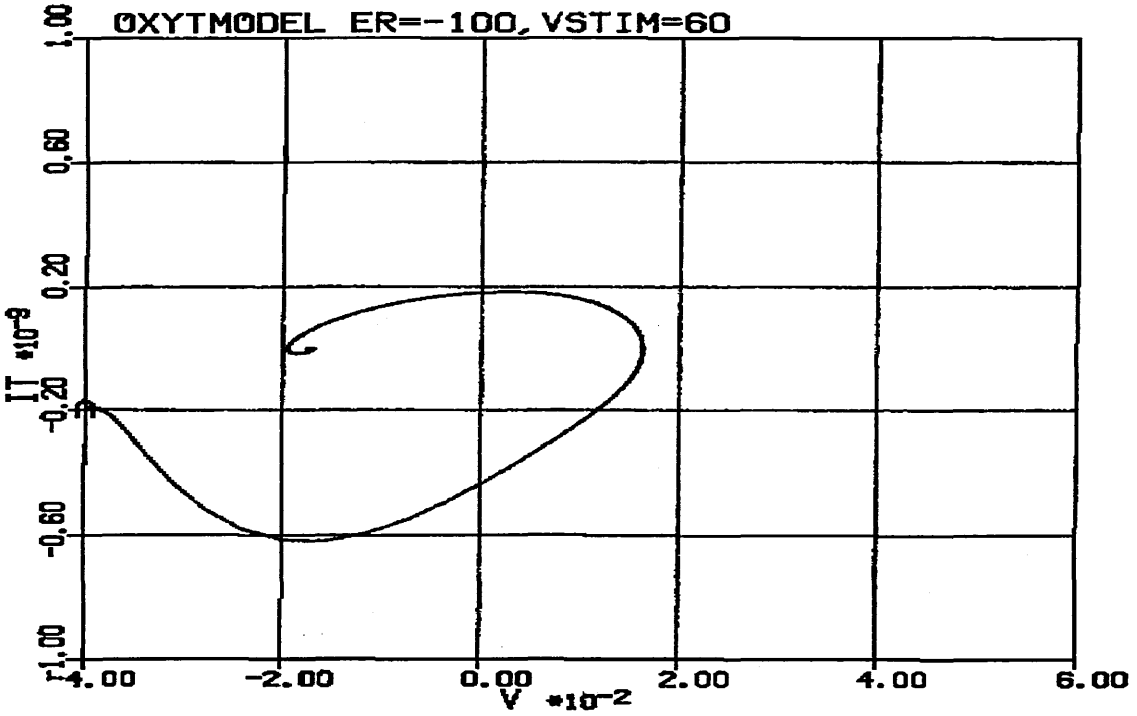


**Figure 4.1**

Current-voltage characteristic of oxytocin cell model. The total membrane current is plotted against membrane voltage.

## MATHEMATICAL ANALYSIS

As part of the investigation into the H-H model, an attempt was made to write down a state-space description of the equations. A mathematical analysis of a system of equations can be useful in revealing the general features of system behaviour without resorting to numerical integration of the full set of equations. The Hodgkin-Huxley equations given by equations 2.1 to 2.5 may be rewritten in a form more amenable to a state-space description as follows:-

$$\dot{V} = -\frac{1}{C_m}[\bar{g}_{Na}\, m^3 h(V-V_{Na}) + \bar{g}_K n^4(V-V_K) + \bar{g}_L(V-V_L)] \quad \ldots\ldots (4.1)$$

$$\dot{m} = \alpha_m - (\alpha_m+\beta_m)m \quad \ldots\ldots (4.2)$$

$$\dot{h} = \alpha_h - (\alpha_h+\beta_h)h \quad \ldots\ldots (4.3)$$

$$\dot{n} = \alpha_n - (\alpha_n+\beta_n)n \quad \ldots\ldots (4.4)$$

The voltage-dependence of the rate functions has been omitted for clarity. The state variables chosen are V,m,n and h as shown here.

The usual form of a state-space description of a multivariable system is as follows :-

$$\dot{\underline{x}} = A\underline{x} \quad \ldots\ldots (4.5)$$

for a system with no external inputs. The vector x is a vector containing the state variables and the matrix A is

known as the system matrix.

Attempting to write a state-space description in this format using the state variables as shown gives rise to a difficulty in that the H-H equations as shown here do not fit neatly into the standard format for a state-space description. This is due to the high order nonlinearities and mutual coupling present in the equations. This means that there are a number of ways of writing a state-space description, one of which is shown below:-

$$\begin{bmatrix} \dot{V} \\ \dot{n} \\ \dot{m} \\ \dot{h} \end{bmatrix} = A \begin{bmatrix} V \\ n \\ m \\ h \end{bmatrix} \quad \ldots\ldots\ldots\ldots\ldots\ldots\ldots\ldots\ldots\ldots \quad (4.6)$$

where the A matrix is:-

$$\begin{bmatrix} a_{11} & a_{12} & a_{13} & a_{14} \\ 0 & a_{22} & 0 & 0 \\ 0 & 0 & a_{33} & 0 \\ 0 & 0 & 0 & a_{44} \end{bmatrix} \quad \ldots\ldots\ldots\ldots\ldots\ldots\ldots\ldots\ldots\ldots \quad (4.7)$$

With elements :-

$$a_{11} = -\frac{1}{C_m}(\bar{g}_{Na}\, m^3 h + \bar{g}_K\, n^4 + \bar{g}_L) \quad \ldots\ldots\ldots\ldots\ldots\ldots \quad (4.8)$$

$$a_{12} = \bar{g}_K\, V_K\, n^3 \quad \ldots\ldots\ldots\ldots\ldots\ldots\ldots\ldots \quad (4.9)$$

$$a_{13} = \bar{g}_{Na}\, V_{Na}\, m^2 h \quad \ldots\ldots\ldots\ldots\ldots\ldots\ldots \quad (4.10)$$

$$a_{14} = 0 \quad \ldots\ldots\ldots\ldots\ldots\ldots\ldots\ldots \quad (4.11)$$

$$a_{22} = -(\alpha_n + \beta_n) \quad \ldots\ldots\ldots\ldots\ldots\ldots\ldots \quad (4.12)$$

$$a_{33} = -(\alpha_m + \beta_m) \quad \ldots\ldots\ldots\ldots\ldots\ldots\ldots \quad (4.13)$$

$$a_{44} = -(\alpha_h + \beta_h) \quad \ldots\ldots\ldots\ldots\ldots\ldots\ldots \quad (4.14)$$

With an additional vector of constants given in equation 4.15.

$$\begin{bmatrix} 0 \\ \alpha_n \\ \alpha_m \\ \alpha_h \end{bmatrix} \quad \ldots\ldots\ldots\ldots\ldots\ldots\ldots\ldots \quad (4.15)$$

As stated previously (Chapter 2 p13), the Hodgkin-Huxley model is a set of non-linear differential equations. There is

no single standard method of analysis for non-linear systems. However, a number of techniques are available. Some of these are: linearisation of the system around an operating point; describing function analysis; Lyapunov methods; pertubation theory; and bifurcation analysis. Most of these techniques are concerned with analysis of the stability of the system and testing for the existence of limit cycles. They generally give qualitative information about the solutions of the differential equations rather than detailed quantitative results.

The state-space description shown above in equations 4.6 to 4.15 were written down at an early stage in the project but this analysis was not taken further when it was realised that the equations did not fit the standard format and that there was no unique way of writing such a description. Patton (Patton 1980) however, takes this analysis a stage further by performing a linearisation of the state-space description around the resting potential. The derivation of the linearised model is quite lengthy and will not be reproduced here. The linearised H-H system is expressed in a specific matrix format known as mammillary compartmental form as shown below. Troy (Troy 1975) also derives a linearised H-H model in this form.

$$\begin{bmatrix} \alpha_1 & \alpha_2 & \alpha_3 & \alpha_4 \\ \beta_1 & \beta_2 & 0 & 0 \\ \gamma_1 & 0 & \gamma_3 & 0 \\ \varepsilon_1 & 0 & 0 & \varepsilon_4 \end{bmatrix} \quad \ldots\ldots\ldots\ldots\ldots\ldots\ldots\ldots \quad (4.16)$$

with elements :-

$$\alpha_1 = \frac{1}{C_m}[\bar{g}_{Na\,\infty} + \bar{g}_{K\,\infty} + \bar{g}_{l\,\infty}] \quad \ldots\ldots\ldots\ldots\ldots \quad (4.17)$$

$$\alpha_2 = 3\bar{g}_{Na}\, m_\infty^3\, h_\infty\, (V_\infty - V_{Na}) \quad \ldots\ldots\ldots\ldots\ldots \quad (4.18)$$

$$\alpha_3 = 4\bar{g}_K\, n_\infty^3\, (V_\infty - V_K) \quad \ldots\ldots\ldots\ldots\ldots \quad (4.19)$$

$$\alpha_4 = \bar{g}_{Na}\, m_\infty^3\, (V_\infty - V_{Na}) \quad \ldots\ldots\ldots\ldots\ldots \quad (4.20)$$

$$\beta_1 = \left(\frac{\partial \dot{m}}{\partial V}\right)_\infty \quad \ldots\ldots\ldots\ldots\ldots \quad (4.21)$$

$$\beta_2 = -(\alpha_m + \beta_m) \quad \ldots\ldots\ldots\ldots\ldots \quad (4.22)$$

$$\gamma_1 = \left(\frac{\partial \dot{n}}{\partial V}\right)_\infty \quad \ldots\ldots\ldots\ldots\ldots \quad (4.23)$$

$$\gamma_3 = -(\alpha_n + \beta_n) \quad \ldots\ldots\ldots\ldots\ldots \quad (4.24)$$

$$\varepsilon_1 = \left(\frac{\partial \dot{h}}{\partial V}\right)_\infty \quad \ldots\ldots\ldots\ldots\ldots \quad (4.25)$$

$$\varepsilon_4 = -(\alpha_h + \beta_h) \quad \ldots\ldots\ldots\ldots\ldots\ldots \quad (4.26)$$

The fact that the linearised system matrix is in this form has relevance to the analysis of system stability (see Patton 1980). As with all linearisation exercises, the approximation is only valid for small pertubations around the operating point. In the case of the Hodgkin-Huxley model, the threshold for stimulus is such that it represents a significant pertubation.

As stated previously in relation to Guttman and Barnhill's work, a constant suprathreshold current stimulus causes repetitive firing. Troy (Troy 1975) uses bifurcation theory with the applied current as the bifurcation parameter to show that as the current passes through a critical value a bifurcation of periodic solutions occurs. Patton (1980) also discusses bifurcation analysis and the describing function method. The describing function method is an involved procedure for the H-H equations and yields inconclusive results.

The aim of this project is to create a mathematical model of the characteristic patterns of electrical activity exhibited by the oxytocin-secreting cell. The approach taken in this project was to study the literature on similar systems to gain familiarity with previous work and to decide upon a suitable strategy for building a model for this system.

The characteristic behaviour of interest in the system under study is the unique bursting activity. This entails repetitive firing that is initiated and terminated at regular

intervals. Part of the process of building up a model for this behaviour is to determine how repetitive firing may be induced in nerve cells. There are several ways of modifying the Hodgkin-Huxley equations so that they become oscillatory or autorhythmic. Patton (Patton 1980) discusses several of these. The first way is to add an additional conductance in parallel with the normal sodium conductance (Patton 1980; Kamaluddin and Power 1974; Noble 1962). The second method mentioned is to increase the power of the potassium activation from four to six. Cole and Moore (Cole and Moore 1960) state that a sixth power relation describes the potassium current data more accurately than the Hodgkin-Huxley fourth order relationship.

As stated in the introduction, there are several characteristic features of the system that a successful model should reproduce. These are the 'shoulder' on the repolarising phase of the action potential, the acceleration and deceleration of firing during a burst, the frequency of firing and the generation of the burst itself. Mathematical analyses such as those described above are useful in predicting the stability of the system and defining the conditions for oscillation, but not in describing the details of the characteristic patterns of electrical discharge. FitzHugh's work shows what state variables are needed to describe the on-off bursting behaviour of the cell and the work done by Rinzel and co-workers; Plant and Kim and Smith give good models on which to base this work. Rather than spend time on intricate analyses, ideas taken from Rinzel's model of the pancreatic ß-cell and the models for the cell

R15 were used. A brief summary of the main features follows. The model developed by Rinzel exhibits bistability. One state is characterised by electrical silence and the other by continuous firing. The cell is driven between these two states by an underlying slow oscillation of the intracellular calcium concentration. The patterns of firing are similar to those exhibited by the oxytocin-secreting cell. The main components of Rinzel's model are a potassium current, a calcium current, a calcium-gated potassium current and a model for the intracellular calcium concentration. Feedback from the slow calcium dynamics to the faster dynamics of the membrane voltage is provided by the calcium-gated potassium current.

Maintaining the Hodgkin-Huxley model in a state of depolarization leads to a constant train of action potentials as can be seen in Figures 4.2 to 4.5. The scale of the time axis of the graphs is such that the numbers given represent milliseconds. Likewise the voltages are expressed in millivolts and the leakage current $I_L$ is given in microamps. per square centimetre. The results shown here confirm the results of Cooley and Dodge (Cooley & Dodge 1966) and Guttman and Barnhill's work (Guttman & Barnhill 1970). The model used is Hodgkin and Huxley's translated into a program using the ACSL simulation language. Figures 4.2 and 4.3 show the effect of a 10mV sustained depolarization. Figure 4.3 is the same as 4.2 but simulated over a longer time period. Figure 4.4 shows the simulated leakage current during firing and Figure 4.5 is the same as Figure 4.3 but with a different vertical scale.

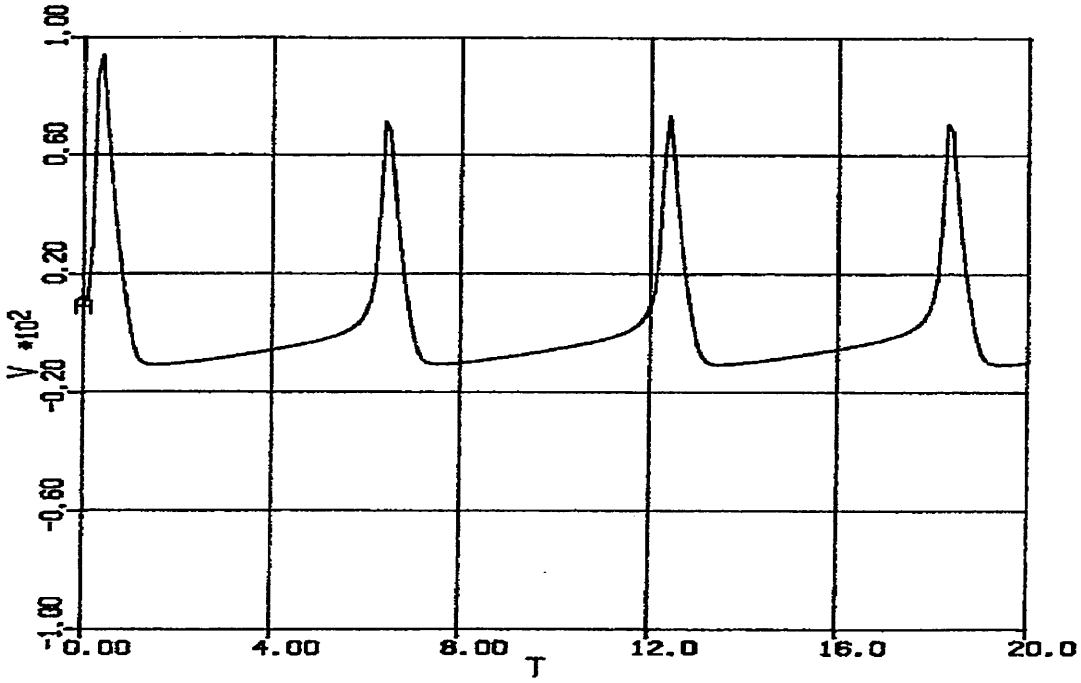


**Figure 4.2**

Result of simulation of H-H model with a maintained depolarization.

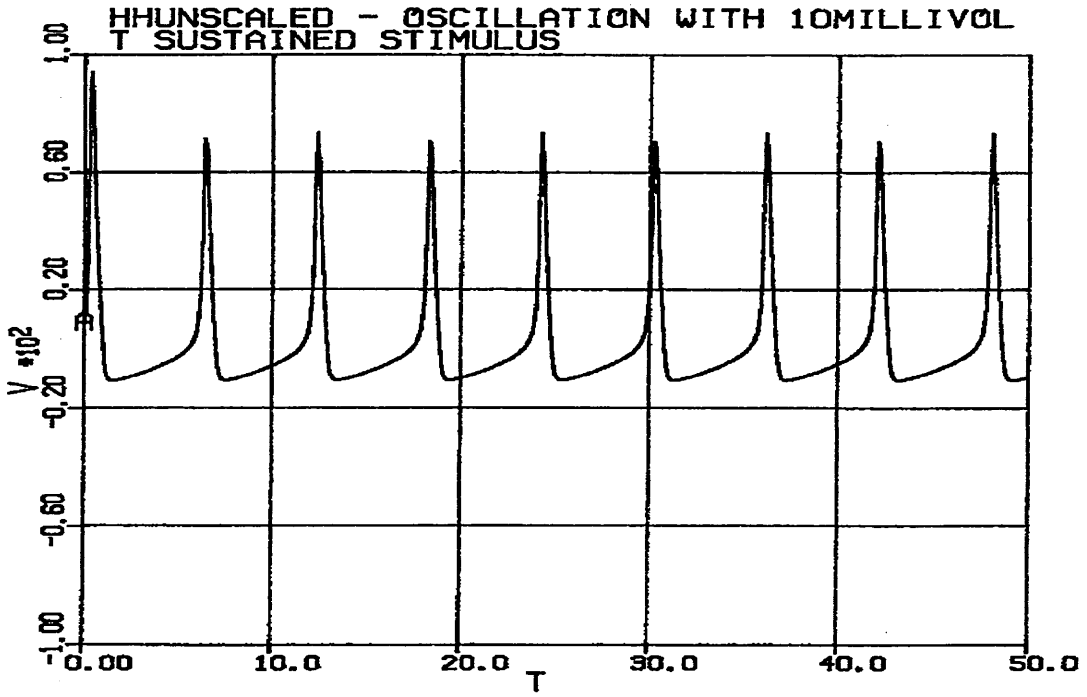


**Figure 4.3**

Simulation result as Figure 4.2 over a longer time period.

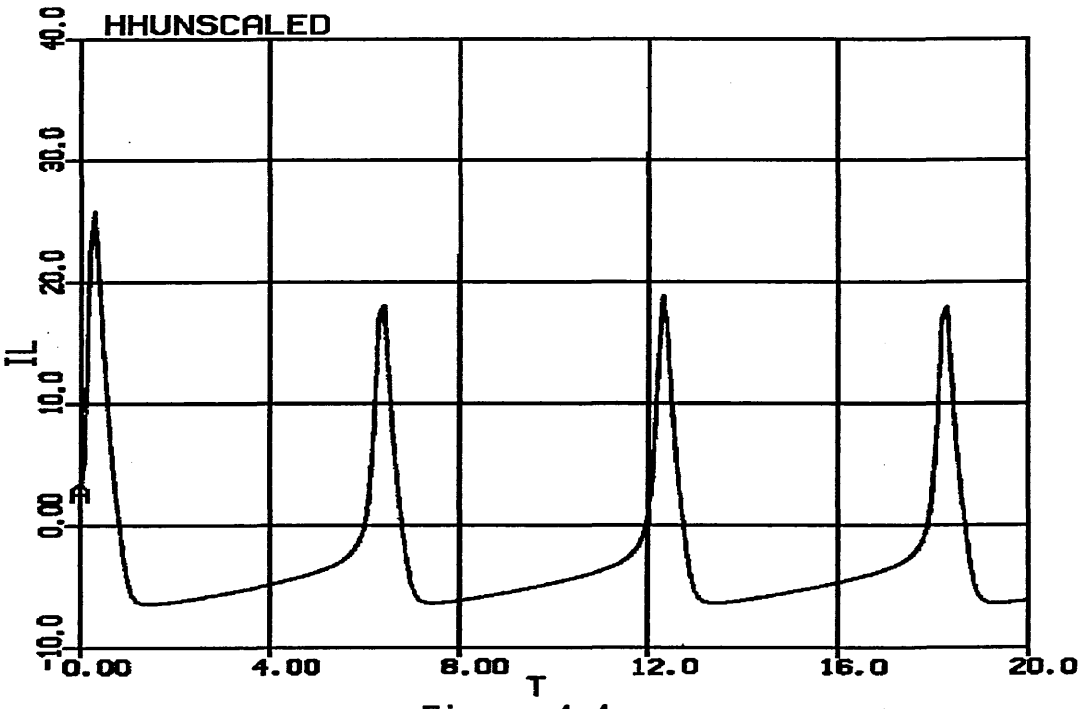


**Figure 4.4**

Graph of leakage current against time during a simulated train of impulses.

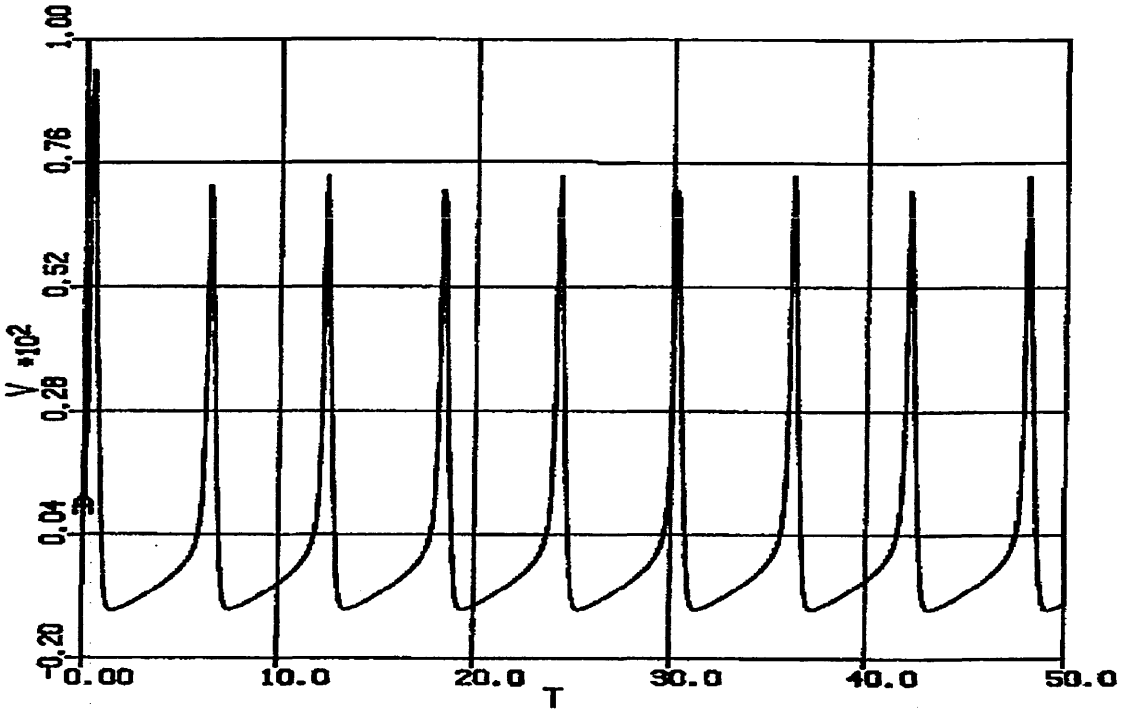


**Figure 4.5**

As Figure 4.3 but displayed on a different vertical scale.

It was then reasoned that if the input stimulus voltage could be raised above the threshold for firing and then returned to resting potential then this might simulate a burst of action potentials. It was therefore decided to stimulate the H-H model equations with an input forcing function designed to simulate a change in calcium concentration. It is known that treatment of the squid axon with low calcium concentration bathing solutions increases the excitability of the membrane and can lead to oscillations (Noble 1966; Guttman & Barnhill 1970). The effect of the reduction in calcium concentration is an apparent shift in membrane potential (Huxley 1959). The form of the forcing function was chosen purely on the grounds of its shape, the function used having a fairly steep rise to a peak followed by a long exponential tail (see Fig. 4.6). This change in calcium concentration was translated into a change in the membrane potential according to an equation derived by Huxley (Huxley 1959).

$$VSHIFT = 9.3 \ln([Ca]/44) \quad (4.1)$$

Where [Ca] is in mM

The resulting burst of action potentials is shown in Figure 4.8. There are several features to note. One is the acceleration of firing rate at the beginning of the burst. This is observed in recordings from bursting neurones. The variation in spike amplitude is also noted in recordings from real neurones (see Fig. 1.3, also Leng 1988). The first spike

of the burst has a lower amplitude than the succeeding spike, a feature that is also often present in experimental recordings. What is not apparent in the simulated trace is the existence of a plateau potential. R15 neurones show a pronounced depolarizing plateau on which the action potential spikes are superimposed. Recordings from supraoptic neurones show a slight dip in the baseline voltage during the period of maximum firing frequency (see Fig. 1.3). From the above experiment it appears possible to model bursting behaviour by driving the H-H model equations by a slow oscillation in calcium concentration. However such a model would be incomplete for the reasons stated above and a more sophisticated model should be sought. Such a simple model also fails to take account of various ionic currents known to be present in oxytocin-secreting cells. Connor & Stevens used a modified H-H model to simulate bursting in R15 neurones (Connor & Stevens 1971) by incorporating a transient potassium current that they had previously identified and modelled. A transient potassium current has also been recorded in the oxytocin-secreting neurone (Cobbett, Legendre & Mason 1989). This current is also incorporated into a model of bursting in R15 neurones by Smith (Smith 1978). Calcium currents have also been recorded in oxytocin-secreting cells and such cells produce reduced amplitude action potentials even in the absence of sodium currents. Calcium-dependent potassium currents have also been recorded (but not fully characterised) in supraoptic neurones (Cobbett, Legendre & Mason 1989). Smith's model (Smith 1978) incoporates such a current. Any complete model of the electrical behaviour of

the oxytocin-secreting neurone should incorporate mathematical descriptions of all the currents that have been observed. If such a model fails to demonstrate bursting behaviour and the model is known to be accurate then it may be assumed that there is another mechanism present responsible for driving the bursting activity.

Figure 4.6 shows the assumed change in calcium concentration. Figure 4.7 shows how this appears as the apparent shift in voltage. Figure 4.8 shows the resulting train of action potentials. Figure 4.9 shows the combination of membrane voltage and the apparent membrane voltage shift. Figures 4.10, 4.11 and 4.12 show the variation in the sodium activation, inactivation and potassium activation variables respectively during a the burst of action potentials. Unless stated otherwise membrane voltages are expressed in millivolts and time in milliseconds.

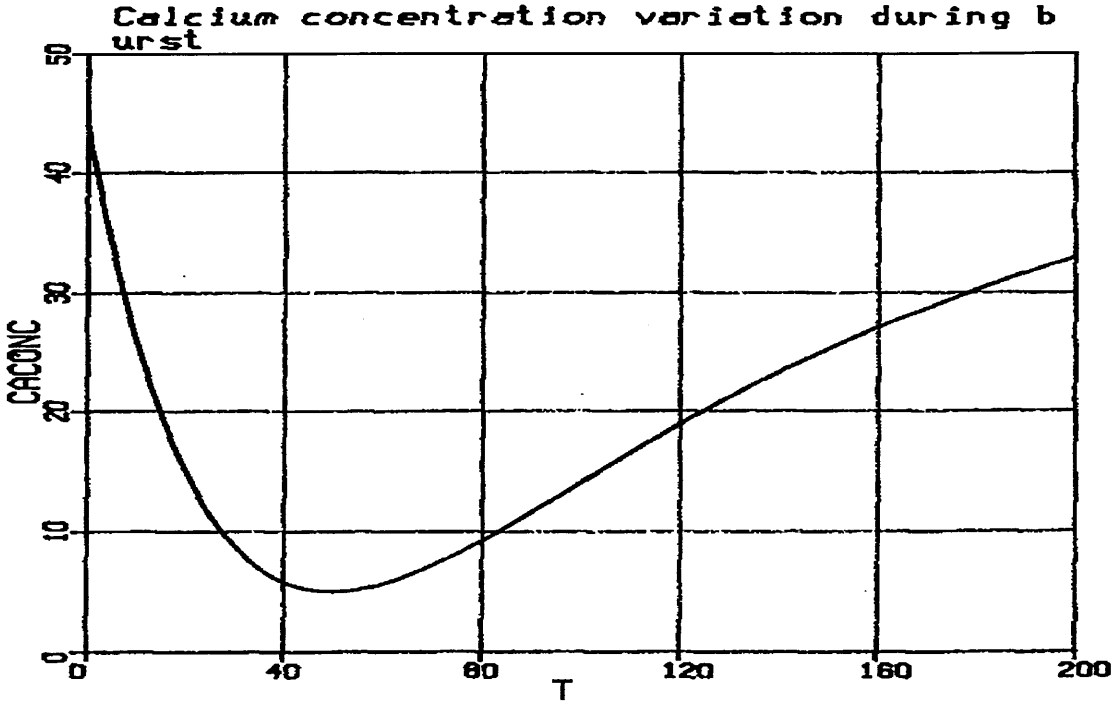


Figure 4.6

Graph of the postulated variation in calcium concentration (mM).

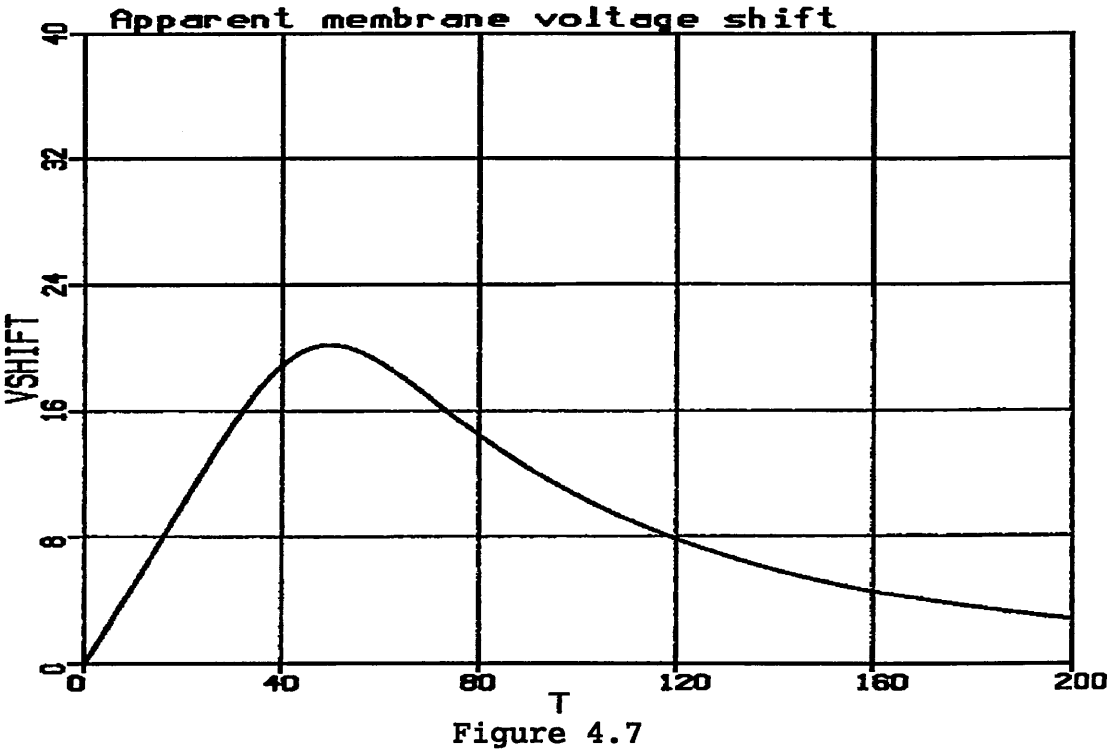


Figure 4.7

Graph showing the variation in calcium concentration translated into an equivalent shift in membrane voltage.

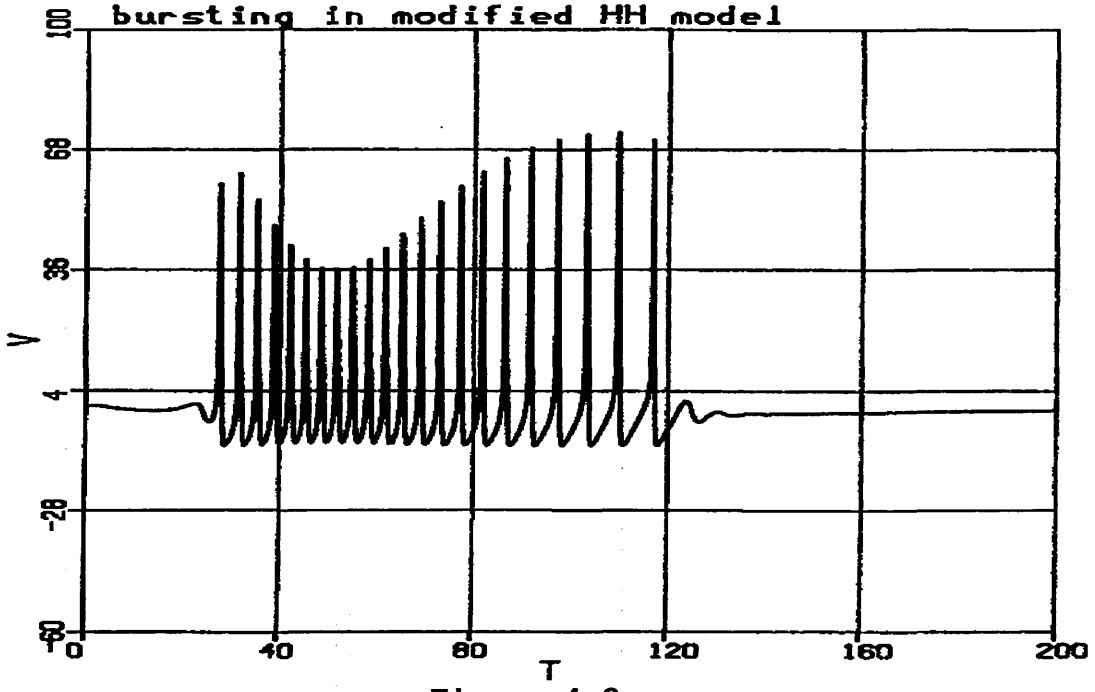


Figure 4.8

Burst of action potentials resulting from the postulated change in apparent membrane potential.

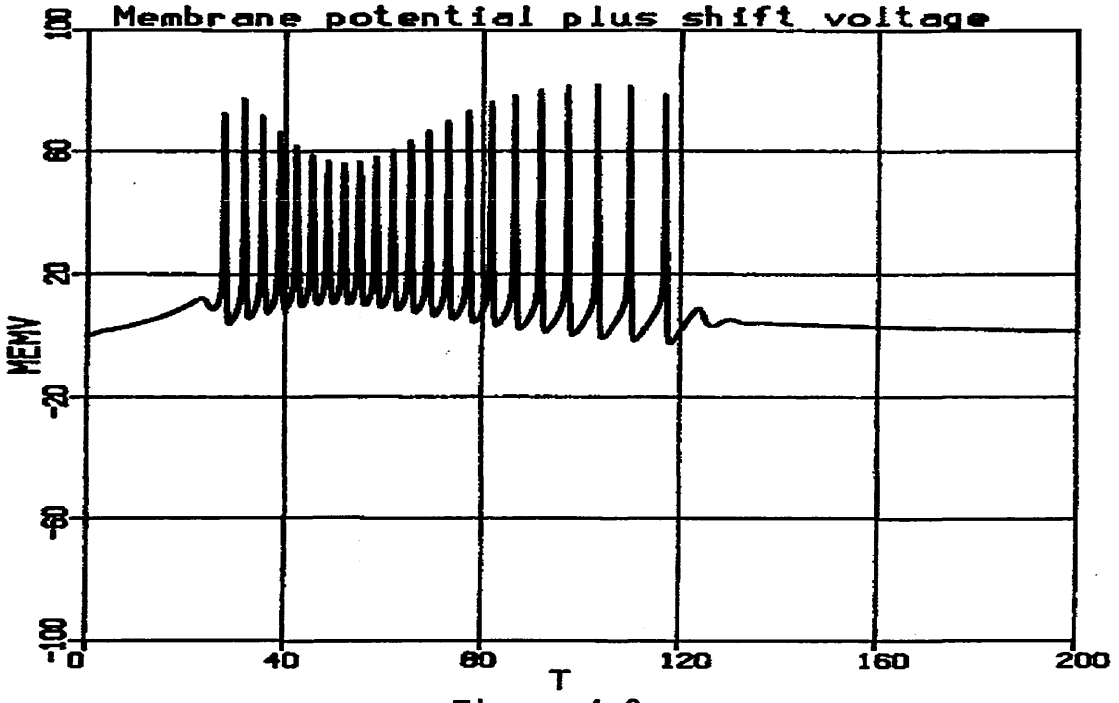


Figure 4.9

This Figure shows the result of adding the apparent shift in membrane potential to the calculated membrane potential.

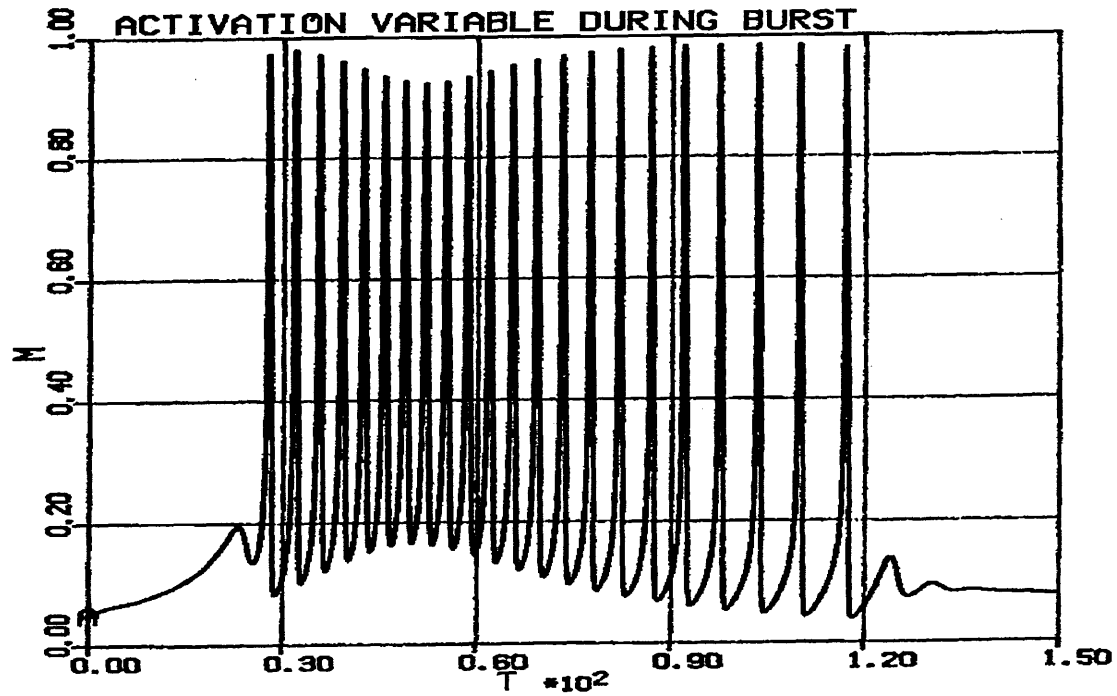


**Figure 4.10**

Graph showing the variation in sodium activation variable during the burst.

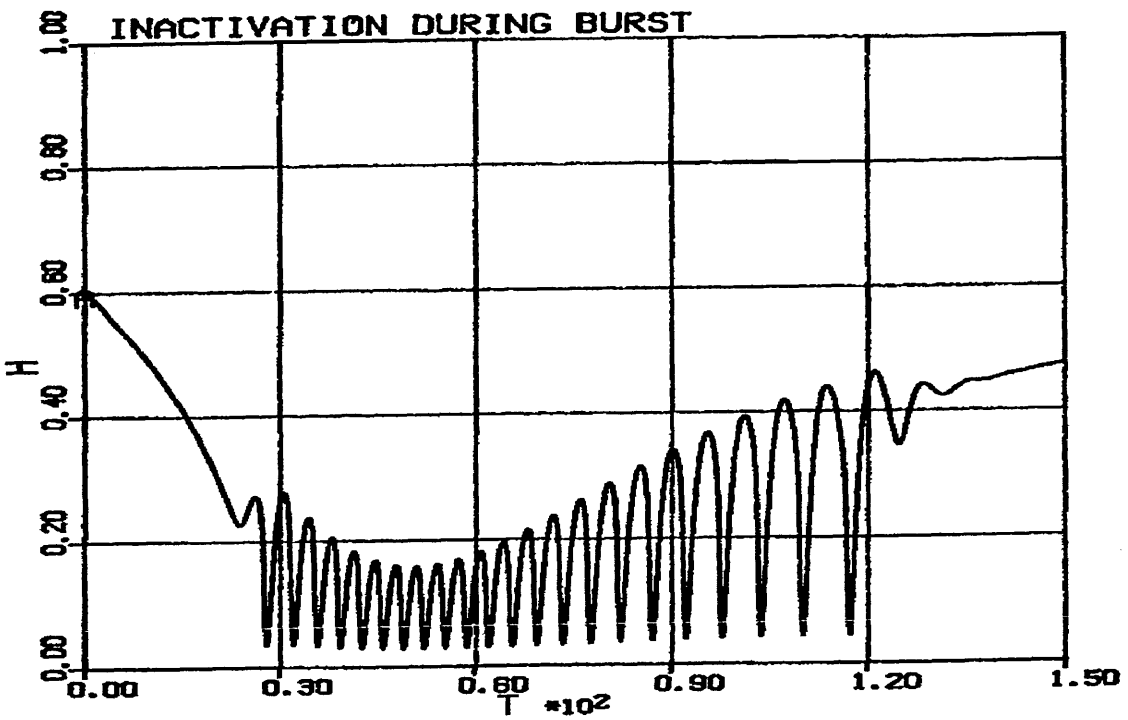


**Figure 4.11**

Graph showing the variation in the sodium inactivation variable during the burst.

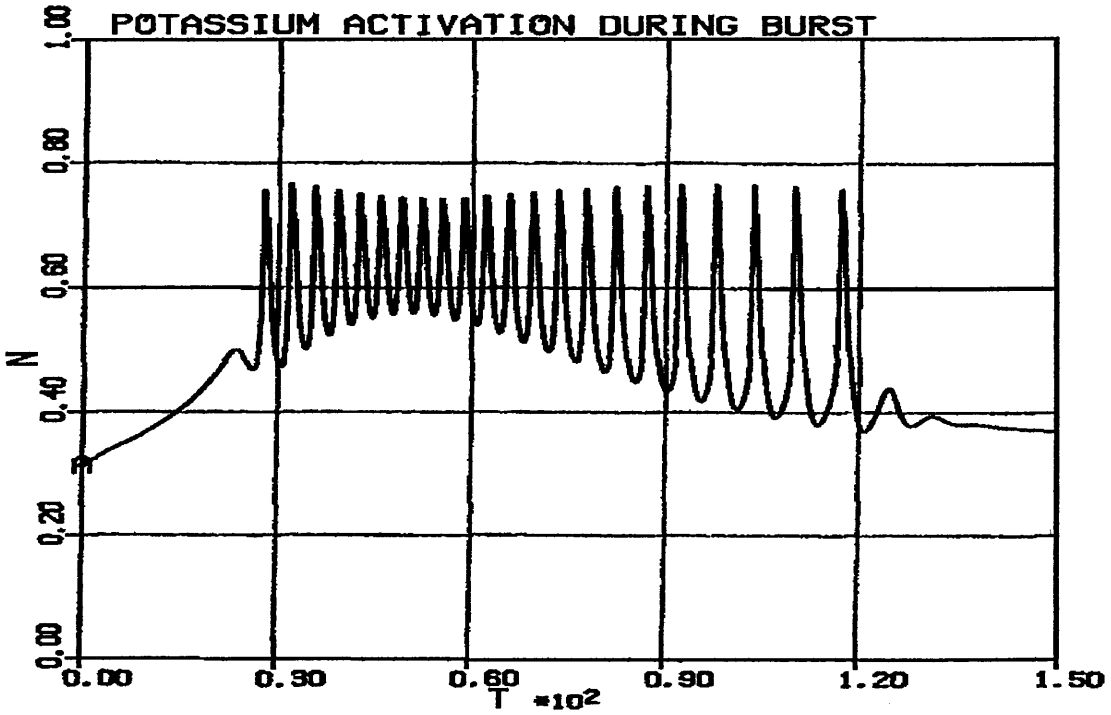


**Figure 4.12**

Graph showing the variation in the potassium activation variable during the burst.

The changes in the sodium activation and inactivation variables are interesting as is the graph showing the variation in potassium activation. Sodium activation shows a large excursion over virtually the full range of allowed values. Sodium inactivation and potassium activation show much smaller excursions during the burst. The sodium inactivation for example starts off at a value of 0.6 and rapidly falls to near zero. The maximum value of inactivation then slowly increases during the burst. The end of the burst shows the inactivation gradually returning to its pre burst value. Potassium activation shows virtually the inverse behaviour, with the value starting off near 0.3 and then rising. The maximum value during the burst does not appear to exceed about 0.75. It would therefore seem as though that the potassium current is never fully activated. The minimum value

of the potassium activation variable rises in a way that follows the general shape of the apparent membrane voltage shift in Figure 4.7. The variable then returns back to its resting value.

The above H-H model, with the inclusion of a term that models changes in calcium concentration, faithfully reproduces some of the observed behaviour of squid axons bathed in low calcium solutions in that at low (around 10μM) calcium concentrations, the model shows spontaneous activity. Changes in intracellular calcium concentration have also been measured using photosensitive calcium-binding compounds such as aequorin and arsenazo III (Gorman & Thomas 1978,1980; Hille 1984). The changes measured by Gormann and Thomas show a similar shape to the forcing function used here. Smith's 1978 model of bursting pacemaker neurones in the mollusc *Tritonia diomedia* incorporates changes in intracellular calcium concentration (Smith 1978). Several studies have shown that calcium plays an important part in regulating the electrical behaviour of certain cell types (Plant & Kim 1978 ;Gorman & Thomas 1980; Barish & Thompson 1983; Igusa & Miyazaki 1983; Barrett & Barrett 1976; Frankenhaeuser & Hodgkin 1957; Huxley 1959; Brink 1954; Bourque 1985).

As mentioned earlier, much work on bursting activity has centred on the neurone labelled R15 by Frazier, Kandel, Kupferman, Waziri & Coggeshall in the mollusc *Aplysia* (Gorman & Thomas 1980). Plant & Kim's model has been mentioned previously (Page 44 Chapter 2). The behaviour of this model will now be examined in more detail.

The model comprises eight ionic currents, three voltage sources and the membrane capacitance. The standard value of capacitance for lipid membranes ($1\mu F/cm^2$) is used. The membrane is modelled as a $1\mu F$ capacitor in parallel with the ionic conductances. One of the currents is the externally applied current controlled by the experimenter and is denoted $I_{ext}$. The transient potassium current $I_A$ described by Connor and Stevens (Connor & Stevens 1971) is included along with a third potassium conductance having a long activation time constant. Also included in the model is a current due to the electrogenic sodium pump denoted $I_{ep}$. Another non-inactivating inward current modelled by a straightforward conductance $g_T$ is included to take account of additional experimental results. No mention is made of calcium or calcium-dependent potassium currents. The later paper (Plant & Kim 1978) identifies the slow potassium conductance with the calcium-dependent potassium current while acknowledging the differences that exist between the postulated current and the experimentally measured current. The other slow inward current $g_T$ is insensitive to the presence of tetrodotoxin (TTX) in the bathing solution which implies that the current is either not carried by sodium ions (since normal sodium

channels are blocked by TTX see Page 95 ) or that there is a TTX-insensitive sodium selective channel present. If the first explanation is correct then it may be that the current is due to calcium.

Plant & Kim describe the use of so-called S and Z functions to describe steady-state activation and inactivation. These functions are themselves functions of $\alpha(V)$ and $\beta(V)$ , the rate "constants" used by Hodgkin and Huxley. Unlike Hodgkin and Huxley the S and Z functions are given explicitly.

The model derived by Plant and Kim was translated into a FORTRAN program and the equations numerically integrated using a fourth-order Runge-Kutta method on an IBM 370/168 computer. The results show a reasonable match to the observed behaviour of the cell R15 under varying experimental conditions. The model demonstrates either beating (continuous firing) behaviour and bursting behaviour depending upon the value of the external current $I_{ext}$. A slow wave is also observed. Some details of the waveforms produced by the model show slight differences from the experimental traces. The underlying plateau potential (see Fig.5a & Fig.6 Plant & Kim 1976) is not reproduced by the model. Acceleration of firing rate at the beginning of the burst is present in the model. The bursting behaviour demonstrated by the model shows a very strong resemblance to recording taken by Carnevale and Wachtel (Carnevale & Wachtel 1980). The model of Plant and Kim can therefore be regarded as successfully describing bursting in the neurone R15.

Sherman, Rinzel and Keizer note (Sherman, Rinzel & Keizer 1988) that the behaviour of pancreatic ß-cells in isolation is different from the behaviour in clusters. The authors propose that channel sharing is necessary and responsible for producing the bursting activity. The channel in question is the K-Ca channel and sharing is accomplished by tight coupling between cells. The model for this system is given in Chapter 2.

## SUMMARY

The models of cells showing bursting activity described in this chapter share several common features. By considering these features it is possible to deduce which characteristics are necessary to enable a cell to exhibit bursting behaviour. One feature is that the overall current-voltage relation for an active neurone should have a region of negative resistance (conductance). A calcium-dependent potassium channel appears to be required to provide a link between the internal calcium concentration and the membrane voltage. These features will therefore be included in the model of the oxytocin-secreting cell. The calcium-dependent calcium current has been recorded in these cells (Bourque & Renaud 1985; Cobbett, Legendre & Mason 1989) and is discussed in more detail in Chapter 6. Also essential is a basic spike generating mechanism.

# CHAPTER FIVE

## SODIUM CURRENT

Due to the polarity of the sodium reversal potential, sodium current is an inward and hence depolarizing current. It is the sodium current that is primarily responsible for the steep upstroke or rising phase of the action potential in most cells. A valuable pharmacological tool that is useful in separating the various ionic currents that are present in nerve membranes is the neurotoxin tetrodotoxin (TTX), a poison derived from puffer fish (Agnew 1984; Catterall, Gonoi & Costa 1985; Hille 1984). This molecule binds very selectively to the outside of the sodium channel where it blocks the flow of sodium current.

Sodium channels have the property of activation and inactivation as described by Hodgkin and Huxley (Hodgkin & Huxley 1952d). Activation refers to the fact that under the influence of a depolarizing stimulus, sodium channels open to allow sodium ions to enter the cell. However, associated with this process is a second process that acts to close the channel in response to a depolarization of the membrane. This process is known as inactivation. It is the combined action of these two processes that produce the characteristic sodium current trace seen under voltage clamp conditions. Two such recordings taken from cells in the rat supraoptic nucleus are reproduced here (Cobbett & Mason, personal communication) in Figs. 5.1 and 5.2. The two processes are taken to be entirely independent in the model of the squid giant axon described by Hodgkin and Huxley. This means that the activation and inactivation processes do not interact. The description of

the sodium current in that model is given by Equations 5.1, 5.2 and 5.3. An action potential occurs due to the difference in time constant of the two processes. (This is not strictly true since repolarization occurs due to potassium currents, but inactivation reduces the amount of charge that would otherwise have to be removed and hence increases the efficiency of the process.) The inactivation time constant $\tau_h$ is at least twice the magnitude of the activation time constant $\tau_m$ at all potentials according to Hodgkin and Huxley's results (Hodgkin & Huxley 1952d). This is illustrated in Figure 5.3 (drawn using Hodgkin and Huxley's conventions). Activation is a more rapid process, so that the channels open in response to a depolarizing stimulus and allow a pulse of sodium ions into the cell before the slightly slower process of inactivation causes the channel to close. Activation has a characteristic sigmoidal time course and a noticeable delay. In the H-H model, activation is given the symbol m and inactivation the symbol h. The product of the two terms determines the fraction of the maximum available sodium conductance active at any given voltage.

$$I_{Na} = \bar{g}_{Na}\, m^3 h (V - V_{Na}) \quad . . . . . (5.1)$$

$$m = [m_\infty - (m_\infty - m_0)\exp(-t/\tau_m)] \quad . . . . . (5.2)$$

$$h = [h_\infty - (h_\infty - h_0)\exp(-t/\tau_h)] \quad . . . . . (5.3)$$

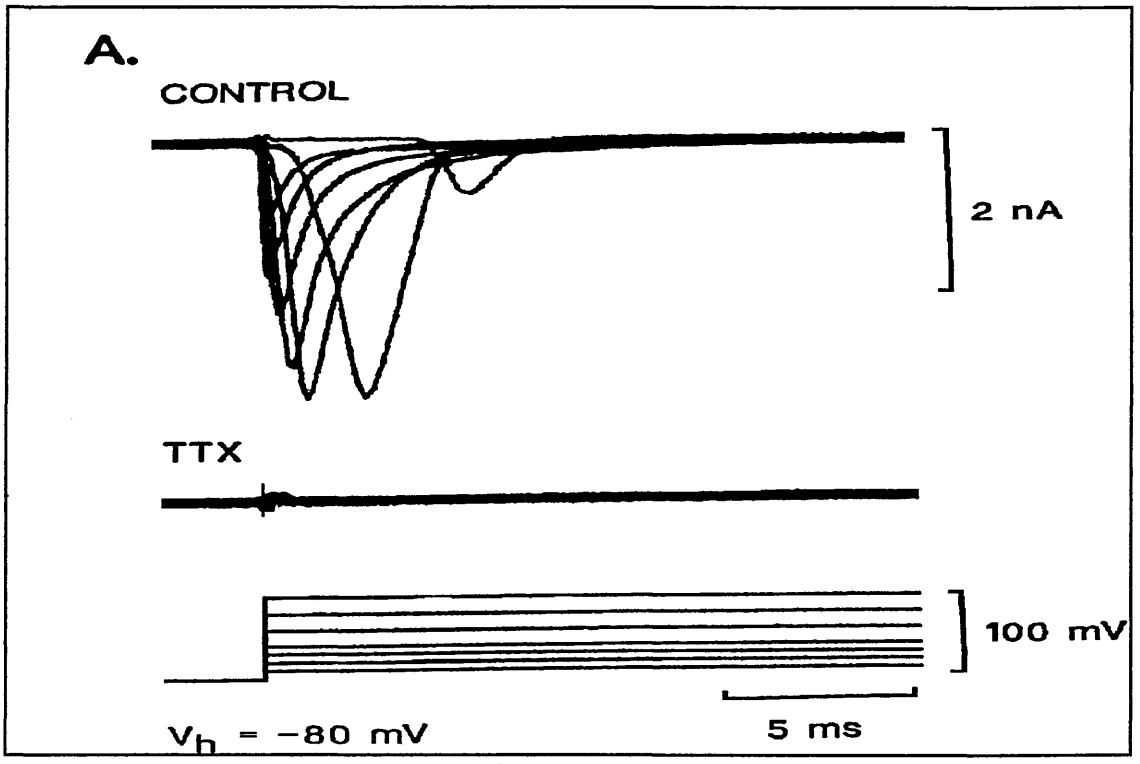


**Figure 5.1**

Experimental recordings of sodium current in supraoptic neurones courtesy P. Cobbett.

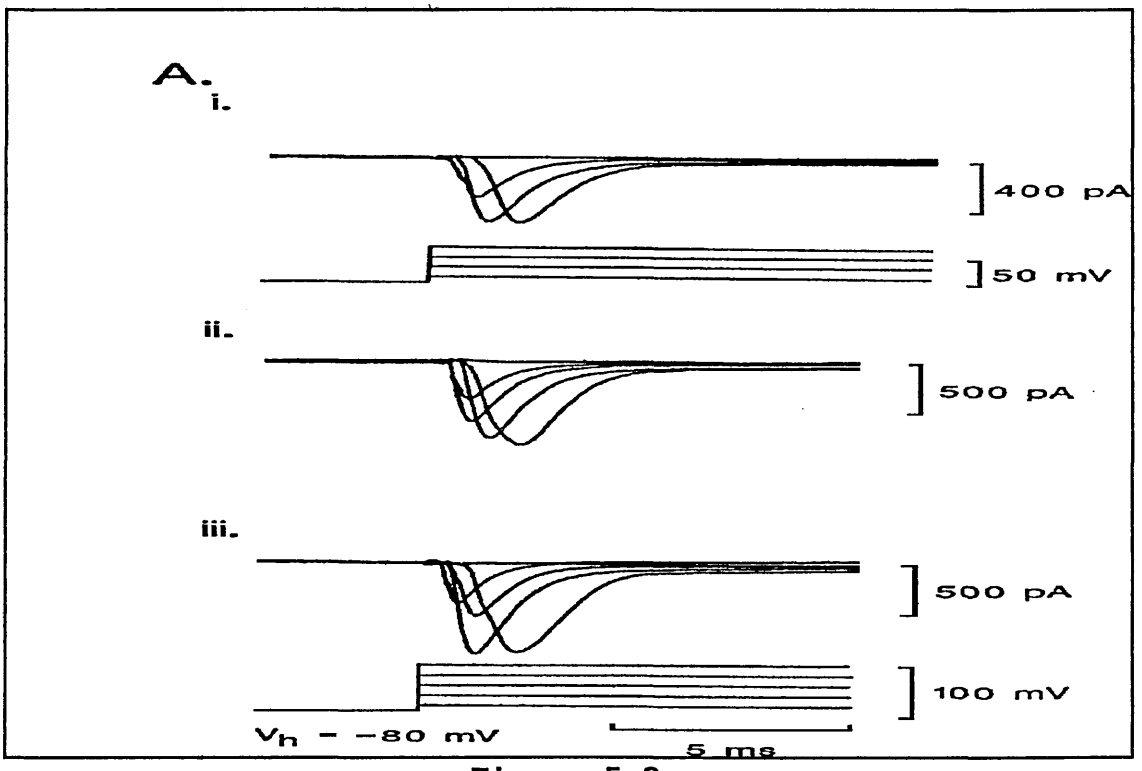


**Figure 5.2**

Recordings of sodium current from supraoptic neurones, courtesy P. Cobbett.

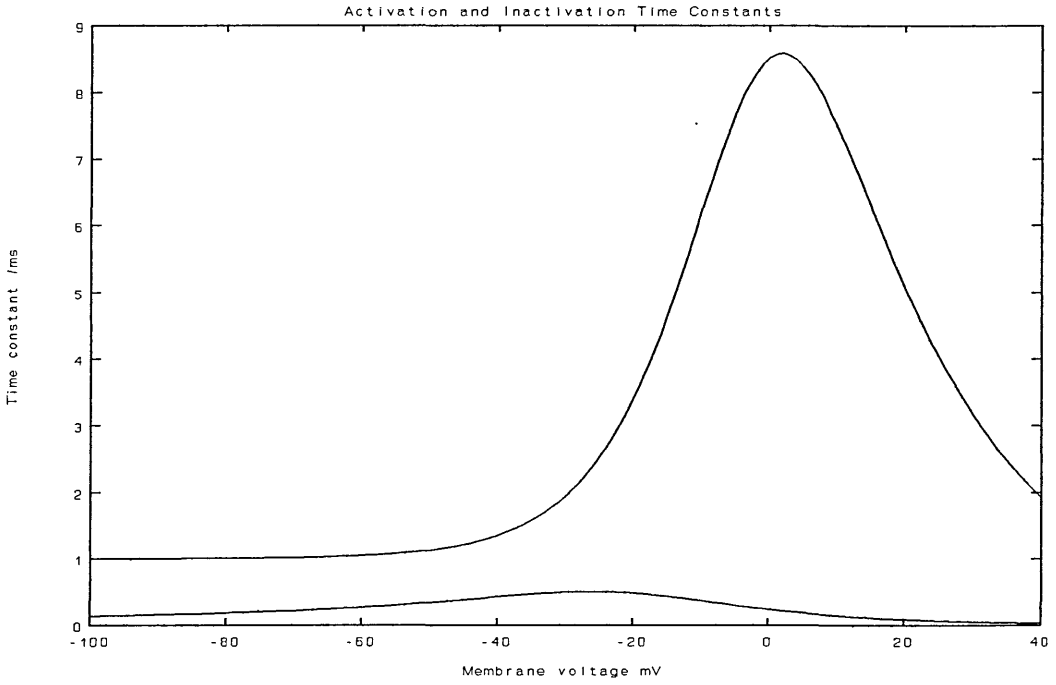


**Figure 5.3**
Graph showing the voltage dependence of sodium current activation and inactivation time constants in the H-H model.

Typical activation and inactivation curves are shown in Figure 5.4. They are shown in the form of the steady-state values $m_\infty$ and $h_\infty$ versus voltage. These curves were drawn using data from the H-H model. Note that these curves were obtained using the original data without correction for membrane resting potential or modern sign conventions for voltage and current (as is Fig. 5.3). To compensate for these factors and to generate curves that reflect modern conventions, the curves should be mirrored about the zero volt axis and the entire curve shifted along the voltage axis by an amount equal to the resting potential of the squid axon (-62mV). The curves as shown here are as drawn by Hodgkin and Huxley. Hille (Hille 1984 p.47) shows similar curves drawn according to present conventions.

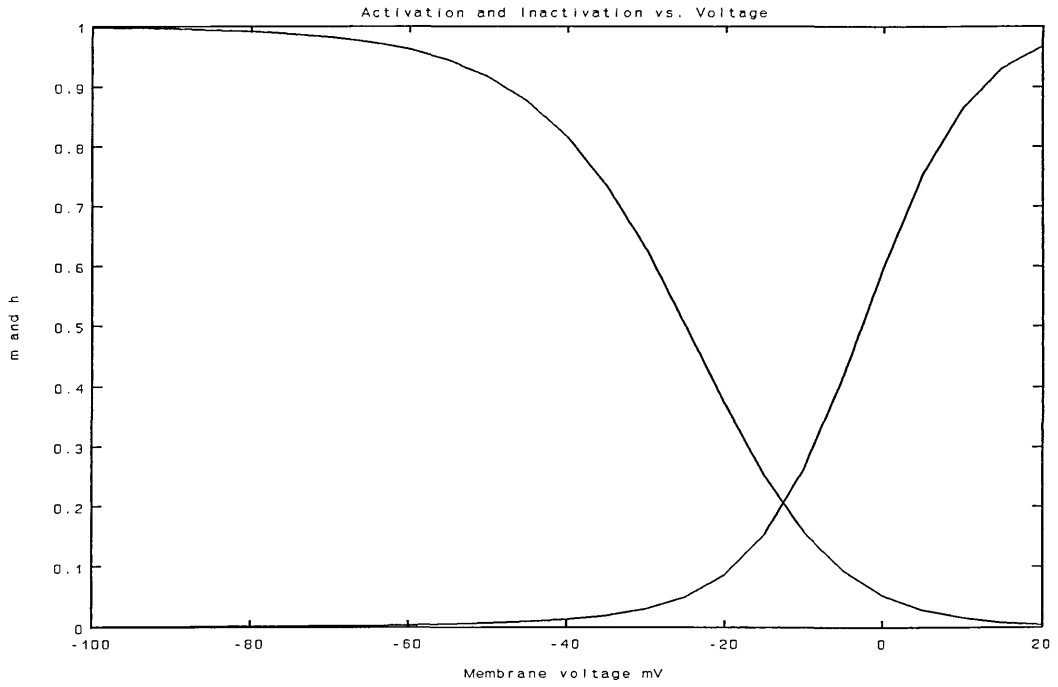


**Figure 5.4**
Graph showing the voltage dependence of the steady-state activation and inactivation variables in the H-H model.

Analysis of the sodium current by voltage clamp methods is complicated by the existence of the two processes and a more complicated experimental procedure is necessary to separate them. The time constants involved are of the same order which creates more difficulties. The problem is that a step depolarization triggers both processes, making it difficult to identify the contribution of each process to the total current. In the instance of the potassium current $I_K$ (see Chapter 6) there is no inactivation, so a depolarizing step triggers the activation process and gives rise to a current that rises to a maximum and remains there. With the two processes of activation and inactivation it is not certain that the activation process has gone to completion before the inactivation process starts to reduce the current.

In other words, the time courses of the two processes overlap (French & Horn 1983). Similarly, following a step depolarization it is not possible to ascertain when and at what voltage the inactivation process started. To overcome these problems a more sophisticated pulse protocol is used. By using a double pulse method it is possible to ensure that the steady state values of activation and inactivation have been reached before making a test depolarization. The double pulse protocol involves the use of a conditioning pulse followed by a test pulse. The test pulse usually has a fixed amplitude. The conditioning pulse may be a fixed amplitude pulse of variable duration or a variable amplitude pulse of fixed duration. This method allows the time course of the recovery from inactivation to be examined (Adams & Gage 1979). Cobbett et al. (Cobbett, Ingram & Mason 1987) give more detail of this technique.

Analysis of sodium current is further complicated in some cells by the existence of more than one inactivation process. Belluzzi and Sacchi (Belluzzi & Sacchi 1986), amongst others note the presence of a slow component in the inactivation process (see Hille 1984 for further references). However, since the time constants associated with slow inactivation are long compared with the duration of the action potential, this additional complication will be ignored in the following model of sodium current in oxytocin-secreting cells.

Hodgkin and Huxley's derivation of their model for sodium current has not been given in previous chapters and so will be covered briefly here. Starting with their assumptions

regarding the shape of the sodium conductance curve and the differential equations governing the gating particles, equations 5.2 and 5.3 (Page 96) were obtained. The initial and steady-state values of activation and inactivation are given the symbols $m_0$, $m_\infty$, $h_0$ and $h_\infty$. Derivation of 5.2 and 5.3 is straightforward and involves finding the general and particular solutions to equations 2.3 and 2.4 in Chapter 2. The rate "constants" are related to the steady-state values of activation and inactivation by the following equations.

$$m_\infty(V) = \frac{\alpha_m(V)}{(\alpha_m(V) + \beta_m(V))} \quad \ldots\ldots\ldots\ldots\ldots\ldots (5.4)$$

$$h_\infty(V) = \frac{\alpha_h(V)}{(\alpha_h(V) + \beta_h(V))} \quad \ldots\ldots\ldots\ldots\ldots\ldots (5.5)$$

The activation and inactivation time constants are related to the rate constants in a similar manner.

$$\tau_m(V) = \frac{1}{(\alpha_m(V) + \beta_m(V))} \quad \ldots\ldots\ldots\ldots\ldots\ldots (5.6)$$

$$\tau_h = \frac{1}{(\alpha_h(V) + \beta_h(V))} \quad \ldots\ldots\ldots\ldots\ldots\ldots (5.7)$$

Rearranging 5.4 and 5.5 and substituting in for $\alpha$ and ß from 5.6 and 5.7 yields the following expressions for the rate "constants" as a function of voltage.

$$\alpha_m(V) = \frac{m_\infty(V)}{\tau_m(V)} \quad \ldots\ldots\ldots\ldots\ldots\ldots\ldots\ldots \quad (5.8)$$

$$ß_m(V) = \frac{1 - m_\infty(V)}{\tau_m(V)} \quad \ldots\ldots\ldots\ldots\ldots\ldots\ldots\ldots \quad (5.9)$$

$$\alpha_h(V) = \frac{h_\infty(V)}{\tau_h(V)} \quad \ldots\ldots\ldots\ldots\ldots\ldots\ldots\ldots \quad (5.10)$$

$$ß_h(V) = \frac{1 - h_\infty(V)}{\tau_h(V)} \quad \ldots\ldots\ldots\ldots\ldots\ldots\ldots\ldots \quad (5.11)$$

By stepping the membrane voltage to various levels from a holding potential and recording the resultant sodium current, Hodgkin and Huxley were able to measure the sodium conductance as a function of time. Then by neglecting $m_0$ and $h_\infty$ (the justification for which is given in their 1952d paper) a simplified version of equations 5.2 and 5.3 (5.12) was fitted to the conductance curves for each of the voltage steps.

$$g_{Na} = g'_{Na}[1 - \exp(-t/\tau_m)]^3 \exp(-t/\tau_h) \quad \ldots\ldots\ldots \quad (5.12)$$

where

$$g'_{Na} = \bar{g}_{Na}\, m_\infty^3\, h_0 \quad \ldots\ldots\ldots\ldots\ldots\ldots \quad (5.13)$$

Equations 5.8, 5.9, 5.10 and 5.11 were then used to plot curves of $\alpha_m$, $\beta_m$, $\alpha_h$ and $\beta_h$ as a function of voltage having obtained $g'_{Na}$ as the cube root of 5.13 and $\tau_m$ indirectly from 5.10. Equations were fitted to the curves obtained to give functions relating the rate "constants" to the membrane voltage. These functions were then used in Equations 2.3 and 2.4 during simulation trials.

Referring back to the state diagrams in Chapter 2, it is noted that the original Hodgkin-Huxley model does not require that activation and inactivation occur in a set sequence. However there are alternative models to the simple one proposed by Hodgkin and Huxley, known as coupled models in which the two aspects of channel behaviour are not independent (Jakobsson 1976). There is experimental evidence that the activation and inactivation processes are independent and occur at different sites in the sodium selective channel (Armstrong 1981).

The observation that inactivation is removed by pronase, iodate ions and N-bromoacetamide and other agents (French & Horn 1983; Hille 1984), while leaving the activation process intact suggests very strongly that the two processes are separate. However, activation and inactivation are almost

certainly not independent since it appears that activation must take place before the inactivation process can operate. One pictorial representation of the interaction between activation and inactivation in the sodium channel is of an activation "gate" and an inactivation particle. The inactivation particle is on the intracellular surface of the channel and can only enter the channel to block ion flow when the activation gate is open. Such a picture is to be found in Armstrong & Bezanilla 1977 and Armstrong 1981.

Creating detailed mathematical models and computer simulations allows various schemes to be discarded as explanations of the behaviour of ionic currents, but is not usually sufficient to determine which of a set of models is the "correct" one. This is because manipulation of model parameters may, in different models, give an equally good fit to the experimental data.

## MODEL DUE TO BELLUZZI AND SACCHI

Belluzzi and Sacchi (Belluzzi & Sacchi 1986) derived a model of the sodium current in the rat sympathetic neurone based on Hodgkin and Huxley's model. In their 1986 paper they do not derive the $\alpha(V)$ and ß(V) functions but fit equations to the $m_\infty$ , $h_\infty$ and $\tau_m$ curves. The following equations summarise their model.

$$I_{Na} = \bar{g}_{Na} m_\infty^3 [1 - \exp(-t/\tau_m)](V - V_{Na}) \quad \ldots\ldots\ldots \quad (5.14)$$

$$\tau_m = 0.06013 + \frac{1}{42.98\exp(0.08915V) + 0.9230\exp(-0.03351V)} \quad (5.15)$$

$$\tau_h = (-0.00455V + 0.2591) +$$

$$\frac{50.85}{2 + \exp[(-59.46 - V)/7.91] + \exp[(V + 40.94)/1.556]} \quad \ldots \quad (5.16)$$

$$m_\infty = \frac{1}{1 + \exp[(-36.0 - V)/7.2]} \quad \ldots\ldots\ldots\ldots \quad (5.17)$$

$$h_\infty = \frac{1}{1 + \exp[(V + 53.219)/6.517]} \quad \ldots\ldots\ldots \quad (5.18)$$

$$S_\infty = \frac{1}{1 + \exp[(V + 62.424)/6.469]} \quad \ldots\ldots\ldots \quad (5.19)$$

Voltages are expressed in millivolts, time constants in milliseconds and conductance in microSiemens.

In this model Belluzzi and Sacchi have used an "S" function to describe the steady-state value of the slow inactivation that they observed.

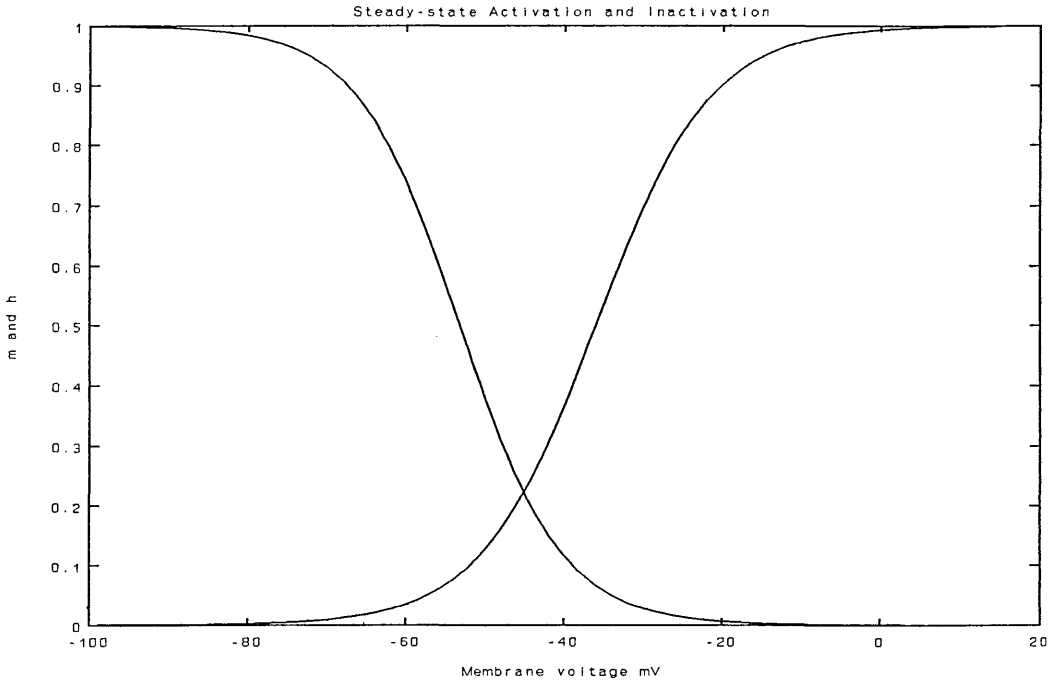


**Figure 5.5**
Graph showing the voltage dependence of the steady-state activation and inactivation variables in Belluzzi and Sacchi's sodium current model.

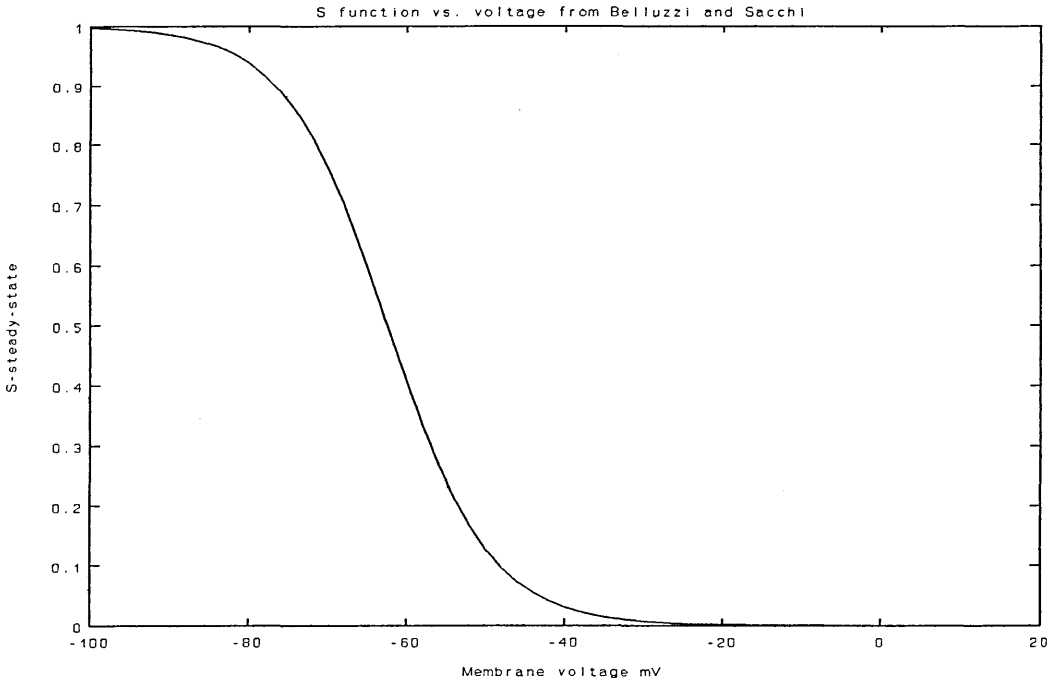


**Figure 5.6**
Graph showing the 'S' function used by Belluzzi and Sacchi in their description of the sodium current in rat sympathetic neurones.

## MODEL DUE TO SMITH

Smith's model (Smith 1978) of the molluscan bursting neurone includes a sodium current model which is reproduced here for purposes of comparison with the other models.

The current may be described using an activation variable raised to the third power multiplied by an activation variable as shown in Equation 5.20.

$$g_{Na} = \bar{g}_{Na}\, m^3 h \quad \ldots\ldots\ldots\ldots\ldots\ldots \quad (5.20)$$

The steady-state activation and inactivation curves are described by Equations 5.21 and 5.22.

$$m^3(V,\infty) = \left\{\frac{1}{\exp[(V+30.1)/-7]+1}\right\}^{8.1} \quad \ldots\ldots\ldots \quad (5.21)$$

$$h(V,\infty) = \left\{\frac{1}{\exp[(V+10.5)/4.5]+1}\right\}^{6} \quad \ldots\ldots\ldots \quad (5.22)$$

The activation and inactivation time constants are described by Equations 5.23 and 5.24.

$$\tau_m(V) = \frac{11.5}{1+\exp[(V+16)/5.75]} + 0.5 \quad \ldots\ldots\ldots \quad (5.23)$$

$$\tau_h(V) = \frac{85}{1+\exp[(V+24)/3.75]} + 4.5 \quad \ldots\ldots\ldots \quad (5.24)$$

The differential equation used to describe the changes in activation and inactivation variables during action potentials are given by 5.25 and 5.26.

$$\tau_m(V)\,\frac{dm(V,t)}{dt} + m(V,t) = m(V,\infty) \quad \ldots\ldots\ldots \quad (5.25)$$

$$\tau_h(V)\,\frac{dh(V,t)}{dt} + h(V,t) = h(V,\infty) \quad \ldots\ldots\ldots \quad (5.26)$$

The curves described by these equations are shown in Figures 5.7 to 5.9.

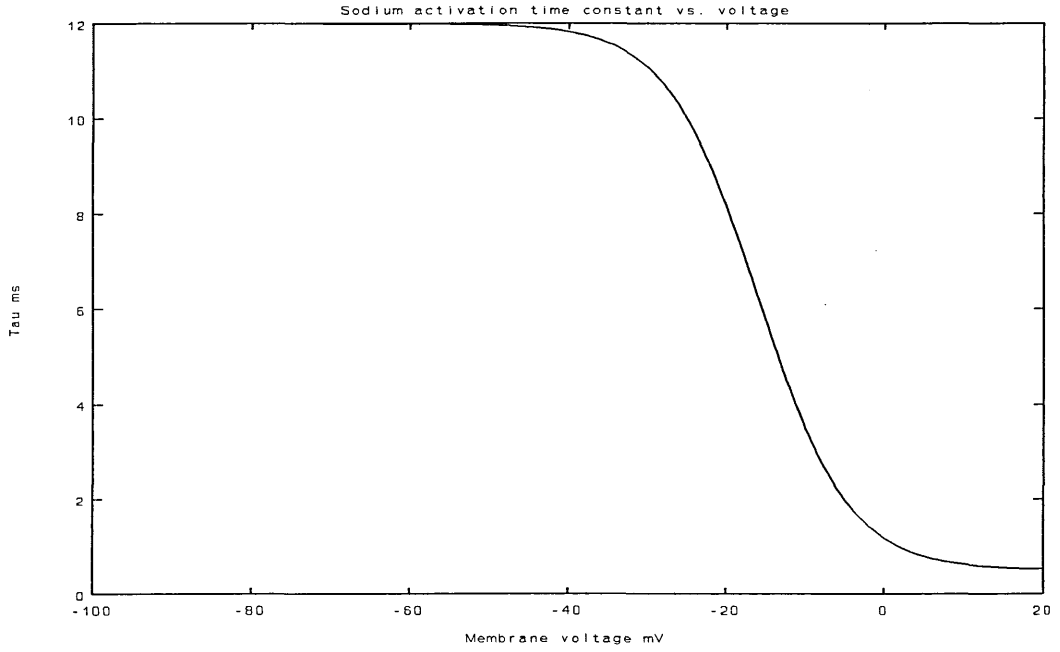


**Figure 5.7**
Graph showing the voltage dependence of activation time constant in Smith's sodium current model.

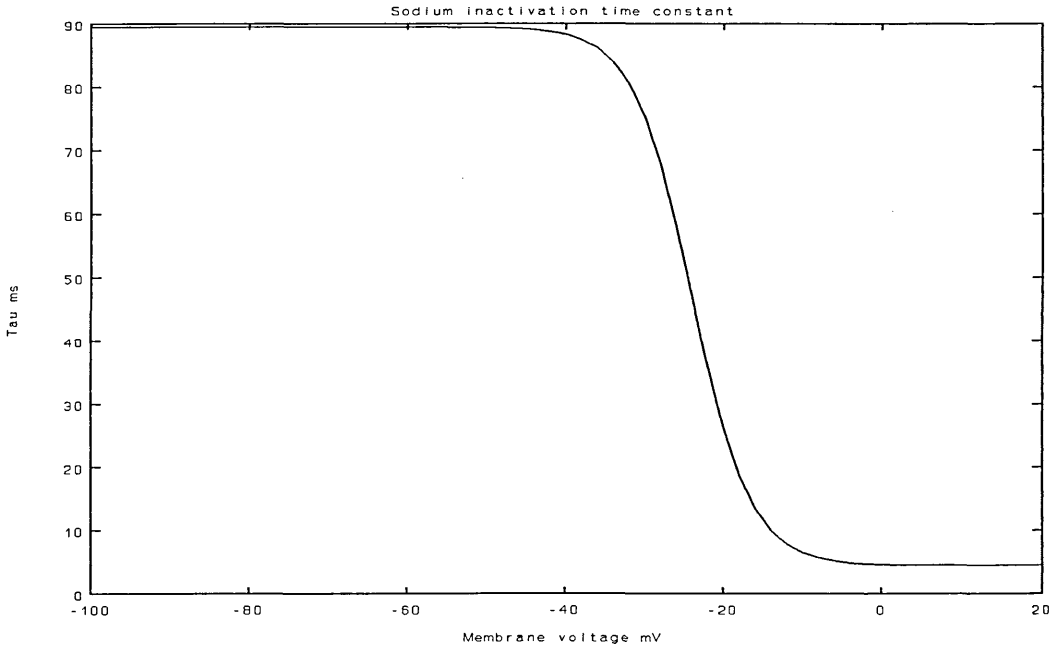


**Figure 5.8**
Graph showing the voltage dependence of the inactivation time constant in Smith's sodium current model.

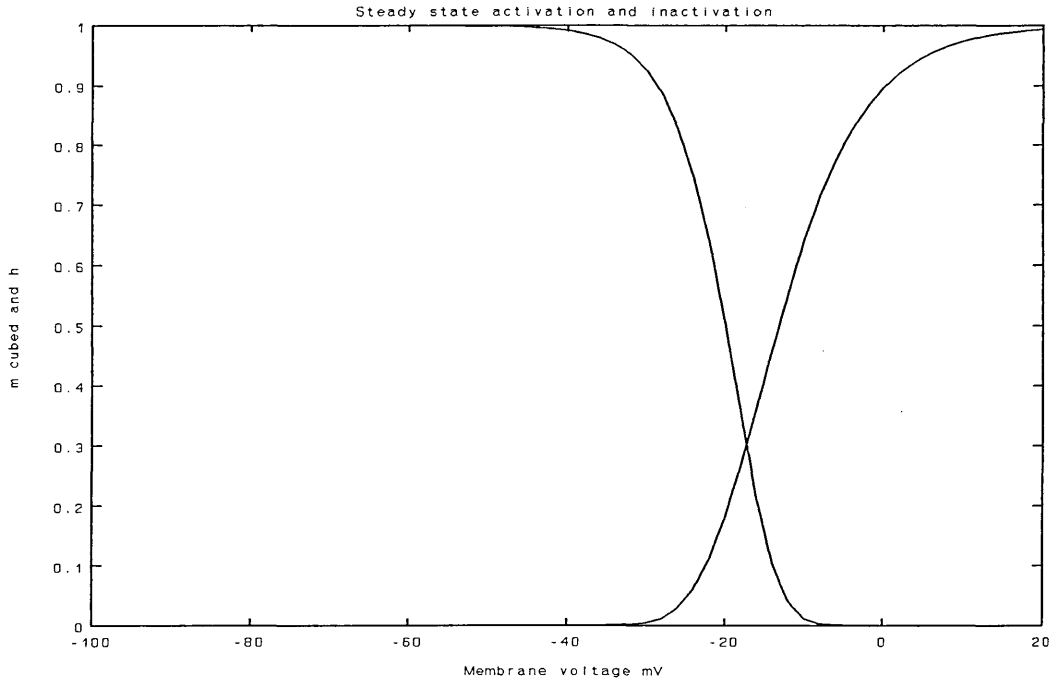


**Figure 5.9**
Graph showing the voltage dependence of the steady-state activation and inactivation variables in Smith's sodium current model.

## MODEL OF SODIUM CURRENT IN OXYTOCIN-SECRETING NEURONE

Using data obtained by Cobbett (personal communication) the following model has been derived to describe the sodium current in the oxytocin-secreting neurone. Voltage-dependent rate equations were fitted to the activation and inactivation time constant curves using methods described in chapter 3. There was insufficient information (no $m_\infty(V)$ curve) to fix the $\alpha_m(V)$ curve prior to fitting to the $\tau_m(V)$ curve so there is considerable freedom in choosing the parameters of the $\alpha_m$ curve. Once that curve has been fixed, the $\beta_m(V)$ is

constrained to fit the curve formed by subtracting the $\alpha_m(V)$ from the $\tau_m(V)$ curve according to equation 5.6. The equations 5.21 to 5.24 were found to fit the data using a Least Squares criterion and manually adjusting the parameters using the computer keyboard. The computer program recalculated the sum of the squared deviations after each trial and replotted the graph. This process was fairly tedious and time-consuming. This approach was used because of the large leeway available for choosing the initial curve. It was felt that a fully automatic data-fitting routine was not justified at this stage. The smooth curves fitted to the data points are shown in Figures 5.10 and 5.11. The data points were included in the original graph but were deleted by the process of importing the graphic into the wordprocessing package.

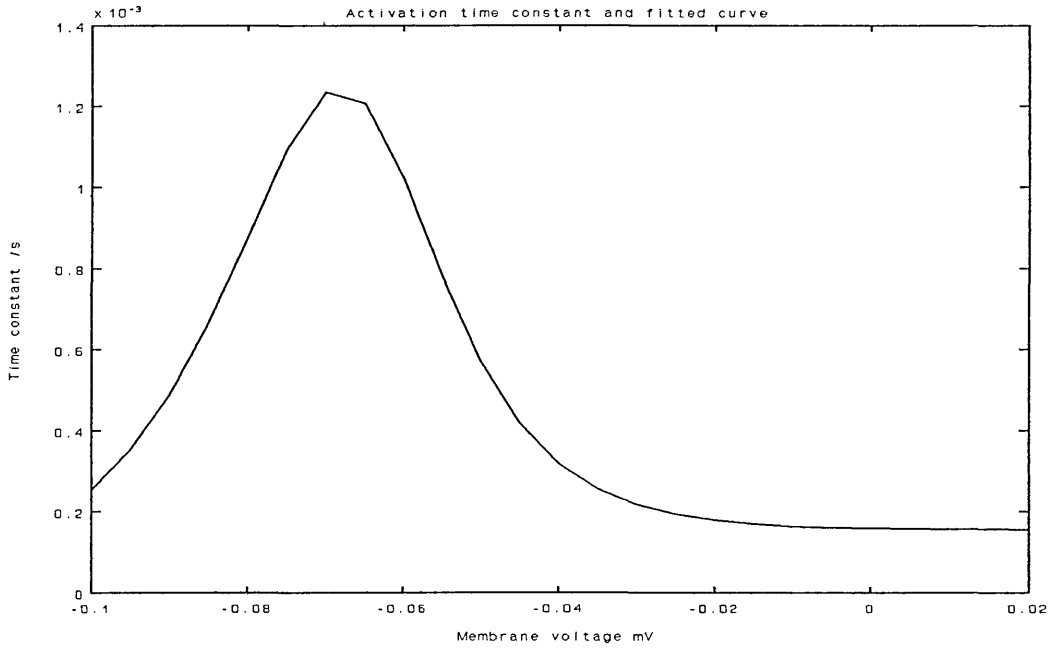


**Figure 5.10**
Graph showing the smooth curve fitted to the activation time constant data.

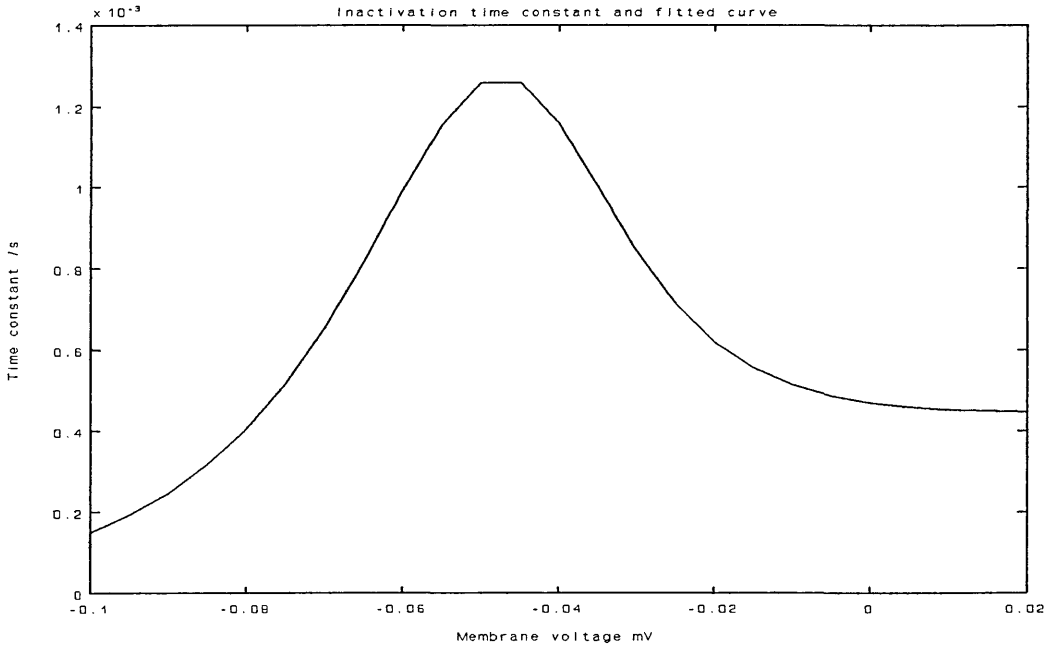


**Figure 5.11**
Graph showing the smooth curve fitted to the inactivation time constant data.

Cobbett found that the sodium current in oxytocin-secreting neurones may be described by the original Hodgkin and Huxley equation as given in equation 5.20.

$$I_{Na} = \bar{g}_{Na}\, m^3 h (V - E_{Na}) \quad \ldots\ldots\ldots\ldots\ldots\ldots \quad (5.20)$$

The range and number of data points available for curve fitting are restricted so the following functions may not be the "best" description of the experimentally observed current.

$$\alpha_m(V) = \frac{6400}{[0.02\exp(-100V) + 1]} \quad . . . . . \quad (5.21)$$

$$\beta_m(V) = 5\exp(-V/0.015) \quad . . . . . \quad (5.22)$$

$$\alpha_h(V) = 45\exp(-V/0.02) \quad . . . . . \quad (5.23)$$

$$\beta_h(V) = \frac{2250}{[0.08\exp(-92.5V) + 1]} \quad . . . . . \quad (5.24)$$

$$\frac{dm}{dt} = \alpha_m(1 - m) - \beta_m m \quad . . . . . \quad (6.25)$$

$$\frac{dh}{dt} = \alpha_h(1 - h) - \beta_h h \quad . . . . . \quad (5.26)$$

TABLE 5.1

SODIUM CURRENT MODEL PARAMETERS

| | |
|---|---|
| $\hat{g}_{Na}$ = 51.6nS | Maximum whole cell sodium conductance |
| $E_{Na}$ = 43.6mV | Nernst potential for sodium |

Using the above equations (5.20 to 5.26) and the parameters given in the table, numerical simulations were performed. The initial conditions were established for a chosen holding potential and a series of step depolarizations given. The numerical integration routine then proceeded to calculate the behaviour of the model for the chosen time period. Graphical results were obtained and are shown in Figures 5.12 and 5.13. It can be seen from the Figure that the model adequately represents the behaviour of the sodium current under voltage clamp conditions. The figures may be compared with figures 5.1 and 5.2. Careful inspection of 5.1, 5.2, 5.12 and 5.13 reveals that the simulated current is slightly smaller in magnitude and slightly faster than the recorded current. It was felt that the model yielded results that were sufficiently close to the actual current that the model could be used. Slight adjustment of the maximum conductance and a slight increase in the time constants would give a more accurate representation should this prove necessary. The model as it stands is within the limits of experimental variation. The program used to obtain these results was named "INAOXY.CSL" and was written using the ACSL simulation language. The sodium current model was then incorporated in later simulations.

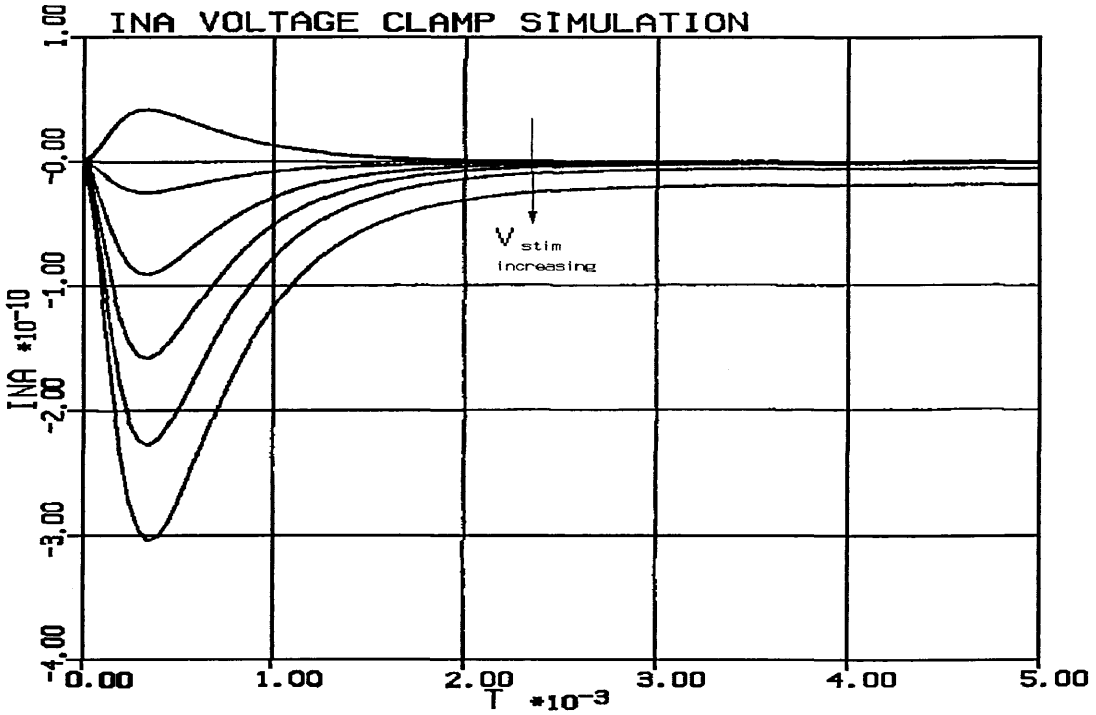


**Figure 5.12**

Simulation of voltage clamp experiment. Holding voltage -80mV as Figs. 5.1 and 5.2

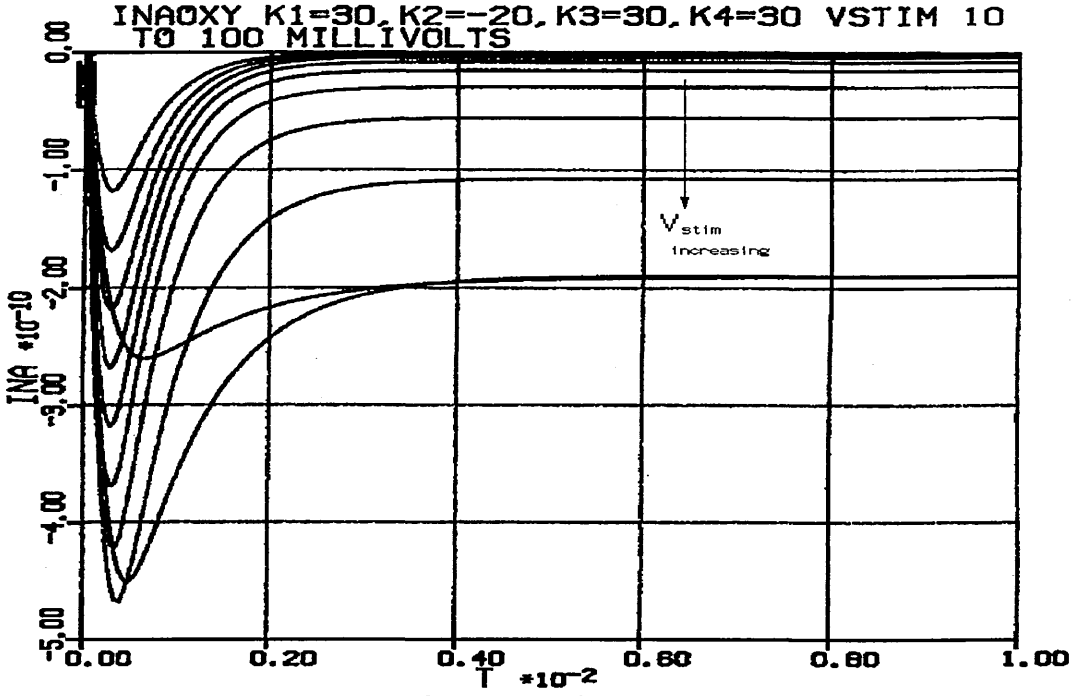


**Figure 5.13**

Results of simulation of voltage-clamp experiment using the model derived for the sodium current.

For comparison, simulations of sodium current using the modified Hodgkin-Huxley model is shown in Fig. 5.14

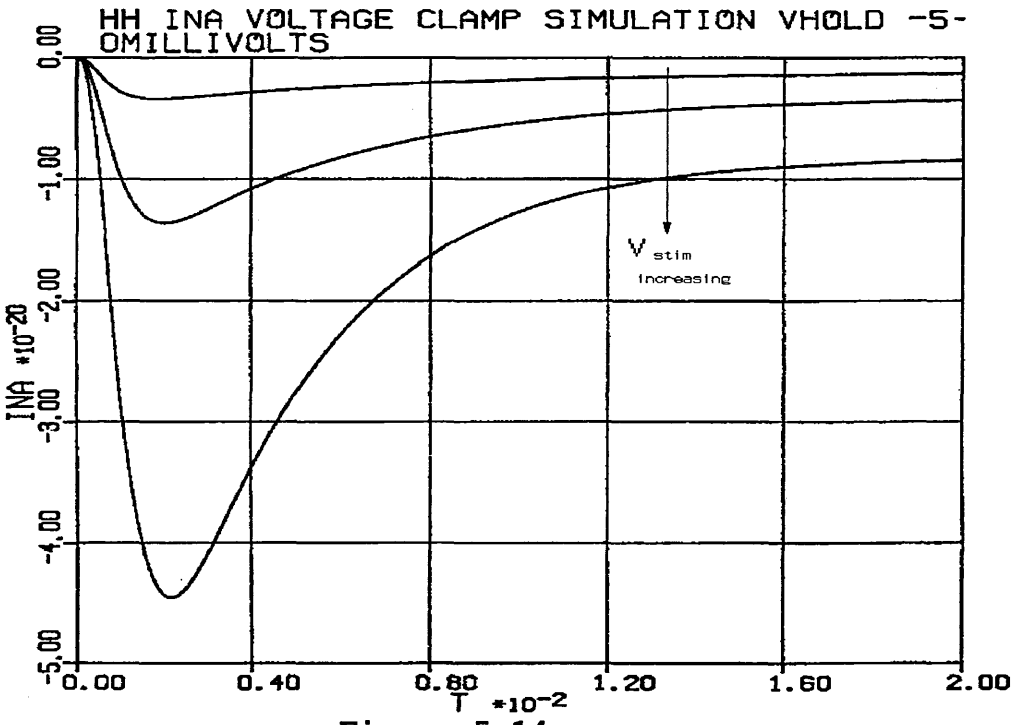


**Figure 5.14**

Results of simulating a voltage-clamp experiment using the H-H sodium current model.

# CHAPTER SIX

## POTASSIUM CURRENTS

Potassium currents are outward currents and therefore have the effect of repolarizing or hyperpolarizing the nerve membrane. The cell resting potential is largely governed by the permeability of the membrane to potassium ions (Hille 1984). Hodgkin and Huxley in their work on the squid giant axon described only one potassium current. Subsequent work in other preparations has shown the existence of a number of different potassium currents that are similar only in the fact that potassium is the major current carrier. These are; transient potassium currents that activate and then inactivate in response to depolarizing stimuli in much the same way as the sodium current does; currents that are controlled by calcium ions on the intracellular membrane surface; M currents that are controlled by chemical messengers. In describing the electrical behaviour of the oxytocin-secreting neurone it will be necessary to model three types of potassium current.

These are; the delayed rectifier current which is given the symbol $I_K$ , a transient potassium current $I_A$ and a calcium-dependent potassium current $I_{K(Ca)}$. These currents were recorded from cultured supraoptic neurones taken from the rat. The $K^+$ currents were recorded during voltage clamp experiments and were identified on the basis of their kinetics, calcium-dependence and response to various channel blocking agents. All these currents have been recorded by Cobbett et al. (Cobbett, Legendre & Mason 1989) and the models in this Chapter have been based on their results. For

the details of the experimental procedure see Cobbett, Legendre & Mason (1989). The nomenclature used to describe the currents is fairly standard although different workers use different symbols, for instance the calcium-gated potassium current is sometimes denoted by $I_C$ whereas here the symbol $I_{K(Ca)}$ is used in line with Hille (1984). Each type of current will be described in more detail under the appropriate subheadings.

The modelling approach that has been used in this project is the same as used by Hodgkin and Huxley and other workers. A mathematical model is found for each of the observed currents taken in isolation and these sets of equations are then put together to form a system of equations that are then solved using computer numerical methods. This chapter describes the fitting of mathematical models to the available data relevant to the three potassium currents recorded by Cobbett et al. Simulation of each of the currents separately (where possible) is also described as a check on the validity of the models.

## MODELLING THE DELAYED RECTIFIER CURRENT $I_K$

The delayed rectifier current $I_K$ exhibits behaviour similar to the potassium current recorded in the squid giant axon by Hodgkin and Huxley (1952d). It is known as the delayed rectifier since there is a marked delay between the onset of a depolarizing stimulus and the appearance of the current. The description rectifier is applied since the channel appears to pass current more easily in the outward direction in much the same way as a semiconductor diode. The channel conductance measured when the current is flowing in the reverse direction (ie. inward) is lower than when passing in the usual direction. The reversal of current is achieved simply by reversal of the potential difference applied to the membrane so as to create a voltage gradient favourable for potassium ions to flow into the cell.

Before describing the derivation of the model for $I_K$ recorded in the oxytocin-secreting cell, it may be useful to describe other models for similar currents that have been recorded from other cell types.

## MODEL DUE TO SMITH

In his 1978 Doctoral Thesis (Smith 1978) Smith describes a model derived from data recorded from molluscan neurones. The model of the delayed potassium current is reproduced here.

$$g_K = \bar{g}_K \, m_K^2(V,t) \quad . . . . . (6.1)$$

$$\tau_{mk}(V) \frac{dm_k(V,t)}{dt} + m_k(V,t) = m_k(V,\infty) \quad . . . . . (6.2)$$

$$\tau_{mk}(V) = \frac{32}{1+\exp((V+18)/4.5)} + 15 \quad . . . . . (6.3)$$

$$m_K^2(V,\infty) = \left\{ \frac{1}{1+\exp((V-V_0)/-14)} \right\}^{2\phi} \quad . . . . . (6.4)$$

Where $V_0$ is -27.6mV, $E_K$ = -52mV, $\phi_K$ = 2.3

This current shows a marked outward rectification.

The threshold for activation of $I_K$ was observed to be about -40mV which is approximately 20mV above the normal resting potential of the cell. The time course of activation is sigmoidal and the maximum current was maintained during voltage steps of less than 300ms duration.

The voltage-clamp recordings were whole-cell recordings and the mean maximum conductance for the channel population recorded at a potential of +30mV was found to be 4.9nS.

The conductance was found to be voltage-dependent as was the time constant for activation of the conductance. At a potential of -30mV the activation time constant was 4.5ms and declined exponentially with voltage to a value of 1.8ms at +50mV. This means that not only does the conductance become greater at greater depolarizations but it also activates more rapidly.

The standard potassium channel blocking agents, tetraethylammonium ions (TEA) and 4-aminopyridine (4-AP), reduced the observed current. This is a way of identifying the type of channel since these blocking agents appear to be fairly channel specific. TEA is known to be a specific potassium channel blocker. The channel kinetics were unaltered.

In order to record $I_K$ in isolation a holding potential of -60mV was used in conjunction with a calcium free bathing medium.

The delayed rectifier is described using a set of

equations similar to those used by Hodgkin and Huxley (1952d).

$$I_K = \bar{g}_K n^3 (V-V_K) \quad \ldots\ldots\ldots\ldots\ldots\ldots\ldots\ldots (6.5)$$

Where $\bar{g}_K$ is the maximum observed conductance

V is the membrane voltage

$V_K$ is the reversal potential for the potassium current

n is the activation variable.

Hodgkin and Huxley used an exponent of 4 for the activation variable to describe the change in conductance whereas Cobbett et al (1989) found that a better fit to the experimental data was obtained by using an exponent of 3.

$V_K$ , the reversal potential for the potassium current was found to be -83mV from experiments on the tail currents recorded when the clamp voltage was stepped to voltages more negative than the holding potential. At these large negative voltages the direction of the current reverses. Changes in potassium ion concentration in the external bathing medium provoked shifts in the reversal potential in accordance with the changes predicted by the Nernst equation.

To complete the mathematical model of the delayed rectifier current the voltage dependence of the activation parameter n needs to be found. Two equations relating the rate of change of activation to the membrane potential are needed. Following the procedure expounded by Hodgkin and Huxley these two equations may be written :-

$$n_\infty = \frac{\alpha_n(V)}{\alpha_n(V)+\beta_n(V)} \quad \ldots\ldots\ldots\ldots\ldots\ldots\ldots\ldots \quad (6.6)$$

$$\tau_n = \frac{1}{\alpha_n + \beta_n} \quad \ldots\ldots\ldots\ldots\ldots\ldots\ldots\ldots \quad (6.7)$$

The variable $n_\infty$ is the value that the activation variable n attains after a long duration pulse. So for a set of current recordings a graph of values of $g_{K\infty}$ versus voltage may be constructed. By using the relationship

$$g_K = \bar{g}_K\, n^3 \quad \ldots\ldots\ldots\ldots\ldots\ldots\ldots\ldots \quad (6.8)$$

values of $n_\infty$ at particular voltages may be found.

$$n_\infty = \frac{g_{K\infty}}{g_K} \quad \ldots\ldots\ldots\ldots\ldots\ldots\ldots\ldots \quad (6.9)$$

By recording values of time constant at various voltages and by using equations 2 and 3 the rate variables $\alpha_n$ and $\beta_n$ may be derived. The results of a curve-fitting procedure that yields the rate variables is shown in Figure 6.1. (See Page 62 Chapter 3 for description of fitting routine.) Additional equations used to derive the expressions used are as given below.

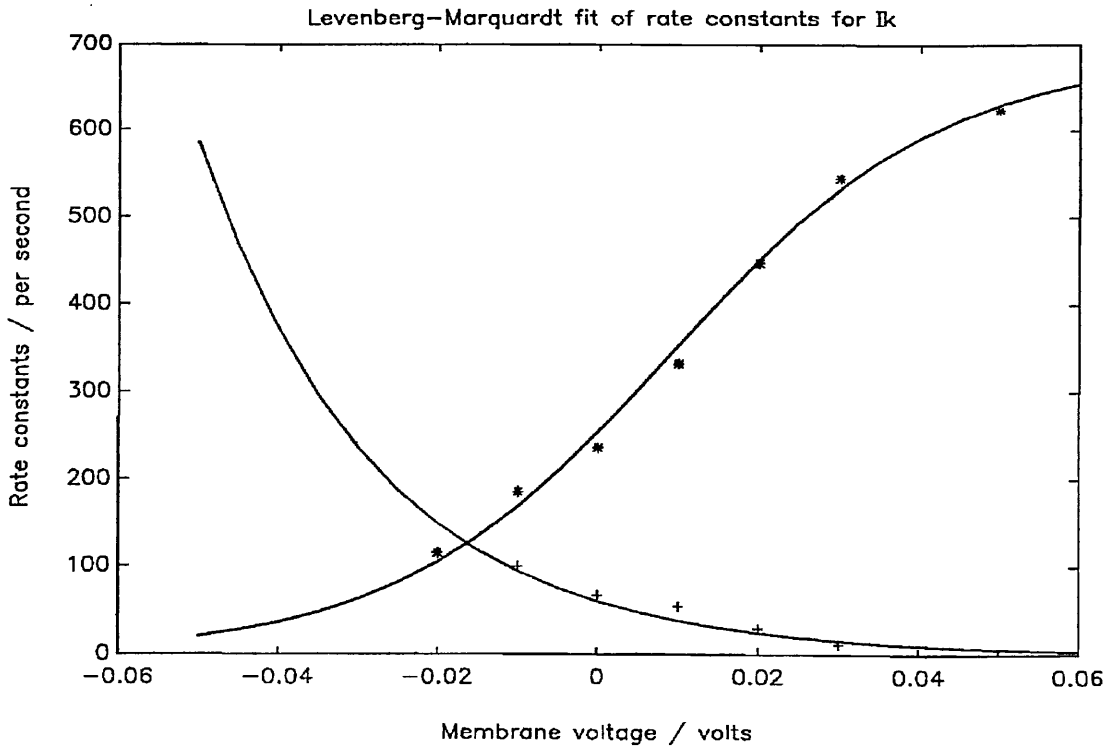


**Figure 6.1**

Graph showing alpha and beta data points and smooth curve fitted to them.

$$\alpha_n(V) = \frac{n_\infty(V)}{\tau_n(V)} \quad \ldots\ldots\ldots\ldots\ldots\ldots \quad (6.10)$$

$$\beta_n(V) = \frac{1 - n_\infty(V)}{\tau_n(V)} \quad \ldots\ldots\ldots\ldots\ldots\ldots \quad (6.11)$$

These functions and the differential equation for n as described in Hodgkin and Huxley's (1952d) model are used to describe the behaviour of the delayed rectifier potassium current. In order to check that the equations do indeed give results that match up with the experimental results a trial simulation of a voltage-clamp experiment was performed and

the graphical output from the simulations are shown in Figures 6.2. to 6.4. The simulations perform numerical integration of the differential equations used to model the potassium current for various given initial conditions (equivalent to stepping the clamp voltage) and presents the results in the form of a sequence of superimposed current traces.

The functions that were obtained by fitting curves to the data points as given are as shown below.

$$\alpha_n = \frac{600.0}{[\exp(-60V) + 1]} \quad . . . . . \quad (6.12)$$

$$\beta_n = 30.0\exp(-V/0.02) \quad . . . . . \quad (6.13)$$

The computer simulation of the voltage-clamp experiments yield current versus time traces that may be described by the equation :-

$$I_K(t) = \bar{g}_K\{n_\infty - (n_\infty - n_0)\exp[-(\alpha_n + \beta_n)t]\}^3 (V-V_K) \quad . . . \quad (6.14)$$

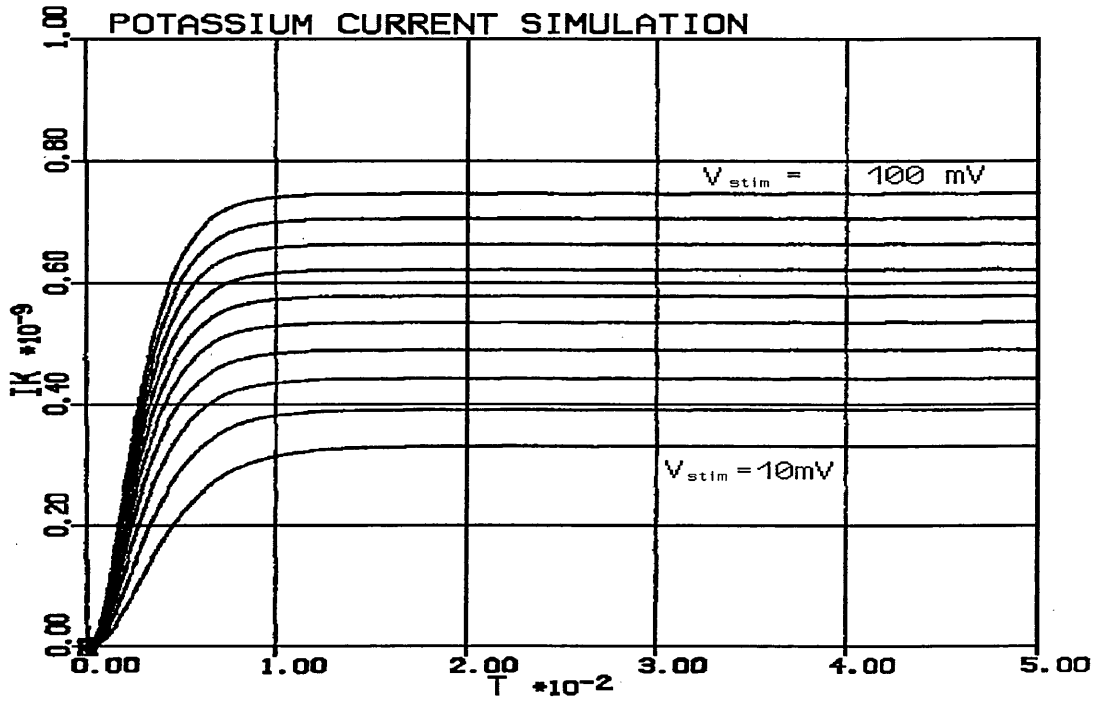


**Figure 6.2**

Result of simulation of voltage-clamp using potassium current model.

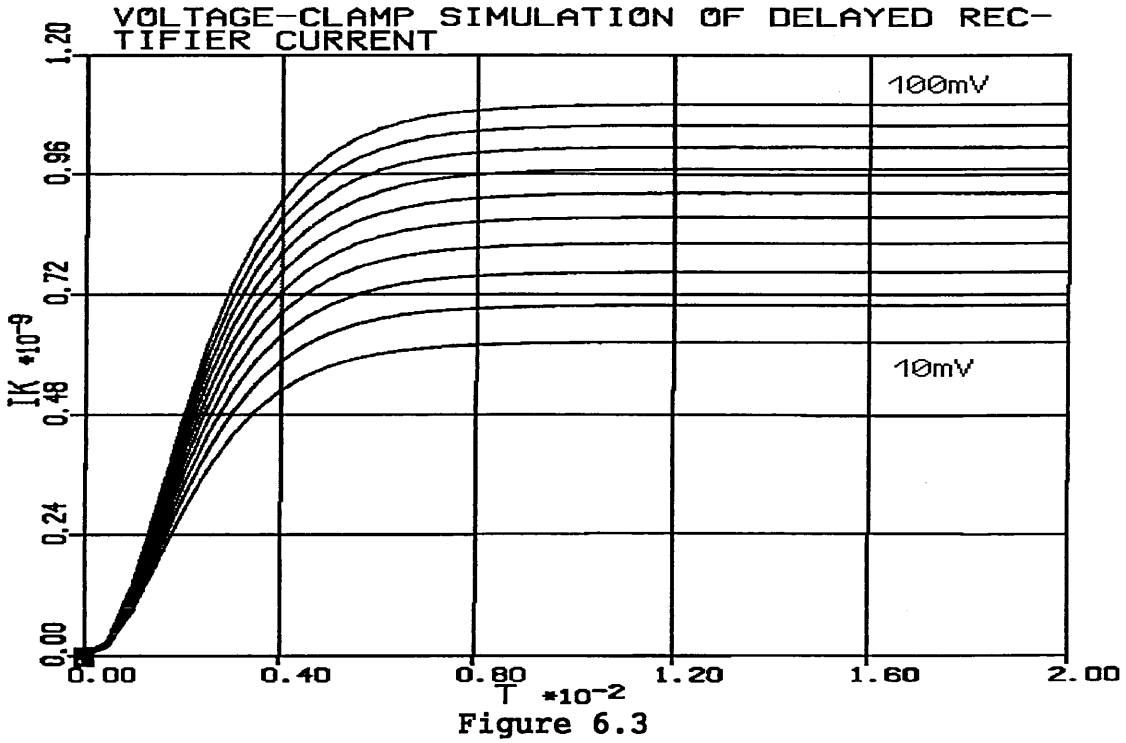


**Figure 6.3**

Results of voltage-clamp simulation on a shorter time scale.

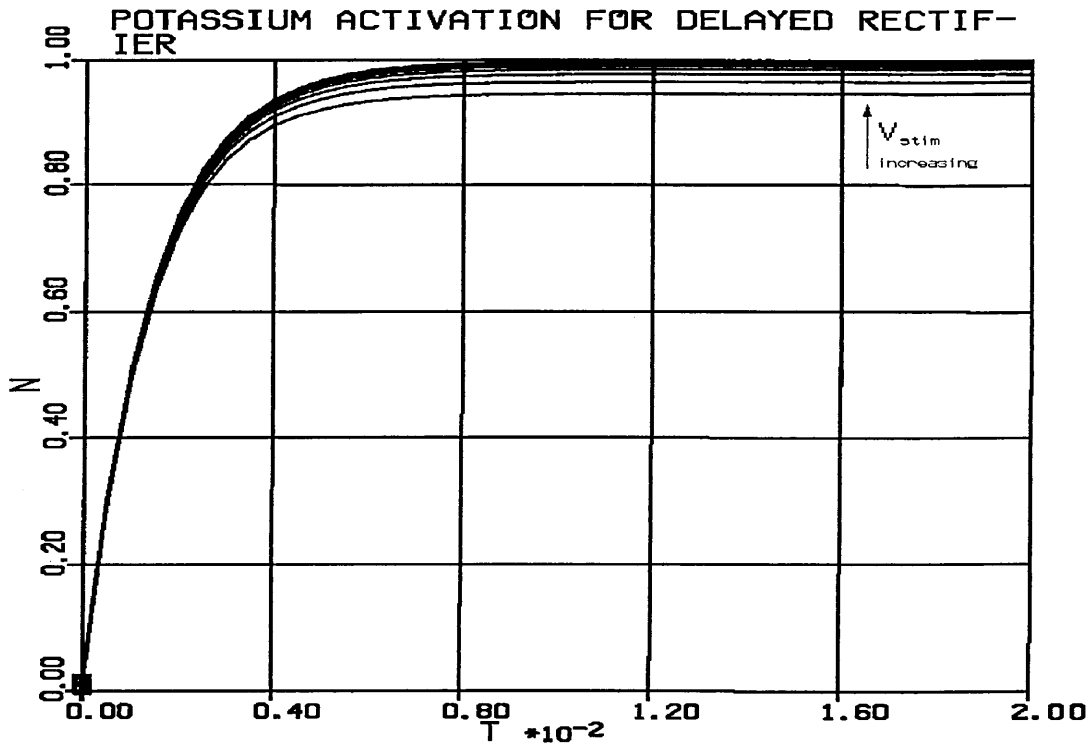


**Figure 6.4**

Graph showing the potassium activation variable during a voltage-clamp simulation.

Inspection of the results shown in Figure 6.2 show a good fit with the experimental data published by Cobbett et al. (1989) in terms of the maximum amplitude and the time course. As a result of the closeness of fit it may be assumed that the equations used do describe the time and voltage behaviour of the observed delayed rectifier current and those equations may be used with confidence in a model of the electrical behaviour of the cell as a whole. It should be noted that the currents in the graphs have units of amperes and time is given in seconds.

The program used to simulate this current is to be found in the Appendix as PROGRAM IKOXY.

## MODELLING THE TRANSIENT POTASSIUM CURRENT $I_A$

Transient potassium currents have been observed in a large number of cells ( Hille B. (1984); Smith S. J. (1978); Connor & Stevens 1971; Bevan & Raff 1985; Cobbett, Legendre & Mason 1989; Thompson 1977; Cooper & Shrier 1985; Belluzzi, Sacchi & Wanke 1985; Champagnat, Jacquin & Richter 1986.) and are thought to increase the interspike intervals of repetitively firing neurones by cancelling out some of the applied stimulus current immediately following the hyperpolarization of the cell after an action potential. Transient potassium currents are described using an activation and an inactivation parameter in a similar manner to sodium currents.

Under the experimental conditions described by Cobbett et al. (1989) which were voltage-clamp experiments on dissociated cell cultures of supraoptic neurones from neonatal rats, bathed in sodium and calcium free media, the current trace following a voltage step from -100mV to 0mV is qualitatively different from a current trace elicited by a voltage step from -60mV to 0mV.

By finding the difference current between the two traces the transient potassium current $I_A$ may be recorded. The current trace obtained by subtraction of the current recorded from a holding potential of -60mV from the current recorded from a holding potential of -100mV is not a true record of the transient potassium current due to contamination from $I_K$ but this has been ignored in the analysis. Pharmacological methods of separating the two currents are not completely successful either. This is due to the fact that the delayed

rectifier current and the transient current are both carried by potassium ions. It appears that the transient current flows through a different type of ionic channel and does not represent a different gating mechanism for $I_K$ or other potassium channels. Blocking agents that prevent current flow through delayed rectifier channels also block the so-called A channels. At present then, imperfect separation of the delayed rectifier and transient potassium current is a restriction on the modelling of the two currents but is an experimental reality. Experimental results were obtained as stated above from sodium - and calcium - free external bathing solutions so it may be assumed that there is no contamination from other sources.

The maximum whole-cell conductance was found to be 5.9 nS ± 1.6 nS (mean ± s.e.m.). The large size of the maximum conductance compared with the maximum conductance of the $I_K$ channels suggests that the transient potassium current is significant in determining the overall behaviour of the oxytocin-secreting neurone. Since the current is carried by potassium ions it is an outward current and therefore has the effect of hyperpolarizing or repolarizing the cell membrane.

A series of voltage-clamp experiments on the cell yielded a family of current records that showed the behaviour of the transient potassium current. The current appears to activate with sigmoidal rise and inactivates following a simple exponential fall. The authors of the paper (Cobbett et al. (1989)) suggest that the kinetic behaviour of the current may be described according to an equation proposed by Connor and Stevens. (Connor J. A. and Stevens C. F. 1971).

$$I_A = g_A\, a^n\, b(V-V_K) \quad \ldots\ldots\ldots\ldots\ldots\ldots \quad (6.15)$$

The exponent n was found to be 4 by plotting :-

$$\ln\left\{K - \left[\frac{I_A}{(K \exp\{-t/\tau_B\})}\right]\right\} \quad \ldots\ldots\ldots\ldots\ldots \quad (6.16)$$

against t for different values of n. K in the above equation is a scaling factor.

The situation is complicated by the fact that the single exponential used to describe the decaying phase of the current does not apply for potentials of +20mV and above. (See Cobbett et al 1989) This should not pose a serious problem since the normal action potential does not exceed this value. ( Membrane resting potential ≈ -60mV and normal spike amplitude ≈70mV .)

The complete transient outward current may thus be described by the equation :-

$$I_A(t) = K[1 - \exp(-t/\tau_A)]^4 \exp(-t/\tau_B) \quad \ldots\ldots\ldots \quad (6.17)$$

Activation ($\tau_A$) and inactivation ($\tau_B$) time constants are found to be voltage-dependent so it may be assumed that the use of voltage-dependent rate "constants" is appropriate.

$$\tau_A = \frac{1}{\alpha_A(V) + \beta_A(V)} \quad \ldots\ldots\ldots\ldots\ldots\ldots \quad (6.18)$$

$$\tau_B = \frac{1}{(\alpha_B + \beta_B)} \quad \ldots\ldots\ldots\ldots\ldots\ldots \quad (6.19)$$

Plots of $\tau_A$ and $\tau_B$ versus voltage are given in Cobbett et al. (1989) but no data is given on the steady-state values of the activation ($a_\infty$) and inactivation ($b_\infty$) parameters as a function of voltage. This means that Equations (6.6) and (6.7) may not be used to find the functions for $\alpha_A(V)$ , $\beta_A(V)$, $\alpha_B(V)$ and $\beta_B(V)$. The functions for the $\alpha$'s and $\beta$'s are constrained such that they satisfy equations (6.14) and (6.15) but apart from that there is a choice as to the exact form and numerical values that constitute the functions. This means that there is no unique description of the rate functions given the available data.

The activation and inactivation time constants have different ranges of values. The activation process is faster than the inactivation process with a range from 2.1 ms to 0.5 ms over the voltage range -40mV to +40mV. This range does not include the normal resting potential of the membrane which limits the accuracy of the modelling equations. This may be important since the A current activates with a threshold close to the resting potential of -60mV. In the absence of this data the curves used to fit the data available are merely extrapolated to cover the full voltage range of

normally firing cells.

With all this in mind the following functions have been found to fit the available data.

$$\alpha_A = \frac{2200}{[\exp(2200(0.00008 - 0.025V)) + 1]} \quad . . . . . \quad (6.20)$$

$$\beta_A = 80\exp(-V/0.03) \quad . . . . . \quad (6.21)$$

$$\alpha_B = 26\exp(-V/0.076) \quad . . . . . \quad (6.22)$$

$$\beta_B = \frac{70}{[\exp(70(0.0017-0.85V)) + 1]} \quad . . . . . \quad (6.23)$$

Computer simulation of voltage-clamp experiments was again used to ensure that the simulated transient potassium current matched the experimentally recorded current closely. The results of a typical simulation are shown in Figure 6.5.

The ACSL listing for the program that simulates the transient potassium current is to be found in the Appendix and is called IKTRAN.

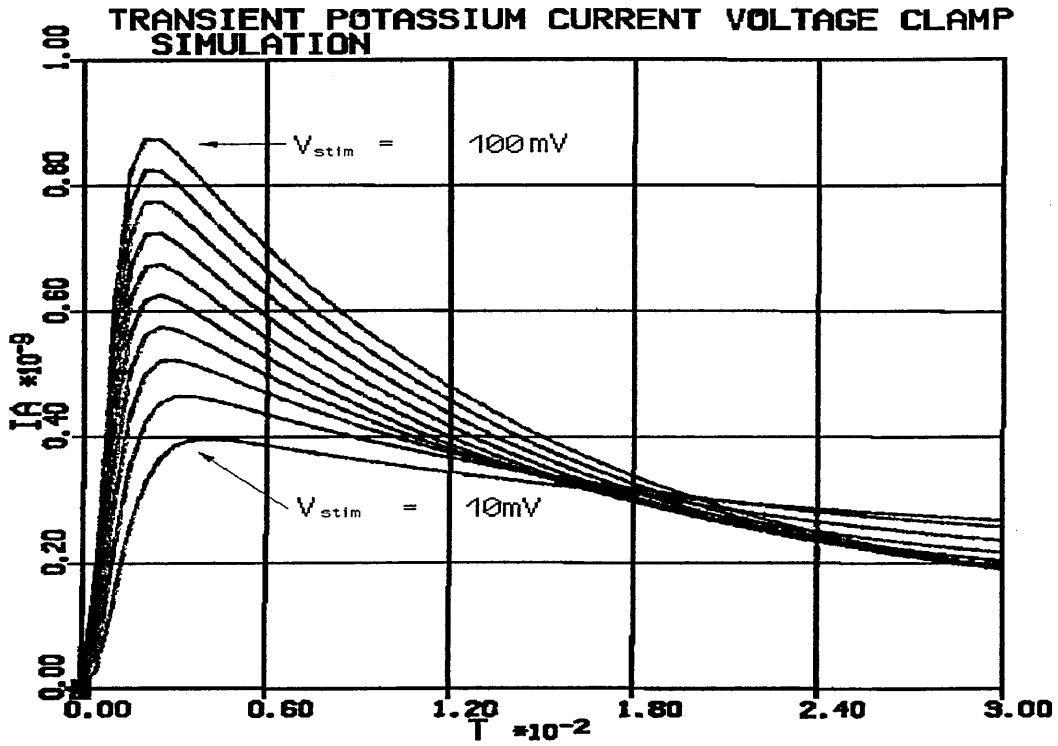


**Figure 6.5**

Results of simulation of voltage-clamp using the model derived for the transient potassium current.

## MODELLING THE CALCIUM - DEPENDENT POTASSIUM CURRENT $I_{K\text{-}Ca}$

The third type of potassium - selective channel is gated not by membrane voltage but rather by changes in the concentration of calcium ions on the inner surface of the membrane. Calcium-dependent potassium current has been recorded in a number of different cells and is thought to play a significant role in bursting behaviour. ( Hille 1984; Smith 1978; Meech 1978; Rinzel (pre publication communication); Cobbett, Legendre & Mason 1989; Belluzzi, Sacchi & Wanke 1985; Cobbett, Ingram & Mason 1987; Thompson 1977; Barrett, Magleby & Pallotta 1982; Pallotta 1985; Magleby & Pallotta 1983a; Magleby & Pallotta 1983b; Gorman & Thomas 1980; Hirst, Johnson & van Helden 1985; Maruyama,

Petersen, Flanagan & Pearson 1983; Adams, Constanti, Brown & Clark 1982; Schwarz & Passow 1983; Petersen & Maruyama 1984; Brown & Griffith 1983; Tanaka & Kuba 1987; Latorre, Coronado & Vergara 1984; Thomas 1984; Meech 1978; Quandt 1988; Bourque 1988; Brown & Higashida 1988; Cook & Haylett 1985; Marty & Neher 1985; Plant & Kim 1978).

The channel is not always insensitive to the membrane voltage however. Deriving a model for this current, usually denoted $I_{K(Ca)}$ , in the oxytocin-secreting cell is not straightforward since there is insufficient experimental data published by Cobbett et al. (1989) to follow the procedures that have been described so far. However, by making suitable assumptions and by using data published by other authors ( Plant & Kim 1978; Bourque 1988; Sherman, Rinzel & Keizer 1988 ), a model may be derived. The validity of the model may be checked by running simulations as with the other models and comparing the results with published data. If a good match with experimental results is not immediately forthcoming, then assuming the basic assumptions and the general model are sound then the model parameters may be "tuned" to produce results that more closely match the published data.

Smith (Smith 1978) describes a model for the calcium-gated potassium current in a molluscan neurone and this model is reproduced here.

MODEL DUE TO SMITH

$$\Delta I_C = \Delta P_C \frac{F^2 V}{RT} \frac{\gamma_K [K^+]_o - \gamma [K^+]_i \, e^{VF/RT}}{1 - \exp(VF/RT)} \quad \ldots\ldots\ldots\ldots \quad (6.24)$$

This equation relates the change in calcium-gated potassium current to changes in the channel permeability $P_C$. Simulated changes in calcium concentration closely follow changes in the current, which indicates that the channel is gated directly by calcium concentration at the inner surface of the membrane. The changes in $I_C$ are converted to corresponding changes in conductance by dividing by the potassium equilibrium potential. The data necessary to use this approach were not available so the calcium-gated potassium current has not been modelled for the oxytocin-secreting cell.

MODEL DUE TO PLANT AND KIM

Plant and Kim (Plant & Kim 1978) model changes in calcium concentration and the effects of those changes on the calcium-gated potassium channel using the following equations.

$$\frac{dc}{dt} = k_{in} \, x_T (V_{Ca} - V) - k_{out} \, c \quad \ldots\ldots\ldots\ldots \quad (6.25)$$

$$g_p = \frac{\bar{g}_p c}{(K_p + c)} \quad \ldots\ldots\ldots\ldots\ldots\ldots \quad (6.26)$$

The above model described by Plant and Kim was used in the model of the pancreatic ß cell derived by Sherman, Rinzel and Keizer (Sherman, Rinzel & Keizer 1988). Their equations are reproduced here.

$$g_{K\text{-}Ca}(Ca) = \bar{g}_{K\text{-}Ca} \frac{Ca_i}{K_d + Ca_i} \quad \ldots\ldots\ldots\ldots\ldots\ldots \quad (6.27)$$

$$\frac{dCa_i}{dt} = f(-\alpha I_{Ca} - k_{Ca} Ca_i) \quad \ldots\ldots\ldots\ldots\ldots\ldots \quad (6.28)$$

This model shows how the calcium-gated potassium conductance depends upon the concentration of intracellular free calcium. It also shows how the calcium current is responsible for the increase in intracellular free calcium. This model was used in the oxytocin cell model.

## SUMMARY

This chapter has described the various potassium currents known to be present in the oxytocin-secreting cell. Using data provided by Cobbett and co-workers, mathematical models of the delayed rectifier and transient potassium currents have been derived. A curve-fitting program written by the author was used to find the parameters of the fitting functions. The resulting model equations were then simulated on a computer in isolation before being included in the overall model for the cell. The simulation programs written in the ACSL modelling language are included in the Appendix.

# CHAPTER SEVEN

## CALCIUM CURRENTS

Calcium plays a very important rôle in cell processes and controls the exocytosis of neurosecretory granules at the axon end-terminals (Hille 1984; Maddrell & Nordmann 1979). Calcium ions are also important for controlling the gating of certain potassium-selective ionic channels as described earlier. Muscle contraction and regulation of various internal cell processes also involve calcium ions (Barish & Thompson 1983; Brink 1954; Carafoli & Penniston; Fox, Nowycky & Tsien 1987a; Gorman & Thomas 1980; Igusa & Miyazaki 1983; Matteson & Armstrong 1986). Calcium is also involved in the processes following egg fertilization (Igusa, Miyazaki & Yamashita 1983). In this respect calcium plays an important role as a second messenger in the cell. In fact it appears that calcium is one of the most biologically important inorganic ions.

In most cells calcium ions also contribute to the total ionic current in an excitable membrane during depolarization. Hodgkin and Huxley's original model of electrical excitability in squid giant axon did not include current due to calcium ions and the squid axon is a fairly simple system in this respect, since calcium currents have been found in most types of cell (Hille 1984). Extensions and modifications to the simple Hodgkin-Huxley model have included the effect of extracellular calcium concentration on the excitability of the membrane (Huxley 1959). Most of the calcium ions within a cell are not free to move around but are held in a bound

form by calcium chelating molecules such as calmodulin. The mitochondria in the cell are also responsible for some of the uptake of calcium (Meech 1974). The concentration of free intracellular calcium is estimated to be between 10nM and 100nM (Gorman & Thomas 1978; Llinás, Steinberg & Walton 1981). In contrast, the extracellular medium contains a significant concentration of free calcium. This creates a Nernst potential $E_{Ca}$ that is larger than the sodium Nernst potential and of the same polarity. Taking figures of 10nM for the intracellular free calcium concentration and 10mM as the extracellular calcium concentration, Hille (Hille 1984 Ch.4) calculates the calcium Nernst potential as +175 mV. In fact, calcium current reversal potentials of this size are not recorded due to the size of the current being unresolvable before this voltage is reached (Adams & Gage 1979; Sánchez & Stefani 1983). This makes the measurement of the calcium equilibrium potential or reversal potential difficult if not impossible using present techniques (Sánchez & Stefani 1983; Kay & Wong 1987). Estimation of the reversal potential by extrapolation of the conductance curve is unreliable due to the way the curve becomes asymptotic to the axis and by the rectifying properties of the calcium channel (Akaike, Lee & Brown 1978; Kay & Wong 1983; Llinás, Steinberg & Walton 1981). Estimates and measurements of calcium potentials taken from various authors are:- +150mV (Sánchez & Stefani 1983 although they measured an apparent reversal potential of only +40mV) , +85mV by extrapolation (Hencek & Zachar 1977), +40mV to +150mv by extrapolation (Hirst, Johnson & van Helden 1985), +139mV (Gorman & Thomas 1980),

+50mV (Standen 1974), +103.7mV (Atwater, Dawson Eddlestone & Rojas 1981), +115mV by extrapolation (Llinás, Steinberg & Walton 1981), +168mV (Akaike, Lee & Brown 1978), +64mV (Adams & Gage 1979) and +130mV (Smith 1978). Internal buffering of calcium ions coupled with active extrusion of calcium from the cell maintains this low internal concentration (Barish & Thompson 1983). The efflux of calcium from the cell is linked with sodium influx (Glitsch, Reuter & Scholz 1970; Meech 1974; Hille 1984). This process is complicated by dependence upon sodium and calcium concentrations and will not be discussed further.

The study of calcium currents is complicated by the diversity of effects that calcium ions have both inside and outside the cell. For instance, not only does an increase in intracellular free calcium ion concentration activate a potassium current ($I_{K(Ca)}$), but also serves to inactivate calcium channels (Hille 1984; Bourque, Brown & Renaud 1986). This makes recording and analyzing calcium currents more difficult than other currents. In addition to this, calcium currents often occur in highly infolded cell membranes which makes the establishment of a good voltage clamp difficult (Hille 1984; Sánchez & Stefani 1983). Even when a good voltage clamp has been established, recording is difficult due to the small size of calcium currents and the possibility of contamination with other currents. There is also evidence that the distribution of calcium ions around the cell membrane is not uniform and that the dendrites are sites of a concentration of calcium channels (Mason & Leng 1984). One of the objectives when recording membrane currents is to

achieve a spatially uniform clamp voltage. The presence of large numbers of calcium channels in the dendrites makes this much more difficult (Kay & Wong 1987).

Another complication is the diversity of calcium channels that have been recorded. Calcium channels may be slow or fast, inactivating or non-inactivating. A slow and a fast current were recorded in chick dorsal root ganglion neurones by Fedulova, Kostyuk and Veselovsky (Fedulova, Kostyuk & Veselovsky 1985). The fast current inactivated rapidly and monoexponentially while the slow current inactivated only slowly with two time constants of inactivation. A single fairly rapidly activating and inactivating current is described by Hencek and Zachar (Hencek & Zachar 1977). A slow calcium current in frog motoneurones is reported by Barrett and Barrett (Barrett & Barrett 1976). A slowly activating and inactivating current in frog twitch muscle fibres was recorded by Sánchez and Stefani (Sánchez & Stefani 1983). Belluzzi, Sacchi and Wanke (Belluzzi, Sacchi & Wanke 1985) recorded a calcium current that activated rapidly and inactivated with two voltage-independent time constants, one fast and one slow. A slowly activating and inactivating calcium current was recorded in an *Aplysia* neurone by Adams and Gage (Adams & Gage 1979). Brown and Griffith (Brown & Griffith 1983) recorded a slowly activating, persistent calcium current in hippocampal neurones of the guinea-pig. A calcium component to the action potential spike in rat supraoptic neurones was reported by Bourque and Renaud (Bourque & Renaud 1985). Geduldig and Junge (Geduldig & Junge 1968) reported a calcium action potential similar to the

normal action potential in *Aplysia* giant neurone. The sodium component was either blocked by the addition of tetrodotoxin or by recording in sodium free solution. A rapidly activating and inactivating calcium current was recorded in *Helix* neurone by Akaike, Lee and Brown (Akaike, Lee & Brown 1978). Three distinct calcium channels were reported in chick sensory neurones by Fox, Nowycky and Tsien (Fox, Nowycky & Tsien 1987 a,b). One current activated rapidly and showed little inactivation, another activated and inactivated rapidly and the third activated rapidly but decayed slowly. In terms of single channel properties, the channels could be distinguished on the basis of single channel conductance, mean open time distribution and voltage dependence. These three channel types were given the designations T, L and N. Two currents were recorded in rat sensory neurones by Bossu, Feltz and Thomann (Bossu, Feltz & Thomann 1985), one persistent and a second which displayed inactivation. Matteson and Armstrong (Matteson & Armstrong 1986) describe two calcium currents in clonal pituitary cells, one which displays inactivation and the other which does not. Two currents, both of which inactivate but one more slowly than the other, were reported by Cobbett, Ingram and Mason (Cobbett, Ingram & Mason 1987). Standen (Standen 1975) describes a fairly rapidly activating and inactivating calcium current in snail neurones. Kramer and Zucker (Kramer & Zucker 1985a,b) note the presence of a calcium-inactivated calcium current in *Aplysia* neurones. A calcium current with two phases of inactivation, fast and slow, is described by Hirst, Johnson and van Helden (Hirst, Johnson & van Helden

1985). The squid giant synapse displays a calcium current with slow activation and little fast inactivation (Llinás, Steinberg & Walton 1981).

Calcium channels are blocked by transition ion metal ions such as manganese, nickel, cobalt and cadmium (Hille 1984). Organic channel blockers specific to calcium also include verapamil, nifedipine, methoxyverapamil (D-600) and D890 (Walden & Speckman 1987; Hille 1984). The dihydropyridine derivative BAY K 8644 acts as an agonist in low concentrations but in higher concentrations reduces calcium current (Walden & Speckmann 1987). A useful agent in the study of calcium currents is the barium ion. This substitutes well for calcium in carrying current through calcium channels and gives rise to faster, larger and more prolonged currents (Bourque, Brown & Renaud 1986). Barium, however does not substitute well for calcium in the inactivation of calcium channels or in activation of the $I_{K(Ca)}$ channel, which are apparently more specific to calcium (Bourque,Brown & Renaud 1986). This is an advantage since the current being recorded will not be contaminated by the potassium current and the current being carried through the calcium channels will be larger and therefore easier to resolve due to the lack of inactivation.

Calcium channels appear to have the property of inward rectification ie. calcium ions flow in through the channels but not out, even when the driving voltage is increased beyond the calcium reversal voltage (Kay & Wong 1987; Tsien 1983).

The influx, diffusion and accumulation of free calcium

in the cytoplasm is treated by Smith (Smith 1978) and Gorman and Thomas (Gorman & Thomas 1980) who derive partial differential equations to describe the process. Gorman and Thomas give an expression for calculating the calcium concentration at any time and any radial distance by assuming spherical geometry and a constant rate of calcium influx. Smith's model was modified slightly to take account of additional calcium binding sites by Barish and Thompson (Barish & Thompson 1983). These diffusion models are based upon a spherical cell having radial symmetry. The effects of calcium accumulation and diffusion have not been addressed in this study due to the additional complexity of introducing computer code to solve partial differential equations into ACSL models. The integration routines in ACSL are only able to integrate with respect to one variable. The diffusion problem requires stepping forward in three spatial dimensions and time. This is beyond the capability of ACSL as it stands. However, it is possible to call FORTRAN subroutines from within an ACSL program. It is therefore possible to write code to solve the diffusion equation (using a Crank-Nicholson or other appropriate algorithm) and call the routine at every time step or communication interval, but it would not be a trivial task to implement such a scheme. According to Hille (Hille 1984), diffusion of calcium throughout a 300μm diameter cell takes longer than 300ms. This is long compared to the time taken for calcium influx to occur during an action potential. Because of the finite time taken for calcium ions to diffuse throughout the cytoplasm, the internal free calcium concentration will not be uniform

during periods of influx. The calcium concentration just inside the cell membrane will be higher than in the bulk cytoplasm. In fact, the concentration of free calcium close to the inner membrane surface is estimated to be approximately 15.5μM according to Glitsch, Reuter & Scholz (Glitsch, Reuter & Scholz 1970), (c.f. 10-100 nM in the bulk cytoplasm). The modulating effect that calcium ions have on various membrane components such as calcium channels themselves and calcium-gated potassium channels will be determined by the concentration just inside the membrane (Meech 1974). This makes any attempt at relating bulk calcium concentration measurements such as those obtained using aequorin or arsenazo III to gating of these channels, difficult (Gorman & Thomas 1980).

Calcium ions are also observed to have a stabilizing effect upon the membrane potential (Brink 1954; Frankenhaeuser & Hodgkin 1957; Huxley 1959). Frankenhaeuser and Hodgkin (Frankenhaeuser & Hodgkin 1957) note that the voltage dependence of sodium and potassium activation and inactivation functions is shifted along the axis in a depolarizing direction as extracellular calcium concentration is decreased. Their results are summarised and given a mathematical expression by Huxley (Huxley 1959), reproduced here as equation 7.1. The same effect is noted in *Helix* neurones by Standen (Standen 1975).

$$\Delta V = k \, Ln([Ca]/[Ca]_n) \quad . . . . . (7.1)$$

Where $\Delta V$ is the change in membrane voltage and $[Ca]_n$ is the normal extracellular calcium concentration and Ln denotes the natural logarithm.

The rôle of calcium ions in bursting behaviour is discussed by several authors and some of the essential points will be discussed here. As noted previously, calcium-gated potassium currents are observed in cells that display bursting behaviour and appear to be responsible for the post-burst hyperpolarization. No system displaying bursting behaviour without this channel has come to the author's attention. (Calcium-gated potassium currents are also responsible for the hyperpolarizing response of hamster eggs to calcium injection, Igusa & Miyazaki 1983.) Evidence for this comes from replacement of calcium by barium which removes the hyperpolarizing after-potential (Bourque, Brown & Renaud 1986). It seems, then, that as calcium accumulates during a burst of action potentials due to voltage-dependent opening of calcium channels, more and more calcium-gated potassium channels open. This leads to an increase in the outward currents which eventually overcome the membrane depolarization and cause the burst to terminate. These potassium currents decrease during the inter-burst interval as calcium is removed and eventually the membrane depolarizes sufficiently for another burst to start.

As noted above, calcium currents are difficult to record and difficult to analyse for various reasons. However, various workers have attempted to characterize and describe them. Hodgkin and Huxley's formalism is still a popular way of doing this, although consideration of the details of the current show that a Hodgkin-Huxley model is not adequate in certain instances (Brown, Tsuda & Wilson 1983). There is a certain amount of doubt as to whether calcium currents display inactivation in the same way that sodium currents do or if the inactivation observed is soley due to the effects of the increased concentration of calcium ions themselves. Calcium activation has been described by an "m" variable raised to the first power (Akaike, Lee & Brown 1978), second power (Byerly, Chase & Stimers 1984; Brown, Tsuda & Wilson 1983; Fedulova, Kostyuk & Veselovsky 1983; Kay & Wong 1987), the third power (Sánchez & Stefani 1983), the fourth power (Belluzzi, Sacchi & Wanke 1985) or to the sixth power (Llinás, Steinberg & Walton 1981; Hencek & Zachar 1977). An exponent of 1 or 2 was needed to describe calcium activation at different potentials in experiments performed by Adams and Gage (Adams & Gage 1979) and the results of Llinás, Steinberg & Walton do not distinguish well between the fifth and sixth powers.

Close examination of the inactivation of calcium current shows that it has two separate phases (Hirst, Johnson & van Helden 1985; Cobbett, Ingram & Mason 1987)

In the absence of detailed data on the calcium currents in the oxytocin-secreting neurone it was necessary to

incorporate a model from a different source. The model derived by Hencek and Zachar (Hencek & Zachar 1977) is complete in terms of giving all the equations and model parameters necessary to reproduce their results, and as such, the equations they used were coded into an ACSL program and used in simulations. The curves derived for the activation and inactivation rate constants are shown plotted against voltage in Figures 7.1 and 7.2. The variation of the steady state activation and inactivation with voltage are shown in Figure 7.3. Activation and inactivation time constants as a function of voltage are shown in Figure 7.4.

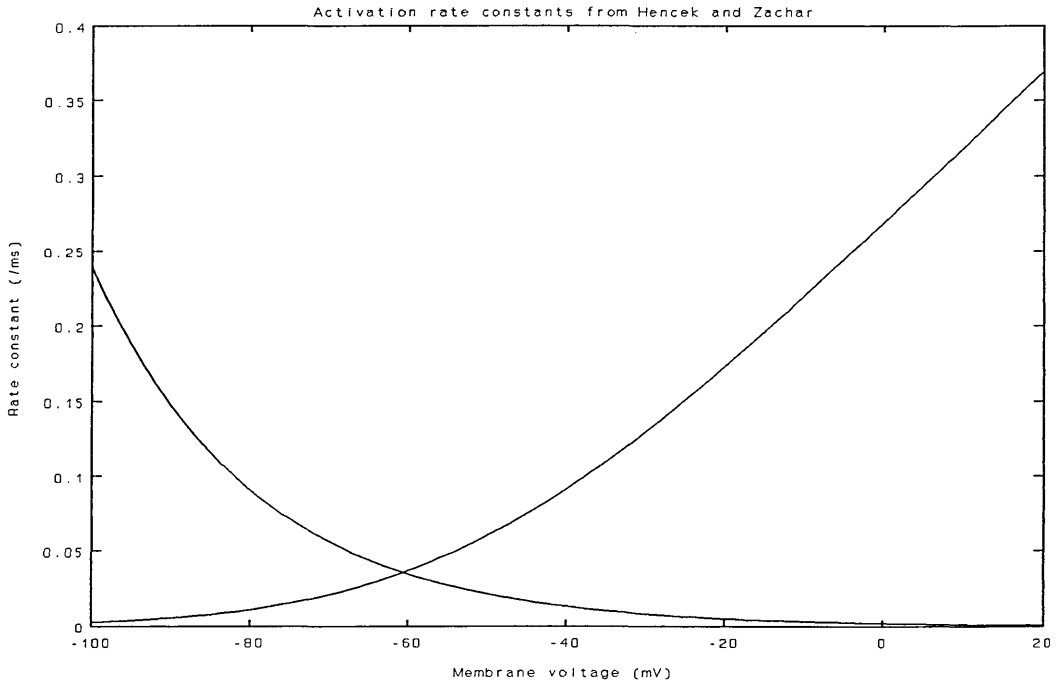


**Figure 7.1**
Graph showing the voltage dependence of the activation rate constants from Hencek and Zachar's calcium current model.

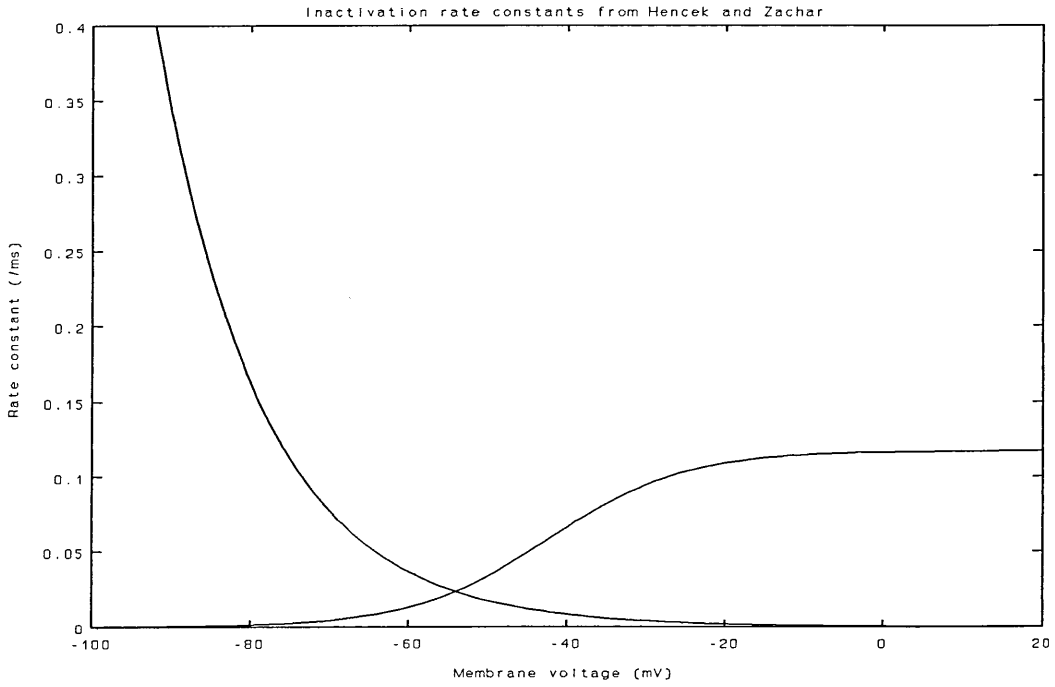


**Figure 7.2**
Graph showing the voltage dependence of the inactivation rate constants derived by Hencek and Zachar.

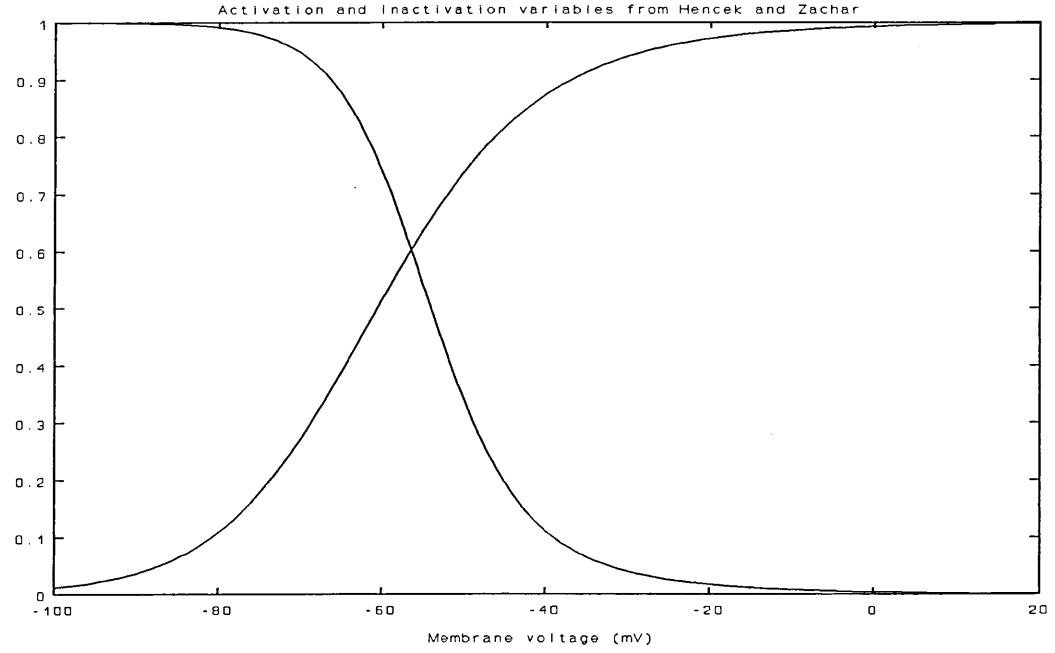


**Figure 7.3**
Graph showing the voltage dependence of the steady-state activation and inactivation in Hencek and Zachar's model.

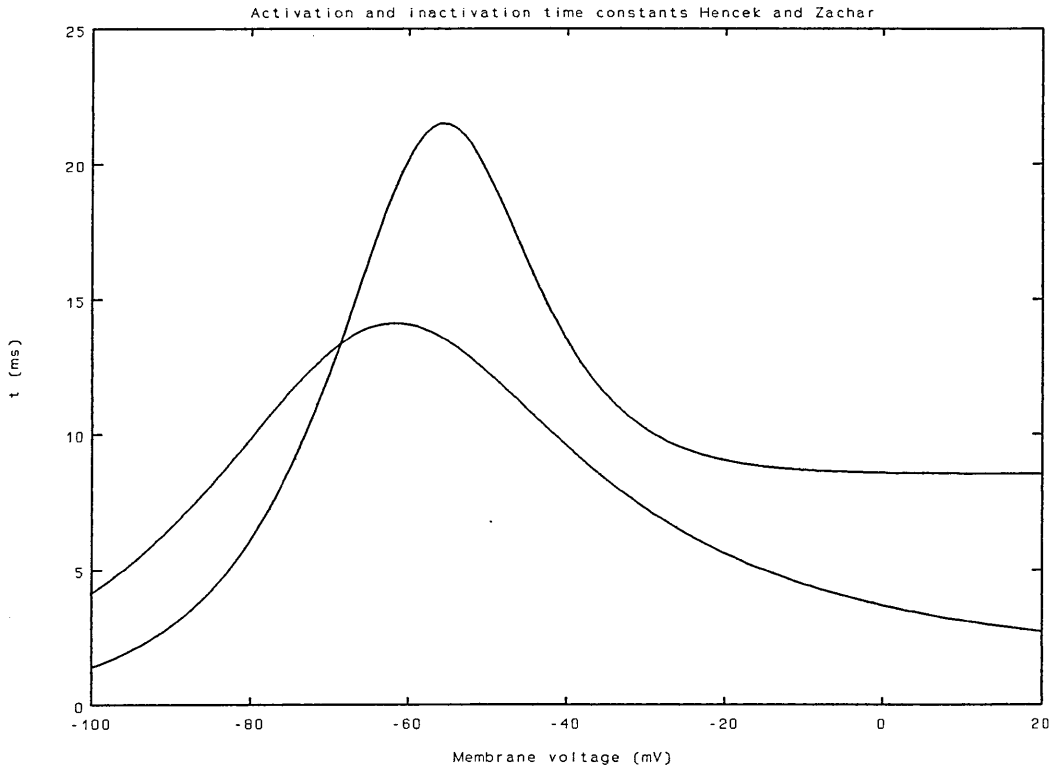


**Figure 7.4**
Graph showing the variation with voltage of the calcium activation and inactivation time constants. Hencek and Zachar's model.

$$I_{Ca} = \bar{g}_{Ca}\, m^6 h( V - V_{Ca} ) \quad . . . . . (7.2)$$

$$\alpha_m(V) = \frac{\bar{\alpha}_m ( V - \bar{V}_m )}{[1-\exp[-(V-\bar{V}_m)/\varepsilon_{\alpha,m}]]} \quad . . . . . (7.3)$$

$$\beta_m(V) = \bar{\beta}_m \exp[-(V-\bar{V}_m)/\varepsilon_{\beta,m}] \quad . . . . . (7.4)$$

$$\alpha_h(V) = \bar{\alpha}_h \exp[-(V-\bar{V}_h)/\varepsilon_{\alpha,h}] \quad . . . . . (7.5)$$

$$\beta_h(V) = \frac{\bar{\beta}_h}{[1+\exp[-(V-\bar{V}_h)/\varepsilon_{\beta,h}]]} \quad . . . . . (7.6)$$

TABLE 7.1

MODEL PARAMETERS

| | |
|---|---|
| $\bar{\alpha}_m = 0.0051 ms^{-1}$ | $\beta_m = 0.024 ms^{-1}$ |
| $\bar{V}_m = 52.45 mV$ | $\varepsilon_{\alpha,m} = 10.5 mV$ |
| $\varepsilon_{\beta,m} = 20.7 mV$ | |
| $\bar{\alpha}_h = 0.0097 ms^{-1}$ | $\beta_h = 0.117 ms^{-1}$ |
| $\bar{V}_h = -42.2 mV$ | $\varepsilon_{\alpha,h} = 13.4 mV$ |
| $\varepsilon_{\beta,h} = 8.54 mV$ | |
| $\bar{g}_{Ca} = 15.0 mS cm^{-2}$ | $V'_{Ca} = 84.9 mV$ |

$V'_{Ca}$ as given here is the reversal potential for the calcium current obtained by extrapolation of the conductance graph. This value may differ significantly from the Nernst or equilibrium potential as determined by considering the relative concentrations of calcium ions inside and outside the cell. Measurement of $E_{Ca}$ is difficult as outlined earlier in this chapter. Because of this, the value may need some adjustment to obtain the amplitude of peak current that is experimentally observed.

The results of the simulation of calcium current using the above model with the parameters in Table 7.1 are given in Figures 7.5 to 7.8. Time is measured in milliseconds and current in $mA/cm^2$. The actual ACSL model appears in the appendix as HENZAK. The results are for voltage-clamp simulations and as can be seen from Figure 7.5 there is a clear discrepancy between the simulated current and the current recorded experimentally by Hencek and Zachar. The simulated current shows no inactivation. The model derived by Hencek and Zachar was examined carefully and the equations given for the $\alpha$ and ß functions do appear to fit the data as shown in their paper. The activation and inactivation variables as plotted against voltage in Figure 7.3 also appear reasonable and were derived from the model equations shown above. The simulated holding potential was -80mV as this is given as the membrane resting potential of the cell. Depolarizing stimuli of 20mV to 100mV were used to simulate the experimental conditions. Comparison of the activation (Fig. 7.6) and inactivation (Fig. 7.8) show that inactivation occurs faster than activation. The activation and inactivation time

constants as a function of voltage in Figure 7.4 show that over the voltage range of interest, the inactivation time constant is larger than the activation time constant apart from a small region at the most polarized end of the graph where the reverse is true. This should be the situation, since Table 1 (Hencek & Zachar 1977) clearly shows the inactivation time constant to be larger than at all voltages. Close inspection of Figure 7.4 here and Table 1 in Hencek and Zachar's paper shows that time constants read from the graph in Figure 7.4 do not match well with the values shown in their Table 1. This model, as it stands does not therefore accurately represent the calcium current described by Hencek and Zachar and cannot be used without modification. The simulation of $I_{Ca}$ was performed independently using data from Hencek and Zachar. The ACSL simulation confirmed Author's results (W A Barraclough personal communication 1991).

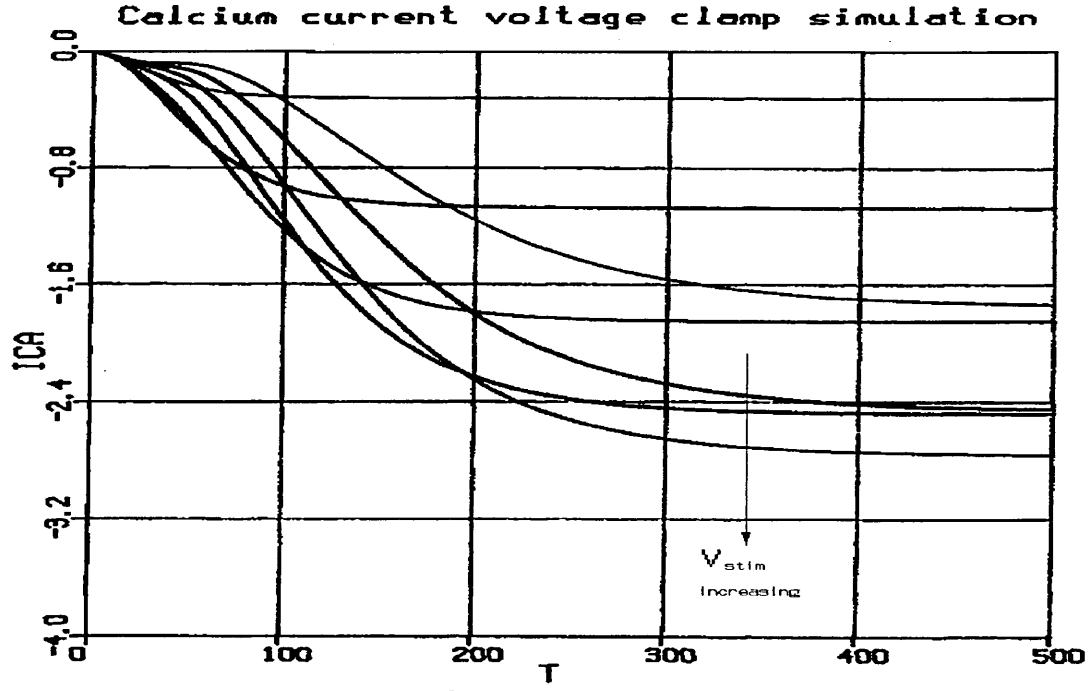


**Figure 7.5**

Results of simulation of voltage-clamp experiment using the model due to Hencek and Zachar.

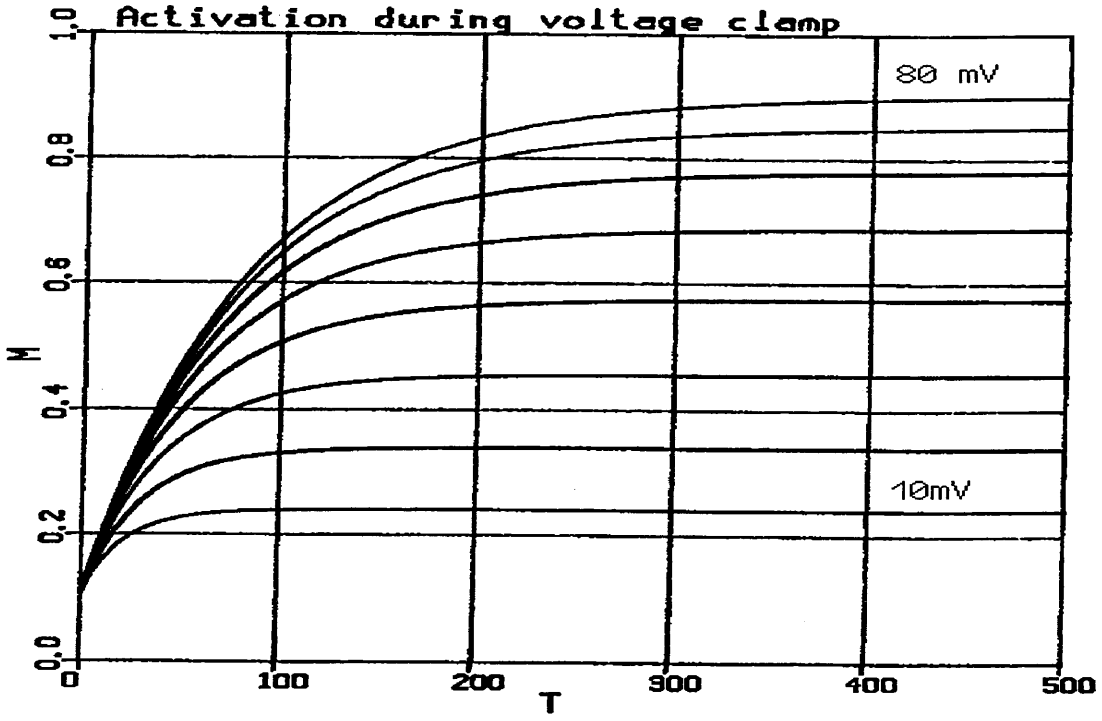


**Figure 7.6**

Graph showing the variation of the calcium activation variable during voltage-clamp simulations.

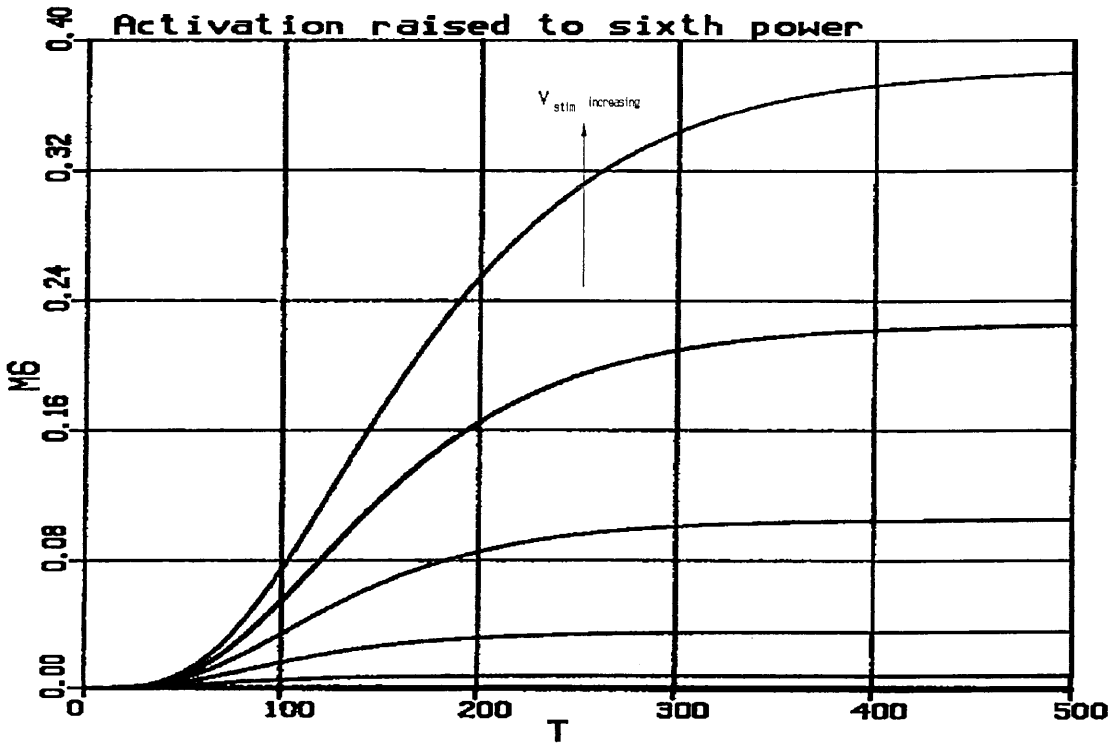


**Figure 7.7**

Graph showing the calcium activation variable raised to the sixth power simulated using Hencek and Zachar's model.

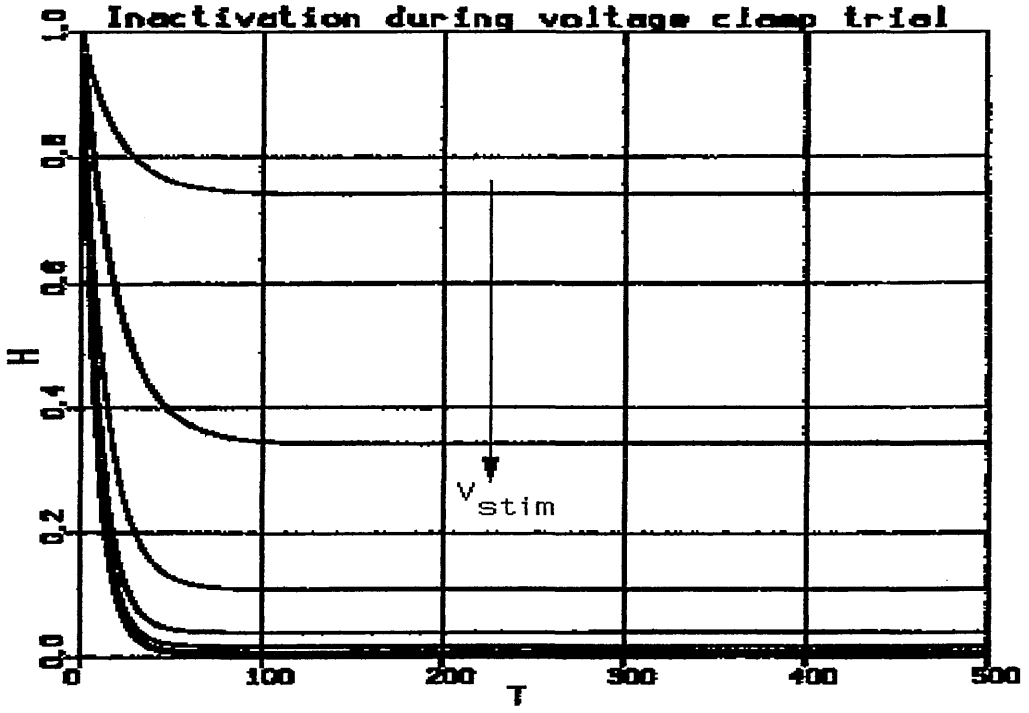


**Figure 7.8**

Calcium inactivation variable simulated using Hencek and Zachar's model.

As with Hencek and Zachar's model, the Hodgkin-Huxley approach is used. The current they observed did not inactivate, so they used the simpler model shown in Equation 7.7.

$$I_{Ca} = g_{Ca}(V)m^2(V,t) \quad \ldots\ldots\ldots\ldots\ldots\ldots \quad (7.7)$$

The rate functions are given by Equations 7.8 and 7.9.

$$\alpha_m(V) = \frac{1.6}{[1 + \exp(-0.072(V-5))]} \quad \ldots\ldots\ldots\ldots \quad (7.8)$$

$$\beta_m(V) = \frac{(0.02(V+8.69))}{[\exp((V+8.69)/5.36)-1]} \quad \ldots\ldots\ldots\ldots \quad (7.9)$$

Note that in the original paper (Kay & Wong 1987) there is an error in the equation for $\alpha_m$ in that the slope factor 0.072 is incorrectly given as 0.0072 (Equation (6) Page 614 Kay & Wong 1987). The rate functions and activation variable m plotted against voltage are reproduced here as Figures 7.9 and 7.10. The time constant of activation as a function of voltage is reproduced in Figure 7.11. The conductance g(V) is given as a function of voltage, reproduced here as Equation 7.10.

$$g(V) = \frac{PV\exp[2FV/RT]}{1 - \exp[-2FV/RT]} \quad \ldots\ldots\ldots\ldots\ldots \quad (7.10)$$

where P is a constant which depends upon the extracellular calcium concentration.

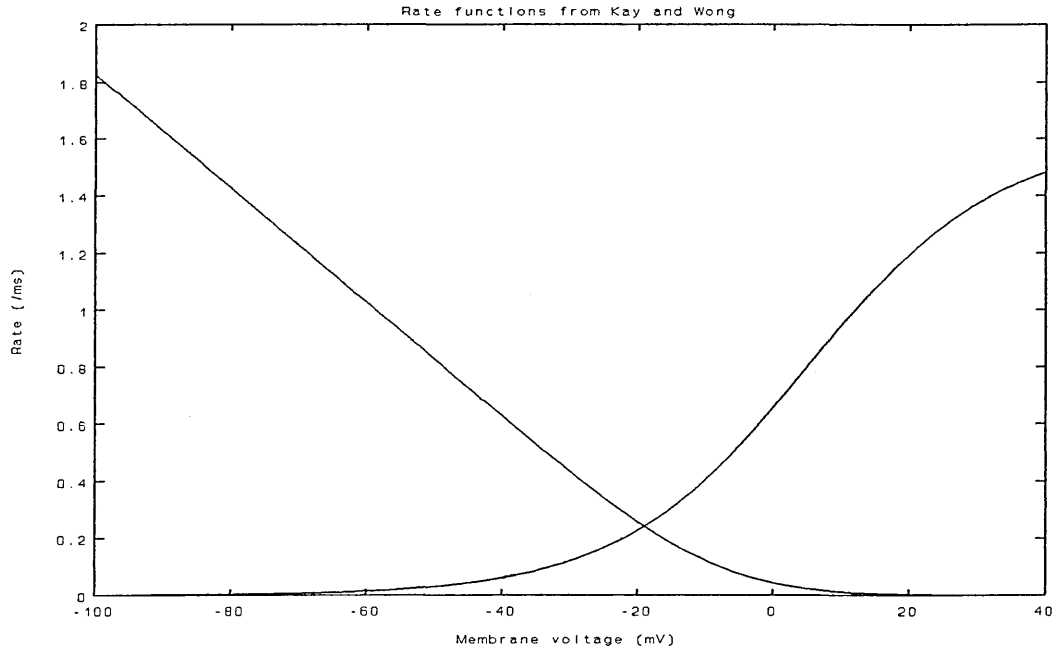


**Figure 7.9**
Graph showing the rate functions from Kay and Wong's calcium current model.

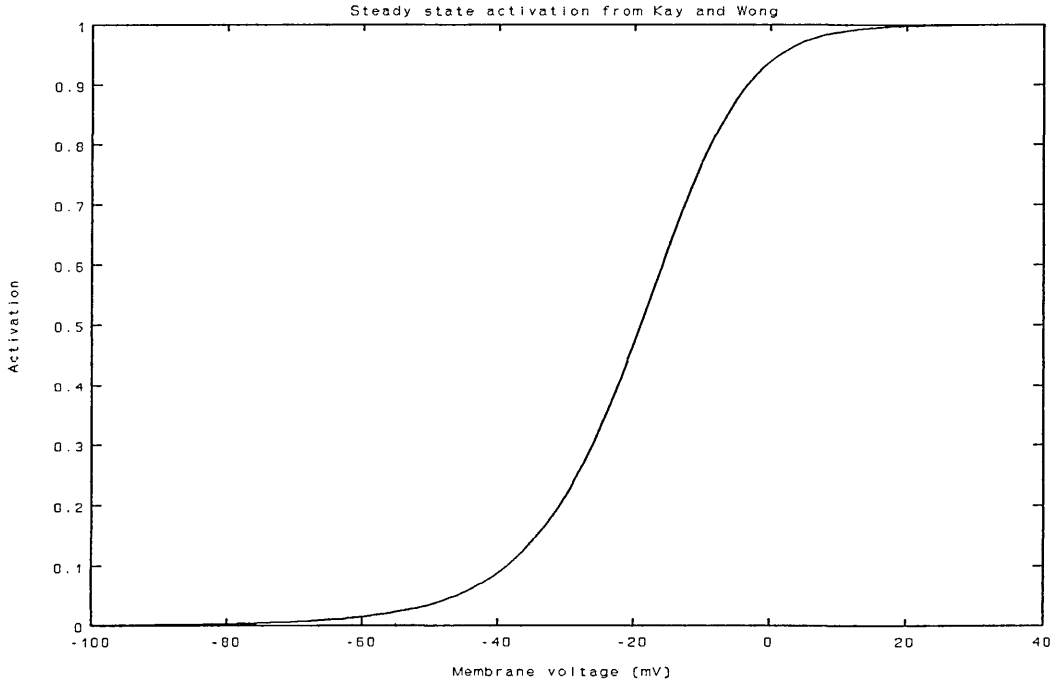


**Figure 7.10**
Graph showing the variation in steady-state calcium activation derived using data from Kay and Wong.

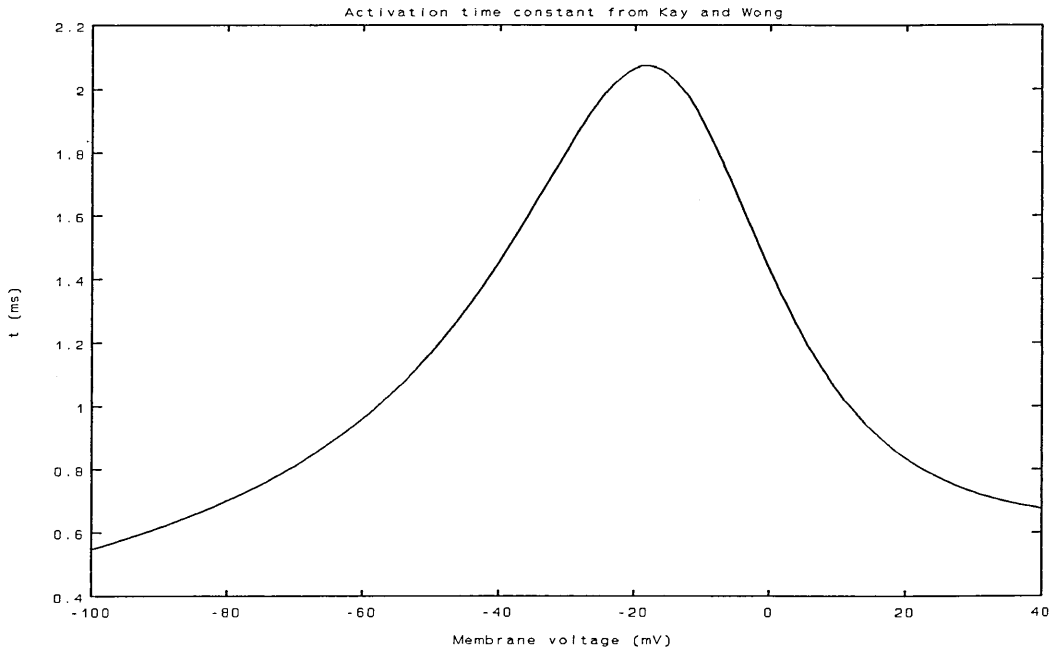


**Figure 7.11**
Graph showing the variation with voltage of the calcium activation time constant from Kay and Wong's model.

$$I_{Ca} = A(1-\exp(-t/\tau_m))^3(h_\infty-(h_\infty-h_0)\exp(-t/\tau_h)) \quad . . . . \quad (7.11)$$

$$h_\infty = \frac{1}{[1+\exp[(E-E_{h_{1/2}})/k_h]]} \quad . . . . . \quad (7.12)$$

$$\alpha_h = \bar{\alpha}_h \exp((E_h-E)/V_{\alpha,h})) \quad . . . . . \quad (7.13)$$

$$\beta_h = \frac{\bar{\beta}_h}{[1 + \exp[(E_h-E)/V_{\beta,h}]]} \quad . . . . . \quad (7.14)$$

$$\alpha_m = \frac{\bar{\alpha}_m(E-E_m)}{1 - \exp[(E_m-E)/V_{\alpha,m}]} \quad . . . . . \quad (7.15)$$

$$\beta_m = \bar{\beta}_m \exp[(E_m-E)/V_{\beta,m}] \quad . . . . . \quad (7.16)$$

The alpha and beta rate functions as a function of voltage are shown in Figures 7.12 and 7.13. The steady-state activation and inactivation curves are given as a function of voltage in Figure 7.14 and activation and inactivation time constants as a function of voltage in Figures 7.15 and 7.16 respectively.

TABLE 7.2

MODEL PARAMETERS

| | | |
|---|---|---|
| $E_{h\frac{1}{2}} = -33mV$ | $k_h = 6.3mV$ | |
| $\hat{\alpha}_h = 0.08s^{-1}$ | $\beta_h = 1.4s^{-1}$ | $E_h = -25.5mV$ |
| $V_{\alpha,h} = 19.7mV$ | $V_{\beta,h} = 6.1mV$ | |
| $\hat{\alpha}_m = 1.74mVs^{-1}$ | $\beta_m = 0.12s^{-1}$ | $E_m = -43.0mV$ |
| $V_{\alpha,m} = 19.2mV$ | $V_{\beta,m} = 23.1mV$ | |

There appears to be a mistake in either the equations given by Sánchez and Stefani or the graph of $\tau_m$ against voltage as given in Figure 8 of their 1983 paper. The equations as given do not reproduce the curve as shown. Figure 7.15 here was produced using Equations 7.15 and 7.16 but with the parameter values from Table 7.2 adjusted by a factor of ten each to give a graph having the same scale as that shown in Figure 8 in the 1983 paper. Due to this uncertainty in the parameter values this model was not investigated further.

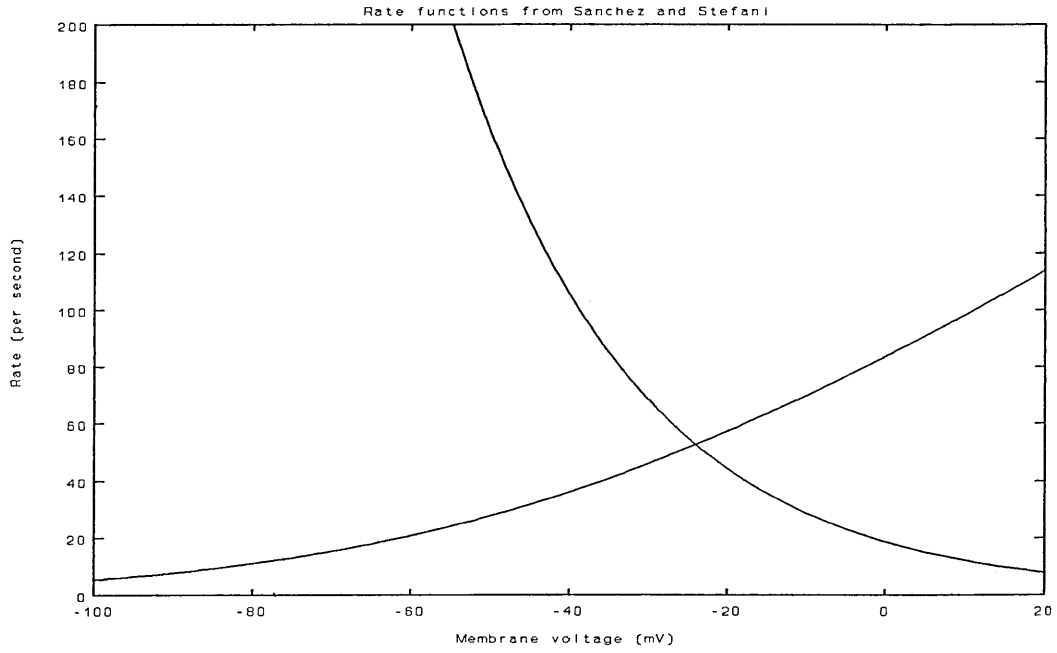


**Figure 7.12**
Graph showing the variation with voltage of the alpha and beta rate functions in Sanchez and Stefani's calcium current model.

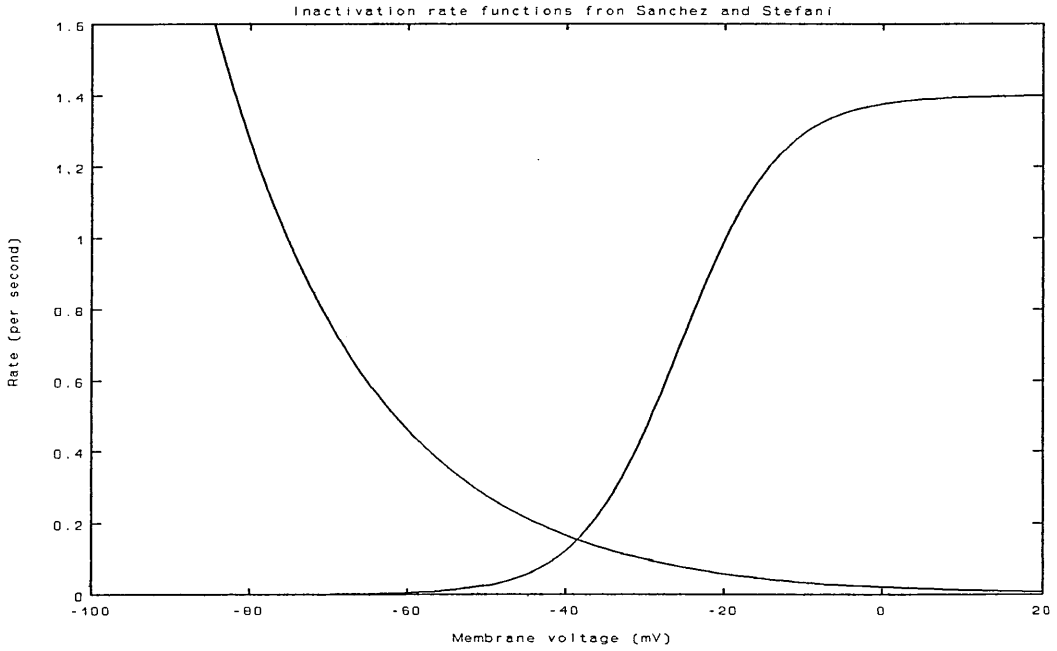


**Figure 7.13**
Graph showing the voltage-dependence of the calcium inactivation rate functions in Sanchez and Stefani's model.

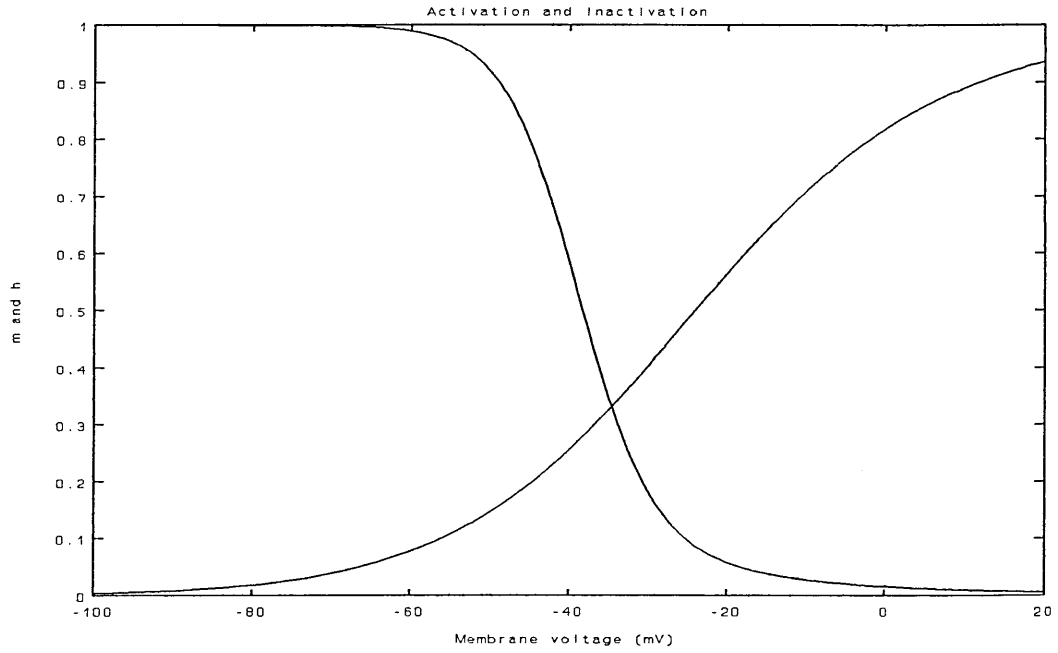


**Figure 7.14**
Graph showing the variation with voltage of the steady-state calcium activation and inactivation variables.

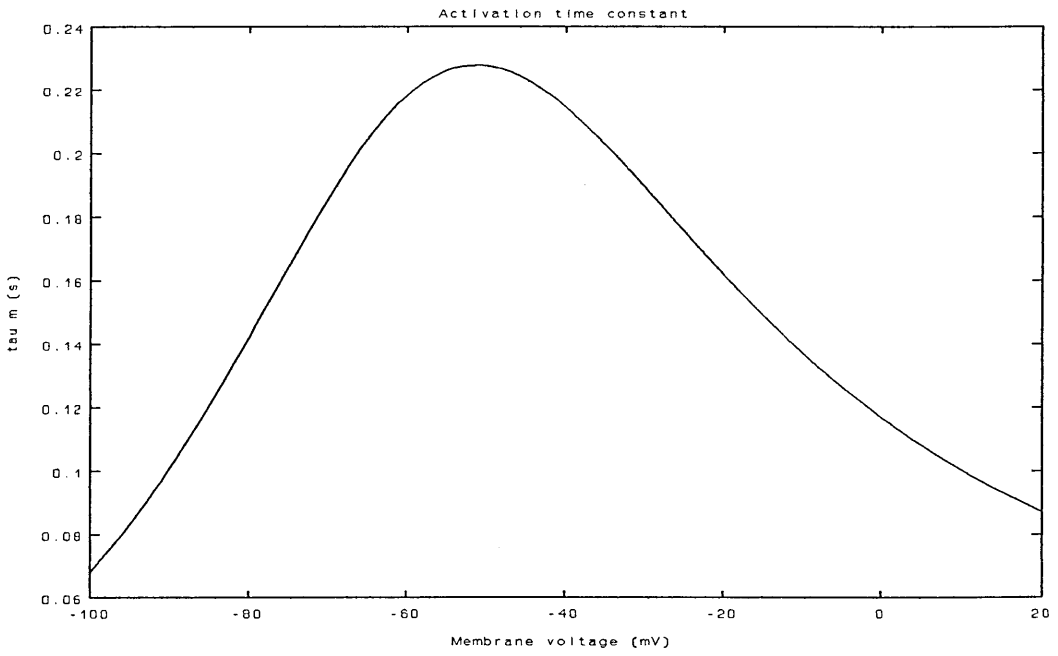


**Figure 7.15**
Graph showing the voltage-dependence of the steady-state activation time constant in Sanchez and Stefani's model.

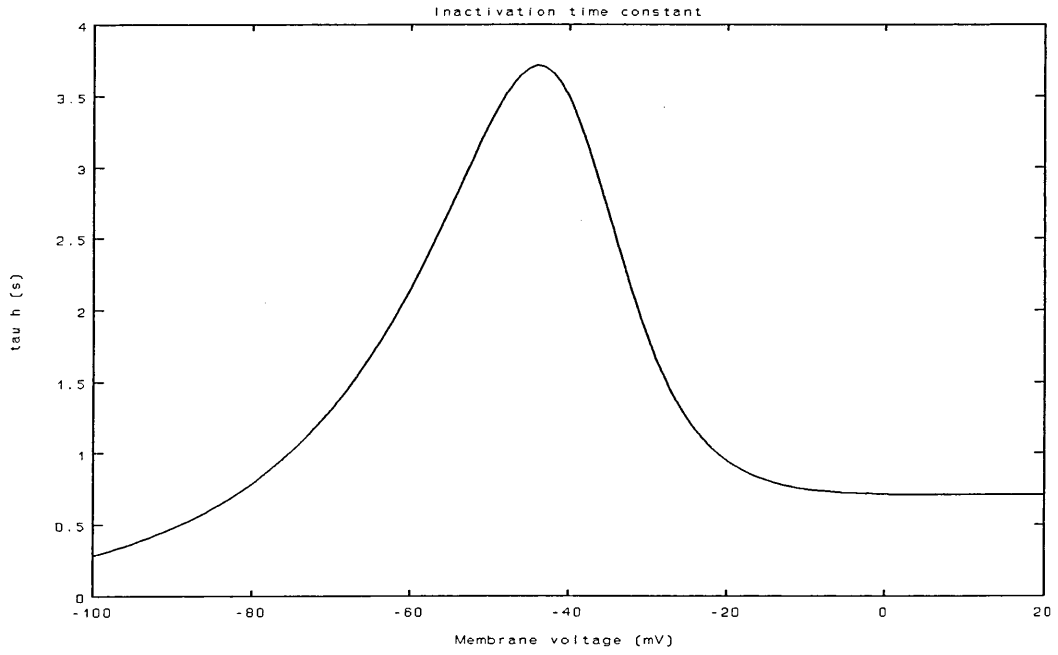


**Figure 7.16**
Graph showing the voltage-dependence of the calcium inactivation time constant in Sanchez and Stefani's model.

## SUMMARY

One of the important features of the oxytocin-secreting cell is the presence of calcium currents. This Chapter has reviewed work by various researchers on calcium currents in related systems. Unfortunately no data is available for building a mathematical model of the calcium current in oxytocin-secreting cells. To overcome this difficulty, a model taken from a paper by Hencek and Zachar has been used. The ACSL program written by the author to simulate their model is included in the Appendix.

# CHAPTER EIGHT

## RESULTS

The preceding chapters have described the derivation of a mathematical model to describe the stereotyped bursting behaviour observed in oxytocin-secreting neurones. This chapter will discuss the experimental results obtained from computer simulations of the model. As a first step in the modelling process, the Hodgkin-Huxley model was simulated on an IBM personal computer (PC) using the FORTRAN-77 programming language. These simulations demonstrated the validity of this approach but highlighted several practical problems. The first of these was simply the speed of computation. Although simulation of a single action potential was achieved fairly rapidly, the simulation of a train of action potentials took about 30 minutes for a 20ms burst. Since the observed milk ejection burst is of the order of seconds with a similar period of silence it was quickly realised that the computation of a complete burst would require an excessive amount of computer time. Dramatic improvements in personal computer technology have now largely alleviated this problem. Another associated problem was the amount of data accumulated during a simulation run. Small time steps are required to maintain accuracy and stability of the numerical integration routine which leads to a large volume of accumulated data which exceeded the storage capacity of the floppy discs then available. Again, improvements have since vastly increased the storage capacity of the magnetic media. In order to overcome the storage problem it was decided to simply store only those values of

output variables which differed from the previous output by a given tolerance, while maintaining the intermediate values actually required for calculation of the next time step. This is a valid approach since the eventual output from the program is in the form of graphs which require less accuracy to represent the variables than is required to maintain the accuracy and stability of the numerical integration routine. A similar approach is used by the ACSL software referred to in Chapter 3. The results are saved at equal intervals of time, the interval being called the communication interval. However, the third problem was instrumental in deciding to move away from the PC-based approach onto a mainframe. This was simply the lack of suitable graph plotting software and hardware for the PC. Program listings for some of the programs developed on the IBM PC appear in the appendix.

Trial simulations of the H-H equations on the IBM 4313 mainframe computer were encouraging and showed a close agreement with published results. At this stage it was decided that the computer program was generating valid data and that the development of the model for the oxytocin secreting cell could proceed with confidence.

Simulation of a single action potential using the oxytocin model and H-H equations is shown here in Figures 8.1 and 8.2. Voltage and time are given in volts and seconds in Figure 8.1 and in millivolts and milliseconds in Figure 8.2. These graphs were generated using the ACSL software to solve the model equations.

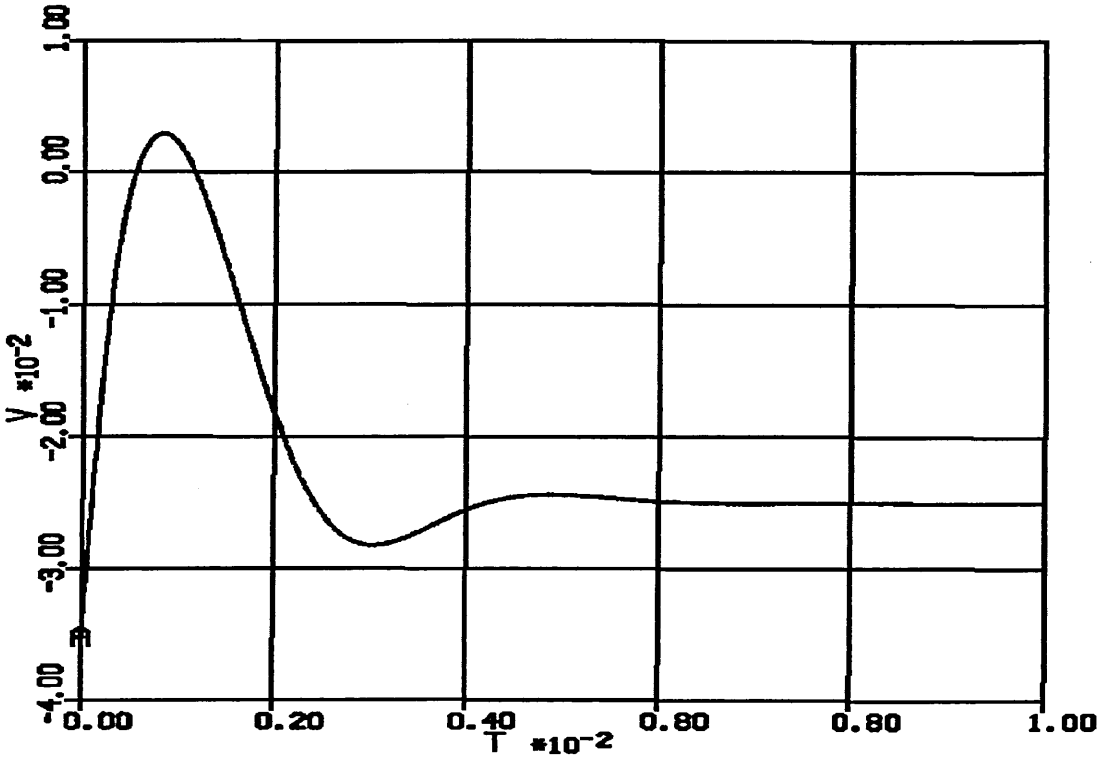


Figure 8.1

Action potential simulation using of oxytocin cell model equations scaled in standard SI units.

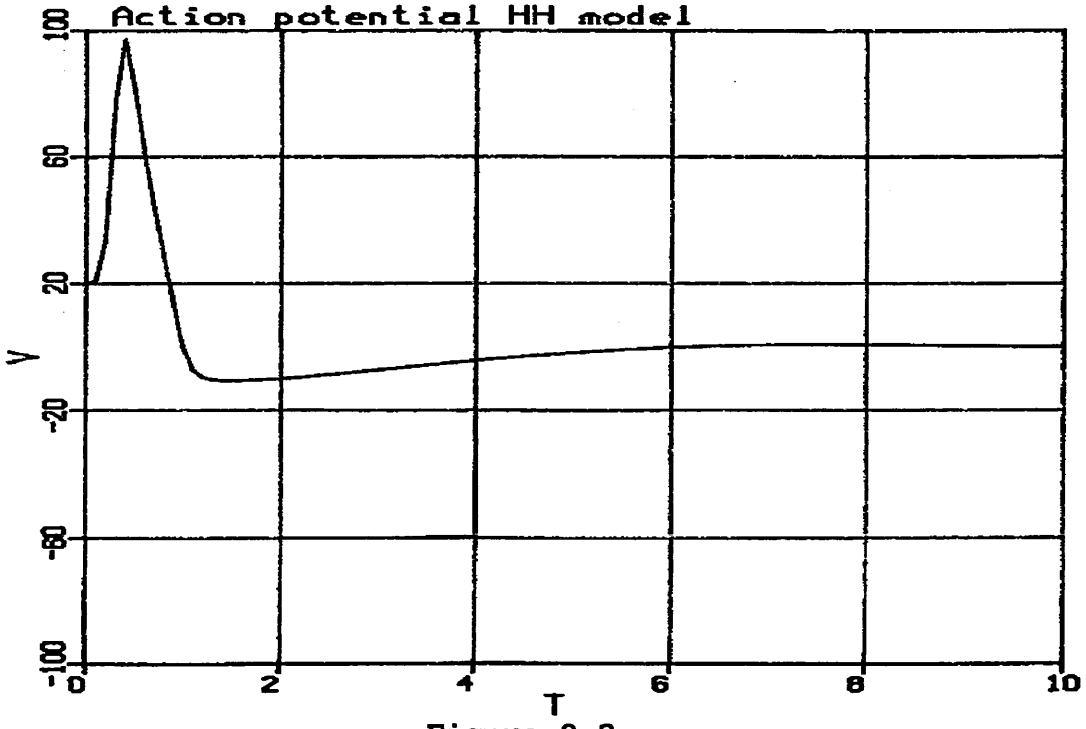


Figure 8.2

Simulation of action potential using H-H model equations.

The literature search revealed that repetitive firing could be induced by lowering the concentration of calcium in the bathing solution. As described on Page 84, a change in external calcium concentration may be modelled as a shift of the model alpha and beta functions along the voltage axis in a depolarizing direction. This feature was then included in the model. It was assumed that a double exponential "forcing function" could be used to simulate changes in the calcium concentration. This was then tried as an experiment and the results are shown in Chapter 4. Hille and Tse (Hille & Tse 1992) discuss oscillations in certain pituitary cells due to oscillatory release of internal calcium triggered by hormones. It seems that the assumption of an endogenous oscillation in internal calcium concentration is very reasonable.

Blocking the passage of sodium ions does not prevent the oxytocin-secreting cell from generating an action potential. A calcium component of the total membrane current is responsible for generating a spike under conditions of sodium channel block (Bourque & Renaud 1985). To take account of this, the H-H model equations were extended to include a calcium channel (using data from Hencek & Zachar). As mentioned in Chapter 7, data on calcium currents in the oxytocin-secreting cell was not available, so the Hencek and Zachar model was used instead. As the results in Chapter 7 demonstrate, the model did not yield satisfactory results. Part of the characteristics of action potentials recorded from oxytocin-secreting cells is the 'shoulder' on the repolarizing phase. This is due to calcium current (Mason &

Leng 1984). This feature does not, therefore appear in the model described here for the reason that the Hencek Zachar model is not appropriate. In order to model the electrical behaviour of the oxytocin-secreting cell fully it will be necessary to perform experiments to obtain the data pertinent to the calcium current.

A suite of computer programs were written which allowed the user to simulate a variety of models and obtain graphical output of different model variables on a graphics terminal and a Calcomp drum plotter. At this stage a problem with the computer system became evident. It was thought useful to have the ability to run simulations on an interactive basis. This entails running a simulation on the computer, viewing the graphical output and sending the resulting plot off to the remote plotter if required, while still remaining within the program environment. Such an approach allows the user to run a series of simulations with differing model parameters and compare the results. Hardcopy output was not immediately available due to the fact that the plotter was at a remote location and plot files were stored until the plotter operator decided to run the plotter. The problem arose due to the limited allowable interaction of the program with the mainframe operating system causing unexpected and unwanted results. Help on resolving this problem was not forthcoming so work with the IBM mainframe was abandoned and the Apollo computer network was used in preference, since the ACSL software package was available which eliminated the above mentioned problems.

Problems involving computer numerical solution of

mathematical models are not uncommon in science and engineering and several computer packages are available that perform this task. One such package is the Advanced Continuous Simulation Language (ACSL), described in Chapter 3. This is available on the Polytechnic's Apollo computer network. ACSL is a trademark of Mitchell Gauthier Associates.

Basically, ACSL is a translation program produced by Mitchell Gauthier Associates that converts programs written in a specialised modelling language into equivalent FORTRAN source code and then compiles and links the resulting code with various support programs such as numerical integration routines and graphics routines to produce an executable file. This software provides all the facilities required to run a series of simulations on an interactive basis and obtain hardcopy of graphical output on a plotter.

In view of all the benefits provided it was decided to learn to use the package. This proved to be a relatively straightforward task. The added advantage of this approach is that the model can be defined in relatively few lines of code and thus greatly enhances the speed with which models may be tested. This is a significant gain since each new model written in FORTRAN on the mainframe requires a substantial amount of source code to be typed into a computer terminal. Again, a first step was to use the well tried and tested H-H model to obtain results that could be compared with published results. This was done with satisfactory results as can be seen from Figure 8.2.

Once it had been established that the ACSL simulations were producing valid results, data on membrane and channel properties taken from oxytocin-secreting cells was needed in order to build up the model. Cell capacitance was derived using data on the cell size and morphology and using the value of $1\mu F/cm^2$ for the capacitance of the cell membrane. Sodium and potassium current data were taken from published results as described in preceding chapters. At this point a major problem with the project was encountered. This was simply the lack of appropriate data for all the channels known to be present in the membrane. Experimental results were not forthcoming so an alternative method was sought. At this stage it may be useful to summarise what data was available and to highlight the deficiencies in the model. Cell capacitance was available. Model equations describing the sodium current, the delayed rectifier potassium current and the transient potassium current had been derived and used in simulations. Data for the calcium-dependent potassium current was incomplete and there was no data on the calcium channel. The membrane resting potential was known.

TABLE 8.1

CURRENTS PRESENT IN OXYTOCIN CELL

| |
|---|
| Sodium Current $I_{Na}$ |
| Potassium Delayed rectifier $I_K$ |
| Transient Potassium current $I_A$ |
| Calcium-gated Potassium current $I_{K(Ca)}$ |
| Calcium current $I_{Ca}$ |
| Leakage current $I_L$ |

TABLE 8.2

SUMMARY OF OXYTOCIN CELL PROPERTIES

| |
|---|
| Cell size : 25 μm diameter |
| Membrane resting potential : -60mV |
| Input resistance : 50M to 1G Ohm |
| Time constant : 9 to 15 ms |
| Cell capacitance : 45 to 300pF |
| Action potential amplitude : 70mV |
| Action potential duration : 2ms |
| Maximum firing frequency : 80Hz |
| $\hat{g}_{Na}$ = 51.6nS $E_{Na}$ = 43.6mV |
| $\hat{g}_K$ = 4.9nS $E_K$ =-83.0mV |
| $\hat{g}_A$ = 5.9nS $E_{Ca}$ =85.0mV |

Table 8.2 summarises the model parameters used. The values given are those quoted in previous chapters. $E_{Ca}$ is taken from Hencek and Zachar (Hencek and Zachar 1977).

The electrical circuit diagram showing the known conductances is shown in Figure 8.3.

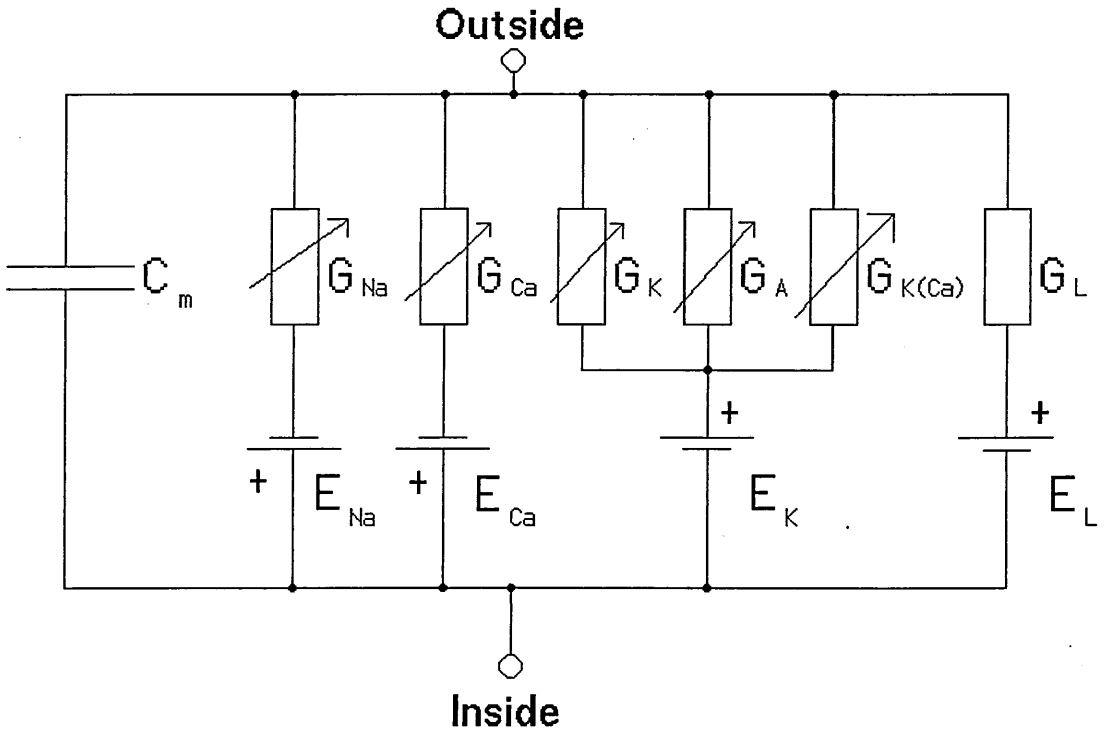


**Figure 8.3**
Circuit diagram of oxytocin-secreting cell membrane showing the various conductances present.

The model equations shown here do not include the equations for Hencek and Zachar's calcium current model.

Results of the simulations are shown in Figures 8.4 to 8.25. It was decided to use SI units in the models. Voltages are therefore expressed in Volts, Currents in Ampères and time in seconds. The appropriate scaling factors appear on the graphs.

The model devised for the electrical behaviour of the oxytocin-secreting cell is given in equations 8.1 to 8.18.

OXYTOCIN CELL MODEL

$$I_{Na} = \bar{g}_{Na}\, m^3 h (V - E_{Na}) \quad (8.1)$$

$$\frac{dm}{dt} = \alpha_m(1 - m) - \beta_m m \quad (8.2)$$

$$\frac{dh}{dt} = \alpha_h(1 - h) - \beta_h h \quad (8.3)$$

$$\alpha_m(V) = \frac{6400}{[0.02\exp(-100V) + 1]} \quad (8.4)$$

$$\beta_m(V) = 5\exp(-V/0.015) \quad (8.5)$$

$$\alpha_h(V) = 45\exp(-V/0.02) \quad (8.6)$$

$$\beta_h(V) = \frac{2250}{[0.08\exp(-92.5V) + 1]} \quad (8.7)$$

$$I_K = \bar{g}_K\, n^3\, (V - V_K) \quad (8.8)$$

$$\frac{dn}{dt} = \alpha_n(1 - n) - \beta_n n \quad (8.9)$$

$$\alpha_n = \frac{600.0}{[\exp(-60V) + 1]} \quad (8.10)$$

$$\beta_n = 30.0\exp(-V/0.02) \quad (8.11)$$

$$I_A = g_A\, a^4\, b(V - V_K) \quad (8.12)$$

$$\frac{da}{dt} = \alpha_a(1 - a) - \beta_a a \quad (8.13)$$

$$\frac{db}{dt} = \alpha_b(1 - b) - \beta_b b \quad (8.14)$$

$$\alpha_A = \frac{2200}{[\exp(2200(0.00008 - 0.025V)) + 1]} \quad (8.15)$$

$$\beta_A = 80\exp(-V/0.03) \quad (8.16)$$

$$\alpha_B = 26\exp(-V/0.076) \quad (8.17)$$

$$\beta_B = \frac{70}{[\exp(70(0.0017 - 0.85V)) + 1]} \quad (8.18)$$

Figures 8.4 to 8.6 show results of simulations under different conditions. For example, the stimulus voltage that produced the results shown in Figure 8.4 is 20mV whereas Figure 8.6 shows the results when no stimulus is given. In Figure 8.5, the model is rerun with an increased stimulus voltage. Figure 8.7 shows the result of removing the leakage current component. As mentioned in Chapter 4, a region of negative resistance is required in order to sustain continuous firing and Figure 8.8 demonstrates that the oxytocin model as described here does possess such a region. The total membrane current is shown plotted against membrane voltage. The effects of a reduction in calcium concentration are modelled as an apparent voltage shift in the alpha and beta rate functions. Figure 8.9 shows the result of running a simulation where a constant offset voltage has been added to the membrane voltage. These initial results showed that the model was capable of demonstrating an action potential given a suitable stimulus. However, close examination of the sodium current traces revealed a problem. The sodium current was not returning to zero as it should under free-run conditions. The sodium currents recorded under voltage-clamp conditions both experimentally and simulated, show that the sodium current does not always return to zero. Figures 5.1, 5.2, 5.12, 5.13 and 5.14 demonstrate this. The simulation results show this to a greater extent. The voltage trace should also return to the resting potential but does not as close examination of the results show. The current-voltage characteristic in Figure 8.8 is particularly useful in highlighting this phenomenon. The leakage current is not

present in the model that generated that particular graph but it does illustrate the point. Observation of the fact that both the membrane voltage and the sodium current do not return to the appropriate values prompted the experiment shown in Figure 8.10. Here, only the graph of sodium current was plotted. The membrane resting potential in the model was varied and a comparison made between the two resulting traces. Curve A, resulted from the higher resting potential and shows that at that voltage, the sodium current is active from the beginning of the simulation. Lowering the membrane resting potential to -70mV generated curve B which shows a more normal trace. The sodium current is initially inactive but the stimulus causes it to activate and then inactivate as is usual for this current. The conclusion to be drawn from this experiment is that this current is very sensitive to changes in membrane resting potential. This point will be discussed later.

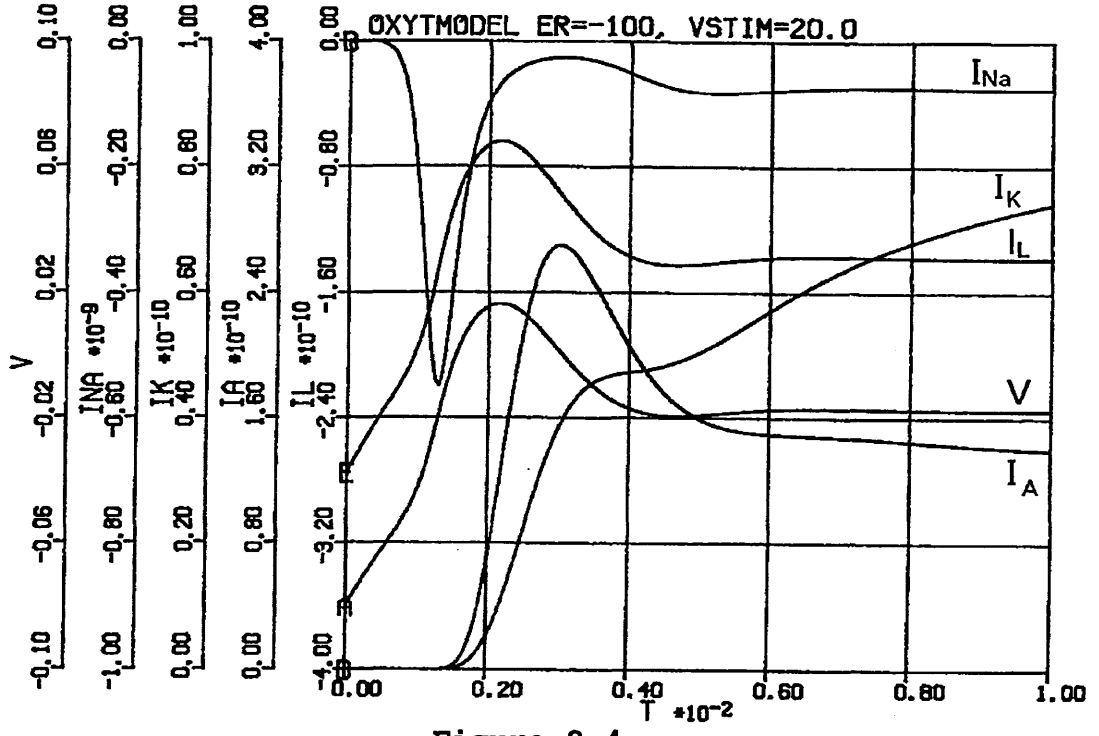


**Figure 8.4**

Simulation results from oxytocin cell model showing voltage, sodium, potassium, transient potassium and leakage currents.

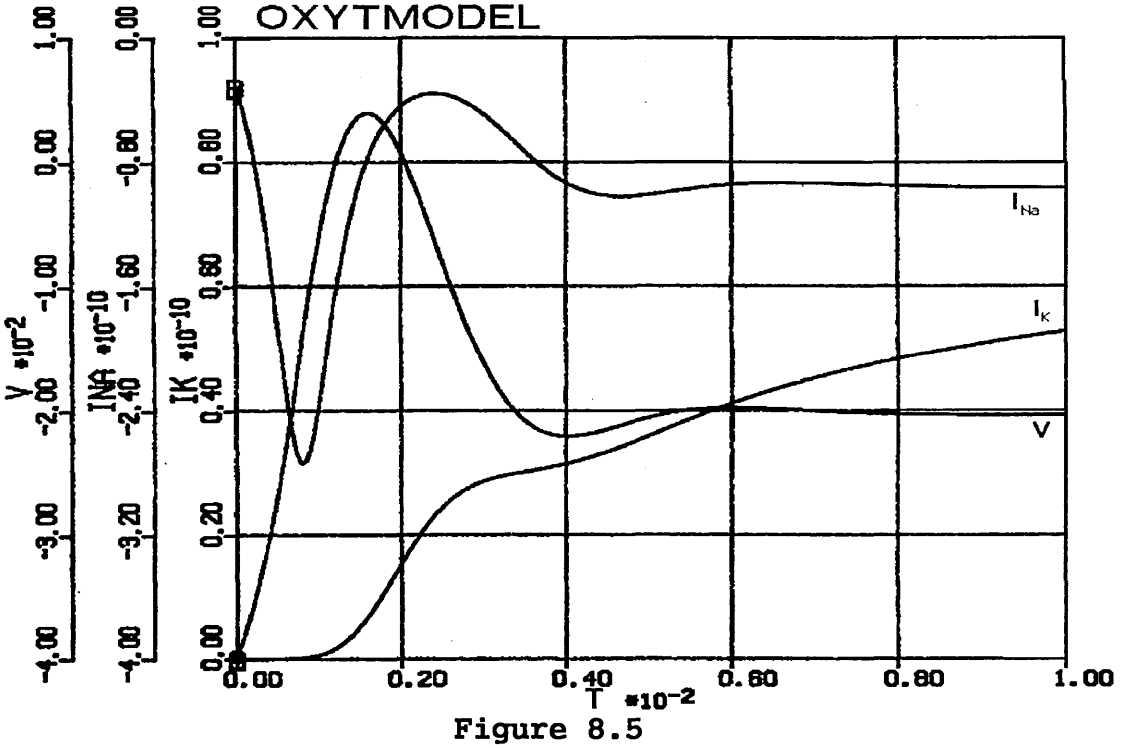


**Figure 8.5**

Simulation of oxytocin-secreting cell from a holding potential of -40mV.

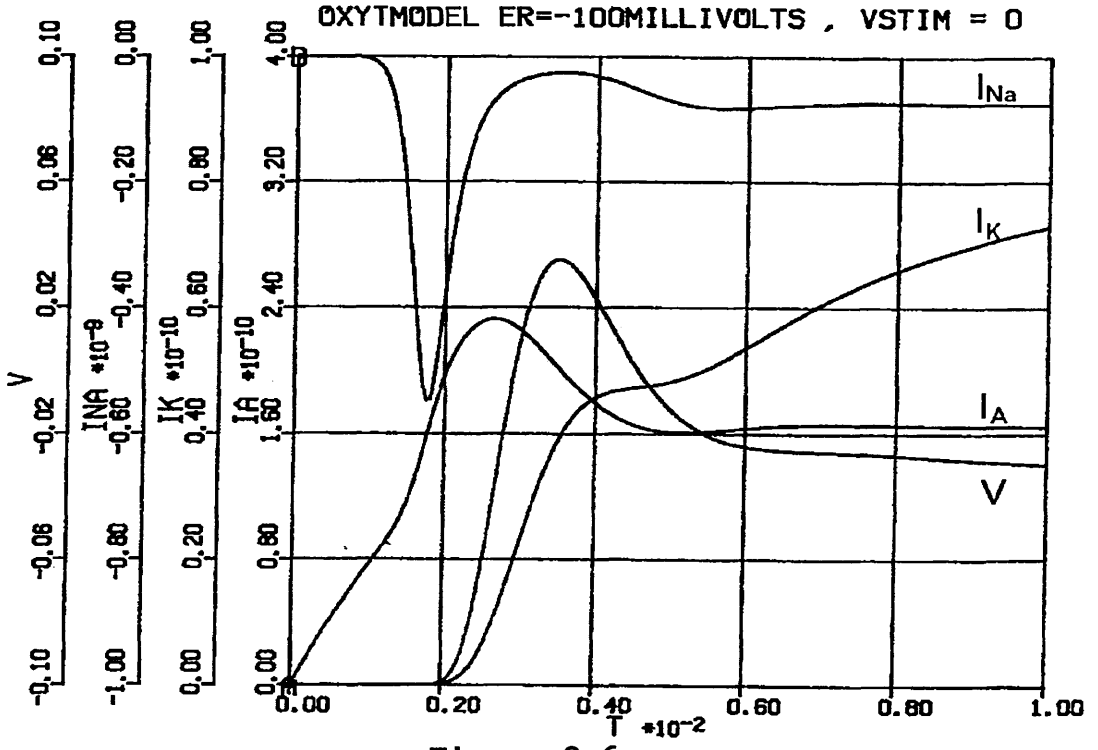


**Figure 8.6**

Action potential generated by model of oxytocin-secreting cell

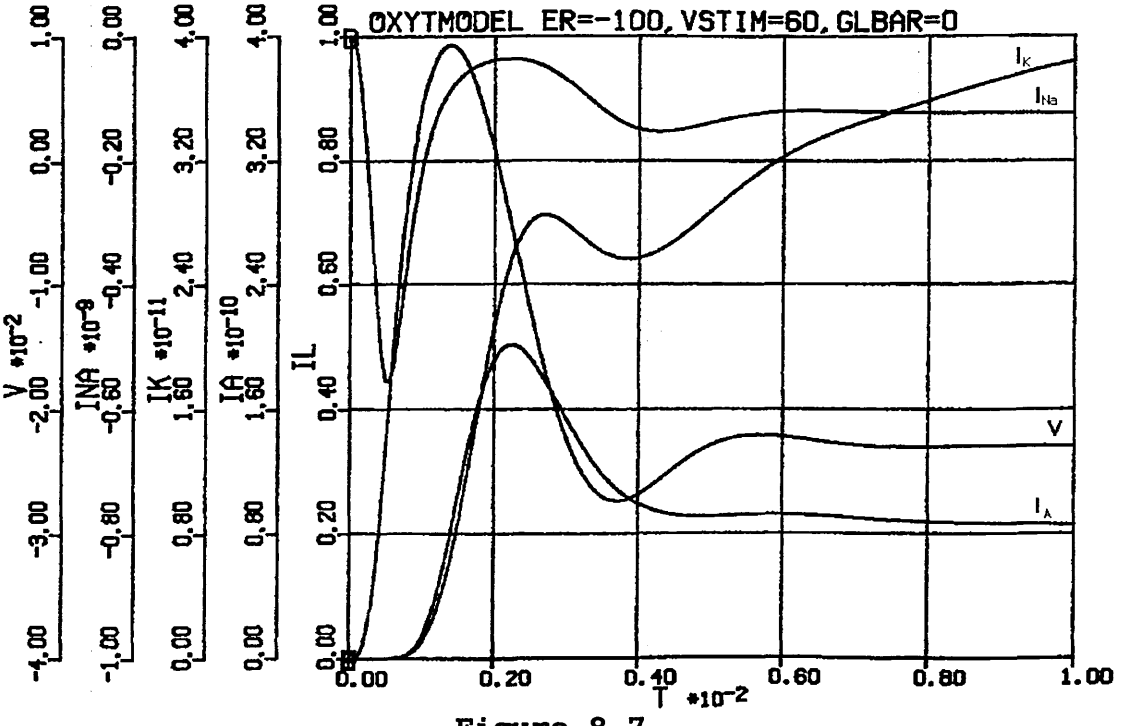


**Figure 8.7**

Simulation of oxytocin cell with the leakage conductance removed from the model.

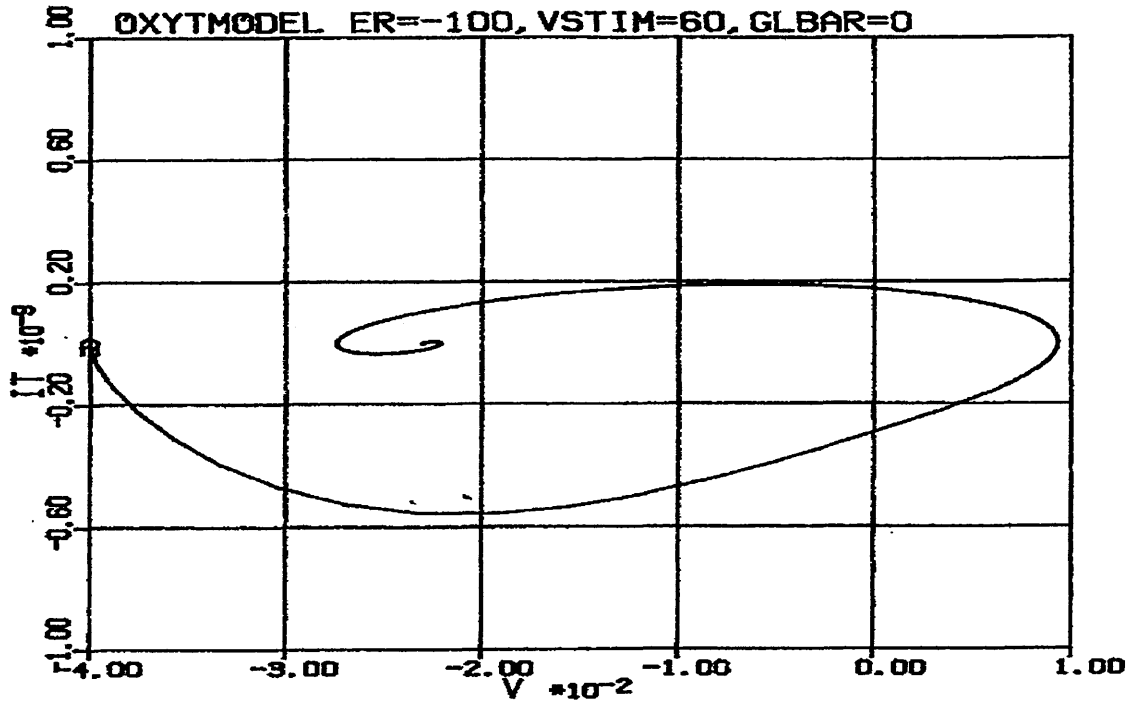


Figure 8.8

Current-voltage characteristic for oxytocin cell model. Total membrane current in amperes plotted against membrane voltage in volts.

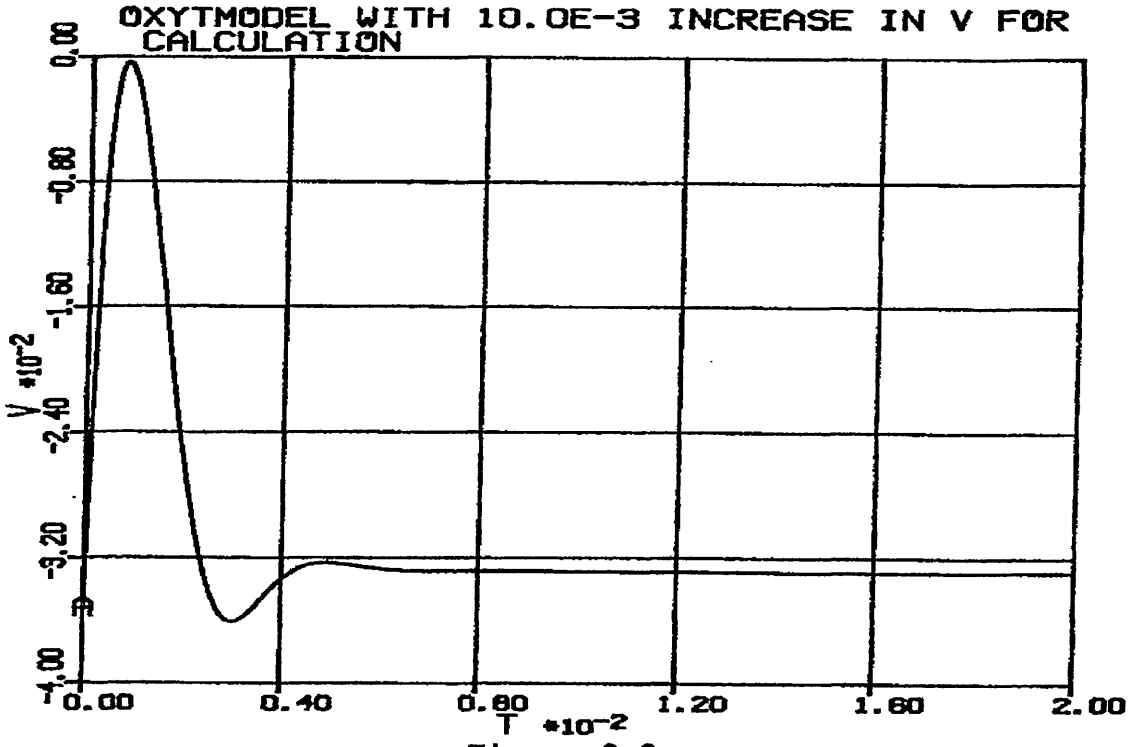


Figure 8.9

This figure shows the effect of adding a constant offset of 10mV to the calculated membrane voltage

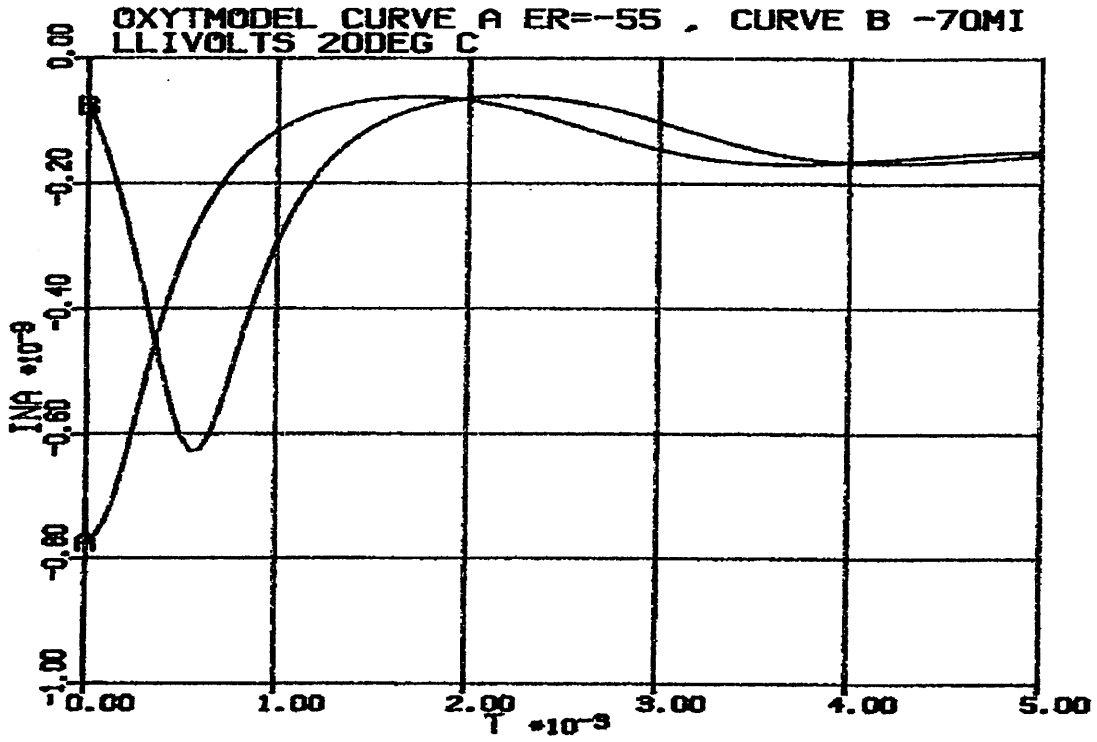


**Figure 8.10**

Simulation results showing the difference in sodium current due to a difference in the resting potential.

The model used to generate these results does not include a calcium-gated potassium current, the data for this channel being unavailable. It is known that such a channel is present in the membrane and contributes significantly to the total membrane current (Cobbett et al 1989). It was therefore decided to include this channel in the model by using data from other sources. An additional repolarizing current should have the effect of bringing the membrane voltage back to the resting potential at which point all the currents should be inactive. Rinzel's model (see Page 41) includes a mathematical description of the calcium-gated potassium current observed in pancreatic beta cells so it was decided to use this model. Apart from a change of units, the model

was used unaltered. Figures 8.11 to 8.20 show the results obtained from this extended model. Figure 8.11 shows the membrane voltage, sodium current and potassium delayed rectifier current. The potassium current is a repolarizing current and should have the effect of bringing the membrane voltage back to its resting value. At the end of a 10ms simulation the potassium current has not stopped increasing in amplitude. This is clearly not in line with experimentally observed behaviour. Figure 8.12 shows the voltage time graph for a simulated action potential and clearly shows that the voltage does not return to its resting value. Individual currents were then inspected under various conditions to attempt to isolate the cause of this behaviour. At this point the complexity of the model becomes evident. There are so many interacting variables that it is extremely difficult to determine what the effects of changing one parameter has on the overall system behaviour. At first it was thought that the sodium current model was causing these problems since it was not returning to its inactivated state as it should. However, it could be that this behaviour is a symptom of the membrane voltage not returning to the resting potential rather than a cause. Figure 8.13 shows the sodium current during a simulation run. It can be seen that the current is already active at the start of the simulation. This implies that the sodium current is sufficiently activated at the chosen resting potential that a stimulating voltage causes an immediate flow of current. According to Hodgkin and Huxley's model, the inactivation variable has a value of around 0.6 at resting potential (Fig. 10 P. 518 Hodgkin & Huxley 1952d).

The sodium activation variable has a very low value at resting potential which is what prevents the current from flowing under the influence of the transmembrane potential. The idea that the sodium current is already active at the resting potential is bourne out by the result shown in Figure 8.14 which shows the resulting voltage and sodium current during a simulated depolarisation from a more negative resting potential. Close examination of Figures 8.13 and 8.14 reveals some other unusual behaviour of the sodium current. At about 2ms on the timescale, the sodium current has almost returned to zero. However, it then increases in amplitude again before appearing to reach a non-zero steady-state. It is not known what is responsible for this behaviour since during voltage-clamp simulations, the current decays even with a maintained depolarisation. Depolarisation of the membrane has a twofold effect on the sodium channel. It triggers the activation process which causes the channel to open but at the same time triggers the inactivation process which causes the channel to close. What appears to be happening in the sodium current model is that the activation and inactivation processes are not going to completion. It appears that both processes are remaining in a state of partial activation, causing the some of the channels to remain open. It appears, therefore that the sodium current model as described here needs some refinement in order for it to more accurately represent the actual behaviour of sodium current in the oxytocin-secreting cell.

Figure 8.15 shows the potassium current following a depolarisation. It is noticeable here that the current does

not return to zero as anticipated. Since the channel is volotage-gated, this may again be a consequence of the membrane voltage not returning to the resting potential. The transient potassium current in Figure 8.16 also shows this behaviour. Since it is governed by an activation and inactivation variable like the sodium current, the graph shows a similar behaviour to the sodium current but with opposite polarity. The voltage clamp simulation of this current shown in Figure 6.5, Page 133 shows the current declining to zero but with a fairly long time constant. It appears that this current also is not returning to its resting state following the action potential.

The calcium current shows a rising phase followed by a falling phase that also does not return to the zero resting state. Referring back to the project introduction it was noted that the calcium current is thought to be responsible for the 'shoulder' on the experimentally observed action potential. This is not the case here since the current starts to decrease before the membrane potential. Another way of stating this point is that the calcium current spike is too fast. This could probably be corrected by adjustement of the activation and inactivation time constants in the calcium current model. Another important point to note here is that the calcium current starts off from a relatively large negative value (around -200pA) and decreases before increasing again. The current should be an inward (negative) depolarizing current due to the polarity of the driving voltage (see Figure 8.3). It was expected that the current would start off from zero before increasing to a large

negative value and then returning to zero.

Figure 8.18 shows the behaviour of the calcium-gated potassium current taken from Rinzel's model. It can be seen that the current is still increasing at the end of the 10ms simulation. This behaviour is tied in with the behaviour of the calcium concentration shown in Figure 8.19 which also shows a steady increase throughout the period of simulation.

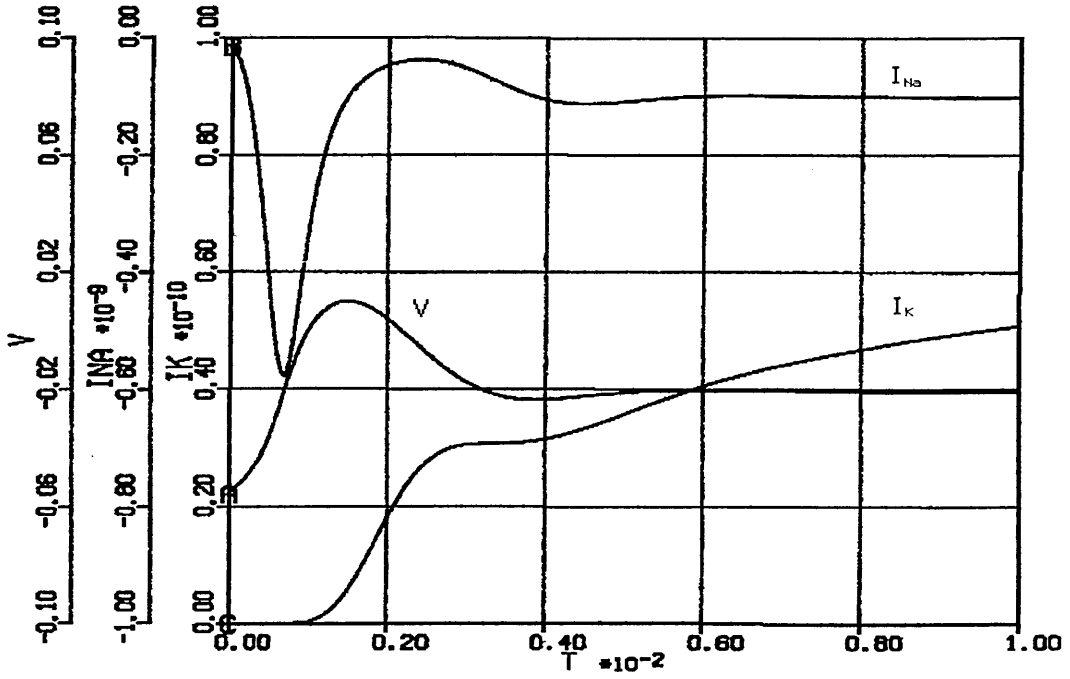


**Figure 8.11**

Graph showing the membrane voltage, sodium current and potassium current during a simulation.

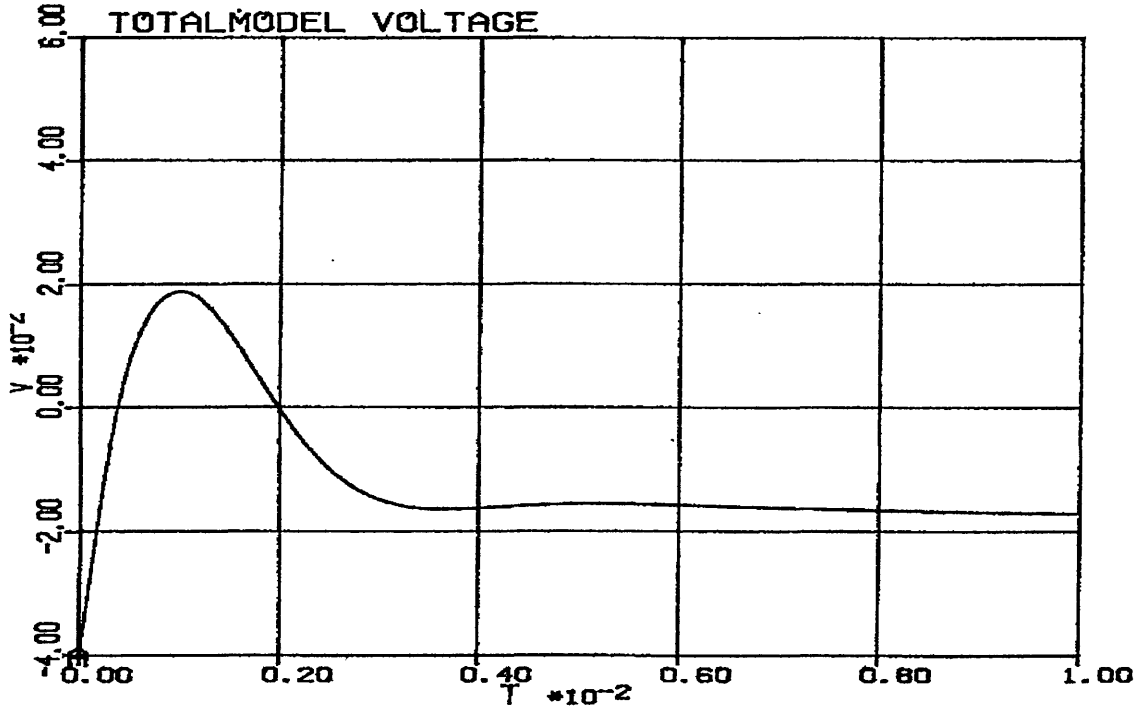


**Figure 8.12**

Simulated action potential resulting from the complete model including calcium and calcium-gated potassium currents.

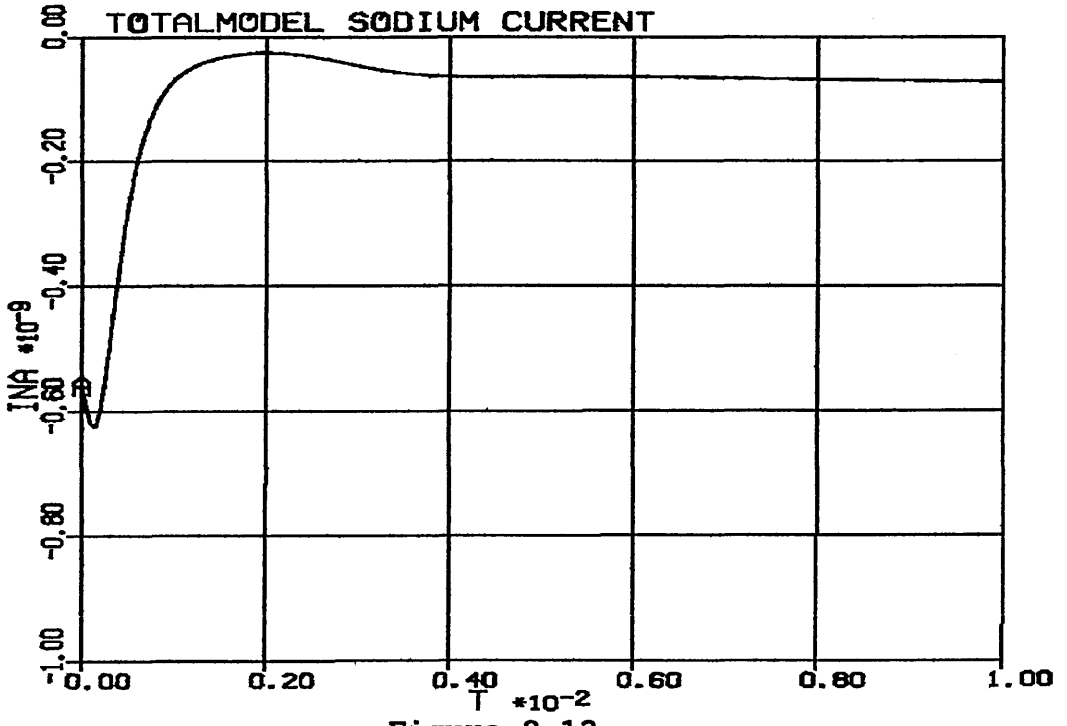


**Figure 8.13**

Sodium current from simulation of complete model.

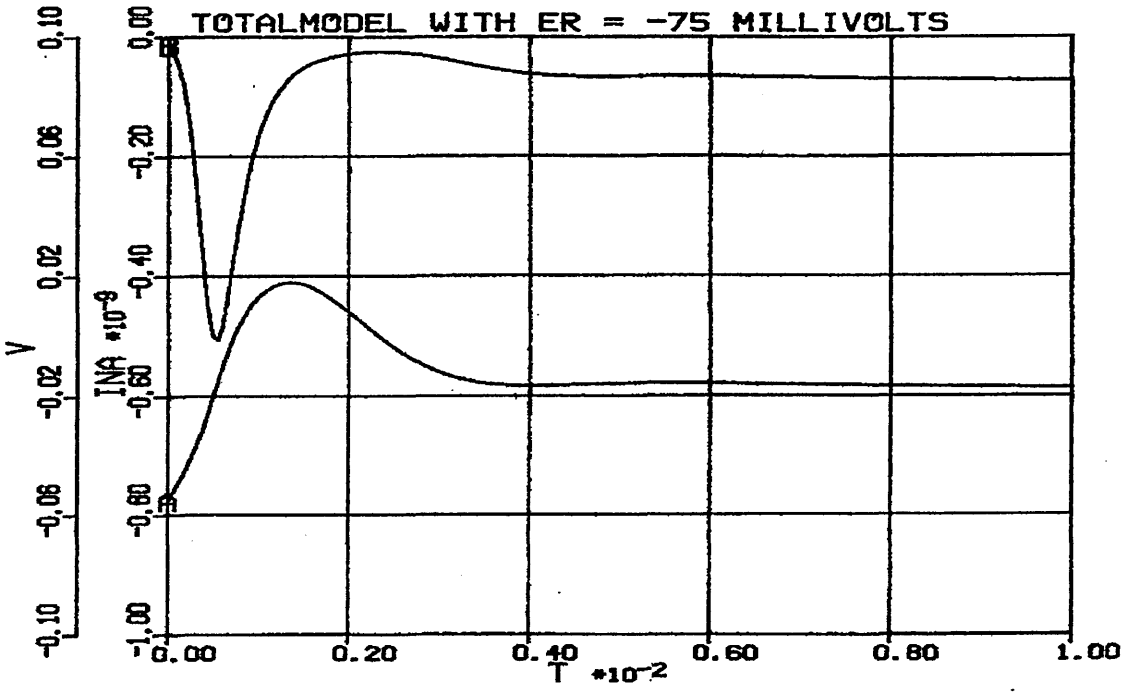


**Figure 8.14**

Simulated membrane voltage and sodium current resulting from the complete model.

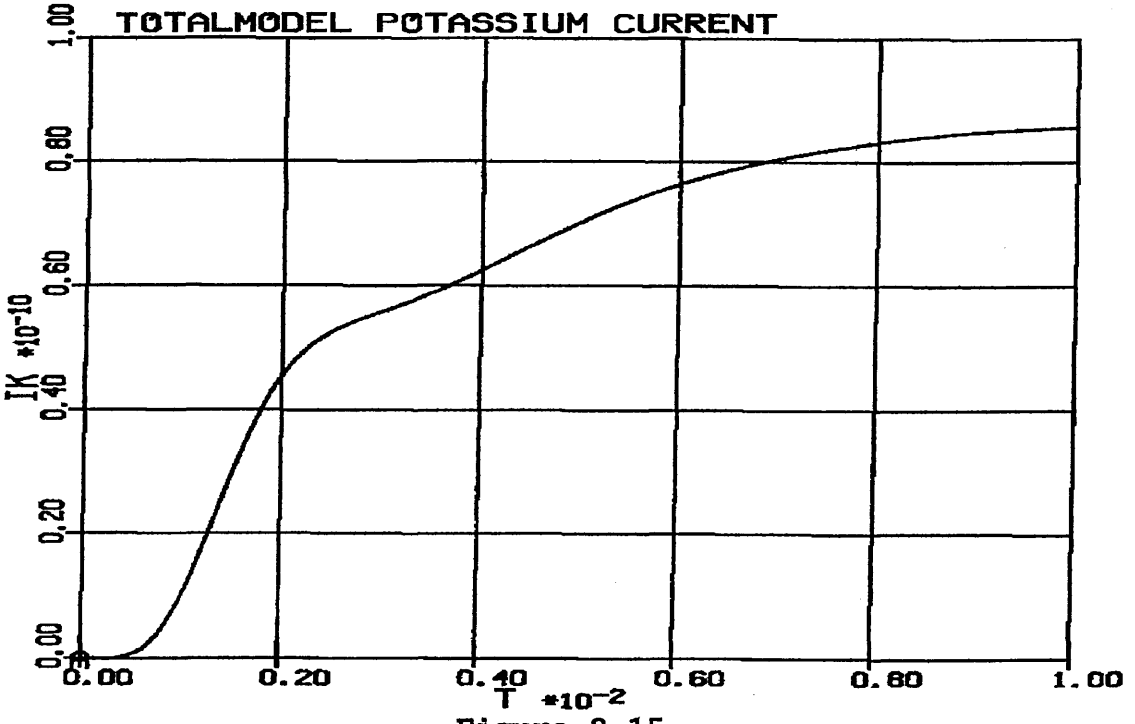


**Figure 8.15**

Graph showing the delayed rectifier potassium current resulting from the simulation of the complete model.

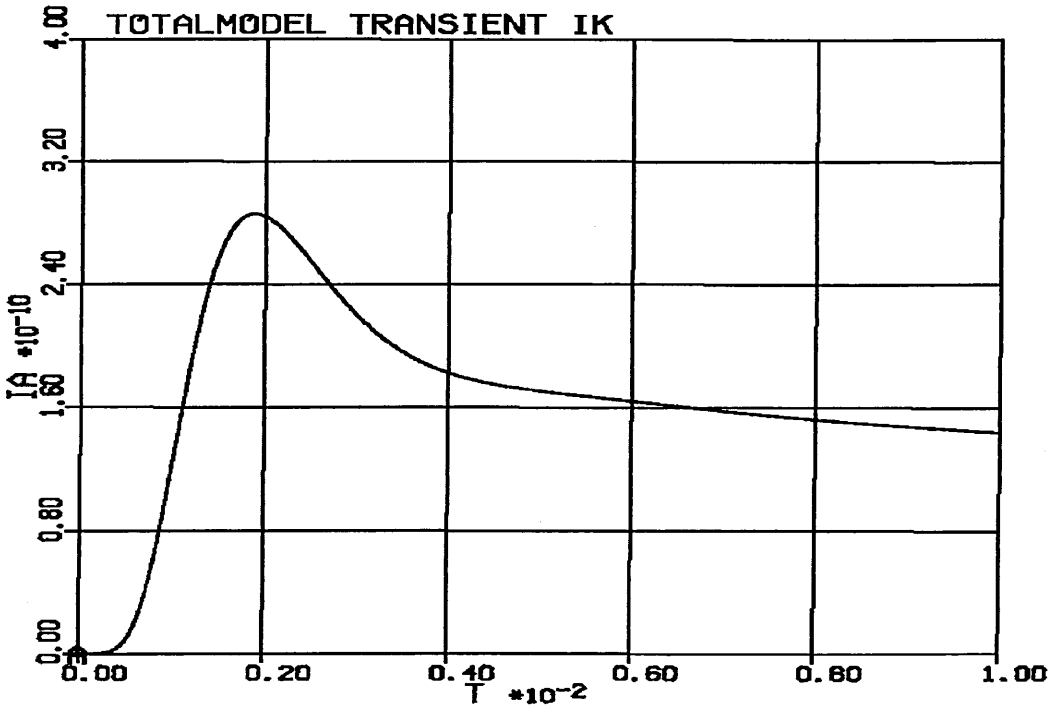


**Figure 8.16**

Graph showing the transient potassium current resulting from the simulation of the completed model.

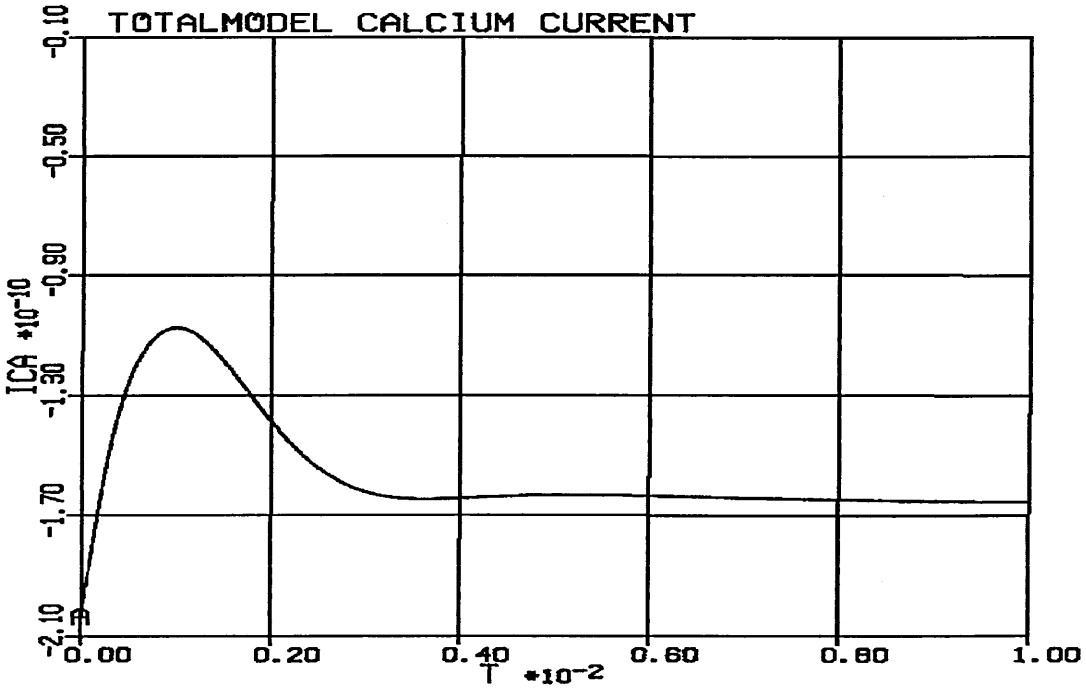


**Figure 8.17**

Graph showing the calcium current resulting from simulation of the completed model.

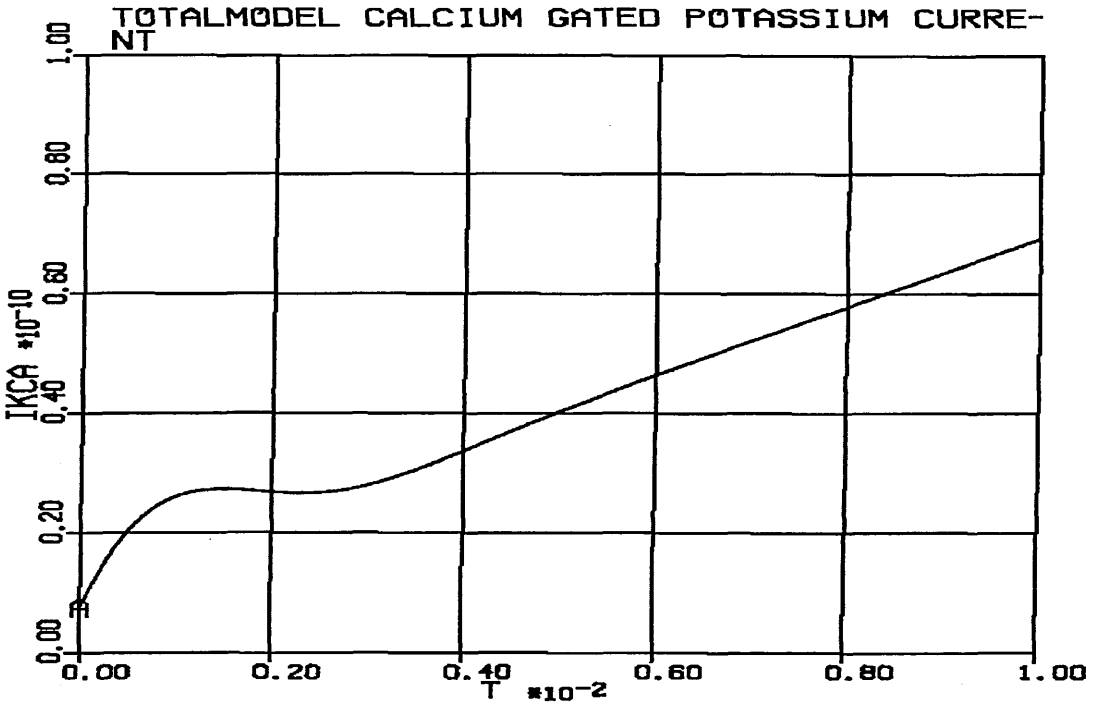


**Figure 8.18**

Graph showing the calcium-gated potassium current in the completed model during a simulated action potential.

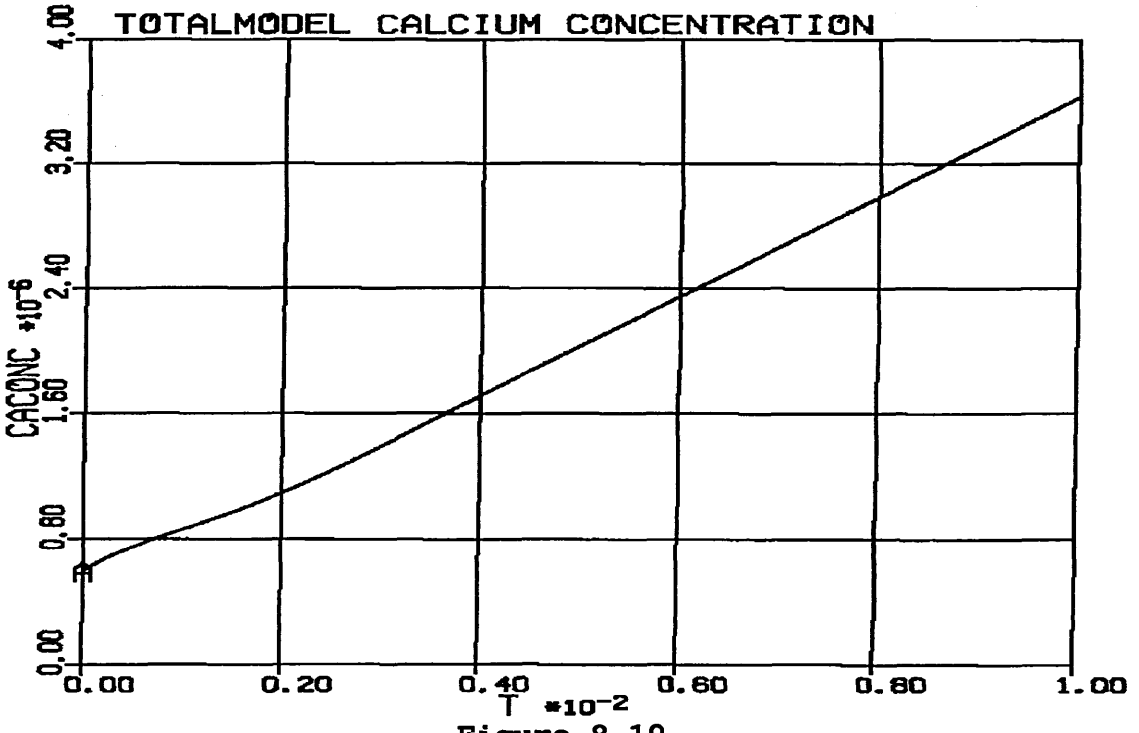


**Figure 8.19**

Graph showing the variation in calcium concentration during a simulated action potential.

It is evident from these results that the model does not describe the electrical behaviour of the oxytocin-secreting cell. Particularly lacking was the inability of the model to demonstrate continuous firing. The observation that the currents involved do not return to their resting values is also of concern. As mentioned previously it is a complex model with many interactions that are difficult to decouple or disentangle. In view of this, it was decided to build up the complete model from simpler blocks and test each part before adding it to the model structure. As a minimal model, the sodium, potassium and leakage currents were chosen. It was anticipated that such a model would then be successively refined by the addition of other channel models until the required results were obtained.

The results of the simplified model are shown here in Figures 8.20 to 8.24.

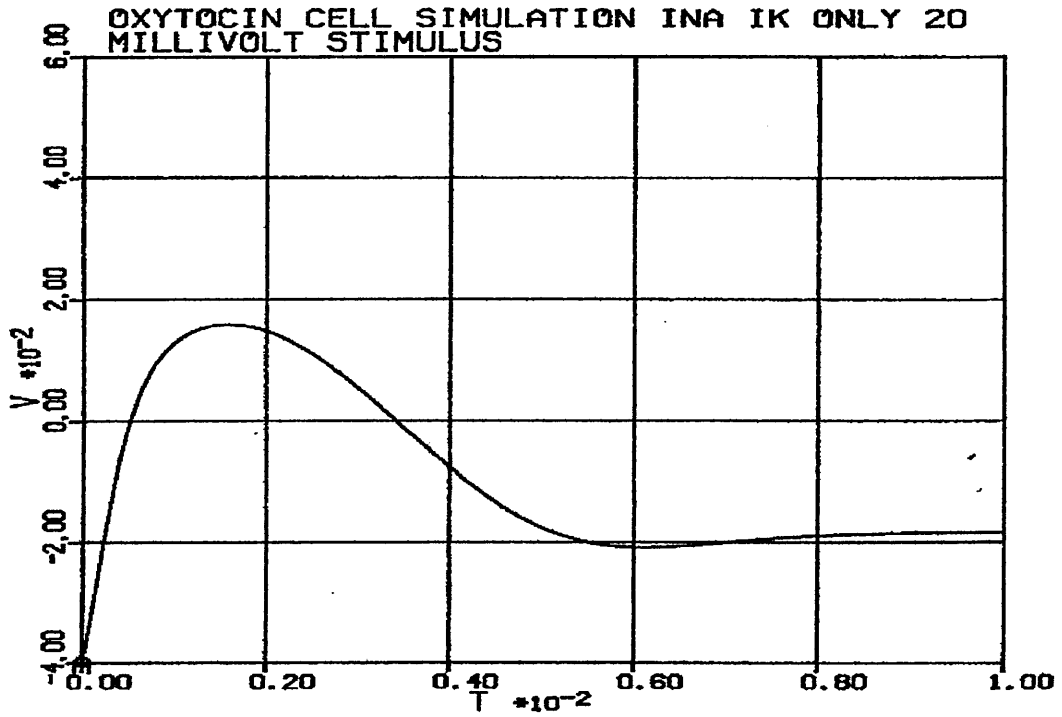


**Figure 8.20**

Action potential generated by simulation of the reduced model.

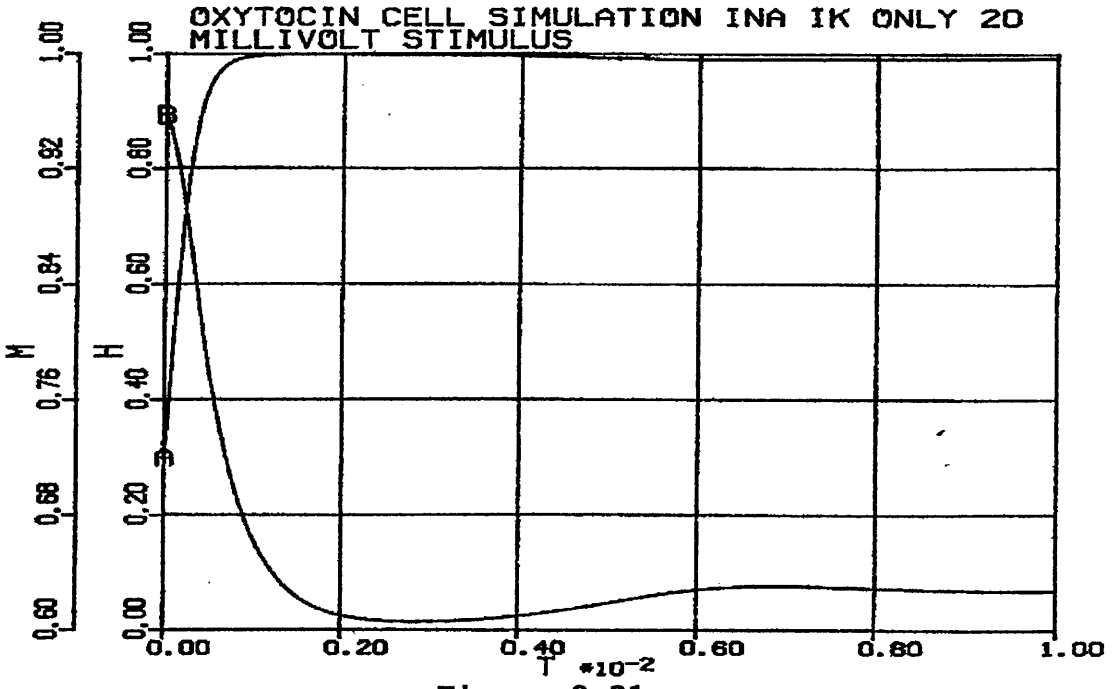


**Figure 8.21**

Graphs showing the variation in sodium activation and inactivation variables during a simulated action potential.

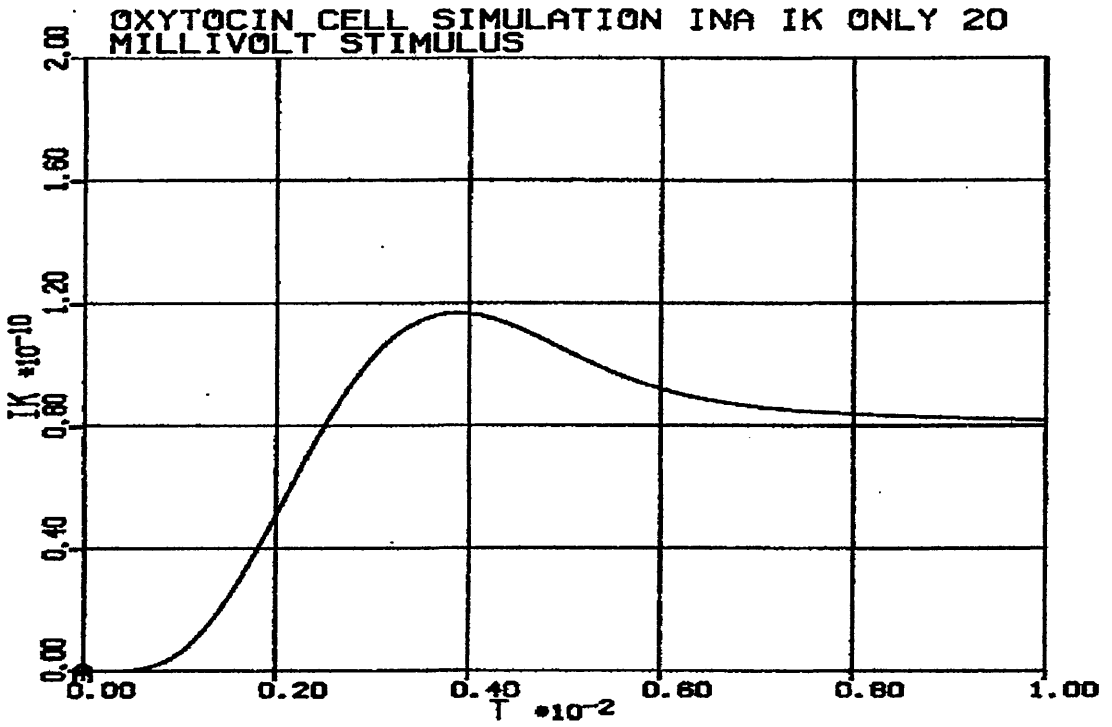


Figure 8.22

Graph showing the potassium current during a simulated action potential in the reduced model.

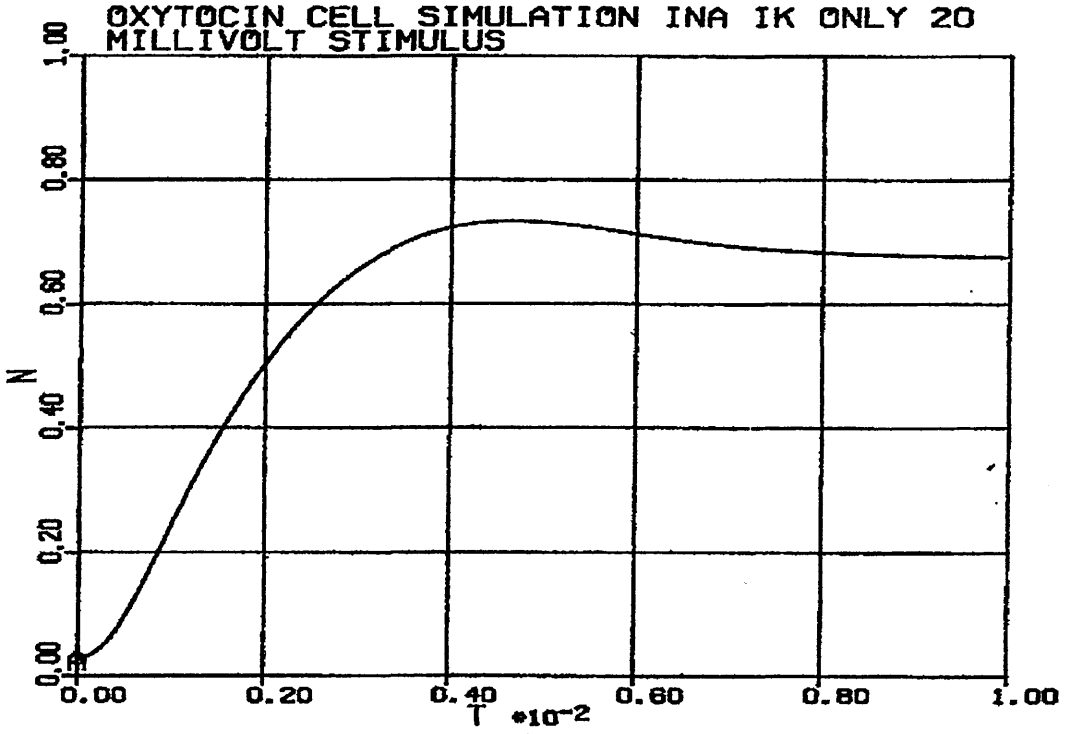


Figure 8.23

Variation of potassium activation in reduced model.

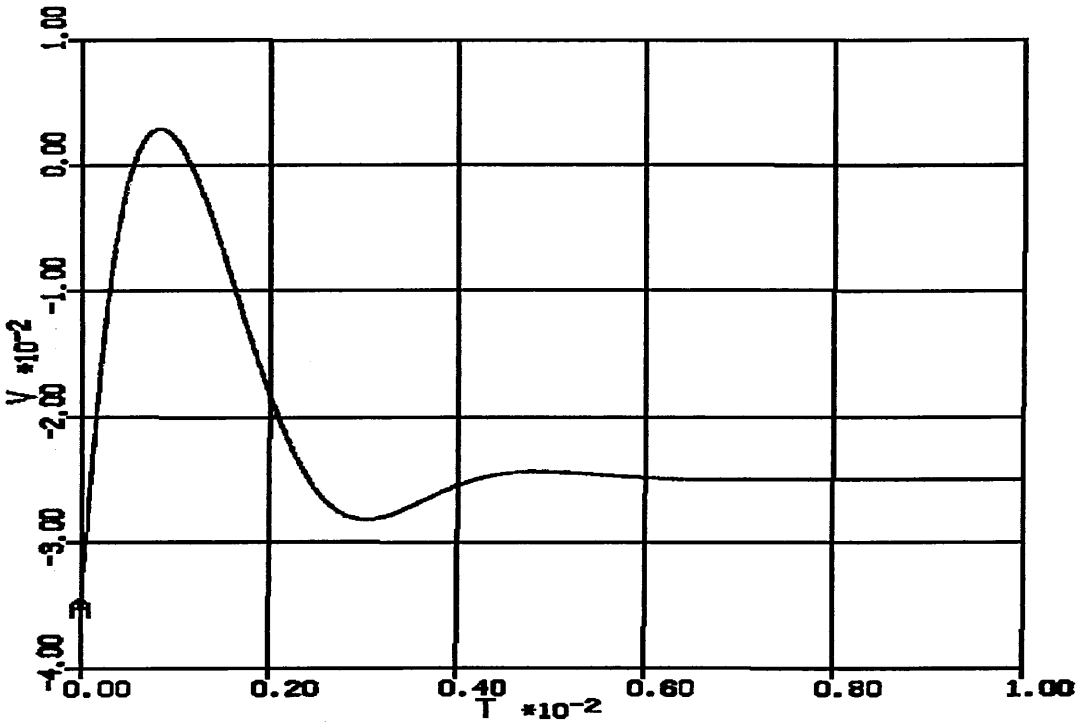


**Figure 8.24**

Action potential generated by reduced model.

Figure 8.20 shows the simulated action potential resulting from this simplified model. Even with these three currents present, the action potential is not returning back to the resting potential. Figure 8.21 shows the activation and inactivation variables responsible for controlling the sodium current. The inactivation starts from a higher value than the Hodgkin-Huxley model. The value is nearer 0.9 than 0.6. The activation variable m also starts out from a higher value than expected. During the course of the simulation, the inactivation variable decreases to near zero but the activation variable quickly reaches a value near 1 and remains there. This is not the behaviour normally seen during an action potential simulation. The modified Hodgkin-Huxley model described in Chapter 4 clearly shows the activation and inactivation variables returning to near their starting

values after an action potential.

The potassium current in Figure 8.22 also shows an incomplete return to the resting state. The steady-state potassium activation n shown in Figure 8.23 starts out from near zero as expected but does not return to zero.

Changing the resting potential to a lower value and giving an increased stimulus results in the action potential shown in Figure 8.24. The membrane voltage does still not return to zero under these conditions. However, the sharpness of the spike has increased and the undershoot of the steady-state value is more pronounced.

Because Hodgkin and Huxley's sodium current does describe the sodium current quite well, it was decided to replace the existing sodium model with Hodgkin and Huxley's by using appropriate scaling factors. In translating the model across so that it becomes relevant to the oxytocin cell, several factors need to be taken into consideration.The first of these is the fact that Hodgkin and Huxley translated all the functions along the voltage axis so that the resting potential became zero. This means that all the functions have to be rescaled by an amount proportional to the resting potential of the squid giant axon. This has been discussed on page 57 and shown in Figures 3.3 and 3.4. The next point to be considered is the units used in their model. This has been discussed on page 59. To determine the effects of altering the units, two programs were written in the ACSL language. These were called HHUNSCALED and HODGHABS respectively to denote the original H-H model and the model scaled by appropriate factors to produce a model whose variables were

expressed in standard SI units. Since this is a fairly routine exercise and yielded the expected results, this piece of work has been omitted from this discussion. Another point to consider is adjusting the maximal conductance to give a current whose amplitude is the same as that observed in the oxytocin cell. The final point to be considered is the change in temperature between the two systems. This is a general point and must be considered when using data from other systems. This point will now be discussed.

## EFFECT OF VARYING TEMPERATURE

Hodgkin and Huxley's work involved making measurements on the squid giant axon at differing temperatures. Some readings were taken at room temperature and others at temperatures similar to those actually encountered in the natural environment. The equations derived were corrected for temperature by using a $Q_{10}$ of 3 and multiplying the rate functions ($\alpha$'s and ß's) by the appropriate factor. The same approach has been used in this project. Many of the experimental results used were derived at room temperature and are therefore not appropriate to describe the behaviour at 37°C. Various workers have derived $Q_{10}$ factors of similar magnitude to that found by Hodgkin and Huxley. In the absence of specific data for temperature correction factors, Hodgkin and Huxley's value has been used. Several experiments were performed to determine the effect of temperature on the various models that have been derived during the development of this project. Figures 8.25 to 8.28 show the effect of temperature on simulated action potentials. The first and most obvious point to note is that action potentials are more brief at elevated temperatures and firing rate in a continuously firing system is increased. This is to be expected since the rate constants are multiplied by a positive number greater than unity at temperatures higher than those appropriate to the actual experimental conditions. What is less obvious is that the action potential amplitude is reduced at higher temperature. Noble (Noble 1966) gives an explanation of why this should occur. His discussion of this phenomenon will not be reproduced in detail here. However, it

will be useful to note that the reasoning is based upon the difference in the effects of temperature upon the rate of depolarization and rate of repolarization of the membrane. The effect of temperature increase on the potassium and sodium current is shown in Figures 8.29 to 8.32.

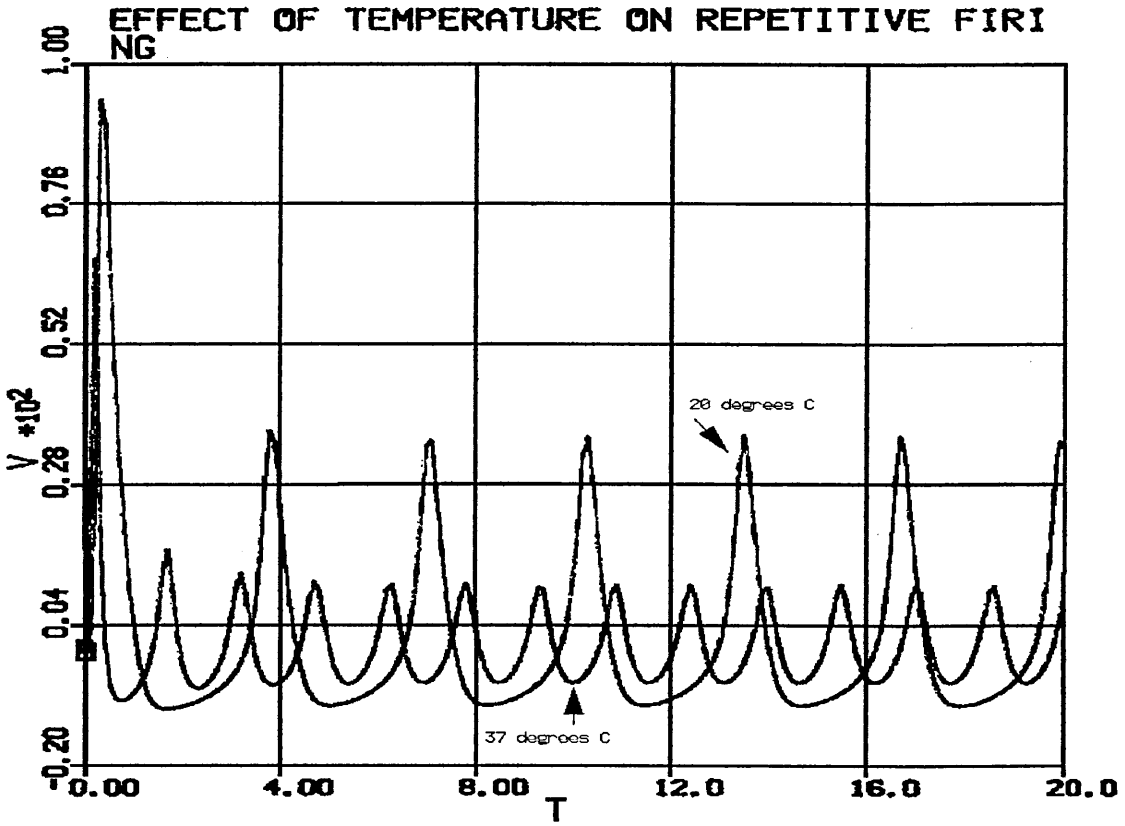


**Figure 8.25**

The effect of increasing the temperature on a repetitively firing neurone model are shown here. The slower, larger amplitude trace results from the lower temperature.

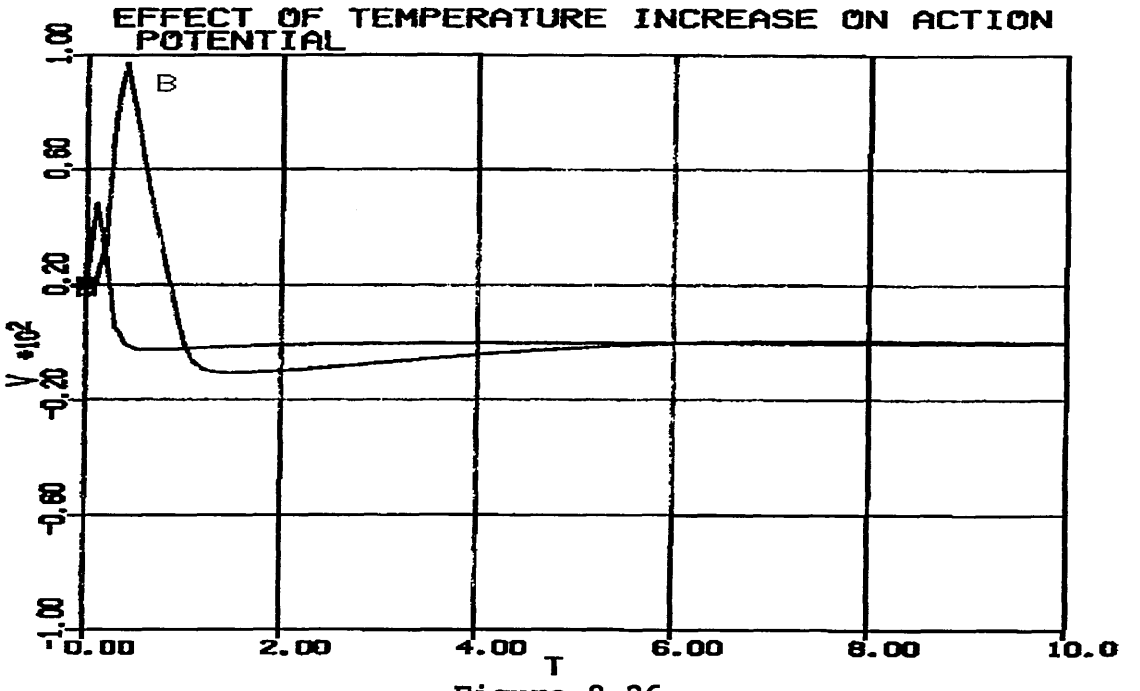


**Figure 8.26**

This figure shows the effect of increasing the temperature in the H-H model. The larger, slower action potential was calculated at the lower temperature.

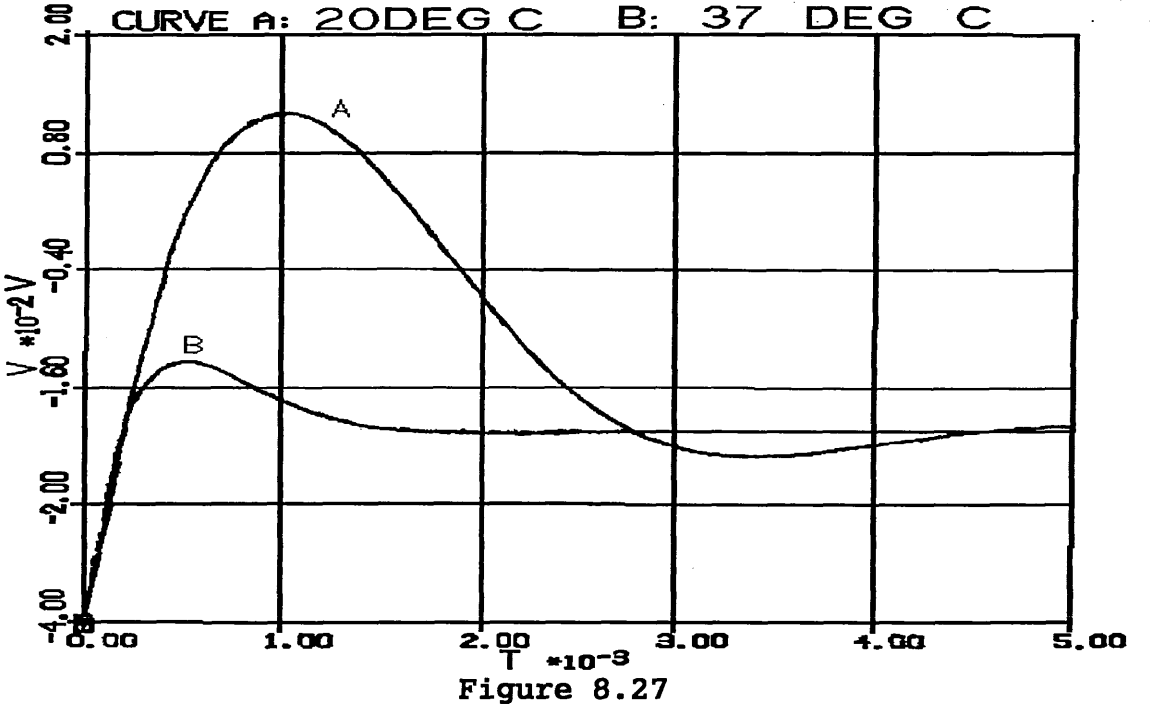


**Figure 8.27**

Action potential simulation from oxytocin cell model shown on an expanded time scale.

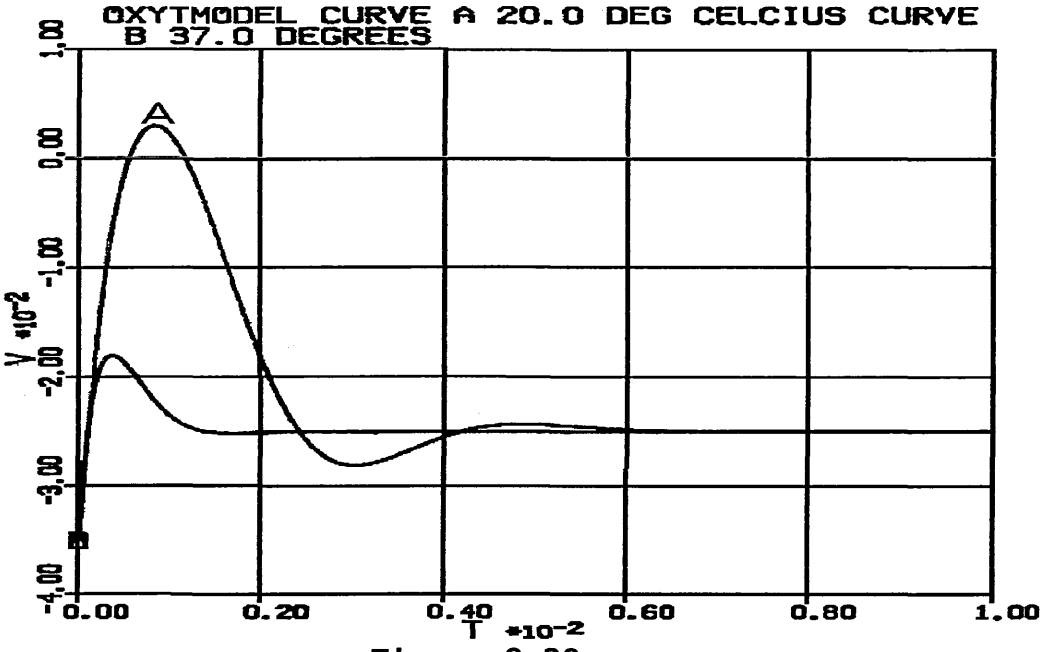


**Figure 8.28**

Simulation showing the effect of temperature change on action potential in oxytocin cell model.

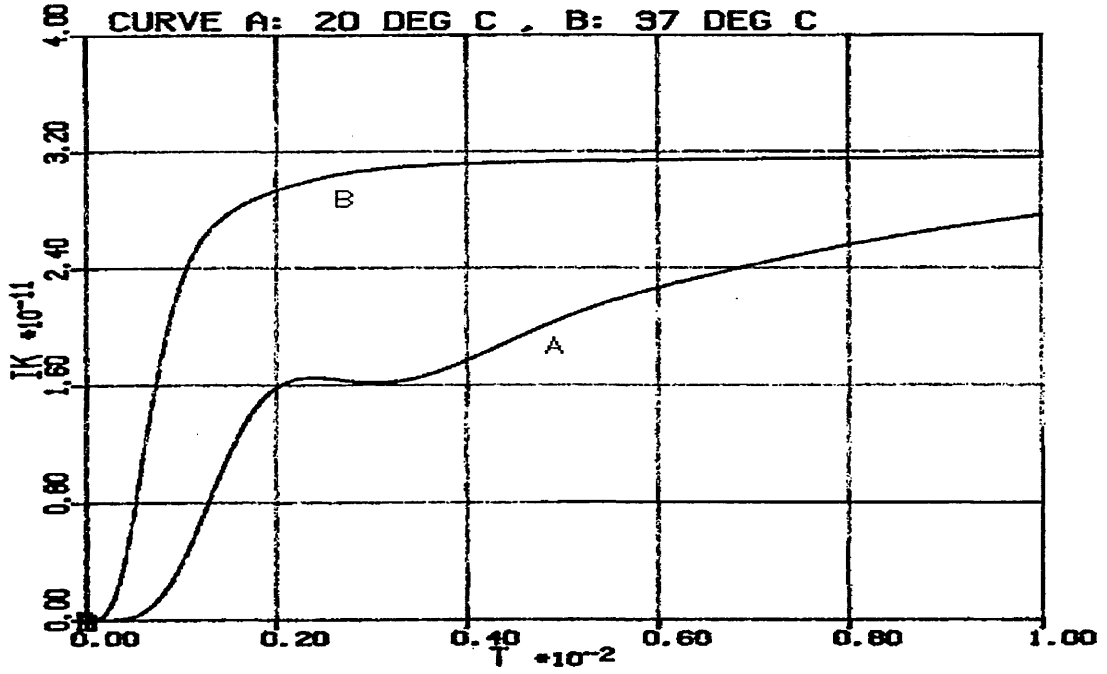


**Figure 8.29**

Graph showing the effect of temperature change on the potassium delayed rectifier current. The slower current is at the lower temperature.

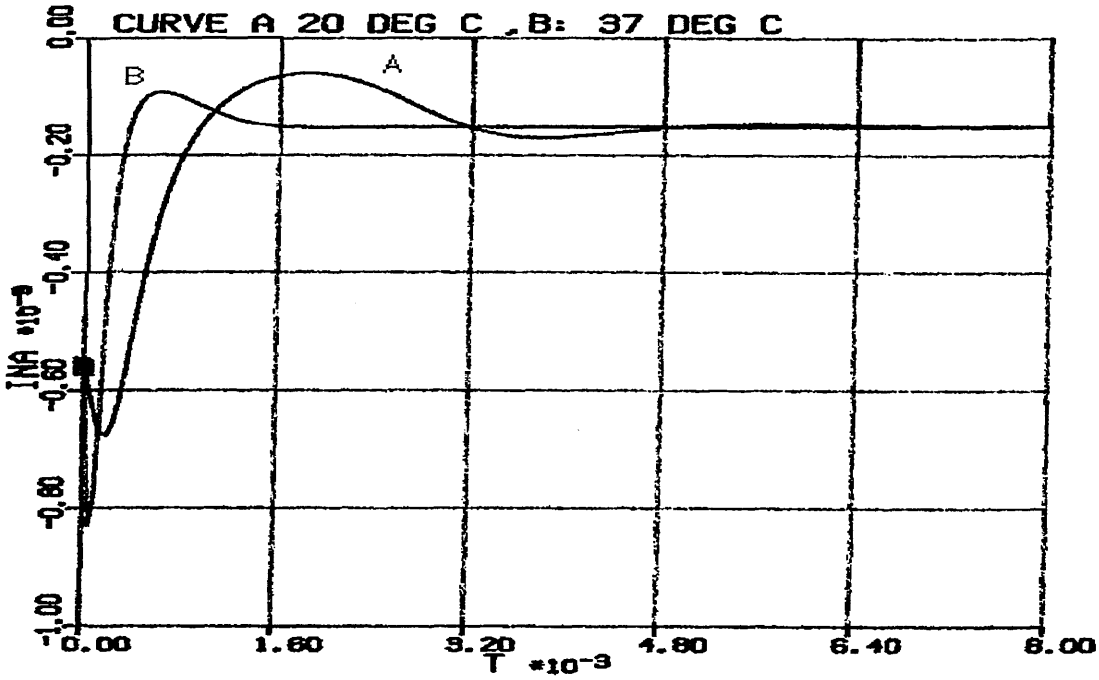


**Figure 8.30**

Plot showing the effect of temperature on the sodium current in the oxytocin cell model. The larger, slower trace corresponds to the lower temperature.

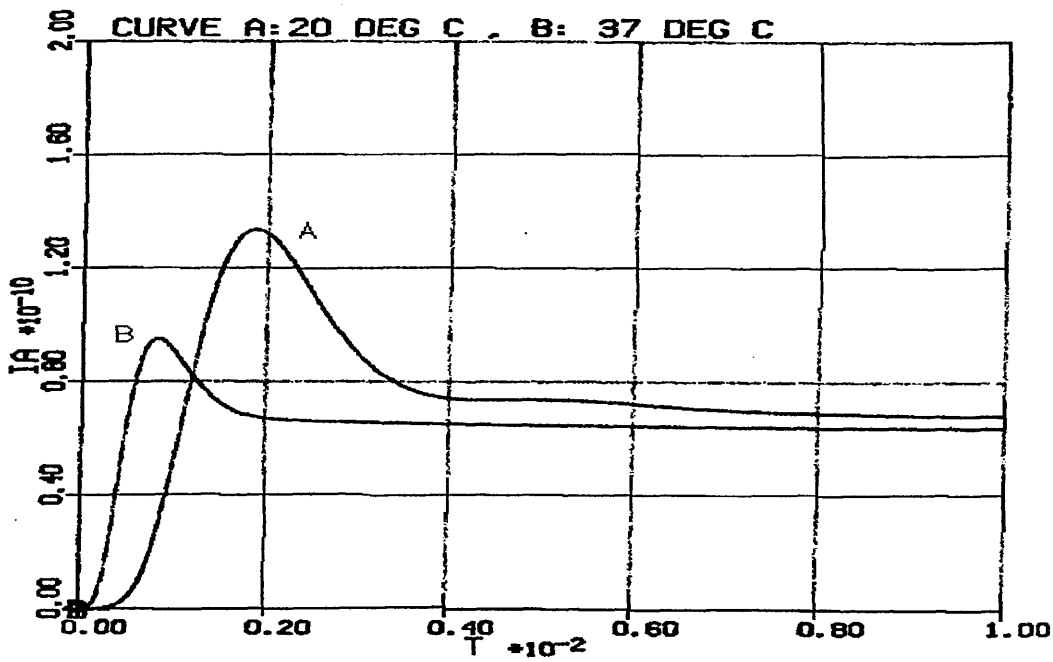


**Figure 8.31**

This figure shows the effect of temperature on the transient potassium current. The smaller, faster trace results from the higher temperature.

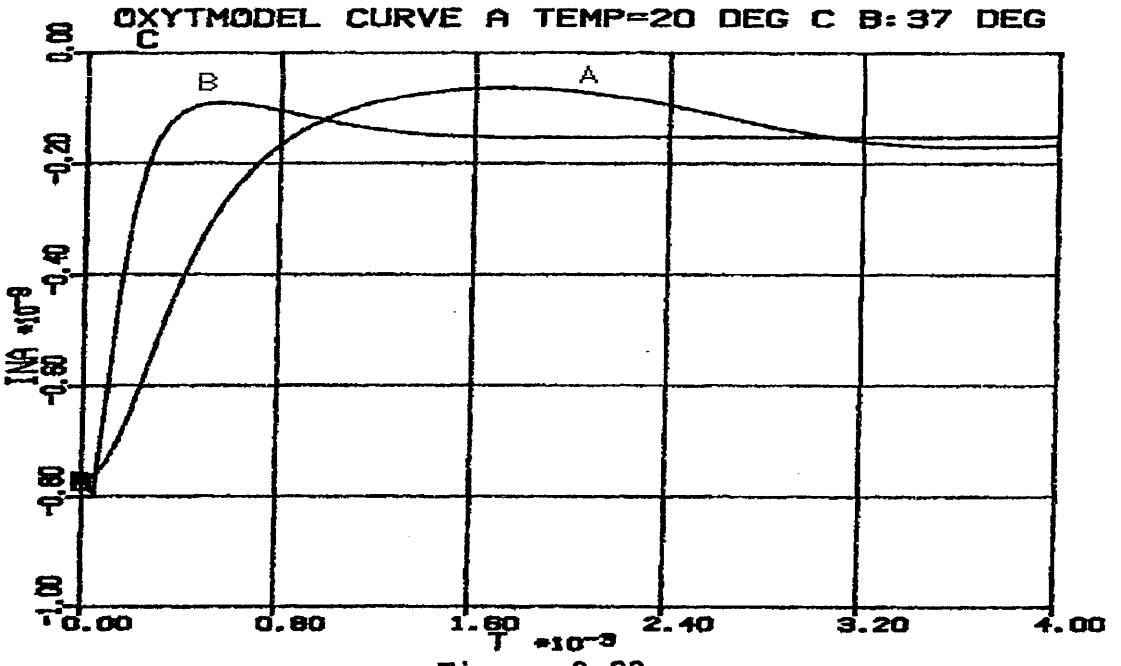


**Figure 8.32**

This figure shows the effect of temperature on the sodium current on an expanded time scale.

Adrian and Almers (Adrian & Almers 1976), and Takashima and Yantorno have investigated the variation of membrane capacitance in nerve membrane. In Hodgkin and Huxley's squid giant axon model, the membrane capacitance appears as a fixed model parameter, having a value of $1\mu F/cm^2$. This figure is generally accepted as representing the capacitance of the lipid bilayer that comprises nerve membranes. The above-mentioned workers have found the membrane capacitance to be voltage-dependent and that capacitance increases with depolarization.

Several trial simulations of the basic Hodgkin-Huxley model were performed, varying the membrane capacitance between runs. The results are shown in Fig. 8.35. The cell capacitance was derived by considering the cells to be smooth spheres. The surface area was calculated to be approximately $2 \times 10^{-9}$ $\mu m^2$ using the formula $A = 4\pi r^2$. The above figure for the specific capacitance of lipid bilayers was then used to calculate the total capacitance of the cell. Consideration of the simulation results show that the effects are as expected from the physics of the situation. Given a fixed current flow, a smaller capacitance will charge up faster and to a higher voltage (in a given time interval) than a larger capacitance. Current is simply the flow of electrical charge and a higher current implies a higher rate of flow of charge. The fundamental relationship between voltage, charge and capacitance is given in equation 8.19.

$$Q = CV \quad \ldots\ldots\ldots\ldots\ldots\ldots\ldots\ldots \quad (8.19)$$

Differentiating with respect to time gives

$$i = C_m \frac{dV}{dt} \quad \ldots\ldots\ldots\ldots\ldots\ldots\ldots\ldots \quad (8.20)$$

This equation confirms that a high rate of change of voltage is associated with a high current. Since the effects described by Adrian et. al. are fairly small it was decided that capacitance variation with membrane voltage would not dramatically affect the membrane dynamics. For this reason, such effects are not considered further.

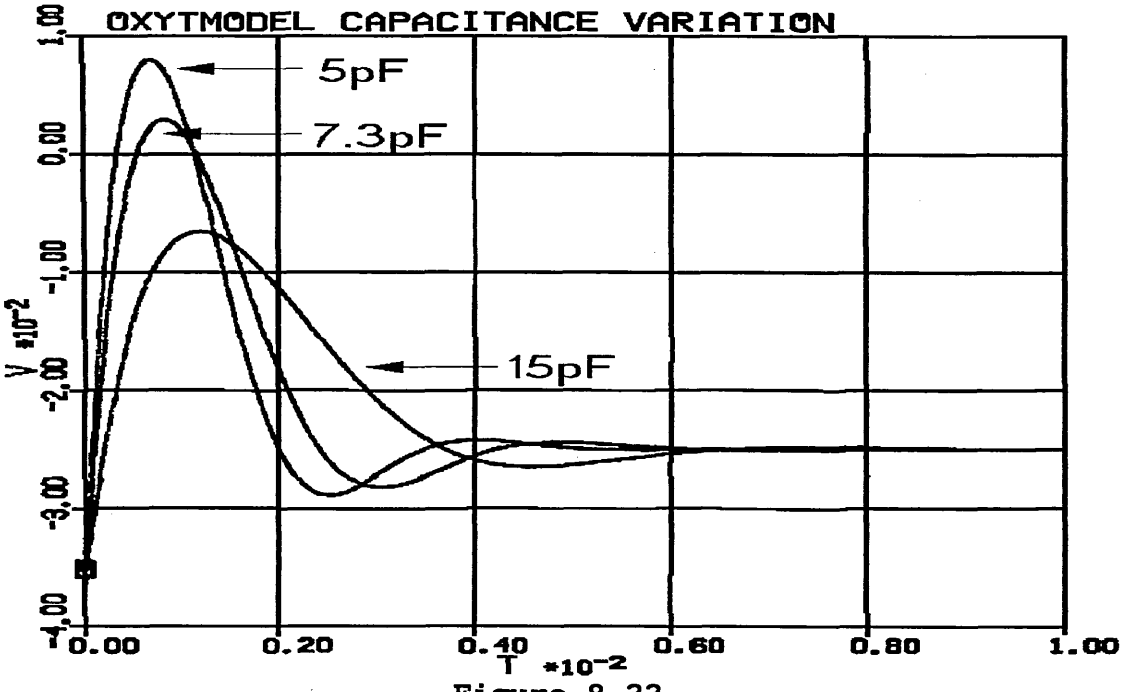


**Figure 8.33**

Figure showing the effects of changing the capacitance of the oxytocin cell model.

## EFFECT OF CHANGING PARAMETERS

One of the important features of a model is its robustness in the face of changes in the parameter values. In this instance it would be useful to determine how widely the behaviour of the model varied, given changes in the model parameters. The model parameters under consideration are the constants used in the alpha and beta rate functions, temperature and membrane capacitance having already been discussed. In order to achieve this aim, the constants in various ACSL models were changed to variables that the user could change at will. In equations 8.4 and 8.7 there are three constants in each equation. In equations 8.5 and 8.6 there are only two. These constants were given variable names and initial values. Rerunning voltage-clamp simulations with widely varying parameter values showed that the behaviour of the equations varied relatively little. A series of graphs showing this are reproduced here in Figs. 8.34 to 8.50.

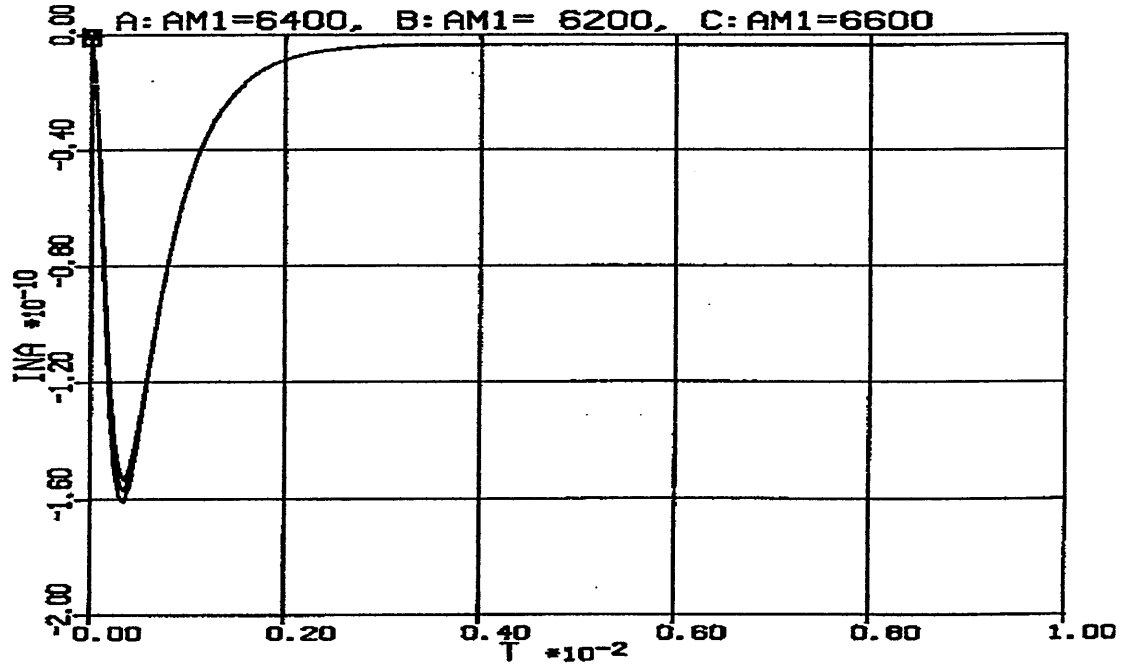


**Figure 8.34**

This shows the effects of varying the parameter alpha-m1 on the sodium current.

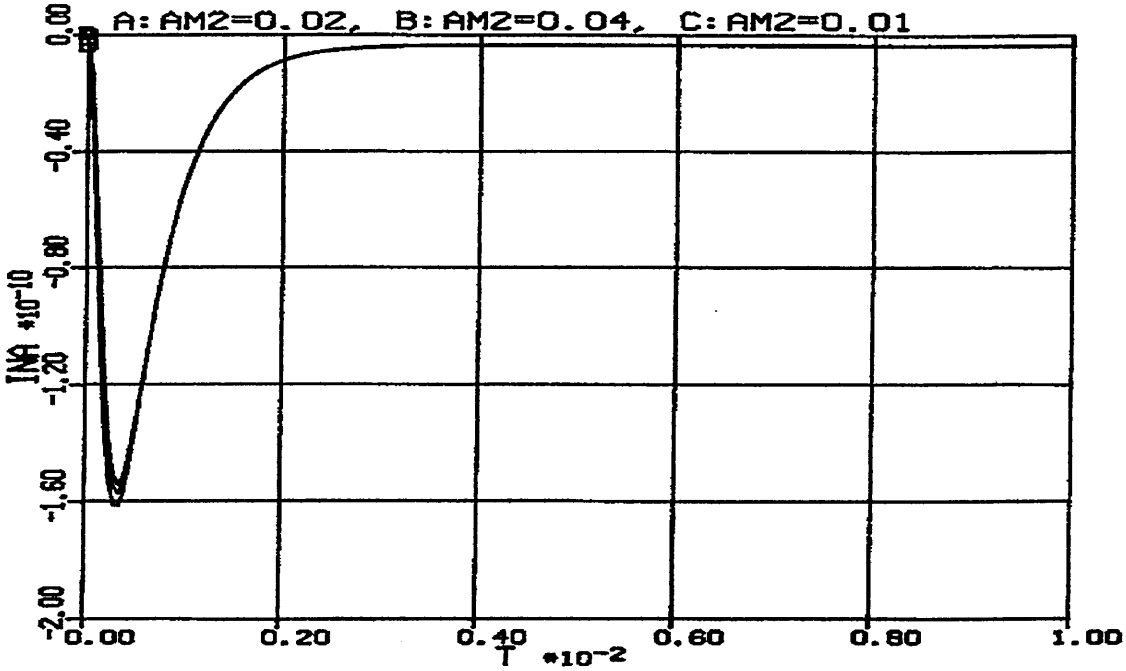


**Figure 8.35**

The effect of varying parameter alpha-m2 on the sodium current is shown here.

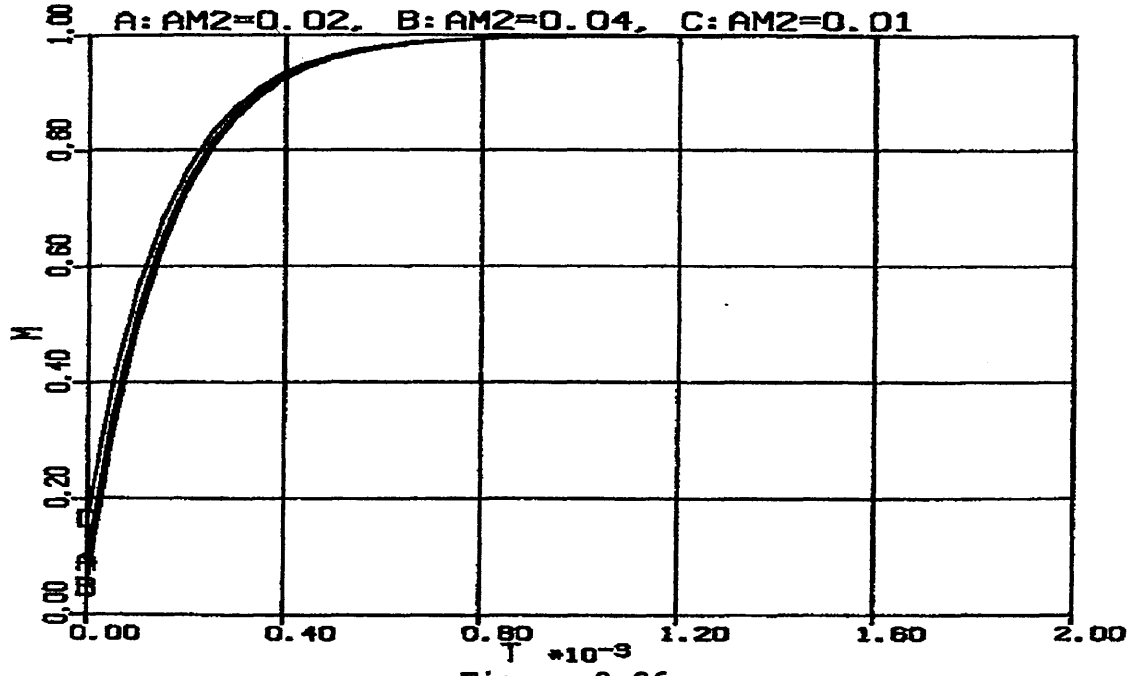


Figure 8.36

This figure shows the effect of varying the parameter alpha-m2 on the steady-state sodium activation.

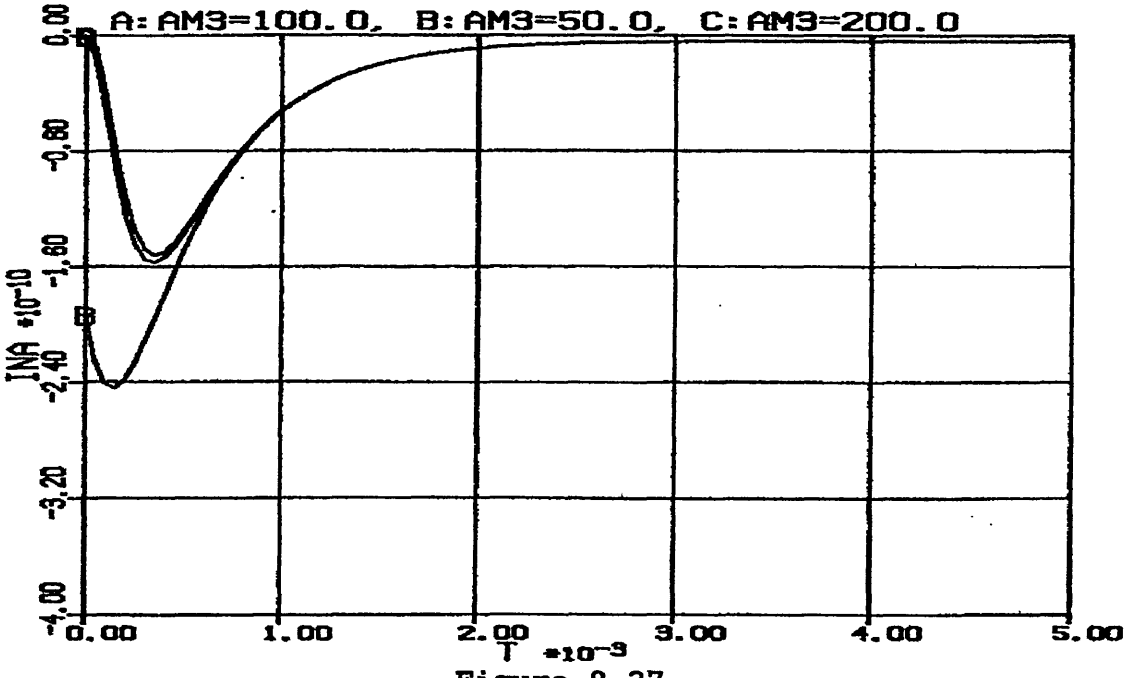


Figure 8.37

This shows the effect of varying the parameter alpha-m3 on the sodium current.

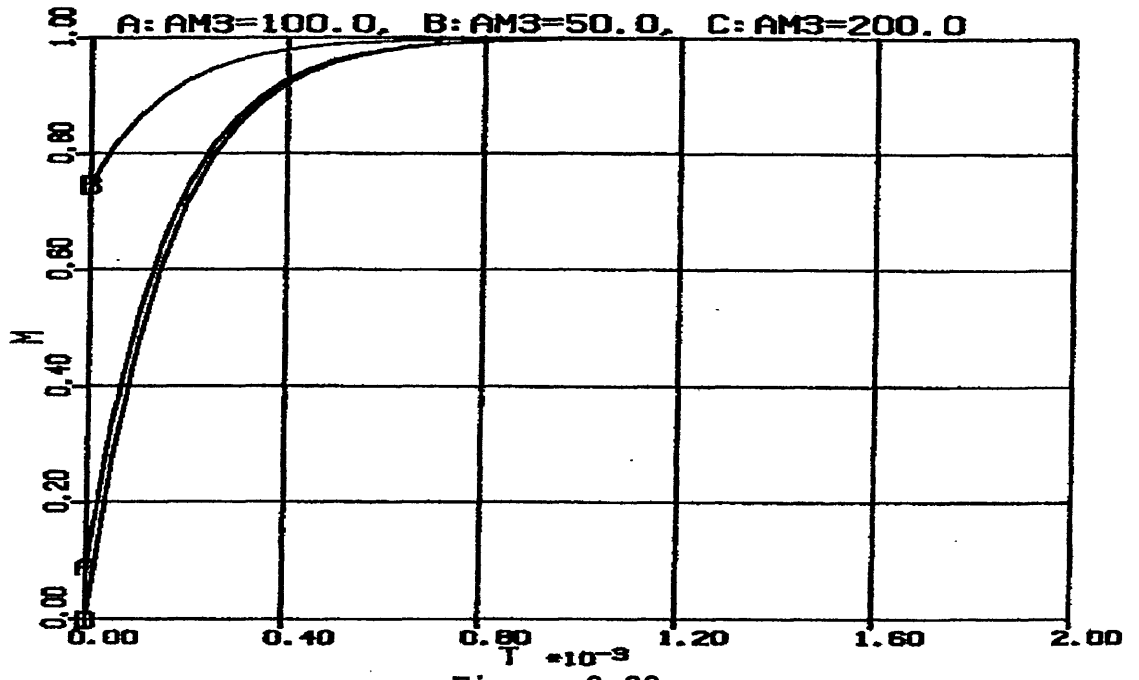


**Figure 8.38**

The effect of changing parameter alpha-m3 on the steady-state sodium activation variable is shown here.

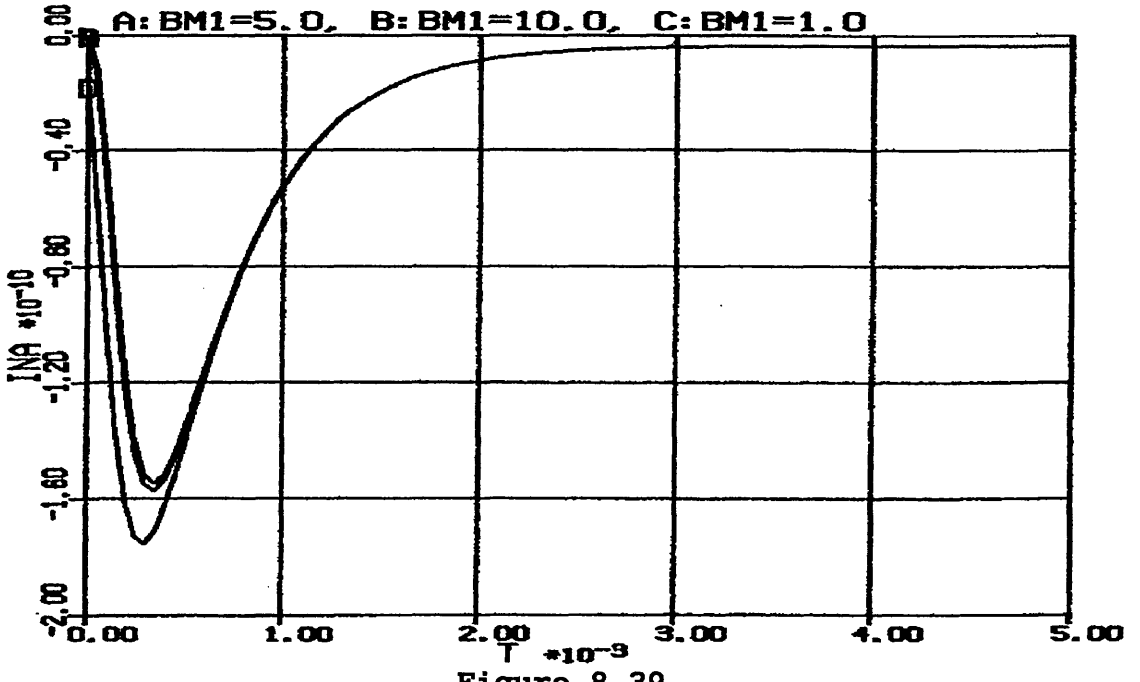


**Figure 8.39**

This figure shows the effect of varying the parameter beta-m1 on the sodium current.

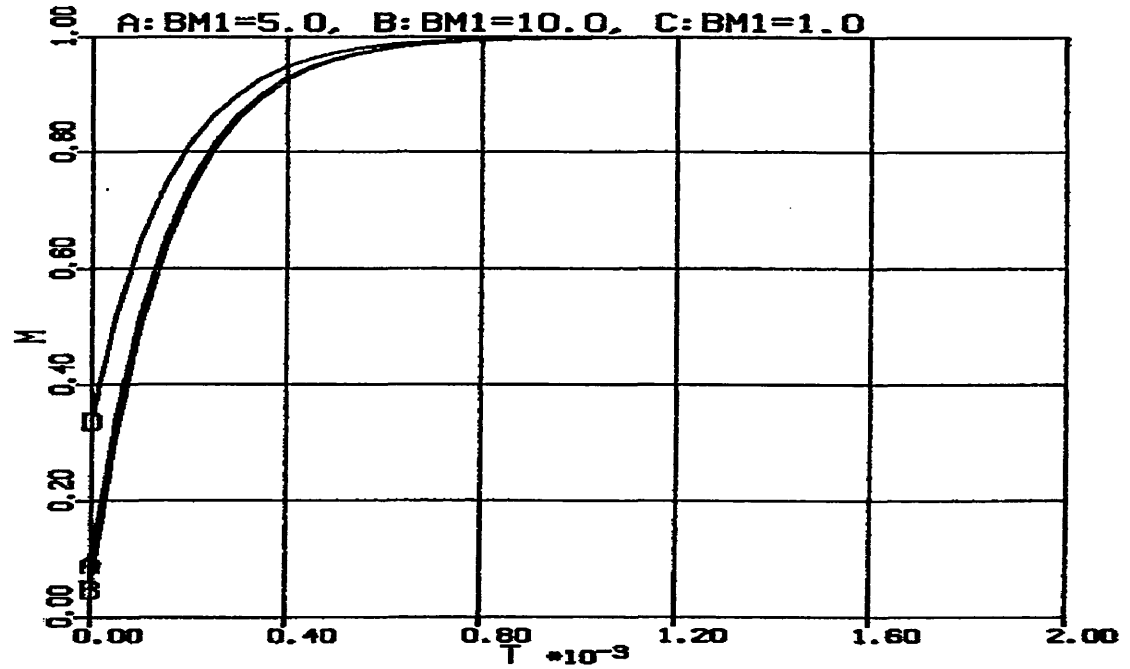


Figure 8.40

The effect of changing the parameter beta-m1 on the steady-state activation is shown here.

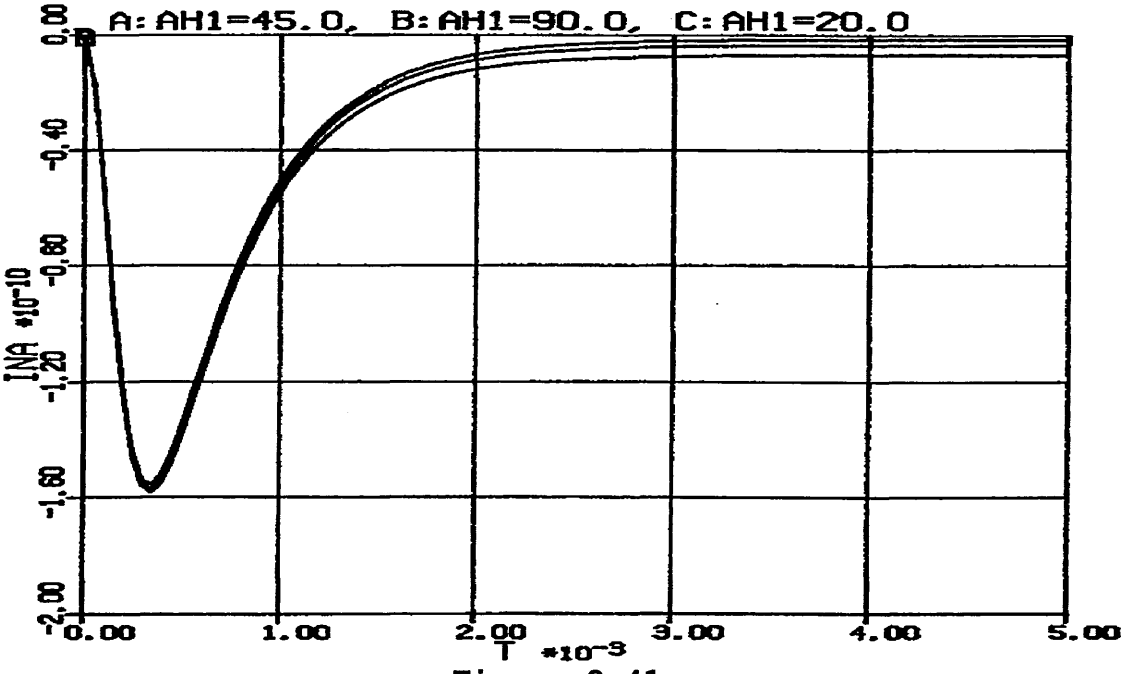


Figure 8.41

This figure shows the effect of varying the parameter alpha-h1 on the sodium current.

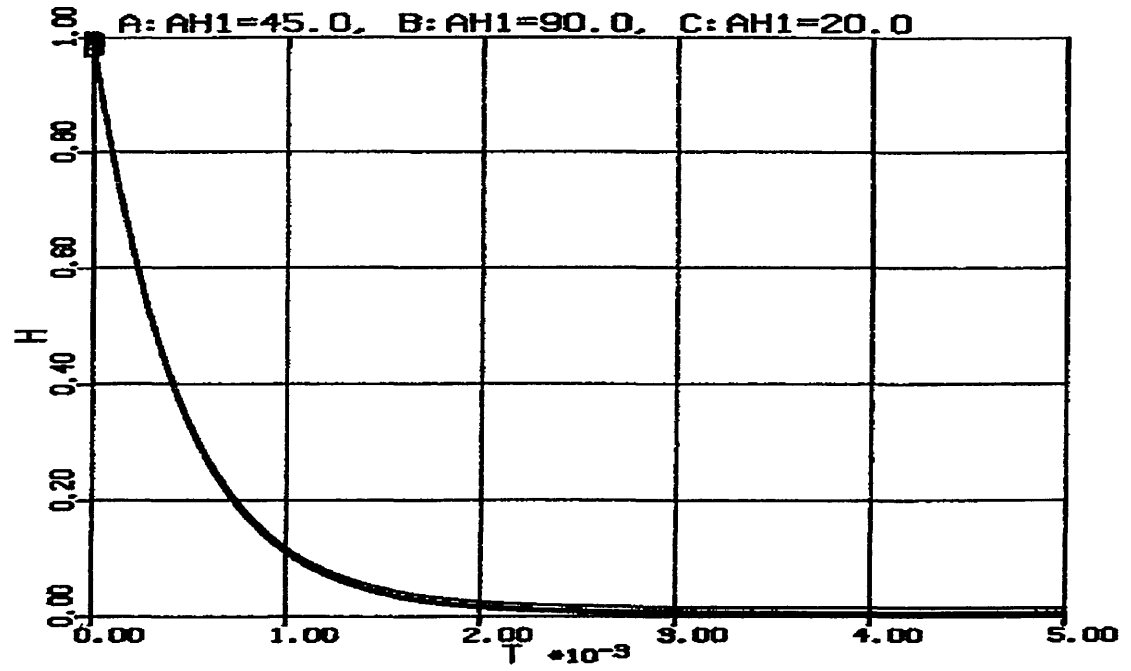


Figure 8.42

The effect of changing the parameter alpha-h1 on the steady-state sodium inactivation is shown here.

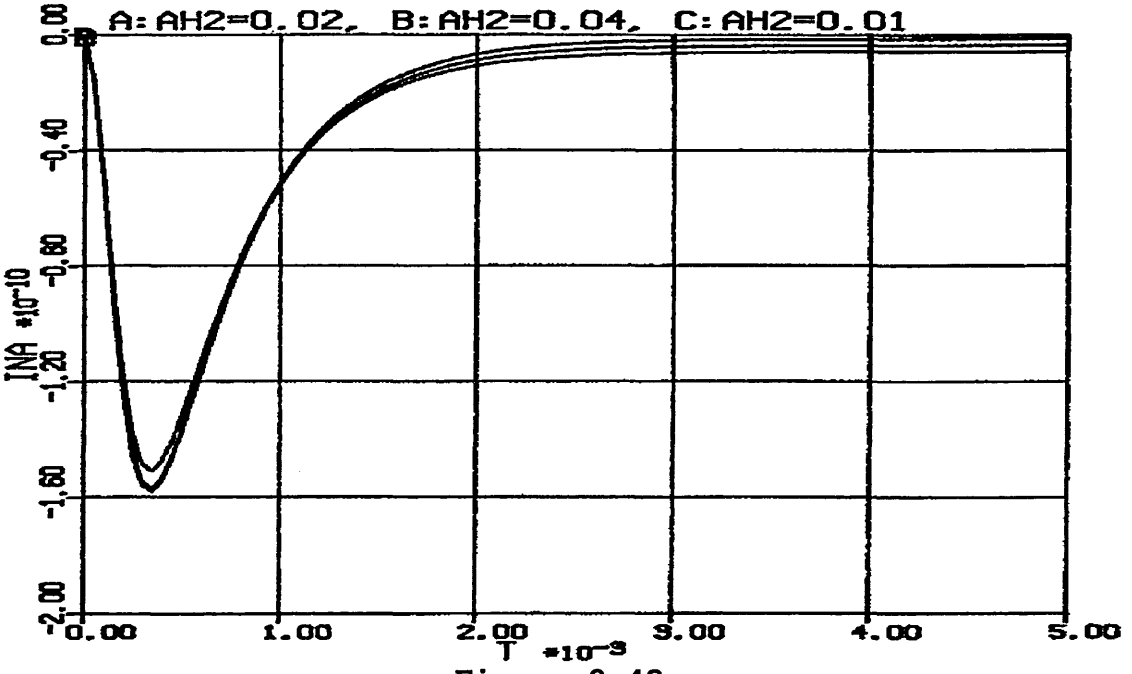


Figure 8.43

This figure shows the effect of varying the parameter alpha-h2, on the sodium current.

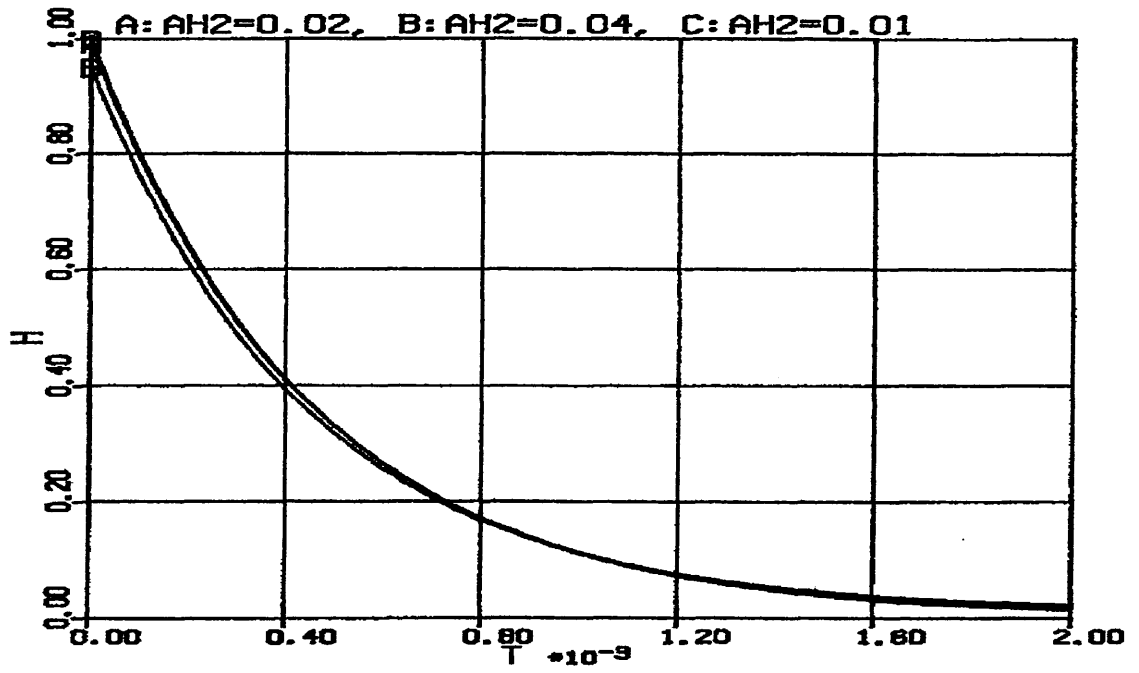


**Figure 8.44**

This figure shows the effect of changing parameter alpha-h2, on the sodium current activation variable.

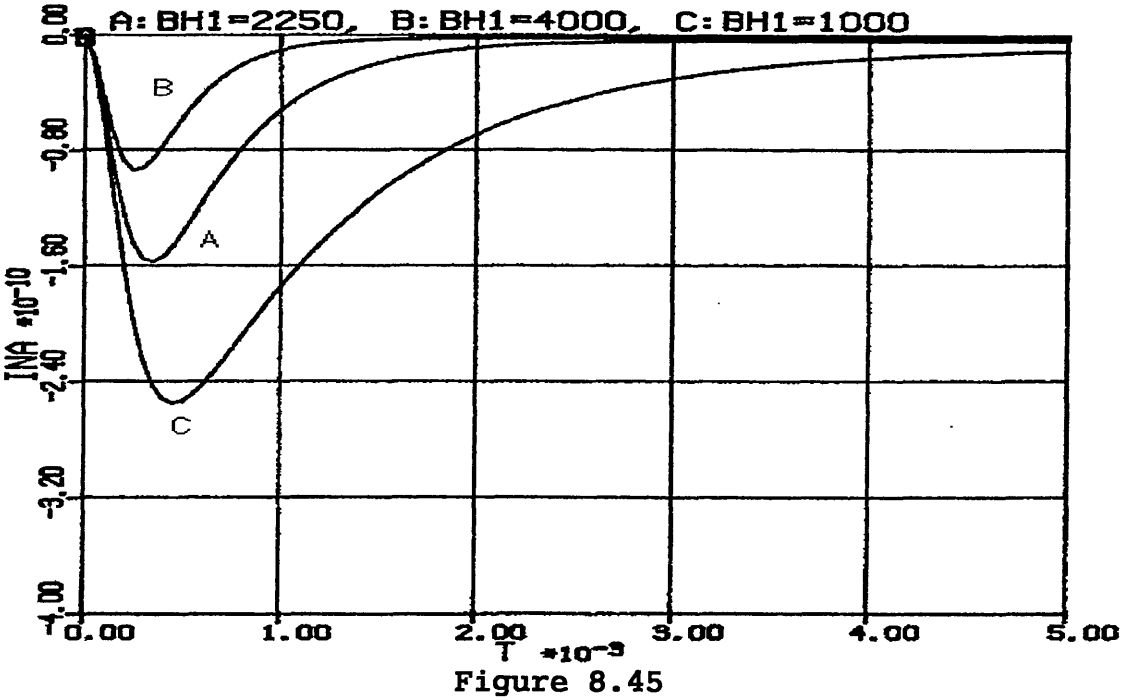


**Figure 8.45**

This figure shows the effect of changing parameter beta-h1, on the sodium current.

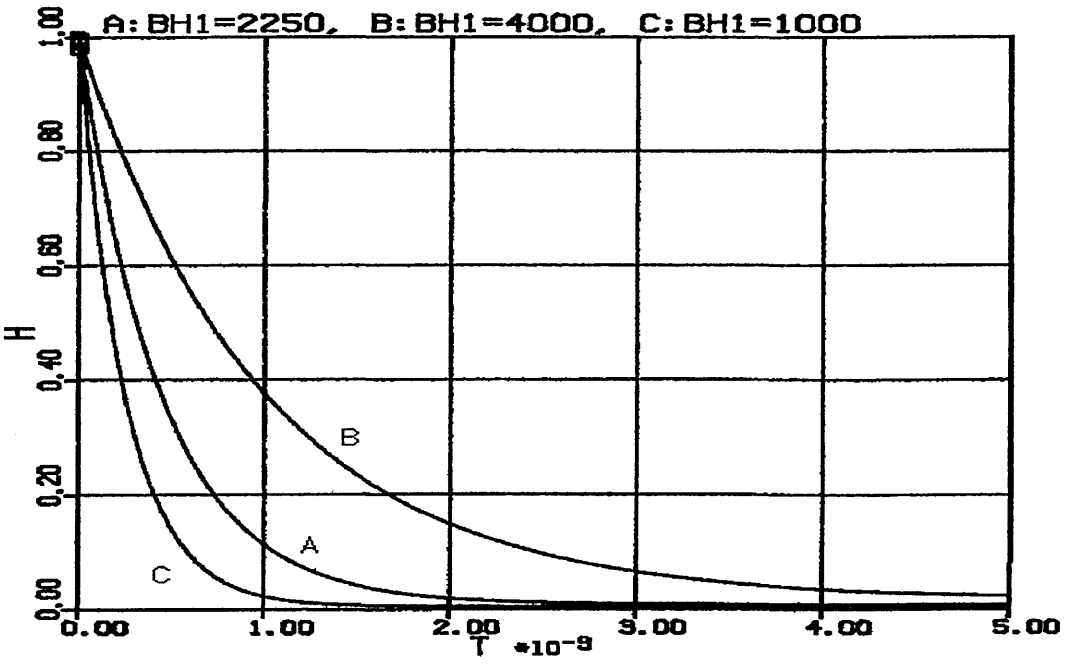


**Figure 8.46**

This figure shows the effect of varying parameter beta-h1, on the sodium current activation variable.

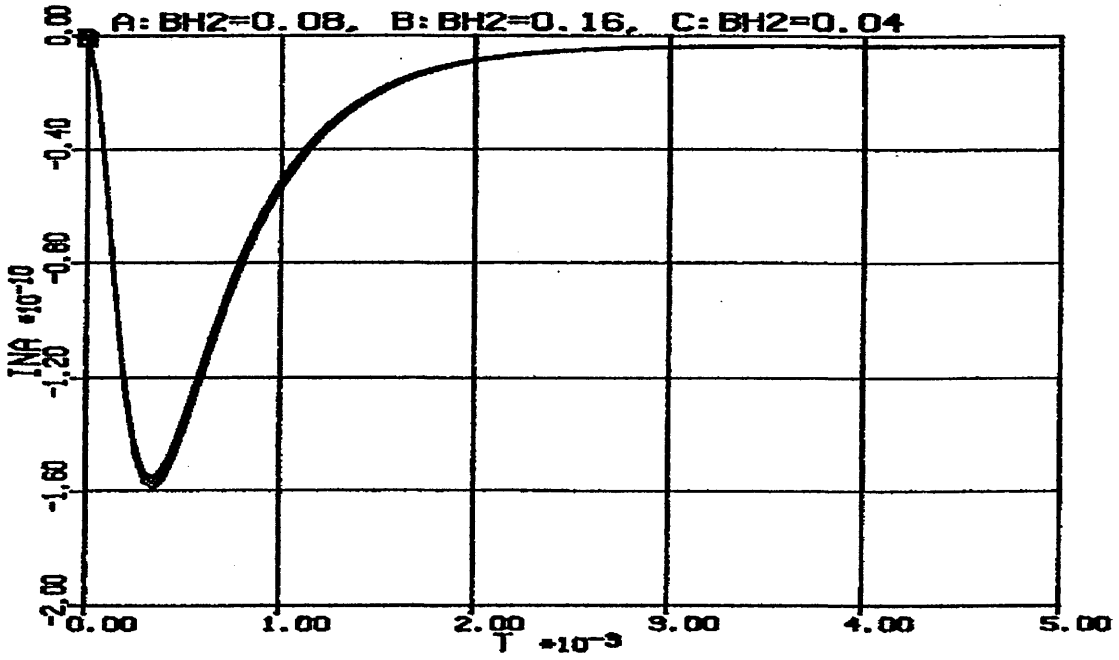


**Figure 8.47**

This figure shows the effect of varying parameter beta-h2, on the sodium current.

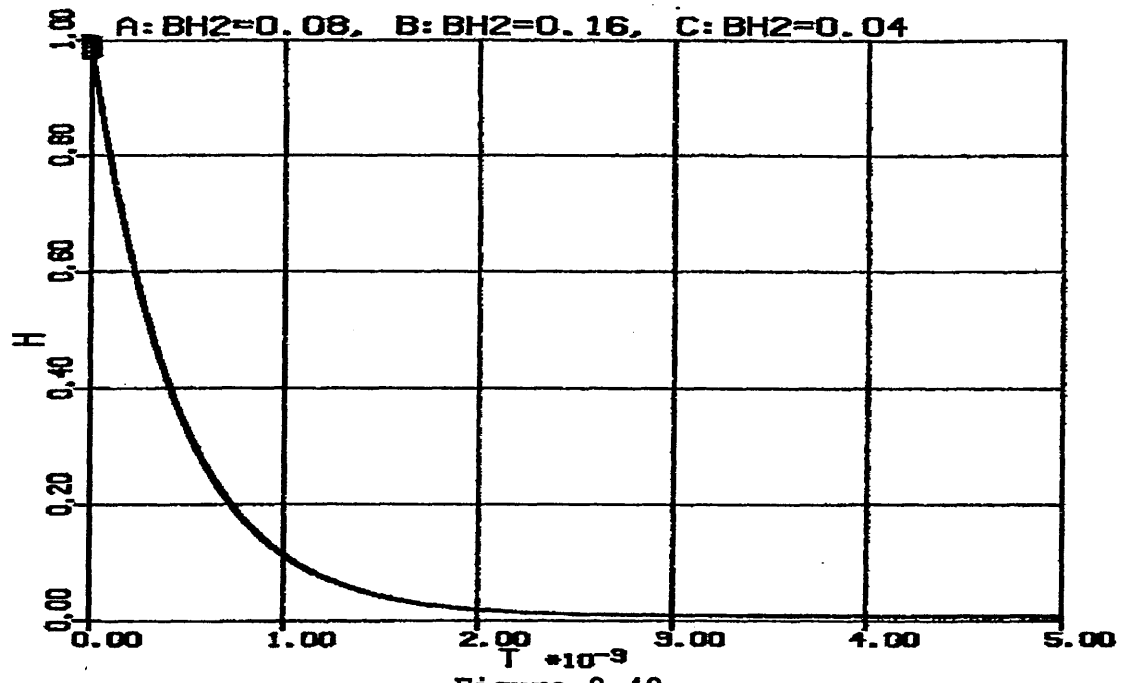


Figure 8.48

This figure shows the effect of changing parameter beta-h2, on the sodium current activation variable.

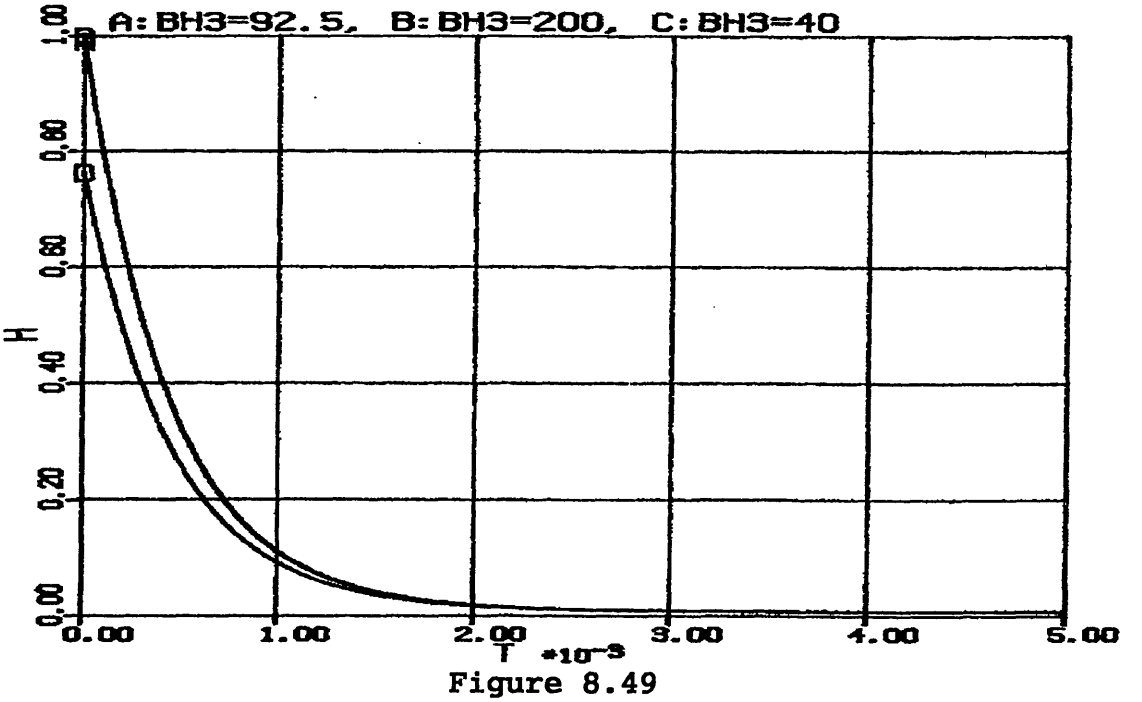


Figure 8.49

This figure shows the effect of changing parameter beta-h3 on the steady-state sodium inactivation variable.

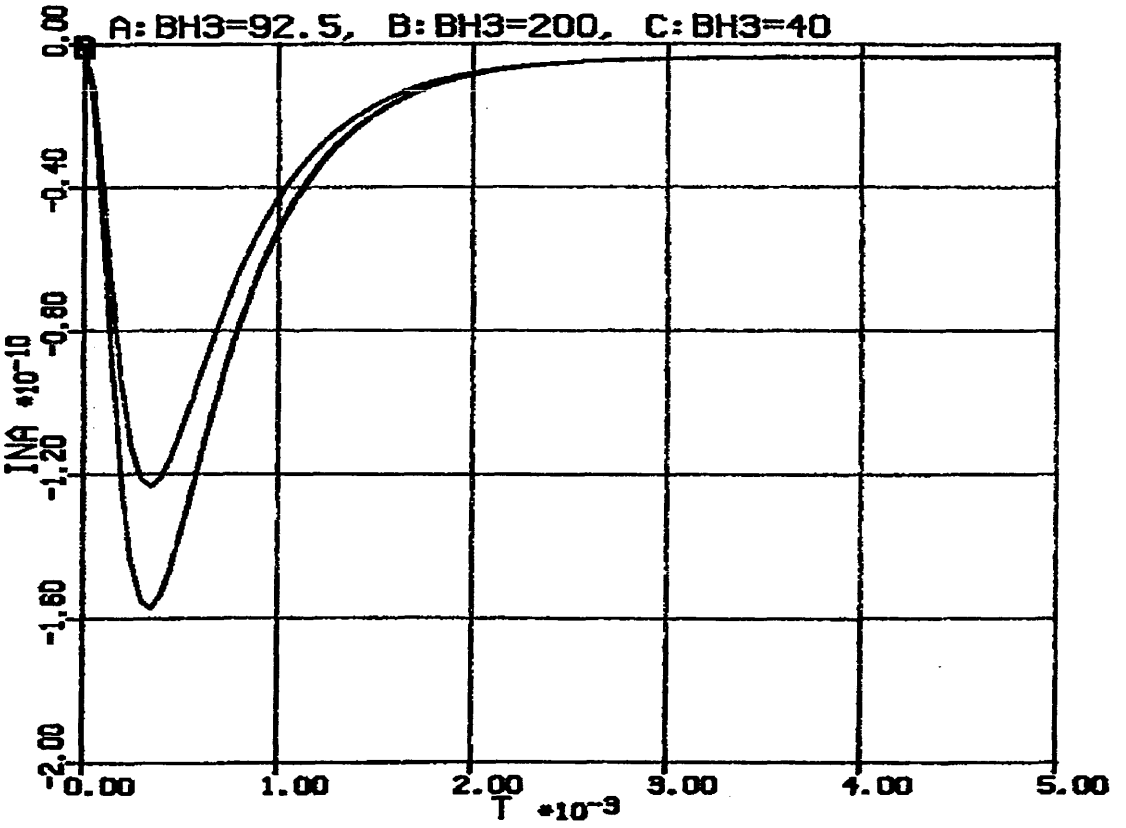


**Figure 8.50**

This figure shows the effect of changing parameter beta-h3, on the sodium current.

As can be seen from these figures, the effects of considerable changes in the parameters has a relatively small effect upon the behaviour of the steady-state activation and inactivation variables and on the sodium current itself. A similar study of the effects of parameter variations on the potassium currents was also performed, but the results are not shown here for reasons of space. These results are as expected for this system. The overall system behaviour is governed by the interactions between the currents and a fairly wide variability is encountered in the system parameters such as maximum conductance and slope factors in the rate equations.

After allowing for the differences in temperature,

maximum conductance and change of units, the Hodgkin-Huxley model for sodium current in squid giant axon was incorporated into a model with the delayed rectifier current from the oxytocin model. The mixed model thus created was used in several trial simulations. The results were not encouraging and are not included here. At that stage in the project, time was limited which precluded further experimentation.

## SUMMARY

This chapter describes work done by the author in building up a mathematical model of the electrical behaviour of the oxytocin-secreting cell. The ACSL programs written by the author are included in the Appendix. The models of the various ionic currents derived in previous chapters were amalgamated to form the model of the entire cell, using parameters such as capacitance, resting potential and temperature from published work.

Many simulations were performed using the APOLLO network and some of the results are shown here.

# CHAPTER NINE

## DISCUSSION AND CONCLUSIONS

Bursting behaviour in cells involves several membrane currents with fairly complex interactions.

As can be seen from the preceding chapters, all of the necessary components for producing bursting activity are present in the oxytocin-secreting cell. These are; an action potential generating mechanism; a feedback mechanism between the membrane potential and the intracellular calcium concentration and a region of negative resistance in the current/voltage characteristic.

However, the results of the simulations are disappointing in that the model as it stands does not show the patterns of firing that are observed experimentally. This may be due to the lack of relevant channel data on which to base the model. Specifically, the data on the calcium-gated potassium channel in a form suitable for detailed mathematical description is unavailable, as is the data for the calcium channel. Data on the leakage current is also unavailable but this presents less of a problem since the form of the model of leakage current is known and manipulation of the parameters is straightforward. In modelling studies on similar systems, workers have built models with known channel models and adjusted the leakage current parameters such that the total current at the resting potential is zero. This approach is the one used here. The three currents that have been modelled are the sodium

current, the delayed rectifier and the transient potassium current. In the absence of data on these channels alternative models from other similar systems have been used. This strategy of using data relevant to other related systems is used by workers in this field and has resulted in several successful studies. In this instance however, doubt has been cast on the validity of the alternative models used.

Specifically, the results of simulation of the calcium current using the model due to Hencek and Zachar do not agree with their findings. It is also not known whether the calcium-gated potassium current model used is appropriate to this system. The changes in calcium concentration are modelled using Rinzel's equations, it is not known whether this is appropriate for the system under study. Another strategy that was used in this study to overcome the lack of relevant data was to assume the form of the model and to adjust the model parameters until the required results were obtained. The problem with this approach is the complexity of the system under study. There are many parameters involved and there are many interactions between the currents. This makes the process very laborious and time-consuming. As discussed previously, the most common techniques for analysis of system behaviour are inappropriate for such a complex system.

The modelling methodology is appropriate and similar studies on other similar systems have proved successful. Chapter 2 discusses several of these.

Due to the complexity of the system, the parameter tuning approach did not yield a successful model in the time

available. However, in developing the model described here, a thorough understanding of the system and the modelling process has been achieved.

The strategy that was adopted in pursuing a model of the system once it had been realised that the initial attempts were not producing the expected results was to build up the model from simpler blocks. The paper by Bourque and Renaud is useful in this endeavour since it gives details of the effects of various channel blocking agents on the recorded response of supraoptic neurones (Bourque & Renaud 1985). The experiments they performed effectively demonstrated the effects of isolating various components of the total ionic current in the membrane. Adding the potassium channel blocker TEA to the bathing solution resulted in an action potential with a much longer duration than the control. Addition of manganese ions (calcium channel blocker) reduced the amplitude of the response and abolished the hyperpolarizing part of the response observed in the control. Addition of the sodium channel blocker TTX reveals a fairly complicated response. Upon application of the stimulus, the voltage increases fairly slowly and reaches a plateau after a few milliseconds. The voltage continues to rise at a slow rate and then "turns the corner" and generates a spike with slightly reduced amplitude and with a rapid repolarization phase. After repolarizing, the voltage rises again at a relatively slow rate up to a cusp and then decays in an exponential manner. Addition of TTX and manganese ions produces a response that rises to a plateau and remains at the depolarized level until the stimulus voltage is removed,

whereupon it decays exponentially. A model in which the calcium current has been ommitted should show a response similar to the trace obtained by Bourque and Renaud after addition of manganese ions. Similarly, a model without the delayed rectifier current should give a response similar to the results obtained by Bourque and Renaud upon application of TEA. By using the results obtained by Bourque and Renaud it should be possible to build up a model by adding various currents to the model one at a time and checking the intermediate simulation results against the experimental recordings. Their results show that a simplified model containing fewer channels than are known to be present can still fire an action potential when stimulated.

The most serious defect of the model for the oxytocin secreting cell as it stands is the fact that the model appears to have a stable state at a depolarized potential which does not allow the various ionic channels to return to their resting states. Put another way, it appears that there is a stable node or attractor that pulls the voltage trajectory towards it. The membrane resting potential should be the only stable resting state of the cell. At equilibrium, the voltage is stabilised by a balance of ionic currents. In the resting state most of the channels are closed and therefore nonconducting. The model appears to stabilise at the depolarised potential due to a balance between inward and outward currents. If inward and outward currents are equal, the net ionic current is zero and hence the membrane capacitance will neither charge nor discharge and the voltage will remain constant. The membrane voltage in the model is

determined by the charge on the membrane capacitor (see Figure 8.3 , Page 171). The rate of change of voltage is determined by the current flowing into the capacitor. If the "capacity current" is zero then the rate of change of voltage is also zero. Because the voltage does not change at the equilibrium point, the voltage-gated channels will not change their conductances and the channels will remain in that condition. One experiment that was tried to overcome this problem was to artificially increase the maximum potassium conductance parameter. This should have the effect of increasing magnitude of the repolarising potassium current and so force the membrane potential back to its resting value. However, even increasing the maximum conductance to an unreasonably large value did not produce the required effect. The location of the depolarised stable state did move towards the resting potential but the complete repolarisation of the membrane did not occur. It would be useful to perform a detailed analysis of the resting state of the membrane by running a simulation with no stimulus voltage. By plotting out the behaviour of all the ionic currents, any unusual behaviour would be highlighted. With no stimulus voltage, all the currents should remain at their resting levels.

In conclusion the model as described here is incomplete due to the lack of relevant data on the system and although these deficiencies have been compensated for by the inclusion of models from related systems, the composite model failed to demonstrate the required behaviour. To complete the model it will be necessary to collect the relevant channel data and include the resulting sub-models into the model.

Alternatively, by re-examining the models for calcium and calcium-gated potassium channels and adjusting the model parameters, it may be possible to produce the desired behaviour.

## SUGGESTIONS FOR FURTHER WORK

As stated previously the approach used here for building up a model of the electrical behaviour of the cell has been used successfully by a number of workers. For example Rinzel's model of bursting behaviour in pancreatic beta cells. This is a good model upon which to base further work.

The calcium current used in the model was taken from Hencek and Zachar's 1977 paper since no data was available for the oxytocin-secreting cell. Numerical integration of their equations does not reproduce their published results and the use of the equations casts doubt on the validity of the model. It would therefore be useful to obtain a calcium current model from another source and to use this in the oxytocin cell model. The equations used to represent the sodium current appear to yield acceptable results when used in voltage-clamp simulations. However, in the total cell model there appears to be the anomaly of the sodium current not returning to zero as described earlier. This needs further investigation before it can be stated categorically that the sodium current model is correct and the anomalous behaviour of the whole model is due to other causes.

It would be useful to undertake a detailed mathematical analysis of the model to ascertain the basis for the

existence of the stable depolarized state as seen in figure 8.12.

The model due to Hindmarsh and Rose (1984) exhibits bursting using three coupled nonlinear differential equations. This is the minimum number needed to describe bursting behaviour according to FitzHugh. Such a minimal mathematical model provides a useful basis for analysis of bursting behaviour. A more detailed investigation of their proposed model would be useful in gaining a deeper understanding of the parts that the various variables play in determining the overall behaviour. The model was simulated using ACSL but the program did not reproduce the stated results with the parameters given. Given the limited time available this line of research was abandoned since it did not appear to be one of the more promising approaches. One of the reasons for this is that the model is of reduced order compared to the H-H model with an additional adaptation variable. Clearly, a model using only three equations would not be able to reproduce the full range of behaviour being sought.

Abe, H. & Ogata, N. (1982)
Ionic mechanisms for the osmotically-induced depolarization in neurones of the guinea-pig supraoptic nucleus *in vitro*.
*J. Physiol.* (1982) **327** pp. 157-171

Adams, D.J. & Gage, P.W. (1976)
Gating currents associated with sodium and calcium currents in an *Aplysia* neuron.
*Science* (1976) **192** pp. 783-784

Adams, D.J. & Gage, P.W. (1979)
Ionic currents in response to membrane depolarization in an *Aplysia* neurone.
*J. Physiol.* (1979) **289** pp. 115-141

Adams, P.R. , Constanti, A., Brown, D.A. & Clark, R.B. (1982)
Intracellular $Ca^{2+}$ activates a fast voltage-sensitive $K^{+}$ current in vertebrate sympathetic neurones.
*Nature* (1982) **296** pp. 746-749

Akaike, T. (1982)
Periodic bursting activities of locus coeruleus neurons in the rat.
*Brain Res.* (1982) **239** pp. 629-633

Andrew, R.D. & Dudek, F.E. (1984)
Analysis of intracellularly recorded phasic bursting by mammalian neuroendocrine cells.
*J. Neurophysiol.* (1984) **51** No.3 pp. 552-566

Armstrong, C.M. (1975)
Ionic pores, gates and gating currents.
*Q. Rev. Biophysics* (1975) **7** No.2 pp. 179-210

Armstrong, C.M. (1981)
Sodium channels and gating currents.
*Physiogical Rev.* (1981) **61** No.3 pp. 644-683

Armstrong, C.M. & Bezanilla, F. (1974)
Charge movement associated with the opening and closing of the activation gates of the Na channels.
*J. Gen. Physiol.* (1974) **63** pp. 533-552

Armstrong, C.M. & Bezanilla, F. (1973)
Currents related to movement of the gating particles of the sodium channels.
*Nature* (1973) **242** pp. 459-461

Attwell, D. & Jack, J. (1978)
The interpretation of membrane current-voltage relations : a Nernst-Planck analysis.
*Prog. Biophys. molec. Biol.* (1978) **34** pp. 81-107

Bader, C.R. , Bernhein, L. & Bertrand, D. (1985)
Sodium-activated potassium current in cultured avian neurones.
*Nature* (1985) **317** pp. 540-542

Barish, M.E. (1986)
Differentiation of voltage-gated potassium current and modulation of excitability in cultured amphibian spinal neurones.
*J. Physiol.* (1986) **375** pp. 229-250

Barrett, J.N. , Magelby, K.L. & Pallotta, B.S. (1982)
Properties of single calcium-activated potassium channels in cultured rat muscle.
*J. Physiol.* (1982) **331** pp. 211-230

Linares-Barranco, B. , Sánchez-Sinencio, E. , Rodriguez-Vázquez, A. & Huertas, J.L. (1991)
A CMOS implementation of the FitzHugh-Nagumo neuron model.
*IEEE J. of solid-state circuits* (1991) **26** No.7 pp.

Bekkers, J.M. , Greeff, N.G. & Keynes, R.D. (1986)
The conductance and density of sodium channels in the cut-open squid giant axon.
*J. Physiol.* (1986) **377** pp. 436-486

Belluzzi, O. & Sacchi, O. (1988)
The interactions between potassium and sodium currents in generating action potentials in the rat sympathetic neurone.
*J. Physiol.* (1988) **397** pp. 127-147

Belluzzi, O. , Sacchi, O. & Wanke, E. (1985a)
A fast transient outward current in the rat sympathetic neurone studied under voltage-clamp condtions.
*J. Physiol.* (1985a) **358** pp. 91-108

Belluzzi, O. , Sacchi. O. & Wanke, E. (1985b)
Identification of delayed potassium and calcium currents in the rat sympathetic neurone under voltage clamp.
*J. Physiol.* (1985b) **358** pp. 109-129

Benson, J.A. & Cooke, I.M. (1984)
Driver potentials and the organization of rhythmic bursting in crustacean ganglia.
*TINS* (March 1984) pp. 85-91

Berman, N.J. , Bush, P.C. & Douglas, R.J. (1989)
Adaptation and bursting in neocortical neurones may be controlled by a single fast potassium conductance.
*Q. J. of Exp. Physiol.* (1989) **74** pp. 223-226

Bezanilla, F. & Armstrong, C.M. (1974)
Gating currents of the sodium channels: Three ways to block them.
*Science* (1974) **183** pp. 753-754

Bicknell, R.J. , Chapman, C. & Leng, G. (1982)
A perifusion system for studying neurosecretion from the isolated rat neurohypophysis *in vitro.*
*J. Neurosci. Methods* (1982) **5** pp. 95-101

Bossu, J.L. , Feltz, A. & Thomann, J.M. (1985)
Depolarization elicits two distinct calcium currents in vertebrate sensory neurones.
*Pflügers Archiv* (1985) **403** pp. 360-368

Bourque, C.W. (1987)
Current- and voltage-clamp studies of transient and pacemaker currents in neurosecretory neurons of the supraoptic nucleus.
*Inactivation of Hypersensitive Neurons* (1987) Alan R. Liss inc. pp. 415-422

Bourque, C.W. (1989)
Ionic basis for the intrinsic activation of rat supraoptic neurones by hyperosmotic stimuli.
*J. Physiol.* (1989) **417** pp. 263-277

Bourque, C.W. (1988)
Transient calcium-dependent potassium current in magnocellular neurosecretory cells of the rat supraoptic nucleus.
*J. Physiol.* (1988) **397** pp. 331-347

Bourque, C.W. & Renaud, L.P. (1985a)
Calcium-dependent action potentials in rat supraoptic neurosecretory neurones recorded *in vitro.*
*J. Physiol.* (1985a) **363** pp. 419-428

Bourque, C.W. & Renaud, L.P. (1985b)
Activity dependence of action potential duration in rat supraoptic neurosecretory neurones recorded *in vitro.*
*J. Physiol.* (1985b) **363** pp. 429-439

Bourque, C.W. , Randle, J.C.R. & Renaud. L.P. (1986)
Non-synaptic depolarizing potentials in rat supraoptic neurones recorded *in vitro.*
*J. Physiol.* (1986) **376** pp. 493-505

Brimble, M.J. & Dyball, R.E.J. (1977)
Characterization of the responses of oxytocin- and vasopressin-secreting neurones in the supraoptic nucleus to osmotic stimulation.
*J. Physiol.* (1977) **271** pp. 253-271

Brown, D.A. & Higashima, H. (1988)
Voltage- and current-activated potassium currents in mouse neuroblastoma and rat glioma hybrid cells.
*J. Physiol.* (1988) **397** pp. 149-165

Byerly, L. & Hagiwara, S. (1981)
Calcium channel
*Ann. Rev. Neurosci.* (1981) **4** pp. 69-125

Champagnat, J. , Jaquin, T. & Richter, D.W. (1986)
Voltage-dependent currents in neurones of the nuclei of the solitary tract of rat brainstem slices.
*Pflügers Archiv* (1986) **406** pp. 372-379

Chay, T.R. & Rinzel, J. (1985)
Bursting, beating and chaos in an excitable membrane model.
*Biophys. J.* (1985) **47** pp. 357-366

Cobbett, P. , Inenaga, K. & Mason, W.T.
Mechanisms of phasic bursting in vasopressin cells.
unpub.

Cobbett, P. , Ingram, C.D. & Mason, W.T. (1987)
Sodium and potassium currents involved in action potential propagation in normal bovine lactotrophs.
*J. Physiol.* (1987) **392** pp. 273-299

Cobbett, P. & Mason, W.T. (1987)
Whole cell voltage clamp recordings from cultured neurons of the supraoptic area of neonatal rat hypothalamus.
*Brain Res.* (1987) **409** pp. 175-180

Cobbett, P. & Weiss, M.L. (1990)
Voltage-clamp recordings from identified dissociated neuro-endocrine cells of the adult rat supraoptic nucleus.
Rapid communication
*J. of Neuroendocrinology* (1990) **2** No.3 pp. 267-269

Coburn, B. & Sin, W.K.
A theoretical study of epidural electrical stimulation of the spinal cord - Part 1: Finite element analysis of stimulus fields.
*IEEE transactions on Biomedical Engineering* (1985) **BME-32** No.11 pp.

Colding-Jorgensen, M. (1976)
A description of adaptation in excitable membranes.
*J. theor. Biol.* (1976) **63** pp. 61-87

Cole, K.S. (1958)
Membrane excitation of the Hodgkin-Huxley axon. Preliminary corrections.
*J. Appl. Physiol.* (1958) **12** pp. 129-130

Cole, K.S. , Antosiewicz, H.A. & Rabinowitz, P. (1955)
Automatic computation of nerve excitation.
*J. Soc. Indust. Appl. Math.* (1955) **3** pp. 153-

Cole, K.S. & Moore, J.W. (1960)
Potassium ion current in the squid giant axon: Dynamic characteristic.
*Biophys. J.* (1960) **1** pp. 1-14

Coles, J.A. & Poulain, D.A. (1991)
Extracellular $K^+$ in the supraoptic nucleus of the rat during reflex bursting activity by oxytocin neurones.
*J. Physiol.* (1991) **439** pp. 383-409

Connor, J.A. (1985)
Neural pacemakers and rhythmicity.
*Ann. Rev. Physiol.* (1985) **47** pp. 17-28

Connor, J.A. & Stevens, C.F. (1971a)
Inward and delayed outward membrane currents in isolated neural somata under voltage clamp.
*J. Physiol.* (1971a) **213** pp. 1-19

Connor, J.A. & Stevens, C.F. (1971b)
Voltage-clamp studies of a transient outward membrane current in gastropod neural somata.
*J. Physiol.* (1971b) **213** pp. 21-30

Connor, J.A. & Stevens, C.F. (1971c)
Prediction of repetetive firing behaviour from voltage-clamp data on an isolated neurone soma.
*J. Physiol.* (1971c) **213** pp. 31-53

Cook, N.S. & Haylett, D.G. (1985)
Effects of apamin, quinine and neuromuscular blockers on calcium-activated potassium channels in guinea-pig hepatocytes.
*J. Physiol.* (1985) **358** pp. 373-394

Cooke, I.M. & Stuenkel, E.L. (1985)
Electrophysiology of invertebrate neurosecretory cells.
Chapter 6 *The electrophysiology of the secretory cell.*
Poisner & Trifaró (eds.) Elsevier 1985

Cooley, J.W. & Dodge, F.A. Jr. (1966)
Digital computer solutions for excitation and propagation of the nerve impulse.
*Biophys. J.* (1966) **6** pp. 583-599

Cooper, E. & Shrier, A. (1985)
Single-channel analysis of fast transient potassium currents from rat nodose neurones.
*J. Physiol.* (1985) **369** pp. 199-208

Deck, K.A. & Trautwein, W. (1964)
Ionic currents in cardiac excitation.
*Pflügers Archiv* (1964) **280** pp. 63-80

Dudek, F.E. , Andrew, R.D. , MacVicar, B.A. , Snow, R.W & Taylor, C.P. (1983)
Recent evidence for and possible significance of gap junctions and electrotonic synapses in the mammalian brain.
*Basic mechanisms of neurona hyperexcitability* pp. 31-73 Alan R. Liss Inc. 1983

Dudek, F.E. , Hatton, G.I. & MacVicar, B.A. (1980)
Intracellular recording from the paraventricular nucleus in slices of rat hypothalamus.
*J. Physiol.* (1980) **301** pp. 101-114

Dutton, A. & Dyball, R.E.J. (1979)
Phasic firing enhances vasopressin release from the rat neurohypophysis.
*J. Physiol.* (1979) **290** pp. 433-440

Dyball, R.E.J. , Barnes, P.R.J. & Shaw, F.D. (1985)
Significance of phasic firing in enhancing vasopressin release from the neurohypophysis.
*Neurosecretion and the biology of neuropeptides* Kobayashi, H. *et al.* (eds.) 1985 pp. 239-246

Dyball, R.E.J. & Leng, G. (1985)
Supraoptic neurones in Brattleboro rats respond normally to changes in plasma osmotic pressure.
*J. Endocr.* (1985) **105** pp. 87-90

Dyball, R.E.J. & Leng, G. (1986)
Regulation of the milk ejection reflex in the rat.
*J. Physiol.* (1986) **380** pp.239-256

Ehrenstein, G. , Lecar, H. & Nossal, R. (1970)
The nature of the negative resistance in bimolecular lipid membranes containing excitability-inducing material.
*J. Gen. Physiol.* (1970) **55** pp. 119-133

Erickson, K.R. , Ronnekleiv, O.K. & Kelly, M.J. (1990)
Inward rectification ($I_h$) in immunocytochemically identified vasopressin and oxytocin neurons of the guinea-pig supraoptic nucleus.
Rapid communication
*J. of Neuroendocr.* (1990) **2** No.3 pp. 261-265

Fidler, J.K. & Nightingale, C. (1978)
Computer aided circuit design.
Nelson 1978

FitzHugh, R. (1969)
Mathematical models of excitation and propagation in nerve.
Chapter 1 *Biological Engineering* Schwan, H.P. (ed.) pp. 1-85
McGraw-Hill Book Co. 1969

ffrench-Mullen, J.M.H. , Tokutomi, N. & Akaike, N. (1988)
The effect of temperature on the GABA-induced chloride current in isolated sensory neurones of the frog.
*Br. J. Pharmacol.* (1988) **95** pp. 753-762

Frankenhaeuser, B. & Huxley, A.F. (1964)
The action potential in the myelinated nerve fibre of *Xenopus Laevis* as computed on the basis of voltage clamp data.
*J. Physiol.* (1964) **171** pp.302-315

French, R.J. & Horn, R. (1983)
Sodium channel gating : Models, mimics and modifiers.
*Ann. Rev. Biophys. Bioeng.* (1983) **12** 319-356

Geduldig, D. & Junge, D. (1968)
Sodium and calcium components of action potentials in the *Aplysia* giant neurone.
*J. Physiol.* (1968) **199** pp. 347-365

George, E.P. & Johnson, E.A. (1961)
Solutions of the Hodgkin-Huxley equations for squid axon treated with tetraethylammonium and in potassium-rich media.
*Aust. J. exp. Biol.* (1961) **39** pp. 275-294

Gillespie, C.J. (1976)
Towards a molecular theory of nerve membrane : The sufficiency of a single ion queue.
*J. theor. Biol.* (1976) **58** pp.477-498

Gillespie, C.J. (1976)
Towards a molecular theory of nerve membrane : Inactivation.
*J.theor. Biol.* (1976) **60** pp. 19-35

Gola, M. (1987)
Calcium interactions with potassium currents may limit or sustain repetetive firing.
*Inactivation of Hypersensitive Neurons* pp. 379-390 Alan R. Liss Inc. 1987

Gorman, A.L.F. & Thomas, M.V. (1978)
Changes in the intracellular concentration of free calcium ions in a pace-maker neurone, measured with the metallochromic indicator dye arsenazo III.
*J. Physiol.* (1978) **275** pp. 357-376

Goulden, P.T. (1976)
The biological membrane potential : Some theoretical considerations.
*J. theor. Biol.* (1976) **58** pp. 425-438

Guttman, R. & Barnhill, R. (1970)
Oscillations and repetetive firing in squid axons.
*J. Gen. Physiol.* (1970) **55** pp. 104-118

Hartung, K. & Rathmayer, W. (1985)
*Anemonia sulcata* toxins modify activation and inactivation of $Na^+$ currents in a crayfish neurone.
*Pflügers Archiv* (1985) **404** pp. 119-125

Hatton, G.I. , Ho, Y.W. & Mason, W.T. (1983)
Synaptic activation of phasic bursting in rat supraoptic nucleus neurones recorded in hypothalamic slices.
*J. Physiol.* (1983) **345** pp. 297-317

Hencek, M. & Zachar, J. (1977)
Calcium currents and conductances in the muscle membrane of the crayfish.
*J. Physiol.* (1977) **268** pp. 51-71

Hille, B. (1976)
Gating in sodium channels of nerve.
*Ann. Rev. Physiol.* (1976) **38**

Hille, B. (1984)
Ionic channels of excitable membranes.
Sinauer Associates Inc. 1984

Hodgkin, A.L. & Huxley, A.F. (1952d)
A quantitative description of membrane current and its application to conduction and excitation in nerve.
*J. Physiol.* (1952d) **117** pp. 500-544

Horn, R. (1984)
Gating of channels in nerve and muscles : A stochastic approach.
*Current topics in membranes and transport* **21** W.D. Stein (ed.)
Academic press 1984 pp. 53-97

Huxley, A.F. (1959)
Ion movement during nerve activity.
*Annals New York Academy of Sciences* (1959) **81** pp. 221-246

Ingram, C.D. , Bicknell, R.J. , Brown, D. & Leng, G. (1982)
Rapid fatigue of neuropeptide secretion during cotinual electrical stimulation.
*Neuroendocrinology* (1982) **35** pp. 424-428

Jack, J.J.B. , Noble, D. & Tsien, R.W. (1985)
Repetetive activity in excitable cells.
Ch. 11 *Electric current flow in excitable cells* pp. 305-378
O.U.P. 1985

Jakobsson, E. (1976)
An assessment of a coupled three-state kinetic model for sodium conductance changes.
*Biophys. J.* (1976) **16** pp. 291-301

Joyner, R.W. , Westerfield, M. , Moore, J.W. & Stockbridge, N. (1978)
A numerical method to model excitable cells.
*Biophys. J.* (1978) **22** pp. 155-170

Kamaluddin, A.K. & Power, H.M. (1974)
A cardiac pacemaker model incorporating frequency control by the autonomic nervous system.
*Int. J. Systems Science* (1974) **5** pp. 673-685

Kay, A.R. & Wong, R.K.S. (1987)
Calcium current activation kinetics in isolated pyramidal neurones of the CA1 region of the mature guinea-pig hippocampus.
*J. Physiol.* (1987) **392** pp. 603-616

Kolb, H.-A. (1984)
Measuring the properties of single channels in cell membranes.
*Current topics in membranes and transport* **21** W.D. Stein (ed.)
pp. 133-179 Academic Press 1984

Kononenko, N.I. (1979)
Modulation of the endogenous electrical activity of the bursting neuron in the snail *Helix Pomatia* -III. A factor modulating the endogenous electrical activity of the bursting neuron.
*Neuroscience* (1979) **4** pp. 2055-2059

Latorre, R. & Alvarez, O. (1981)
Voltage-dependent channels in planar lipid bilayer membranes.
*Physiological Reviews* (1981) **61** pp. 77-150

Latorre, R. , Alvarez, O. , Cecchi, X. & Vergara, C. (1985)
Properties of reconstituted ion channels.
*Ann. Rev. Biophys. Biophys. Chem.* (1985) **14** pp. 79-111

Latorre, R. , Coronado, R. & Vergara, C. (1984)
$K^+$ channels gated by voltage and ions.
*Ann. Rev. Physiol.* (1984) **46** pp. 485-495

Läuger, P. (1984)
Channels with multople conformational states : interrelations with carriers and pumps.
*Current topics in membraanes and transport* **21** W.D. Stein (ed.) Academic Press 1984 pp. 309-326

Legendre, P. , Cooke, I.M. & Vincent, J.-D. (1982)
Regenerative responses of long duration recorded intracellularly from dispersed cell cultures of fetal mouse hypothalamus.
*J. Neurophysiology* (1982) **48** No.5 pp. 1121-1141

Legendre, P. , Poulain, D.A. & Vincent, J.-D. (1988)
A study of ionic conductances involved in plateau potential activity in putative vasopressinergic neurons in primary cell culture.
*Brain Res.* (1988) **457** pp. 386-391

Leng, G. (1981)
Phasically firing neurones in the lateral hypothalamus of anaesthetized rats.
*Brain Res.* (1981) **230** pp. 390-393

Leng, G. (1981)
The effects of neural stalk stimulation upon firing patterns in rat supraoptic neurones.
*Exp. Brain Res.* (1981) **41** pp. 135-145

Leng, G. & Bicknell, R.J. (1984)
Patterns of electrical activity and hormone release from neurosecretory cells.
*Endocrinology* Labrie, F. & Proulx, L. (eds.) Elsevier 1984

Leng, G. & Dyball, R.E.J. (1983)
Intercommunication in the rat supraoptic nucleus.
*Q. J. Exp. Physiol.* (1983) **68** pp. 493-504

Leng, G. Mason, W.T. & Dyer, R.G. (1982)
The supraoptic nucleus as an osmoreceptor.
*Neuroendocrinology* (1982) **34** pp. 75-82

Leng, G. , Shibuki, K. & Way, S.A. (1988)
Effects of raised extracellular potassium on the excitability of, and hormone release from, the isolated rat neurohypophysis.
*J. Physiol.* (1988) **399** pp.591-605

Leng, G. , Shibuki, K. & Way, S. (1987)
Facilitation of stimulus-evoked hormone release from the rat neurohypophysis by elevated extracellular potassium concentrations.
*J. Physiol.* (1987) **14P** p. 388

Levenberg, K. (1944)
A method for the solution of certain non-linear problems in least squares.
*Quart. Appl. Math.* (1944) **2** pp. 164-168

Lincoln, D.W. & Wakerley, J.B. (1974)
Electrophysiological evidence for the activation of supraoptic neurones during the release of oxytocin.
*J. Physiol.* (1974) **242** pp. 533-544

Lundström, I. & Stenberg, M. (1978)
Electrostatic interaction between gating charges in nerve membranes.
*J. theor. Biol.* (1978) **70** pp. 229-244

MacGregor, R.J. & Lewis, E.R. (1977)
Neural Modeling: Electrical signal processing in the nervous system.
Plenum

McKean, H.P. Jr. (1970)
Nagumo's equation.
*Advances in mathematics* (1970) **4** pp. 209-223

McNeal, D. (1976)
Analysis of a model for excitation of myelinated nerve.
*IEEE Transactions on biomedical engineering* (1976) **BME-23** No.4

Madsen, E.L. (1977)
Theory for a test of the electric cable model of the myelinated axon and saltatory conduction.
*J. theor. Biol.* (1977) **67** pp. 203-212

Marmont, G. (1949)
Studies on the axon membrane I. A new method.
*J. Cell. Comp. Physiol.* (1949) **34** pp. 351-382

Marquardt, D.W. (1963)
An algorithm for least squares estimation of nonlinear parameters.
*J. Soc. Indust. Appl. Math.* (1963) **11** No. 2 pp. 431-441

Marty, A. & Neher, E. (1985)
Potassium channels in cultured bovine adrenal chromaffin cells.
*J. Physiol.* (1985) **367** pp. 117-141

Maruyama, Y. & Petersson, O.H. (1982)
Single channel currents in isolated patches of plasma membrane from basal surface of pancreatic acini.
*Nature* (1982) **299** pp. 159-161

Maruyama, Y. , Peterson, O.H. , Flanagan, P. & Pearson, G.T. (1983)
Quantification of $Ca^{2+}$-activated $K^{+}$ channels under hormonal control in pig pancreas acinar cells.
*Nature* (1983) **305** pp. 228-232

Mason, W.T. (1983)
Electrical properties of neurons recorded from the rat supraoptic nucleus *in vitro.*
*Proc. R. Soc. Lond. Ser B* (1983) **217** pp. 141-161

Mason, W.T. (1980)
Supraoptic neurones of rat hypothalamus are osmosensitive.
*Nature* (1980) **287** pp. 154-157

Mason, W.T. & Leng, G. (1984)
Complex action potential waveform recorded from supraoptic and paraventricular neurones of the rat : Evidence for sodium and calcium spike components at different sites.
*Exp. Brain Res.* (1984) **56** pp. 135-143

Mason, W.T. , Cobbett, P. , Inenaga, K. & Legendre, P. (1988)
Ionic currents in cultured supraoptic neurons : actions of peptides and transmitters.
*Brain Res. Bull.* (1988) **20** pp. 757-764

Mason, W.T. & Ingram, C.D.
Techniques for studying the role of electrical activity in control of secretion by normal anterior pituitary cells.
(unpub.)

Matthews, E.K. & O'Connor, M.D.L. (1979)
Dynamic oscillations in the membrane potential of pancreatic islet cells.
*J. Exp. Biol.* (1979) **81** pp. 75-91

Meech, R.W. (1978)
Calcium-dependent potassium activation in nervous tissues.
*Ann. Rev. Biophys. Bioeng.* (1978) **7** pp. 1-18

Merickel, M. & Gray, R. (1980)
Investigation of burst generation by the electrically coupled cyberchron network in the snail *Helisoma* using a single electrode voltage clamp.
*J. Neurobiol.* (1980) **11** No.1 pp. 73-102

Meves, H. (1984)
Hodgkin-Huxley : Thirty years after.
*Current topics in membranes and transport* **22** Baker, P.F. (ed.) (1984) pp. 279-329

Mironov, S.L. (1983)
Theoretical model of slow-wave membrane potential oscillations in molluscan neurons.
*Neuroscience* (1983) **10** No.3 pp. 899-905

Moore, J.W. , Ramón, F. & Joyner, R.W. (1975)
Axon voltage-clamp simulations.
*Biophys. J.* (1975) **15** pp. 11-25

Nagumo, J. , Arimoto, S. & Yoshizawa, S. (1962)
An active pulse transmission line simulating nerve axon.
*Proc. IERE* (1962) **50** pp. 2061-2071

Neher, E. & Stevens, C.F. (1977)
Conductance fluctuations and ionic pores in membranes.
*Ann. Rev. Biophys. Bioeng.* (1977) **6** pp. 345-381

Neyton, J. & Trautmann, A. (1985)
Single-channel currents of an intercellular junction.
*Nature* (1985) **317** pp. 331-335

Noble, D. (1962)
A modification of the Hodgkin-Huxley equations applicable to Purkinje fibre action and pace-maker potentials.
*J. Physiol.* (1962) **160** pp. 317-352

Noble, D. (1966)
Applications of Hodgkin-Huxley equatins to excitable tissues.
*Physiological Rev.* (1966) **46** No.1 pp. 1-50

Noble, D. & Stein, R.B. (1966)
The threshold conditions for initiation of action potentials by excitable cells.
*J. Physiol.* (1966) **187** pp. 129-162

Norton, J.P. (1986)
An introduction to identification.
Academic Press (1986)

Pallotta, B.S. (1985)
Calcium-activated potassium channels in rat muscle inactivate from a short duration open state.
*J. Physiol.* (1985) **363** pp. 501-516

Patton, R.J. (1980)
A mathematical model for intestinal slow waves and spike activity based on the Hodgkin-Huxley equations.
Research report Submitted *IEE Proc.* 1980

Patton, R.J. (1980)
Mathematical and electronic modelling of electrical signals of the gastro-intestinal tract using Hodgkin-Huxley equations.
*PhD thesis* (1980) University of Sheffield

Peterson, O.H. & Maruyama, Y. (1984)
Calcium-activated potassium channels and their role in secretion.
*Nature* (1984) **307** pp. 693-696

Plant, R.E. & Kim, M. (1976)
Mathematical model of a bursting pacemaker neuron by a modification of the Hodgkin-Huxley equations.
*Biophysical J.* (1976) **16** pp. 227-244

Poulain, D.A. & Wakerley, J.B. (1982)
Electrophysiology of hypothalamic magnocellular neurones secreting oxytocin and vasopressin.
*Neuroscience* (1982) **7** No.4 pp. 773-808

Quandt, F.N. (1988)
Three kinetically distinct potassium channels in mouse neuroblastoma cells.
*J. Physiol.* (1988) **395** pp. 401-418

Ramón, F. , Anderson, N.C. , Joyner, R.W. & Moore, J.W. (1976)
A model for propagation of action potentials in smooth muscle.
*J. theor. Biol.* (1976) **59** pp. 381-408

Renaud, L.P. (1987)
Magnocellular neuroendocrine neurons : Update on intrinsic properties, synaptic inputs and neuropharmacology.
*Trends In Neuroscience* (1987) **10** No.12 pp. 498-502

Renaud, L.P. , Bourque, C.W. , Day, T.A. , Ferguson, A.V. & Randle, J.C.R. (1985)
Electrophysiology of mammalian hypothalamic supraoptic and paraventricular neurosecretory cells.
*The electrophysiology of the secretory cell* Poisner & Trifaró (eds.) Elsevier 1985

Rinzel, J. (1986)
A formal classification of bursting mechanisms in excitable systems.
*Proc. of International Congress of Mathematicians* 1986

Rinzel, J.
Bistable behaviour of bursting cells.
pre publication personal communication.

Rinzel, J. (1981)
Models in neurobiology.
*Nonlinear phenomena in physics and biology* Enns, R.H. , Jones, B.L. , Mivra, R.M. & Rangnekar, S.S. (eds.) Plenum 1981

Rinzel, J.
On the electrical activity and glucose response of insulin-secreting cells.
*Biomathematics and related computational problems* Ricciardi, L.M. (ed.) pp. 685-696

Rubinow, S.I. (1975)
Introduction to mathematical biology.
Wiley (1975)

Scales, L.E. (1985)
Introduction to non-linear optimization.
Macmillan (1985)

Seaman, R.L. , Lynch, M.J. & Moss, R.L. (1980)
Effects of hypothalamic peptide hormones on the electrical activity of *Aplysia* neurons.
*Brain Res. Bull.* (1980) **5** pp. 233-237

Sherman, A., Rinzel, J. & Keizer, J. (1988)
Emergence of organised bursting in clusters of pancreatic ß-cells by channel sharing.
*Biophys. J.* (1988) **54** pp. 411-425

Sigworth, F.J. (1980a)
The variance of sodium current fluctuations at the node of Ranvier.
*J. Physiol.* (1980a) **307** pp. 97-129

Sigworth, F.J. (1980b)
The conductance of sodium channels under conditions of reduced current at the node of Ranvier.
*J. Physiol.* (1980b) **307** pp. 131-142

Sikdar, S.K., Waring, D.W. & Mason, W.T. (1986)
Voltage activated ionic current in goadotrophs of the ovine *pars tuberalis.*
*Neuroscience Letters* (1986) **71** pp. 95-100

Smith, S.J. (1978)
The mechanism of bursting pacemaker activity in neurons of the mollusc *Tritonia Diomedia.*
*Ph.D. thesis* (1978) University of Washington

Smythies, J.R., Beaton, J.M., Benington, F., Bradley, R.J. & Morin, R.F. (1976)
On the molecular mechanism of interaction between the neurophysins and oxytocin and vasopressin.
*J. Theor. Biol.* (1976) **63** pp. 33-48

Snow, R.W. & Dudek, F.E. (1984)
Electrical fields directly contribute to action potential synchronization during convulsant - induced epileptiform bursts.
*Brain Res.* (1984) **323** pp. 114-118

Snow, R.W. & Dudek, F.E. (1984)
Synchronous epileptiform bursts without chemical transmission in CA2, CA3 and dentate areas of the hippocampus.
*Brain Res.* (1984) **298** pp. 382-385

Sperelakis, N. & Mann, J.E.Jnr. (1977)
Evaluation of electric field changes in the cleft between excitable cells.
*J. Theor. Biol.* (1977) **64** pp. 71-96

Strandberg, M.W.P. (1976)
Action potential in the giant axon of *Loligo* : a physical model.
*J. Theor. Biol.* (1976) **58** pp. 33-53

Takashima, S. & Yantorno, R.
Investigation of voltage-dependent membrane capacity of Squid giant axons.
*Ann. New York Academy of Sciences* pp. 307-321

Tanaka, K. & Kuba, K. (1987)
The $Ca^{2+}$-sensitive $K^{+}$-currents underlying the slow afterhyperpolarization of bullfrog sympathetic neurones.
*Pflügers Archiv* (1987) **410** pp. 234-242

Taylor, C.P. & Dudek, F.E. (1982)
A physiological test for electrotonic coupling between CA1 pyramidal cells in rat hippocampal slices.
*Brain Res.* (1982) **235** pp. 351-357

Taylor, C.P. & Dudek, F.E. (1984a)
Excitation of hippocampal pyramidal cells by an electrical field effect.
*J. Neurophysiol.* (1984a) **52** No.1 pp. 126-142

Taylor, C.P. & Dudek, F.E. (1984b)
Synchronization without active chemical synapses during hippocampal afterdischarges.
*J. Neurophysiol.* (1984b) **52** No.1 pp. 143-155

Thomas, M.V. (1984)
Voltage-clamp analysis of a calcium-mediated potassium conductance in cockroach (*Periplaneta Americana*) central neurones.
*J. Physiol.* (1984) **350** pp. 159-178

Thompson, S.H. (1977)
Three pharmacologically distinct potassium channels in molluscan neurones.
*J. Physiol.* (1977) **265** pp. 465-488

Trifaró, J.M. & Poisner, A.M. (1985)
Electrophysiological properties of the secretory cell : An overview.
Ch.11 *The electrophysiology of the secretory cell* Poisner & Trifaró (eds.) Elsevier 1985

Troy, W.C. (1975)
Oscillation phenomena in the Hodgkin-Huxley equations.
*Proc. R. Soc. Edinburgh* (1974\75) **74A** 23 pp. 299-310

Tse, A. & Hille, B. (1992)
GnRH-induced $Ca^{2+}$ oscillations and rhythmic hyperpolarizations of pituitary gonadotropes.
*Science* (1992) **255** pp. 462-464

Ulbricht, W. (1977)
Ionic channels and gating currents in excitable membranes.
*Ann. Rev. Biophys. Bioeng.* (1977) **6** pp. 7-31

Volk, K.A. , Matsuda, J.J. & Shibata, E.F. (1991)
A voltage-dependent potassium current in rabbit coronary artery smooth muscle cells.
*J. Physiol.* (1991) **439** pp. 751-768

White, R.L. & Gardner, D. (1981)
Self-inhibition alters firing patterns of neurons in *Aplysia* buccal ganglia.
*Brain Res.* (1981) **209** pp. 77-93

Wilson, W.A. & Wachtel, H. (1974)
Negative resistance characteristic essential for the maintenance of slow oscillations in bursting neurons.
*Science* (1974) **186** pp. 932-934

Yamaguchi, K. & Ohmori, H. (1990)
Voltage - gated and chemically - gated ionic channels in the cultured cochlear ganglion of the chick.
*J. Physiol.* (1990) **420** pp. 185-206

Zeeman, E.C. (1972)
Differential equations for the heartbeat and nerve impulse.
Reprinted from *Towards a Theoretical Biology 4* (1972) Edinburgh University Press and *Dynamical Systems* (1973) Ed. M.M. Peixoto, Academic Press

# BIBLIOGRAPHY


AIDLEY D.J. — The physiology of excitable cells
Cambridge University Press 1971

GERALD C.F. & WHEATLEY P.O. — Applied numerical analysis
Addison - Wesley 1984

HILLE B. — Ionic channels of excitable membranes
Sinauer Associates 1984

JACK, NOBLE & TSIEN — Electric current flow in excitable cells
Oxford University Press 1985

KATZ — Nerve, muscle and synapse
Mc Graw - Hill 1966

MADDRELL S.H.P. NORDMANN J.J — Neurosecretion
Blackie 1979

MILES F.A. — Excitable cells
Heinemann 1969

NOBLE — The initiation of the heartbeat
Oxford University Press 1979

PRESS W.H., FLANNERY B.P., TEUKOLSKY S.A. & VETTERLING W.T. — Numerical Recipes
The Art of Scientific Computing
Cambridge University Press 1986

ROBINSON J.R. — A prelude to physiology
Blackwell Scientific Publications 1975

SAKMANN & NEHER — Single channel recording
Plenum 1983

SCALES L.E. — Introduction to non-linear optimization
Macmillan 1985

# PROGRAM HHMOD

This program solves the Hodgkin-Huxley equations using variables and parameters in units of millivolts, milliseconds, millisiemens per square centimetre and current in microamperes per square centimetre. The model includes a term that simulates the apparent shift in membrane potential due to changing calcium concentration using the model derived by Huxley.

When the program is run (on an IBM compatible PC), the user is prompted for the simulation time. This is the period over which simulation is required. The simulated temperature is then entered from the keyboard at the second prompt. The third prompt is for the calcium concentration. Entering a number lower than 44mM causes the program to generate an apparent membrane depolarization. The stimulus voltage is then entered at the fourth prompt. Once all four values have been entered the initial values for the numerical integration routine are calculated. No default values are set so the user needs to be aware of the range of acceptable values. The program uses a fixed time step for the numerical integration routine which is not available for the user to alter.

The results of the simulation is in the form of a two dimensional array containing corresponding values of voltage and time. At the end of the simulation run the user is prompted for a filename. The data in the array will then be written to a disk in drive a: along with a file header which includes some information pertinent to the simulation such as temperature, date and stimulus voltage.

```
C  ********************************************************
C  ** THIS PROGRAM IMPLEMENTS A MATHEMATICAL MODEL  TO  **
C  ** SIMULATE THE BEHAVIOUR OF A NEURONE.              **
C  ** IT SOLVES THE EQUATIONS DERIVED BY HODGKIN AND    **
C  ** HUXLEY BY USING A NUMERICAL INTEGRATION TECHNIQUE **
C  ********************************************************
C
   PROGRAM HHMOD
C
   DOUBLE PRECISION TIME,TEMP,CACONC,VSTIM,YARRAY(4)
   DOUBLE PRECISION CONSTS(5),ALPHA(3),BETA(3),DYARRY(4)
   DOUBLE PRECISION DATFIL(10000,2),TSTEP
   INTEGER ARYCNT,ERRNUM
C
C  ***** GET DATA IN FROM THE KEYBOARD *****
C
   WRITE (*,*)'ENTER THE TIME DURATION IN MILLISECONDS :'
   READ *,TIME
   WRITE (*,*)'ENTER THE TEMPERATURE IN DEGREES CELCIUS :'
   READ *,TEMP
   WRITE (*,*)'ENTER THE CALCIUM CONCENTRATION MILLIMOLES :'
   READ *,CACONC
   WRITE (*,*)'ENTER THE INITIAL STIMULUS IN MILLIVOLTS :'
   READ *,VSTIM
C
   ARYCNT = 0
   TSTEP  = 0.005
C
C  ***** PUT VALUES IN CONSTANTS ARRAY *****
C
   CONSTS(1) = TEMP
   CONSTS(2) = 0.
   CONSTS(3) = CACONC
   CONSTS(4) = TIME
   CONSTS(5) = VSTIM
C
C  ***** CALL THE INITIALIZATION PROCEDURE *****
C
   CALL INIT(CONSTS,ALPHA,BETA,YARRAY,DYARRY)
C
   YARRAY(1) = VSTIM
C
C  ***** CALL RUNGE-KUTTA DRIVER ROUTINE *****
C
   CALLDRIVER(YARRAY,TIME,TSTEP,DATFIL,ARYCNT,CONSTS,ERRNUM)
C
   IF(ERRNUM.EQ.3)THEN
   GOTO 30
   END IF
C
C  ***** CALL THE OUTPUT ROUTINE *****
C
   CALL OUTPUT(DATFIL,ARYCNT,CONSTS)
C
C
30  CONTINUE
   STOP
   END
```

```
@*************************************************************
C ** INITIALIZATION PROCEDURE: THIS SUBROUTINE SETS UP THE **
C ** INITIAL VALUES OF THE VARIABLES.                       **
@*************************************************************
C
      SUBROUTINE INIT(CONSTS,ALPHA,BETA,YARRAY,DYARRY)
C
      DOUBLE PRECISION CACONC,TEMP,ALPHA(3),BETA(3)
      DOUBLE PRECISION QTEN,V,M,N,H
      DOUBLE PRECISION YARRAY(4),DYARRY(4),CONSTS(5)
      INTEGER I
C
C  ***** GET VALUES OUT OF THE CONSTANTS ARRAY *****
C
      TEMP   = CONSTS(1)
      CACONC = CONSTS(3)
C
C  ***** CALCULATE THE RESTING POTENTIAL *****
C
      V = V + 9.3 * DLOG((44./CACONC))
C
C  ***** CALCULATE THE ALPHA'S AND BETA'S *****
C
      ALPHA(1) = 0.01*(10.-V)/(DEXP(0.1*(10.-V))-1.)
      ALPHA(2) = 0.1*(25.-V)/(DEXP(0.1*(25.-V))-1.)
      ALPHA(3) = 0.07*DEXP(-V/20.)
C
      BETA(1) = 0.125*DEXP(-V/80.)
      BETA(2) = 4.*DEXP(-V/18.)
      BETA(3) = 1./(DEXP(0.1*(30.-V))+1.)
C
C  ***** APPLY TEMPERATURE COMPENSATION IF NEEDED *****
C
      QTEN = 1.
      IF(TEMP.NE.6.3)THEN
C
         QTEN = 3.**((TEMP-6.3)/10.)
C
         CONSTS(2) = QTEN
C
         DO 20 I=1,3
              ALPHA(I) = ALPHA(I)*QTEN
              BETA(I) = BETA(I)*QTEN
      20 CONTINUE
C
      END IF
C
C
C  ***** NOW CALCULATE INITIAL VALUES FOR INTEGRATION *****
C
      N = ALPHA(1)/(ALPHA(1)+BETA(1))
      M = ALPHA(2)/(ALPHA(2)+BETA(2))
      H = ALPHA(3)/(ALPHA(3)+BETA(3))
C
C
C
C
C
```

```
C  ***** PUT THESE VALUES INTO YARRAY *****
C
  YARRAY(1) = V
  YARRAY(2) = N
  YARRAY(3) = M
  YARRAY(4) = H
C  ***** INITIALIZE THE ARRAY OF DERIVATIVES *****
C
  DO 30 I=1,4
     DYARRY(I) =0.
30  CONTINUE
C
C  ALPHAN = ALPHA(1)
C  ALPHAM = ALPHA(2)
C  ALPHAH = ALPHA(3)
C  BETAN  = BETA(1)
C  BETAM  = BETA(2)
C  BETAH  = BETA(3)
C
  RETURN
  END
C
C
C  ********************************************************
C  ** THIS SUBROUTINE INVOKES THE RUNGE-KUTTA ROUTINE   **
C  ** TO CALCULATE THE SIZE OF THE TIME STEP NEEDED FOR **
C  ** THE REQUIRED ACCURACY AND THEN RUNS THE ROUTINE   **
C  ********************************************************
C
  SUBROUTINE DRIVER(YARRAY,TEND,TSTEP,DATFIL,ARYCNT,CONSTS,
   &  ERRNUM)
C
  DOUBLE PRECISION TSTEP,TEND,ERRTOL,YARRAY(4),YSAVE(4)
  DOUBLE PRECISION YINTER(4),YTEST(4),MAXERR,TNEW
  DOUBLE PRECISION CONSTS(5),DATFIL(10000,2),ERROR(4)
  INTEGER I,J,NHALF,STEPNO,ARYCNT,ERRNUM
C
  TNEW = 0.
  ARYCNT = 1
  ERRTOL = 0.00001
C
C  ***** INTEGRATE ONE STEP TWICE NORMAL LENGTH *****
C
7  CONTINUE
  TSTEP  = TSTEP * 2
  STEPNO = 1
  NHALF  =-1
C
  CALL RUNKUT(TNEW,YARRAY,TSTEP,YSAVE,CONSTS)
C
C
C  ***** HALVE THE TIME STEP AND INTEGRATE AGAIN *****
C
12  CONTINUE
  TSTEP  = TSTEP/2.
  STEPNO = STEPNO * 2
  NHALF  = NHALF + 1
C
```

```
C  ***** CHECK NUMBER OF INTERVAL HALVINGS *****
C
   IF(NHALF.GT.10)THEN
      WRITE(*,*)'TOO MANY HALVINGS NEEDED PROGRAM ENDS'
      ERRNUM = 3
      GOTO 53
   END IF
C
C  ***** INTEGRATE TWICE AS MANY STEPS AS BEFORE *****
C  ***** IN ORDER TO END UP AT THE SAME PLACE    *****
C
   DO 23 I=1,4
      YINTER(I) = YARRAY(I)
23  CONTINUE
C
   DO 30 I=1,STEPNO
      CALL RUNKUT(TNEW,YINTER,TSTEP,YTEST,CONSTS)
      TNEW = TNEW + TSTEP
      DO 29 J=1,4
           YINTER(J) = YTEST(J)
29    CONTINUE
30  CONTINUE
C
C  ***** NEW VALUES OF YARRAY ARE RETURNED BY RUNKUT *****
C
   DO 33 I=1,4
      YARRAY(I) = YTEST(I)
33  CONTINUE
C
C  ***** FIND THE DIFFERENCE *****
C
   DO 36 I=1,4
      ERROR(I) = DABS(YTEST(I) - YSAVE(I))
36  CONTINUE
C
C  ***** FIND MAXIMUM ERROR *****
C
   MAXERR = ERROR(1)
   DO 42 I=2,4
      IF(ERROR(I).GT.MAXERR)THEN
           MAXERR = ERROR(I)
      END IF
42  CONTINUE
C
C  ***** CHECK ACCURACY AGAINST ERRTOL *****
C
   IF(MAXERRR.GT.ERRTOL)THEN
      GOTO 12
           ELSE
C
C  ***** WRITE OUT RESULTS TO DATA ARRAY *****
C
           DATFIL(ARYCNT,1) = YTEST(1)
           DATFIL(ARYCNT,2) = TNEW
           ARYCNT = ARYCNT + 1
   END IF
C
C
```

```
C  ***** CHECK FOR END POINT *****
C
   IF(TNEW.LT.TEND)THEN
      GOTO 7
   END IF
C
   ARYCNT = ARYCNT - 1
C
C
53  CONTINUE
   RETURN
   END
C
C
C  ************************************************
C  ** NUMERICAL INTEGRATION SUBROUTINE           **
C  ** THIS SUBROUTINE PERFORMS A FOURTH - ORDER  **
C  ** RUNGE - KUTTA NUMERICAL INTEGRATION OF THE **
C  ** FUNCTION FUNCTN AND OUTPUTS A 2-D ARRAY    **
C  ************************************************
C
   SUBROUTINE RUNKUT(TOLD,YOLD,TSTEP,YNEW,CONSTS)
C
   DOUBLE PRECISION K(4,4),TOLD,TSTEP,YOLD(4),YNEW(4)
   DOUBLE PRECISION YTEMP(4),TTEMP,KTEMP(4),CONSTS(5)
   INTEGER I,J
C
C  ***** CALCULATE K1 *****
C
   CALL FUNCTN(TOLD,YOLD,KTEMP,CONSTS)
   DO 5  J=1,4
      K(J,1) = KTEMP(J)
5  CONTINUE
   DO 10 I=1,4
      K(I,1) = K(I,1)*TSTEP
10  CONTINUE
C
   DO 15 I=1,4
      YTEMP(I) = YOLD(I) + (K(I,1)/2)
15  CONTINUE
   TTEMP = TOLD + TSTEP/2
C
C  ***** CALCULATE K2 *****
C
   CALL FUNCTN(TTEMP,YTEMP,KTEMP,CONSTS)
   DO 18 J=1,4
      K(J,2) = KTEMP(J)
18  CONTINUE
     DO 20 I=1,4
      K(I,2) = K(I,2)*TSTEP
20  CONTINUE
C
   DO 25 I=1,4
      YTEMP(I) = YOLD(I) + (K(I,2)/2)
25  CONTINUE
C
C
C  ***** CALCULATE K3 *****
```

```
      CALL FUNCTN(TTEMP,YTEMP,KTEMP,CONSTS)
      DO 28 J=1,4
         K(J,3) = KTEMP(J)
28    CONTINUE
      DO 30 I=1,4
         K(I,3) = K(I,3)*TSTEP
30    CONTINUE
C
      DO 35 I=1,4
         YTEMP(I) = YOLD(I) + K(I,3)
35    CONTINUE
C
      TTEMP = TOLD + TSTEP
C
C     ***** CALCULATE K4 *****
C
      CALL FUNCTN(TTEMP,YTEMP,KTEMP,CONSTS)
      DO 38 J=1,4
         K(J,4) = KTEMP(J)
38    CONTINUE
      DO 40 I=1,4
         K(I,4) = K(I,4)*TSTEP
40    CONTINUE
C
C     ***** CALCULATE YNEW *****
C
      DO 45 I=1,4
      YNEW(I)=YOLD(I)+(K(I,1)+2.*K(I,2)+2.*K(I,3)+K(I,4))/6
45    CONTINUE
      RETURN
      END
C
C
C     ********************************************************
C     **                                                    **
C     ** FUNCTN SUBROUTINE : THIS SUBROUTINE CALCULATES THE **
C     ** VALUES OF THE VARIABLES THAT ARE REQUIRED BY THE   **
C     ** NUMERICAL INTEGRATION ROUTINE. IT TAKES IN VARIOUS **
C     ** CONSTANTS AND RETURNS WITH THE CURRENT VALUES OF   **
C     ** VDOT,NDOT,MDOT AND HDOT  (DYARRY)                  **
C     **                                                    **
C     ********************************************************
C
      SUBROUTINE FUNCTN(TIME,YARRAY,DYARRY,CONSTS)
C
      DOUBLE PRECISION V,VDOT,N,NDOT,M,MDOT,H,HDOT
      DOUBLE PRECISION ALPHA(3),BETA(3),MEMCAP,GNAMAX,GLMAX
      DOUBLE PRECISION VL,VK,VNA,GK,GNA,GKMAX,QTEN,TIME
      DOUBLE PRECISION CACONC,YARRAY(4),DYARRY(4),CONSTS(5)
      INTEGER I
C
      V    = YARRAY(1)
      N    = YARRAY(2)
      M    = YARRAY(3)
      H    = YARRAY(4)
C
C
C
```

```
      VNA = 115.
      VK  = -12.
      VL  = 10.58921
C
C
      MEMCAP =   1.
      GNAMAX = 120.
      GKMAX  =  36.
      GLMAX  =   0.3
C
      QTEN   = CONSTS(2)
      CACONC = CONSTS(3)
C
      V = V+9.3 * DLOG((44./CACONC))
C
C  ***** ERROR TRAP FOR V = 10 mV *****
C
      IF(V.GT.9.999.AND.V.LT.10.001)THEN
         ALPHA(1) = 0.1
      ELSE
         ALPHA(1) = 0.01*(10.-V)/(DEXP(0.1*(10.-V))-1.)
      END IF
C
C  ***** ERROR TRAP FOR V = 25mV *****
C
      IF(V.GT.24.999.AND.V.LT.25.001)THEN
         ALPHA(2) = 1.0
      ELSE
         ALPHA(2) = 0.1*(25.-V)/(DEXP(0.1*(25.-V))-1.)
      END IF
C
      BETA(1) = 0.125*DEXP(-V/80.)
      BETA(2)  = 4.*DEXP(-V/18.)
      ALPHA(3) = 0.07*DEXP(-V/20.)
      BETA(3)  = 1./(DEXP(0.1*(30.-V))+1.)
C
C  ***** TEMPERATURE COMPENSATION *****
C
      DO 30 I=1,3
         ALPHA(I) = ALPHA(I)*QTEN
         BETA(I)  = BETA(I)*QTEN
30    CONTINUE
C
C  ***** CALCULATE THE CONDUCTANCES *****
C
      GK  = GKMAX*(N**4)
      GNA = GNAMAX*(M**3)*H
C
C  ***** CALCULATE THE DERIVATIVES *****
C
      V = V - 9.3 * DLOG((44./CACONC))
C
      VDOT = (-1./MEMCAP)*(GK*(V-VK)+GNA*(V-VNA)+GLMAX*(V-VL))
C
      NDOT = ALPHA(1)*(1-N)-BETA(1)*N
      MDOT = ALPHA(2)*(1-M)-BETA(2)*M
      HDOT = ALPHA(3)*(1-H)-BETA(3)*H
C
```

```
C  ***** PLACE THESE VALUES IN AN ARRAY FOR CONVENIENCE *****
C
   DYARRY(1) = VDOT
   DYARRY(2) = NDOT
   DYARRY(3) = MDOT
   DYARRY(4) = HDOT
C
   RETURN
   END
C
C  ********************************************************
C  ** OUTPUT SUBROUTINE : THIS SUBROUTINE WRITES THE     **
C  ** CALCULATED VALUES OF THE VOLTAGE AND TIME TO A     **
C  ** DATA FILE CREATED ON A FLOPPY DISC.                **
C  ********************************************************
C
   SUBROUTINE OUTPUT(DATFIL,ARYCNT,CONSTS)
C
   DOUBLE PRECISION DATFIL(10000,2),CONSTS(5)
   INTEGER ARYCNT,ERROR
   CHARACTER FILNAM*6,FILE*12,DATE*8
C
   DATA FILE,DATE/'A:FILNAM.DAT','DD:MM:YY'/
C
C  ***** GET THE FILE NAME AND DATE FROM USER *****
C
   WRITE(*,*)'ENTER THE FILE NAME (6 CHARS) : '
   READ(*,100) FILNAM
C
   WRITE(*,*)'ENTER THE DATE (DD:MM:YY)  : '
   READ(*,400) DATE
C
   FILE(3:8) = FILNAM
C
C  ***** OPEN THE FILE ON DRIVE A: *****
C
   OPEN(UNIT=4,FILE=FILE,STATUS='NEW',IOSTAT=ERROR,
      &     ERR=50)
C
   PAUSE 'INSERT DATA DISC THEN PRESS ENTER'
C
C  ***** NOW WRITE THE ARRAY TO DISC *****
C
   WRITE(4,100) FILNAM
   WRITE(4,200) DATE
   WRITE(4,600)'ARRAY  SIZE'
   WRITE(4,500) ARYCNT
   WRITE(4,200)'DURATION'
   WRITE(4,700) CONSTS(4)
   WRITE(4,600)'TEMPERATURE'
   WRITE(4,700) CONSTS(1)
   WRITE(4,100)'CACONC'
   WRITE(4,700) CONSTS(3)
   WRITE(4,200)'STIMULUS'
   WRITE(4,700) CONSTS(5)
   DO 20 I=1,ARYCNT
   WRITE(4,300) DATFIL(I,1),DATFIL(I,2)
20 CONTINUE
```

```
C
C  ***** ERROR HANDLING ROUTINE *****
C
50  IF(ERROR.EQ.2009)THEN
     WRITE(*,*)'INCORRECT STATUS ARGUMENT'
  ELSE IF(ERROR.EQ.2011)THEN
     WRITE(*,*)'RECORD LENGTH SPECIFIER TOO LARGE'
  ELSE IF(ERROR.EQ.2013)THEN
     WRITE(*,*)'FILENAME HAS BEEN USED BEFORE'
  ELSE IF(ERROR.EQ.2014)THEN
     WRITE(*,*)'FILENAME NOT SPECIFIED'
  END IF
C
C  ***** FORMAT STATEMENTS *****
C
100  FORMAT(A6)
200  FORMAT(A8)
300  FORMAT(D14.6,5X,D14.6)
400  FORMAT(A8)
500  FORMAT(I5)
600  FORMAT(A11)
700  FORMAT(D10.5)
C
C  ***** CLOSE FILE *****
C
  CLOSE(UNIT=4)
C
  RETURN
  END
```

```
C ********************************************************
C ** THIS PROGRAM IMPLEMENTS A MATHEMATICAL MODEL  TO  **
C ** SIMULATE THE BEHAVIOUR OF A NEURONE.             **
C ** IT SOLVES THE EQUATIONS DERIVED BY HODGKIN AND    **
C ** HUXLEY BY USING A NUMERICAL INTEGRATION TECHNIQUE **
C ** THIS PROGRAM HAS BEEN MODIFIED TO COPE WITH MORE  **
C ** OUTPUT VARIABLES TO ENABLE THE USER TO LOOK AT THE**
C ** BEHAVIOUR OF M,N,H,I & V AGAINST TIME.            **
C ********************************************************
C
  PROGRAM HHMDNEW
  DOUBLE PRECISION TIME,TEMP,CACONC,VSTIM,YARRAY(4),TSTEP
  DOUBLE PRECISION CONSTS(5),ALPHA(3),BETA(3),DYARRY(4)
  REAL DATFIL(10000,6)
  INTEGER ARYCNT,ERRNUM
C
C  ***** GET DATA IN FROM THE KEYBOARD *****
C
  WRITE (*,*)'ENTER THE TIME DURATION IN MILLISECONDS :'
  READ *,TIME
  WRITE (*,*)'ENTER THE TEMPERATURE IN DEGREES CELCIUS :'
  READ *,TEMP
  WRITE(*,*)'ENTER THE CALCIUM CONCENTRATION IN MILLIMOLES :'
  READ *,CACONC
  WRITE (*,*)'ENTER THE INITIAL STIMULUS IN MILLIVOLTS :'
  READ *,VSTIM
C
  ARYCNT = 0
  TSTEP  = 0.005
C
C  ***** PUT VALUES IN CONSTANTS ARRAY *****
C
  CONSTS(1) = TEMP
  CONSTS(2) = 0.
  CONSTS(3) = CACONC
  CONSTS(4) = TIME
  CONSTS(5) = VSTIM
C
C  ***** CALL THE INITIALIZATION PROCEDURE *****
C
  CALL INIT(CONSTS,ALPHA,BETA,YARRAY,DYARRY)
C
  YARRAY(1) = VSTIM
C
C  ***** CALL RUNGE-KUTTA DRIVER ROUTINE *****
C
  CALLDRIVER(YARRAY,TIME,TSTEP,DATFIL,ARYCNT,CONSTS,ERRNUM)
C
  IF(ERRNUM.EQ.3)THEN
  GOTO 30
  END IF
C
C  ***** CALL THE OUTPUT ROUTINE *****
C
  CALL OUTPUT(DATFIL,ARYCNT,CONSTS)
30  CONTINUE
    STOP
    END
```

```
@*************************************************************
C ** INITIALIZATION PROCEDURE: THIS SUBROUTINE SETS UP THE **
C ** INITIAL VALUES OF THE VARIABLES.                       **
@*************************************************************
C
  SUBROUTINE INIT(CONSTS,ALPHA,BETA,YARRAY,DYARRY)
C
  DOUBLE PRECISION CACONC,TEMP,ALPHA(3),BETA(3)
  DOUBLE PRECISION QTEN,V,M,N,H
  DOUBLE PRECISION YARRAY(4),DYARRY(4),CONSTS(5)
  INTEGER I
C
C  ***** GET VALUES OUT OF THE CONSTANTS ARRAY *****
C
  TEMP   = CONSTS(1)
  CACONC = CONSTS(3)
C
C  ***** CALCULATE THE RESTING POTENTIAL *****
C
  V = V + 9.3 * DLOG((44./CACONC))
C
C  ***** CALCULATE THE ALPHA'S AND BETA'S *****
C
  ALPHA(1) = 0.01*(10.-V)/(DEXP(0.1*(10.-V))-1.)
  ALPHA(2) = 0.1*(25.-V)/(DEXP(0.1*(25.-V))-1.)
  ALPHA(3) = 0.07*DEXP(-V/20.)
C
  BETA(1) = 0.125*DEXP(-V/80.)
  BETA(2) = 4.*DEXP(-V/18.)
  BETA(3) = 1./(DEXP(0.1*(30.-V))+1.)
C
C  ***** APPLY TEMPERATURE COMPENSATION IF NEEDED *****
C
  QTEN = 1.
  IF(TEMP.NE.6.3)THEN
C
     QTEN = 3.**((TEMP-6.3)/10.)
C
     CONSTS(2) = QTEN
C
     DO 20 I=1,3
          ALPHA(I) = ALPHA(I)*QTEN
          BETA(I) = BETA(I)*QTEN
20   CONTINUE
C
  END IF
C
C  ***** NOW CALCULATE INITIAL VALUES FOR INTEGRATION *****
C
  N = ALPHA(1)/(ALPHA(1)+BETA(1))
  M = ALPHA(2)/(ALPHA(2)+BETA(2))
  H = ALPHA(3)/(ALPHA(3)+BETA(3))
C
C  ***** PUT THESE VALUES INTO YARRAY *****
C
C
C
C
```

```
      YARRAY(1) = V
      YARRAY(2) = N
      YARRAY(3) = M
      YARRAY(4) = H
C     ***** INITIALIZE THE ARRAY OF DERIVATIVES *****
C
      DO 30 I=1,4
         DYARRY(I) =0.
30    CONTINUE
C
      ALPHAN = ALPHA(1)
      ALPHAM = ALPHA(2)
      ALPHAH = ALPHA(3)
      BETAN  = BETA(1)
      BETAM  = BETA(2)
      BETAH  = BETA(3)
C
      RETURN
      END
C
C
C     ********************************************************
C     ** THIS SUBROUTINE INVOKES THE RUNGE-KUTTA ROUTINE    **
C     ** TO CALCULATE THE SIZE OF THE TIME STEP NEEDED FOR **
C     ** THE REQUIRED ACCURACY AND THEN RUNS THE ROUTINE    **
C     ********************************************************
C
      SUBROUTINE DRIVER(YARRAY,TEND,TSTEP,DATFIL,ARYCNT,CONSTS,
     &   ERRNUM,MEMCUR)
C
      DOUBLE PRECISION TSTEP,TEND,ERRTOL,YARRAY(4),YSAVE(4)
      DOUBLE PRECISION YINTER(4),YTEST(4),MAXERR,TSTART,MEMCUR
      DOUBLE PRECISION CONSTS(5),ERROR(4)
      REAL DATFIL(10000,6)
      INTEGER I,J,NHALF,STEPNO,ARYCNT,ERRNUM
C
      TSTART = 0.
      ARYCNT = 1
      ERRTOL = 0.00001
C
C     ***** LOAD THE OUTPUT ARRAY WITH INITIAL VALUES *****
C
      DATFIL(1,1) = SNGL(TSTART)
      DATFIL(1,2) = SNGL(YARRAY(1))
      DATFIL(1,3) = SNGL(YARRAY(2))
      DATFIL(1,4) = SNGL(YARRAY(3))
      DATFIL(1,5) = SNGL(YARRAY(4))
      DATFIL(1,6) = SNGL(MEMCUR)
C
C     ***** INTEGRATE ONE STEP TWICE NORMAL LENGTH *****
C
7     CONTINUE
      TSTEP  = TSTEP * 2
      STEPNO = 1
      NHALF  =-1
C
      CALL RUNKUT(TNEW,YARRAY,TSTEP,YSAVE,CONSTS)
C
```

```
C  ***** HALVE THE TIME STEP AND INTEGRATE AGAIN *****
C
12  CONTINUE
  TSTEP  = TSTEP/2.
  STEPNO = STEPNO * 2
  NHALF  = NHALF + 1
C
C  ***** CHECK NUMBER OF INTERVAL HALVINGS *****
C
  IF(NHALF.GT.10)THEN
     WRITE(*,*)'TOO MANY HALVINGS NEEDED PROGRAM ENDS'
     ERRNUM = 3
     GOTO 53
  END IF
C
C  ***** INTEGRATE TWICE AS MANY STEPS AS BEFORE *****
C  ***** IN ORDER TO END UP AT THE SAME PLACE    *****
C
  DO 23 I=1,4
     YINTER(I) = YARRAY(I)
23  CONTINUE
C
  DO 30 I=1,STEPNO
     CALL RUNKUT(TNEW,YINTER,TSTEP,YTEST,CONSTS)
     TNEW = TNEW + TSTEP
     DO 29 J=1,4
          YINTER(J) = YTEST(J)
29   CONTINUE
30  CONTINUE
C
C  ***** NEW VALUES OF YARRAY ARE RETURNED BY RUNKUT *****
C
  DO 33 I=1,4
     YARRAY(I) = YTEST(I)
33  CONTINUE
C
C  ***** FIND THE DIFFERENCE *****
C
  DO 36 I=1,4
     ERROR(I) = DABS(YTEST(I) - YSAVE(I))
36  CONTINUE
C
C  ***** FIND MAXIMUM ERROR *****
C
  MAXERR = ERROR(1)
  DO 42 I=2,4
     IF(ERROR(I).GT.MAXERR)THEN
          MAXERR = ERROR(I)
     END IF
42  CONTINUE
C
C  ***** CHECK ACCURACY AGAINST ERRTOL *****
C
  IF(MAXERRR.GT.ERRTOL)THEN
     GOTO 12
          ELSE
C
C
```

```
C  ***** WRITE OUT RESULTS TO DATA ARRAY *****
C
           DATFIL(ARYCNT+1,1) = SNGL(TNEW)
           DATFIL(ARYCNT+1,2) = SNGL(YTEST(1))
           DATFIL(ARYCNT+1,3) = SNGL(M)
           DATFIL(ARYCNT+1,4) = SNGL(H)
           DATFIL(ARYCNT+1,5) = SNGL(N)
           DATFIL(ARYCNT+1,6) = SNGL(MEMCUR)
           ARYCNT = ARYCNT + 1
  END IF
C
C  ***** CHECK FOR END POINT *****
C
  IF(TNEW.LT.TEND)THEN
     GOTO 7
  END IF
C
  ARYCNT = ARYCNT - 1
C
53  CONTINUE
  RETURN
  END
C
C
C  ****************************************************
C  ** NUMERICAL INTEGRATION SUBROUTINE                **
C  ** THIS SUBROUTINE PERFORMS A FOURTH - ORDER       **
C  ** RUNGE - KUTTA NUMERICAL INTEGRATION OF THE      **
C  ** FUNCTION FUNCTN AND OUTPUTS A 2-D ARRAY         **
C  ****************************************************
C
  SUBROUTINE RUNKUT(TOLD,YOLD,TSTEP,YNEW,CONSTS)
C
  DOUBLE PRECISION TOLD,TSTEP,YOLD(4),YNEW(4),HLFSTP,SIXSTP
  DOUBLE PRECISION YTEMP(4),TTEMP,DYT(4),DYM(4),CONSTS(5)
  INTEGER I
C
C
  HLFSTP = TSTEP * 0.5
  SIXSTP = TSTEP/6.
  TTEMP  = TOLD + HLFSTP
C
  DO 10 I=1,4
     YTEMP(I) = YOLD(I) + HLFSTP * YOLD(I)
10  CONTINUE
C
  CALL FUNCTN(TTEMP,YTEMP,DYT,CONSTS)
C
  DO 14 I=1,4
     YTEMP(I) = YOLD(I) + HLFSTP * DYT(I)
14  CONTINUE
C
  CALL FUNCTN(TTEMP,YTEMP,DYM,CONSTS)
C
  DO 19 I=1,4
     YTEMP(I) = YOLD(I) + TSTEP * DYM(I)
     DYM(I)   = DYT(I)  + DYM(I)
19  CONTINUE
```

```
C
      CALL FUNCTN(TOLD+TSTEP,YTEMP,DYT,CONSTS)
      DO 23 I=1,4
      YNEW(I)=YOLD(I)+SIXSTP*(YOLD(I)+DYT(I)+2.*DYM(I))
23    CONTINUE
C
      RETURN
      END
C
C
C     ************************************************************
C     **                                                        **
C     ** FUNCTN SUBROUTINE : THIS SUBROUTINE CALCULATES THE    **
C     ** VALUES OF THE VARIABLES THAT ARE REQUIRED BY THE       **
C     ** NUMERICAL INTEGRATION ROUTINE. IT TAKES IN VARIOUS     **
C     ** CONSTANTS AND RETURNS WITH THE CURRENT VALUES OF       **
C     ** VDOT,NDOT,MDOT AND HDOT  (DYARRY)                      **
C     **                                                        **
C     ************************************************************
C
      SUBROUTINE FUNCTN(TIME,YARRAY,DYARRY,CONSTS)
C
      DOUBLE PRECISION V,VDOT,N,NDOT,M,MDOT,H,HDOT,MEMCUR
      DOUBLE PRECISION ALPHA(3),BETA(3),MEMCAP,GNAMAX,GLMAX
      DOUBLE PRECISION VL,VK,VNA,GK,GNA,GKMAX,QTEN,TIME
      DOUBLE PRECISION CACONC,YARRAY(4),DYARRY(4),CONSTS(5)
      INTEGER I
C
      V    = YARRAY(1)
      N    = YARRAY(2)
      M    = YARRAY(3)
      H    = YARRAY(4)
C
      VNA = 115.
      VK  = -12.
      VL  = 10.58921
C
C
      MEMCAP =   1.
      GNAMAX = 120.
      GKMAX  =  36.
      GLMAX  =   0.3
C
      QTEN   = CONSTS(2)
      CACONC = CONSTS(3)
C
      V = V+9.3 * DLOG((44./CACONC))
C
C     ***** ERROR TRAP FOR V = 10 mV *****
C
      IF(V.GT.9.999.AND.V.LT.10.001)THEN
         ALPHA(1) = 0.1
      ELSE
         ALPHA(1) = 0.01*(10.-V)/(DEXP(0.1*(10.-V))-1.)
      END IF
C
C
C
```

```
C  ***** ERROR TRAP FOR V = 25mV *****
C
   IF(V.GT.24.999.AND.V.LT.25.001)THEN
      ALPHA(2) = 1.0
   ELSE
      ALPHA(2) = 0.1*(25.-V)/(DEXP(0.1*(25.-V))-1.)
   END IF
C
   BETA(1) = 0.125*DEXP(-V/80.)
   BETA(2)  = 4.*DEXP(-V/18.)
   ALPHA(3) = 0.07*DEXP(-V/20.)
   BETA(3)  = 1./(DEXP(0.1*(30.-V))+1.)
C
C  ***** TEMPERATURE COMPENSATION *****
C
   DO 30 I=1,3
      ALPHA(I) = ALPHA(I)*QTEN
      BETA(I)  = BETA(I)*QTEN
30  CONTINUE
C
C  ***** CALCULATE THE CONDUCTANCES *****
C
   GK  = GKMAX*(N**4)
   GNA = GNAMAX*(M**3)*H
C
C  ***** CALCULATE THE DERIVATIVES *****
C
   V = V - 9.3 * DLOG((44./CACONC))
C
   MEMCUR = (GK*(V-VK)+GNA*(V-VNA)+GLMAX*(V-VL))
   VDOT = (-1./MEMCAP)*MEMCUR
C
   NDOT = ALPHA(1)*(1-N)-BETA(1)*N
C
   MDOT = ALPHA(2)*(1-M)-BETA(2)*M
C
   HDOT = ALPHA(3)*(1-H)-BETA(3)*H
C
C  ***** PLACE THESE VALUES IN AN ARRAY FOR CONVENIENCE *****
C
   DYARRY(1) = VDOT
   DYARRY(2) = NDOT
   DYARRY(3) = MDOT
   DYARRY(4) = HDOT
C
   RETURN
   END
C
C
C
C
C
C
C
C
C
C
C
```

```
C  ********************************************************
C  ** OUTPUT SUBROUTINE : THIS SUBROUTINE WRITES THE     **
C  ** CALCULATED VALUES OF THE VOLTAGE AND TIME TO A     **
C  ** DATA FILE CREATED ON A FLOPPY DISC.                **
C  ********************************************************
C
   SUBROUTINE OUTPUT(DATFIL,ARYCNT,CONSTS)
C
   DOUBLE PRECISION CONSTS(5)
   REAL DATFIL(10000,6)
   INTEGER ARYCNT,ERROR
   CHARACTER FILNAM*6,FILE*12,DATE*8
C
   DATA FILE,DATE/'A:FILNAM.DAT','DD:MM:YY'/
C
C  ***** GET THE FILE NAME AND DATE FROM USER *****
C
   WRITE(*,*)'ENTER THE FILE NAME (6 CHARS) : '
   READ(*,100) FILNAM
C
   WRITE(*,*)'ENTER THE DATE (DD:MM:YY)  : '
   READ(*,400) DATE
C
   FILE(3:8) = FILNAM
C
C  ***** OPEN THE FILE ON DRIVE A: *****
C
   OPEN(UNIT=4,FILE=FILE,STATUS='NEW',IOSTAT=ERROR,
       &   ERR=50)
C
   PAUSE 'INSERT DATA DISC THEN PRESS ENTER'
C
C  ***** NOW WRITE THE ARRAY TO DISC *****
C
   WRITE(4,100) FILNAM
   WRITE(4,200) DATE
   WRITE(4,600)'ARRAY  SIZE'
   WRITE(4,500) ARYCNT
   WRITE(4,200)'DURATION'
   WRITE(4,700) CONSTS(4)
   WRITE(4,600)'TEMPERATURE'
   WRITE(4,700) CONSTS(1)
   WRITE(4,100)'CACONC'
   WRITE(4,700) CONSTS(3)
   WRITE(4,200)'STIMULUS'
   WRITE(4,700) CONSTS(5)
   DO 20 I=1,ARYCNT
   WRITE(4,300) DATFIL(I,1),DATFIL(I,2),DATFIL(I,3),
       &  DATFIL(I,4),DATFIL(I,5),DATFIL(I,6)
20  CONTINUE
C
C
C
C
C
C
C
C
```

```
C
C  ***** ERROR HANDLING ROUTINE *****
C
50  IF(ERROR.EQ.2009)THEN
      WRITE(*,*)'INCORRECT STATUS ARGUMENT'
  ELSE IF(ERROR.EQ.2011)THEN
      WRITE(*,*)'RECORD LENGTH SPECIFIER TOO LARGE'
  ELSE IF(ERROR.EQ.2013)THEN
      WRITE(*,*)'FILENAME HAS BEEN USED BEFORE'
  ELSE IF(ERROR.EQ.2014)THEN
      WRITE(*,*)'FILENAME NOT SPECIFIED'
  END IF
C
C  ***** FORMAT STATEMENTS *****
C
100  FORMAT(A6)
200  FORMAT(A8)
300  FORMAT(F10.5,X,F10.5,X,F10.5,X,F10.5,X,F10.5,X,F10.5)
400  FORMAT(A8)
500  FORMAT(I5)
600  FORMAT(A11)
700  FORMAT(D10.5)
C
C  ***** CLOSE FILE *****
C
  CLOSE(UNIT=4)
C
  RETURN
  END
```

```
C  ********************************************************
C  ** THIS PROGRAM IMPLEMENTS A MATHEMATICAL MODEL  TO  **
C  ** SIMULATE THE BEHAVIOUR OF A NEURONE.              **
C  ** IT SOLVES THE EQUATIONS DERIVED BY HODGKIN AND    **
C  ** HUXLEY BY USING A NUMERICAL INTEGRATION TECHNIQUE **
C  ********************************************************
C
   PROGRAM OXYMOD
C
   DOUBLE PRECISION TIME,TEMP,VSTIM,YARRAY(4),TSTEP
   DOUBLE PRECISION CONSTS(4),ALPHA(3),BETA(3),DYARRY(4)
   REAL DATFIL(10000,2)
   INTEGER ARYCNT,ERRNUM
   CHARACTER RERUN*3
C
10  CONTINUE
   ERRNUM = 0
C
C  ***** GET DATA IN FROM THE KEYBOARD *****
C
   WRITE (*,*)'ENTER THE TIME DURATION IN MILLISECONDS :'
   READ *,TIME
   WRITE (*,*)'ENTER THE TEMPERATURE IN DEGREES CELCIUS :'
   READ *,TEMP
   WRITE (*,*)'ENTER THE INITIAL STIMULUS IN MILLIVOLTS :'
   READ *,VSTIM
C
   ARYCNT = 0
   TSTEP  = 0.005
C
C  ***** PUT VALUES IN CONSTANTS ARRAY *****
C
   CONSTS(1) = TEMP
   CONSTS(2) = 0.
   CONSTS(3) = TIME
   CONSTS(4) = VSTIM
C
C  ***** CALL THE INITIALIZATION PROCEDURE *****
C
   CALL INIT(CONSTS,ALPHA,BETA,YARRAY,DYARRY)
C
   YARRAY(1) = VSTIM
C
C  ***** CALL RUNGE-KUTTA DRIVER ROUTINE *****
C
   CALLDRIVER(YARRAY,TIME,TSTEP,DATFIL,ARYCNT,CONSTS,ERRNUM)
C
   IF(ERRNUM.EQ.3)THEN
   GOTO 20
   END IF
C
C  ***** CALL THE OUTPUT ROUTINE *****
C
   CALL OUTPUT(DATFIL,ARYCNT,CONSTS)
C
C
C
C
```

```
C  ***** ASK USER IF THEY WANT ANOTHER RUN *****
C
20  CONTINUE
  WRITE(*,*)'DO YOU WANT ANOTHER RUN (Y/N) ? : '
  READ *,RERUN
C
      IF(RERUN.EQ.'Y')THEN
     GOTO 10
  END IF
C
30  CONTINUE
  STOP
  END
C
C
C ***********************************************************
C ** INITIALIZATION PROCEDURE: THIS SUBROUTINE SETS UP    **
C ** THE INITIAL VALUES OF THE VARIABLES.                 **
C ***********************************************************
C
  SUBROUTINE INIT(CONSTS,ALPHA,BETA,YARRAY,DYARRY)
C
  DOUBLE PRECISION TEMP,ALPHA(3),BETA(3)
  DOUBLE PRECISION QTEN,V,M,N,H
  DOUBLE PRECISION YARRAY(4),DYARRY(4),CONSTS(4)
  INTEGER I
C
C  ***** GET VALUES OUT OF THE CONSTANTS ARRAY *****
C
  TEMP    = CONSTS(1)
  V       = 0.0
C
C  ***** CALCULATE THE ALPHA'S AND BETA'S *****
C
  ALPHA(1) = 0.01*(10.-V)/(DEXP(0.1*(10.-V))-1.)
  ALPHA(2) = 0.1*(25.-V)/(DEXP(0.1*(25.-V))-1.)
  ALPHA(3) = 0.07*DEXP(-V/20.)
C
  BETA(1) = 0.125*DEXP(-V/80.)
  BETA(2) = 4.*DEXP(-V/18.)
  BETA(3) = 1./(DEXP(0.1*(30.-V))+1.)
C
C  ***** APPLY TEMPERATURE COMPENSATION IF NEEDED *****
C
  QTEN = 1.
  IF(TEMP.NE.6.3)THEN
C
     QTEN = 3.**((TEMP-6.3)/10.)
C
     CONSTS(2) = QTEN
C
     DO 20 I=1,3
          ALPHA(I) = ALPHA(I)*QTEN
          BETA(I) = BETA(I)*QTEN
20   CONTINUE
C
  END IF
C
```

```
C  ***** NOW CALCULATE INITIAL VALUES FOR INTEGRATION *****
C
   N = ALPHA(1)/(ALPHA(1)+BETA(1))
   M = ALPHA(2)/(ALPHA(2)+BETA(2))
   H = ALPHA(3)/(ALPHA(3)+BETA(3))
C
C  ***** PUT THESE VALUES INTO YARRAY *****
C
   YARRAY(1) = V
   YARRAY(2) = N
   YARRAY(3) = M
   YARRAY(4) = H
C
C  ***** INITIALIZE THE ARRAY OF DERIVATIVES *****
C
   DO 30 I=1,4
      DYARRY(I) =0.
30  CONTINUE
C
   ALPHAN = ALPHA(1)
   ALPHAM = ALPHA(2)
   ALPHAH = ALPHA(3)
   BETAN  = BETA(1)
   BETAM  = BETA(2)
   BETAH  = BETA(3)
C
   RETURN
   END
C
C
C  ********************************************************
C  ** THIS SUBROUTINE INVOKES THE RUNGE-KUTTA ROUTINE    **
C  ** TO CALCULATE THE SIZE OF THE TIME STEP NEEDED FOR **
C  ** THE REQUIRED ACCURACY AND THEN RUNS THE ROUTINE    **
C  ********************************************************
C
   SUBROUTINE DRIVER(YARRAY,TEND,TSTEP,DATFIL,ARYCNT,CONSTS,
     &  ERRNUM)
C
   DOUBLE PRECISION TSTEP,TEND,ERRTOL,YARRAY(4),YSAVE(4)
   DOUBLE PRECISION YINTER(4),YTEST(4),MAXERR,TNEW
   DOUBLE PRECISION CONSTS(4),ERROR(4)
   REAL DATFIL(10000,2)
   INTEGER I,J,NHALF,STEPNO,ARYCNT,ERRNUM
C
   TNEW = 0.
   ARYCNT = 2
   ERRTOL = 0.00001
C
C  ***** LOAD THE OUTPUT ARRAYS WITH THE INITIAL VALUES *****
C
   DATFIL(1,1) = SNGL(YARRAY(1))
   DATFIL(1,2) = SNGL(TNEW)
C
C
C
C
C
```

```
C  ***** INTEGRATE ONE STEP TWICE NORMAL LENGTH *****
C
7  CONTINUE
   TSTEP  = TSTEP * 2
   STEPNO = 1
   NHALF  =-1
C
   CALL RUNKUT(TNEW,YARRAY,TSTEP,YSAVE,CONSTS)
C
C
C  ***** HALVE THE TIME STEP AND INTEGRATE AGAIN *****
C
12  CONTINUE
   TSTEP  = TSTEP/2.
   STEPNO = STEPNO * 2
   NHALF  = NHALF + 1
C
C  ***** CHECK NUMBER OF INTERVAL HALVINGS *****
C
   IF(NHALF.GT.10)THEN
      WRITE(*,*)'TOO MANY HALVINGS NEEDED PROGRAM ENDS'
      ERRNUM = 3
      GOTO 53
   END IF
C
C  ***** INTEGRATE TWICE AS MANY STEPS AS BEFORE *****
C  ***** IN ORDER TO END UP AT THE SAME PLACE    *****
C
   DO 23 I=1,4
      YINTER(I) = YARRAY(I)
23  CONTINUE
C
DO 30 I=1,STEPNO
      CALL RUNKUT(TNEW,YINTER,TSTEP,YTEST,CONSTS)
      TNEW = TNEW + TSTEP
      DO 29 J=1,4
           YINTER(J) = YTEST(J)
29    CONTINUE
30    CONTINUE
C
C  ***** NEW VALUES OF YARRAY ARE RETURNED BY RUNKUT *****
C
   DO 33 I=1,4
      YARRAY(I) = YTEST(I)
33  CONTINUE
C
C  ***** FIND THE DIFFERENCE *****
C
   DO 36 I=1,4
      ERROR(I) = DABS(YTEST(I) - YSAVE(I))
36  CONTINUE
C
C
C
C
C
C
C
```

```
C  ***** FIND MAXIMUM ERROR *****
C
  MAXERR = ERROR(1)
  DO 42 I=2,4
     IF(ERROR(I).GT.MAXERR)THEN
          MAXERR = ERROR(I)
     END IF
42  CONTINUE
C
C  ***** CHECK ACCURACY AGAINST ERRTOL *****
C
  IF(MAXERRR.GT.ERRTOL)THEN
     GOTO 12
          ELSE
C
C  ***** WRITE OUT RESULTS TO DATA ARRAY *****
C
          DATFIL(ARYCNT,1) = SNGL(YTEST(1))
          DATFIL(ARYCNT,2) = SNGL(TNEW)
          ARYCNT = ARYCNT + 1
  END IF
C
C  ***** CHECK FOR END POINT *****
C
  IF(TNEW.LT.TEND)THEN
     GOTO 7
  END IF
C
53  CONTINUE
C
  ARYCNT = ARYCNT - 1
C
  RETURN
  END
C
C
C  ****************************************************
C  ** NUMERICAL INTEGRATION SUBROUTINE                **
C  ** THIS SUBROUTINE PERFORMS A FOURTH - ORDER       **
C  ** RUNGE - KUTTA NUMERICAL INTEGRATION OF THE      **
C  ** FUNCTION FUNCTN AND OUTPUTS A 2-D ARRAY         **
C  ****************************************************
C
  SUBROUTINE RUNKUT(TOLD,YOLD,TSTEP,YNEW,CONSTS)
C
  DOUBLE PRECISION K(4,4),TOLD,TSTEP,YOLD(4),YNEW(4)
  DOUBLE PRECISION YTEMP(4),TTEMP,KTEMP(4),CONSTS(4)
  INTEGER I,J
C
C  ***** CALCULATE K1 *****
C
  CALL FUNCTN(TOLD,YOLD,KTEMP,CONSTS)
  DO 5  J=1,4
     K(J,1) = KTEMP(J)
5  CONTINUE
  DO 10 I=1,4
     K(I,1) = K(I,1)*TSTEP
10  CONTINUE
```

```
C
C
  DO 15 I=1,4
     YTEMP(I) = YOLD(I) + (K(I,1)/2)
15  CONTINUE
  TTEMP = TOLD + TSTEP/2
C
C  ***** CALCULATE K2 *****
C
  CALL FUNCTN(TTEMP,YTEMP,KTEMP,CONSTS)
  DO 18 J=1,4
     K(J,2) = KTEMP(J)
18  CONTINUE
  DO 20 I=1,4
     K(I,2) = K(I,2)*TSTEP
20  CONTINUE
C
  DO 25 I=1,4
     YTEMP(I) = YOLD(I) + (K(I,2)/2)
25  CONTINUE
C
C  ***** CALCULATE K3 *****
C
  CALL FUNCTN(TTEMP,YTEMP,KTEMP,CONSTS)
  DO 28 J=1,4
     K(J,3) = KTEMP(J)
28  CONTINUE
  DO 30 I=1,4
     K(I,3) = K(I,3)*TSTEP
30  CONTINUE
C
  DO 35 I=1,4
     YTEMP(I) = YOLD(I) + K(I,3)
35  CONTINUE
C
  TTEMP = TOLD + TSTEP
C
C  ***** CALCULATE K4 *****
C
  CALL FUNCTN(TTEMP,YTEMP,KTEMP,CONSTS)
  DO 38 J=1,4
     K(J,4) = KTEMP(J)
38  CONTINUE
  DO 40 I=1,4
     K(I,4) = K(I,4)*TSTEP
40  CONTINUE
C
C  ***** CALCULATE YNEW *****
C
  DO 45 I=1,4
  YNEW(I)=YOLD(I)+(K(I,1)+2.*K(I,2)+2.*K(I,3)+K(I,4))/6
45  CONTINUE
  RETURN
  END
C
C
C
C
```

```
C  ********************************************************
C  **                                                    **
C  ** FUNCTN SUBROUTINE : THIS SUBROUTINE CALCULATES THE **
C  ** VALUES OF THE VARIABLES THAT ARE REQUIRED BY THE   **
C  ** NUMERICAL INTEGRATION ROUTINE. IT TAKES IN VARIOUS **
C  ** CONSTANTS AND RETURNS WITH THE CURRENT VALUES OF   **
C  ** VDOT,NDOT,MDOT AND HDOT  (DYARRY)                  **
C  **                                                    **
C  ********************************************************
C
   SUBROUTINE FUNCTN(TIME,YARRAY,DYARRY,CONSTS)
C
   DOUBLE PRECISION V,VDOT,N,NDOT,M,MDOT,H,HDOT
   DOUBLE PRECISION ALPHA(3),BETA(3),MEMCAP,GNAMAX,GLMAX
   DOUBLE PRECISION VL,VK,VNA,GK,GNA,GKMAX,QTEN,TIME
   DOUBLE PRECISION CACONC,YARRAY(4),DYARRY(4),CONSTS(4)
   DOUBLE PRECISION TAU1,TAU2,VSHIFT
   INTEGER I
C
   V    = YARRAY(1)
   N    = YARRAY(2)
   M    = YARRAY(3)
   H    = YARRAY(4)
C
   VNA = 115.
   VK  = -12.
   VL  = 10.58921
C
C
   MEMCAP =   1.
   GNAMAX = 120.
   GKMAX  =  36.
   GLMAX  =   0.3
C
   QTEN   = CONSTS(2)
C
C  ***** CALCULATE THE CALCIUM CONCENTRATION FUNCTION *****
C  ***** AND THE RESULTANT CHANGE IN VOLTAGE          *****
C
   TAU1   = 0.01098 * TIME
   TAU2   =-0.02197 * TIME
   CACONC = 44.- 202.65*(DSINH(TAU1)*DEXP(TAU2))
   VSHIFT = 9.3 * DLOG((44./CACONC))
   V      = V + VSHIFT
C
C  ***** ERROR TRAP FOR V = 10 mV *****
C
   IF(V.GT.9.999.AND.V.LT.10.001)THEN
      ALPHA(1) = 0.1
   ELSE
      ALPHA(1) = (0.01*(10.-V))/(DEXP(0.1*(10.-V))-1.)
   END IF
C
C
C
C
C
C
```

```
C  ***** ERROR TRAP FOR V = 25mV *****
C
   IF(V.GT.24.999.AND.V.LT.25.001)THEN
      ALPHA(2) = 1.0
   ELSE
      ALPHA(2) = (0.1*(25.-V))/(EXP(0.1*(25.-V))-1.)
   END IF
C
   BETA(1) = 0.125*DEXP(-V/80.)
   BETA(2)  = 4.*DEXP(-V/18.)
   ALPHA(3) = 0.07*DEXP(-V/20.)
   BETA(3)  = 1./(DEXP(0.1*(30.-V))+1.)
C
C  ***** TEMPERATURE COMPENSATION *****
C
   DO 30 I=1,3
      ALPHA(I) = ALPHA(I)*QTEN
      BETA(I)  = BETA(I)*QTEN
30  CONTINUE
C
C  ***** CALCULATE THE CONDUCTANCES *****
C
   GK  = GKMAX*(N**4)
   GNA = GNAMAX*(M**3)*H
C
C  ***** CALCULATE THE DERIVATIVES *****
C
    V = V - VSHIFT
C
   VDOT = (-1./MEMCAP)*(GK*(V-VK)+GNA*(V-VNA)+GLMAX*(V-VL))
C
   NDOT = ALPHA(1)*(1-N)-BETA(1)*N
C
   MDOT = ALPHA(2)*(1-M)-BETA(2)*M
C
   HDOT = ALPHA(3)*(1-H)-BETA(3)*H
C
C  ***** PLACE THESE VALUES IN AN ARRAY FOR CONVENIENCE *****
C
   DYARRY(1) = VDOT
   DYARRY(2) = NDOT
   DYARRY(3) = MDOT
   DYARRY(4) = HDOT
C
   RETURN
   END
C
C
C
C
C
C
C
C
C
C
C
C
```

```
C  ********************************************************
C  ** OUTPUT SUBROUTINE : THIS SUBROUTINE WRITES THE     **
C  ** CALCULATED VALUES OF THE VOLTAGE AND TIME TO A     **
C  ** DATA FILE CREATED ON A FLOPPY DISC.                **
C  ********************************************************
C
   SUBROUTINE OUTPUT(DATFIL,ARYCNT,CONSTS)
C
   DOUBLE PRECISION CONSTS(4)
   REAL DATFIL(10000,2)
   INTEGER ARYCNT,ERROR
   CHARACTER FILNAM*6,FILE*12,DATE*8
C
   DATA FILE,DATE/'A:FILNAM.DAT','DD:MM:YY'/
C
C  ***** GET THE FILE NAME AND DATE FROM USER *****
C
   WRITE(*,*)'ENTER THE FILE NAME (6 CHARS) : '
   READ(*,100) FILNAM
C
   WRITE(*,*)'ENTER THE DATE (DD:MM:YY)  : '
   READ(*,400) DATE
C
   FILE(3:8) = FILNAM
C
C  ***** OPEN THE FILE ON DRIVE A: *****
C
   OPEN(UNIT=4,FILE=FILE,STATUS='NEW',IOSTAT=ERROR,
     &     ERR=50)
C
   PAUSE 'INSERT DATA DISC THEN PRESS ENTER'
C
C  ***** NOW WRITE THE ARRAY TO DISC *****
C
   WRITE(4,100) FILNAM
   WRITE(4,200) DATE
   WRITE(4,600)'ARRAY  SIZE'
   WRITE(4,500) ARYCNT
   WRITE(4,200)'DURATION'
   WRITE(4,700) CONSTS(3)
   WRITE(4,600)'TEMPERATURE'
   WRITE(4,700) CONSTS(1)
   WRITE(4,200)'STIMULUS'
   WRITE(4,700) CONSTS(4)
   DO 20 I=1,ARYCNT
   WRITE(4,300) DATFIL(I,1),DATFIL(I,2)
20  CONTINUE
C
C  ***** ERROR HANDLING ROUTINE *****
C
50  IF(ERROR.EQ.2009)THEN
      WRITE(*,*)'INCORRECT STATUS ARGUMENT'
   ELSE IF(ERROR.EQ.2011)THEN
      WRITE(*,*)'RECORD LENGTH SPECIFIER TOO LARGE'
   ELSE IF(ERROR.EQ.2013)THEN
      WRITE(*,*)'FILENAME HAS BEEN USED BEFORE'
   ELSE IF(ERROR.EQ.2014)THEN
      WRITE(*,*)'FILENAME NOT SPECIFIED'
```

```
      END IF
C
C     ***** FORMAT STATEMENTS *****
C
100   FORMAT(A6)
200   FORMAT(A8)
300   FORMAT(F10.6,5X,F10.6)
400   FORMAT(A8)
500   FORMAT(I5)
600   FORMAT(A11)
700      FORMAT(D10.5)
C
C     ***** CLOSE FILE *****
C
      CLOSE(UNIT=4)
C
      RETURN
      END
```

This program simulates the sodium current recorded from the oxytocin-secreting cell. It is based upon data obtained by Cobbett (personal communication). The simulation is of a voltage-clamp experiment whereby a step input voltage is applied to the model equations and the resulting current is calculated.

It is an ACSL-based model and is run by simply invoking the file name from within the ACSL environment. As is normal with ACSL models, the prepare list must be set up before running the program. There is a set of default values for all the main model parameters so these do not need setting up in order to produce results. In an ACSL program all the main variables may be set to desired values which allows a series of simulations to be performed using different starting conditions and model parameters.

Using the plotting commands and selection of variables using the prepare list, any variable may be plotted as a function of time or any variable may be plotted as a function of any other variable.

```
PROGRAM INAOXY

INITIAL
$"----- SET UP THE INITIAL CONDITIONS -----"

REAL M , MDOT , H , HDOT , ALPHAM , BETAM , VDRIV
REAL V , ALPHAH , BETAH , VSTIM , INA , MIC , HIC
REAL K1 , K2 , K3 , K4
CONSTANT VNA = 43.6E-3 , GNABAR = 19.8E-9 , TSTP = 10.0E-3
CONSTANT VSTIM = 20.0E-3 , VHOLD = -80.0E-3 , K1 = 0.0
CONSTANT K2 = 0.0 , K3 = 0.0 , K4 = 0.0 , TEMP = 20.0

QTEN = 3.0**((TEMP - 20.0)/10.0)

ALPHAM = 6400.0/(0.02*(EXP(-100.0*(VHOLD+K1))) + 1.0)*QTEN
BETAM  = 5.0*EXP(-(VHOLD+K2)/0.015)*QTEN
ALPHAH = 45.0*EXP(-(VHOLD+K3)/0.02)*QTEN
BETAH  = 2250.0/(0.08*EXP(-92.5*(VHOLD+K4))) + 1.0)*QTEN

MIC    = ALPHAM/(ALPHAM + BETAM)
HIC    = ALPHAH/(ALPHAH + BETAH)

VDRIV  = (VHOLD + VSTIM) - VNA
V      = VHOLD + VSTIM

ALPHAM = 6400.0/(0.02*(EXP(-100.0*(V+K1))) + 1.0)*QTEN
BETAM  = 5.0*EXP(-(V+K2)/0.015)*QTEN
ALPHAH = 45.0*EXP(-(V+K3)/0.02)*QTEN
BETAH  = 2250.0/(0.08*EXP(-92.5*(V+K4))) + 1.0)*QTEN

END $"OF INITIAL SECTION"

DYNAMIC

IALG           = 5
NSTEPS NSTP    = 1
MAXTERVAL MAXT = 1.0E-4
MINTERVAL MINT = 1.0E-6
CINTERVAL CINT = 5.0E-5

DERIVATIVE

MDOT = ALPHAM - (ALPHAM + BETAM) * M
HDOT = ALPHAH - (ALPHAH + BETAH) * H

M    = INTEG(MDOT , MIC)
H    = INTEG(HDOT , HIC)

END $"OF DERIVATIVE SECTION"

INA = GNABAR*(M**3)*H*VDRIV

TERMT(T .GE. TSTP)

END $"OF DYNAMIC SECTION"

END $"OF PROGRAM"
```

This program simulates the delayed rectifier potassium current recorded in the oxytocin-secreting cell. It is based upon data obtained by Cobbett et al. As with the sodium current, the program performs a simulation of a voltage-clemp experiment which allows the user to compare the calculated results with the experimentally recorded results. The model parameters are easily changed which allows the user to experiment with different values of the conditions (stimulus voltage, temperature).

```
PROGRAM IKOXY
INITIAL
        "----- SET UP THE INITIAL CONDITIONS -----"

      REAL N, NDOT , ALPHAN , BETAN
      REAL VSTIM , IK , VDRIV , V , QTEN

      CONSTANT VK = -83.0E-3 ,GKBAR = 4.09E-9 ,TSTP = 10.0E-3
      CONSTANT VSTIM = 20.0E-3 , VHOLD = -40.0E-3
      CONSTANT TEMP = 20.0

      QTEN = 3.0**((TEMP - 20.0)/10)
      ALPHAN = 600.0 /(EXP(600.0*(0.0-0.1*VHOLD)) +1.0)*QTEN
      BETAN  = 30.0(EXP(-VHOLD/0.02)) * QTEN
      NIC = ALPHAN/(ALPHAN + BETAN)
      V = VHOLD + VSTIM
      VDRIV = V - VK
      ALPHAN = 600.0/(EXP(600.0*(0.0-0.1*V)) +1.0)*QTEN
      BETAN = 30.0*(EXP(-V/0.02))*QTEN

END   $"OF INITIAL SECTION"
DYNAMIC
      IALG = 5
      NSTEPS NSTP = 1
      MAXTERVAL MAXT = 1.0E-4
      MINTERVAL MINT = 1.0E-6
      CINTERVAL CINT = 5.0E-4
DERIVATIVE
      NDOT = ALPHAN - (ALPHAN + BETAN)
      N = INTEG(NDOT , NIC)
END $"OF DERIVATIVE SECTION"
      IK = GKBAR*(N**3)*VDRIV
      TERMT(T .GE. TSTP)
END $"OF DYNAMIC SECTION"
END $"OF PROGRAM"
```

This program performs a simulation of a voltage-clamp experiment involving the transient potassium current recorded by Cobbett et al.

```
PROGRAM IKTRAN

INITIAL
          "----- SET UP THE INITIAL CONDITIONS -----"

     REAL M, MDOT, H, HDOT, ALPHAM, BETAM
     REAL ALPHAH, BETAH, VSTIM, IA, MIC, HIC, VDRIV

     CONSTANT VK = -80.0E-3, GABAR = 5.9E-9, TSTP = 10.0E-3
     CONSTANT VSTIM = 20.0E-3, VHOLD = -100.0E-3

     ALPHAM = 2200/(EXP(2200*(8.0E-5-0.025*VHOLD)) + 1.0)
     BETAM  = 80*EXP(-VHOLD/0.03)
     ALPHAH = 26*EXP(-VHOLD/0.076)
     BETAH  = 70/(EXP(70*(17.0E-3-0.85*VHOLD)) + 1.0)

     MIC    = ALPHAM/(ALPHAM + BETAM)
     HIC    = ALPHAH/(ALPHAH + BETAH)

     VDRIV  = VSTIM - VK

     ALPHAM = 2200/(EXP(2200*(8.0E-5-0.025*VSTIM)) + 1.0)
     BETAM  = 80*EXP(-VSTIM/0.03)
     ALPHAH = 26*EXP(-VSTIM/0.076)
     BETAH  = 70/(EXP(70*(17.0E-3-0.85*VSTIM)) + 1.0)

END $"OF INITIAL SECTION"

DYNAMIC

     IALG           = 5
     NSTEPS NSTP    = 1
     MAXTERVAL MAXT = 1.0E-4
     MINTERVAL MINT = 1.0E-6
     CINTERVAL CINT = 5.0E-4

DERIVATIVE

     MDOT = ALPHAM - (ALPHAM + BETAM) * M
     HDOT = ALPHAH - (ALPHAH + BETAH) * H

     M    = INTEG(MDOT , MIC)
     H    = INTEG(HDOT , HIC)

END $"OF DERIVATIVE SECTION"

     IA   = GABAR*(M**4)*H*VDRIV

     TERMT(T .GE. TSTP)

END $"OF DYNAMIC SECTION"

END $"OF PROGRAM"
```

This program uses the equations for calcium current in crayfish as provided by Hencek and Zachar. The variable names are generally self-explanatory, Hencek and Zachar's notation has been used. The only variable name that warrants explanation is X and this was used as a matter of convenience only. The original equation was too long to fit comfortably on one line and so has been split up. X therefore is an intermediate variable. The units used are millivolts and milliseconds as used by Hencek and Zachar.

```
PROGRAM HENZAK
INTITIIAL
     "----- SET UP THE INITIAL CONDITIONS -----"

REAL M, MDOT, H, HDOT, ALPHAM, BETAM, VDRIV, V
REAL ALPHAH, BETAH, VSTIM, ICA, MIC, HIC

CONSTANT VCA=85.0, GCABAR=15.0, TSTP=10.0
CONSTANT VSTIM=20.0, VHOLD=-80.0
CONSTANT TEMP=20.0

QTEN      = 3.0**((TEMP - 20.0)/10.0)

X         = 1.0 - EXP(-(VHOLD+52.45)/10.5)
ALPHAM    = (0.0051*(VHOLD+52.45)/X) * QTEN

BETAM     = 0.024*EXP(-(VHOLD+52.45)/20.7) * QTEN

ALPHAH    = 0.0097*EXP(-(VHOLD+42.2)/13.4) * QTEN

BETAH     = 0.117/(EXP(-(VHOLD+42.2)/8.5) * QTEN

MIC       = ALPHAM/(ALPHAM + BETAM)
HIC       = ALPHAH/(ALPHAH + BETAH)

VDRIV     = (VHOLD + VSTIM) - VCA
V         =  VHOLD + VSTIM

X         = 1.0 - EXP(-(V+52.45)/10.5)
ALPHAM    = (0.0051*(V+52.45)/X) * QTEN

BETAM     = 0.024*EXP(-(V+52.45)/20.7) * QTEN

ALPHAH    = 0.0097*EXP(-(V+42.2)/13.4) * QTEN

BETAH     = 0.117/(EXP(-(V+42.2)/8.5) * QTEN

END $"OF INITIAL SECTION"
DYNAMIC
DERIVATIVE
     M6   = M**6
     ICA  = GCABAR*M6*H*VDRIV

     MDOT = ALPHAM - (ALPHAM + BETAM) * M
     HDOT = ALPHAH - (ALPHAH + BETAH) * H

     M    = INTEG(MDOT , MIC)
     H    = INTEG(HDOT , HIC)

END $"OF DERIVATIVE SECTION"

     TERMT(T .GE. TSTP)

END $"OF DYNAMIC SECTION"

END $"OF PROGRAM"
```

This is the initial model of the oxytocin-secreting cell coded using ACSL. It includes the calcium current model provided by Hencek and Zachar's equations and the change in calcium concentration as used by Rinzel et al. The calcium-dependent potassium current model is also based on the equations used by Rinzel et al. Sodium current, potassium current and transient potassium current models are based upon data provided by the work of Cobbett et al.

```
PROGRAM OXYMODEL

REAL M , MDOT , H , HDOT , ALPHAM , BETAM , V , VDOT
REAL ALPHAH , BETAH , VSTIM , INA , MIC , HIC , PIC
REAL QIC , N , NDOT , ALPHAN , BETAN , ALPHAP , BETAP
REAL IA , IK , P , PDOT , Q , QDOT , ALPHAQ , BETAQ
REAL IT , IL , QTEN , CACONC , CADOT , ICA , FDOT
REAL D , DDOT , ALPHAD , BETAD , ALPHAF , BETAF

CONSTANT VNA = 43.6E-3 , GNABAR = 19.8E-9 , TSTP = 10.0E-3
CONSTANT VK = -83.0E-3 , GKBAR = 4.09E-9 , GABAR = 5.9E-9
CONSTANT CM = 7.3E-12 , GLBAR = 2.19E-9 , VL = 10.0E-3
CONSTANT ER = -75.0E-3 , VSTIM = 20.0E-3 , VSHIFT = 0.0
CONSTANT GKCABAR = 30.0E-9 , TEMP = 20.0 , KD = 100.0E-6
CONSTANT GCABAR = 109.5E-9 , KCA = 30.0 , ALPHA = 1.95E3
CONSTANT MULF = 0.001 , KCA = 30.0 , VCA = 85.0E-3
CONSTANT CAIC = 1.0E-6

INITIAL "----- SET UP INITIAL CONDITIONS -----"

QTEN = 3.0**((TEMP - 20.0)/10.0)

ALPHAM = (6400.0/(0.02*(EXP(-100.0*ER)) + 1.0))*QTEN
BETAM = (5.0*EXP((-ER/0.015))*QTEN
ALPHAH = (45.0*EXP(-ER/0.02))*QTEN
BETAH = (2250.0/(0.08*EXP(-92.5*ER))+1.0))*QTEN
ALPHAN = (600.0/(EXP*(0.0-0.1*ER))+1.0))*QTEN
BETAN = (30.0*(EXP(-ER/0.02)))*QTEN
ALPHAP = (2200.0/(EXP(2200.0*(8.0E-5-0.025*ER))+1.0))*QTEN
BETAP = (80.0*EXP(-ER/0.03))*QTEN
ALPHAQ = (26.0*EXP(-ER/0.076))*QTEN
BETAQ = (70.0/(EXP(70.0*(17.0E-3 - 0.85*ER))+1.0)*QTEN
ALPHAD=(5.1*ER-0.053)/(1.0-EXP(-((ER+0.053)/0.0105))))*QTEN
BETAD = (24.4*EXP(-((ER+0.053)/0.0207)))*QTEN
ALPHAF = (9.7*EXP(-((ER+0.0422)/0.0134)))*QTEN
BETAF = (117.0/(1.0+EXP(-((ER+0.0422)/0.00854)))))*QTEN

MIC = ALPHAM/(ALPHAM+BETAM)
HIC = ALPHAH/(ALPHAH+BETAH)
NIC = ALPHAN/(ALPHAN+BETAN)
PIC = ALPHAP/(ALPHAP+BETAP)
QIC = ALPHAQ/(ALPHAQ+BETAQ)
DIC = ALPHAD/(ALPHAD+BETAD)
FIC = ALPHAF/(ALPHAF+BETAF)
VIC = ER +VSTIM

END $"OF INITIAL SECTION"

DYNAMIC

IALG = 5
NSTEPS NSTP = 1
MAXTERVAL MAXT = 1.0E-4
MINTERVAL MINT = 1.0E-7
CINTERVAL CINT = 5.0E-5
```

```
DERIVATIVE
          PROCEDURAL

INA   = GNABAR*(M**3)*H*(V-VNA)
IA    = GABAR*(P**4)*Q*(V-VK)
IK    = GKBAR*(N**3)*(V-VK)
IL    = GLBAR*(V-VL)
ICA   = GCABAR*(D**6)*F*(V-VCA)
IKCA = GKCABR*(CACONC/(CACONC+KD))*(V-VK)
IT    = INA + IA + IK + IK + IL + ICA + IKCA

MDOT = ALPHAM - (ALPHAM + BETAM) * M
HDOT = ALPHAH - (ALPHAH + BETAH) * H
NDOT = ALPHAN - (ALPHAN + BETAN) * N
PDOT = ALPHAP - (ALPHAP + BETAP) * P
QDOT = ALPHAQ - (ALPHAQ + BETAQ) * Q
DDOT = ALPHAD - (ALPHAD + BETAD) * D
FDOT = ALPHAF - (ALPHAF + BETAF) * F
CADOT = MULF * (-ALPHA*ICA - KCA * CACONC)
VDOT = -1/CM * IT

M = INTEG(MDOT , MIC)
H = INTEG(HDOT , HIC)
N = INTEG(NDOT , NIC)
P = INTEG(PDOT , PIC)
Q = INTEG(QDOT , QIC)
D = INTEG(DDOT , DIC)
F = INTEG(FDOT , FIC)
CACONC = INTEG(CADOT , CAIC)
V = INTEG(VDOT , VIC)

V = V + VSHIFT

ALPHAM = (6400.0/(0.02*(EXP(-100.0*V)) + 1.0))*QTEN
BETAM = (5.0*EXP((-V/0.015))*QTEN
ALPHAH = (45.0*EXP(-V/0.02))*QTEN
BETAH = (2250.0/(0.08*EXP(-92.5*V))+1.0))*QTEN
ALPHAN = (600.0/(EXP*(0.0-0.1*V))+1.0))*QTEN
BETAN = (30.0*(EXP(-ER/0.02)))*QTEN
ALPHAP = (2200.0/(EXP(2200.0*(8.0E-5-0.025*V))+1.0))*QTEN
BETAP = (80.0*EXP(-V/0.03))*QTEN
ALPHAQ = (26.0*EXP(-V/0.076))*QTEN
BETAQ = (70.0/(EXP(70.0*(17.0E-3 - 0.85*V))+1.0)*QTEN
ALPHAD = (5.1*V-0.053)/(1.0-EXP(-((V+0.053)/0.0105))))*QTEN
BETAD = (24.4*EXP(-((V+0.053)/0.0207)))*QTEN
ALPHAF = (9.7*EXP(-((V+0.0422)/0.0134)))*QTEN
BETAF = (117.0/(1.0+EXP(-((V+0.0422)/0.00854)))))*QTEN

V = V - VSHIFT

END $"OF PROCEDURAL BLOCK"
END $"OF DERIVATIVE SECTION"

TERMT(T .GT. TSTP)

END $"OF DYNAMIC SECTION"

END $"OF PROGRAM"
```

```
PROGRAM BASICMODEL

REAL M , MDOT , H , HDOT , ALPHAM , BETAM
REAL ALPHAH , BETAH , VSTIM , INA , MIC , HIC
REAL N , NDOT , ALPHAN , BETAN , IK , IL , IT , QTEN

CONSTANT VNA = 43.6E-3 , GNABAR = 19.8E-9 , TSTP = 10.0E-3
CONSTANT KV = -83.0E-3 , GKBAR = 4.09E-9 , TEMP = 20.0
CONSTANT CM = 7.3E-12 , GLBAR = 2.19E-9 , VL = 10.59E-3
CONSTANT ER = -75.0E-3 , VSTIM = 20.0E-3 , VSHIFT = 0.0

INITIAL "----- SET UP THE INITIAL CONDITIONS -----"

QTEN = 3.0**((TEMP - 20.0)/10.0)
ALPHAM = (6400.0/(0.02*EXP(-100.0*ER))+1.0)*QTEN
BETAM = (5.0*EXP(-ER/0.015))*QTEN
ALPHAH = (45.0*EXP(-ER/0.02))*QTEN
BETAH = (22500.0/(0.08*(EXP(-92.5*ER)) + 1.0)*QTEN
ALPHAN = (600.0/(EXP(600.0*(0.0-0.1*ER))+1.0)*QTEN
BETAN = (30.0*EXP(-ER/0.02)))*QTEN

MIC = ALPHAM/(ALPHAM+BETAM)
HIC = ALPHAH/(ALPHAH+BETAH)
NIC = ALPHAN/(ALPHAN+BETAN)
VIC = ER + VSTIM

END $"OF INITIAL SECTION"

DYNAMIC

      IALG = 5
      NSTEPS NSTP = 1
      MAXTERVAL MAXT = 1.0E-4
      MINTERVAL MINT = 1.0E-7
      CINTERVAL CINT = 5.0E-5

DERIVATIVE

      PROCEDURAL

INA = GNABAR*(M**3)*H*(V-VNA)
IK  = GKBAR*(N**3)*(V-VK)
IL  = GLBAR*(V-VL)
IT  = INA + IK + IL

MDOT = ALPHAM - (ALPHAM+BETAM)*M
HDOT = ALPHAH - (ALPHAH+BETAH)*H
NDOT = ALPHAN - (ALPHAN+BETAN)*N
VDOT = -1/CM * IT

M = INTEG(MDOT , MIC)
H = INTEG(HDOT , HIC)
N = INTEG(NDOT , NIC)
V = INTEG(VDOT , VIC)

V = V + VSHIFT
```

```
ALPHAM = (6400.0/(0.02*EXP(-100.0*ER))+1.0)*QTEN
BETAM = (5.0*EXP(-ER/0.015))*QTEN
ALPHAH = (45.0*EXP(-ER/0.02))*QTEN
BETAH = (22500.0/(0.08*(EXP(-92.5*ER)) + 1.0)*QTEN
ALPHAN = (600.0/(EXP(600.0*(0.0-0.1*ER))+1.0)*QTEN
BETAN = (30.0*EXP(-ER/0.02)))*QTEN

V = V - VSHIFT

END $"OF PROCEDURAL BLOCK"
END $"OF DERIVATIVE SECTION"

     TERMT(T .GT. TSTP)

END $"OF DYNAMIC SECTION"

END $"OF PROGRAM"
```

This program was written in order to duplicate and verify the model of the pancreatic beta cell as derived by Rinzel et al. The equations are taken from the papers cited in the main body of this thesis. The model as written initially did not reproduce Rinzel's results but after tuning the model parameters, the desired bursting behaviour was observed. The model variables are generally self-explanatory and Rinzel's notation has been adhered to generally.

```
PROGRAM RINZEL

REAL T , ALPHAM , ALPHAN , ALPHAH , BETAM , BETAN , BETAH
REAL NDOT , CADOT , VDOT , V , CACONC , N , M , H

CONSTANT RECIPC = -1.0E-6 , VCA = 100.0E-3 , VK = -75.0E-3
CONSTANT VL = -40.0E-3 , GCABAR = 1.79934E-3
CONSTANT GKBAR = 1.69765E-3
CONSTANT GKCABR = 0.0104998E-3 , GLBAR = 0.00698514E-3
CONSTANT LAMBDA = 0.3 , KCA = 0.00513 , F = 0.0058
CONSTANT ALPHA = 0.0259102 , VREST = -60.0E-3 , CIC = 0.4E-6
CONSTANT TSTP = 20.0E-3

INITIAL
          "SET UP THE INITIAL CONDITIONS"

     V      = VREST
     VSTIM  = 20.0E-3
     ALPHAN = 0.01*(-V-20.0)/(EXP(0.1*9-V-20.0)) - 1.0)
     ALPHAM = 0.1*(-V-25.0)/(EXP(0.1*(-V-25.0)) - 1.0)
     ALPHAH = 0.07 * EXP((-V-50.0)/20.0)

     BETAN  = 0.125 * EXP((-V-30.0)/80.0)
     BETAM  = 4.0 * EXP((-V-50.0)/18.0)
     BETAH  = 1.0/(EXP((-V-30.0)/80.0) + 1.0)

     NIC    = ALPHAN/(ALPHAN + BETAN)
     VIC    = VREST + VSTIM

END

DYNAMIC

     IALG           = 5
     NSTEPS NSTP    = 1
     MAXTERVAL MAXT = 1.0E-4
     MINTERVAL MINT = 1.0E-6
     CINTERVAL CINT = 5.0E-5

DERIVATIVE

     M     = ALPHAM/(ALPHAM + BETAM)
     H     = ALPHAH/(ALPHAH + BETAH)
     NDOT  = LAMBDA * (ALPHAN - (ALPHAN + BETAN) * N)
     CADOT = F * (ALPHA * ICA - KCA * CACONC)
     VDOT  = RECIPC * (ICA + IK + IKCA + IL)

     CACONC = INTEG(CACONC , CIC)
     V      = INTEG(VDOT , VIC)
     N      = INTEG(NDOT , NIC)
     ICA    = GCABAR * ((M**3) * H) * (V - VCA)
     IK     = GKBAR * (N**4) * (V - VK)
     IKCA   = GKCABR * (CACONC/(CACONC + 1)) * (V - VK)
     IL     = GLBAR * (V - VL)
```

```
      ALPHAN = 0.01*(-V-20.0)/(EXP(0.1*(-V-20.0)) - 1.0)
      BETAN  = 0.125 * EXP((-V-30.0)/80.0)
      ALPHAM = 0.1*(-V-25.0)/(EXP(0.1*(-V-25.0)) - 1.0)
      BETAM  = 4.0 * EXP((-V-50.0)/18.0)
      ALPHAH = 0.07 * EXP((-V-50.0)/20.0)
      BETAH  = 1.0/(EXP(0.1*(-V-20.0)) + 1.0)

END $"OF DERIVATIVE SECTION"

      TERMT(T .GE. TSTP)

END $"OF DYNAMIC SECTION"

END $"OF PROGRAM"
```

```
PROGRAM BETACELL

" This program is based upon a model described in a paper by"
" Arthur Sherman , John Rinzel and Joel Keizer entitled :  "
" EMERGENCE OF ORGANIZED BURSTING IN CLUSTERS OF PANCREATIC"
" BETA CELLS BY CHANNEL SHARING "

REAL V , VDOT , CACONC , CADOT , N , NDOT , M , H , TAUN
REAL GKCA , IK , ICA , IKCA , NSS

CONSTANT VIC = -65.0E-3 , CAIC = 0.6E-6
CONSTANT LAMDA = 1.7 , KCA = 30.0 , F = 0.001
CONSTANT ALPHA = 4506.2 , GKCAMX = 30.0E-9 , KD = 100.0E-6
CONSTANT INVCAP = -1.88E11 , VK = -75.0E-3 , VCA = 110.0E-3
CONSTANT TSTP = 20.0 , GKMAX = 2.5E-9 , GCAMAX = 1.4E-9

INITIAL

NIC = 1.0/(1.0 + EXP((-15.0E-3 - VIC)/5.6E-3))
V   = VIC

END $"OF INITIAL SECTION"

DYNAMIC

ALGORITHM IALG = 4
NSTEPS    NSTP = 1
CINTERVAL CINT = 1.0E-5
MINTERVAL MINT = 1.0E-7
MAXTERVAL MAXT = 1.0E-4

DERIVATIVE

V      = INTEG(VDOT , VIC)
N      = INTEG(NDOT , NIC)
CACONC = INTEG(CADOT , CAIC)

M   = 1.0/(1.0 + EXP((4.0E-3 - V)/14.0E-3))
H   = 1.0/(1.0 + EXP((V + 10.0E-3)/10.0E-3))
NSS = 1.0/(1.0 + EXP((-15.0E-3 - V)/5.6E-3))

TAUN = 60.0E-3/(EXP((V + 75.0E-3)/65.0E-3 ) + ...
EXP(-(V + 75.0E-3)/20.0E-3))

GKCA  = GKMAX * ( CACONC/(CACONC + KD))
IK    = GKMAX * N * (V -VK)
ICA   = GCAMAX * M * H * (V - VCA)
IKCA  = GKCA * (V - VK)
NDOT  = LAMDA * ((NSS - N)/TAUN)
CADOT = F * (ALPHA * ICA - KCA * CACONC)
VDOT  = INCAP * (IK + ICA + IKCA)
END $"OF DERIVATIVE"

TERMT(T .GE. TSTP)
END $"OF DYNAMIC"
END $"OF  PROGRAM"
```

# Levenberg-Marquardt Curve Fitting Program

This program is based on the programs given in "Numerical Recipes" (Press, Flannery, Teukolsky and Vetterling 1986).

The function to which the data is to be fitted is defined in the subroutine FUNCS. A different subroutine has to be written for each new function. The name must be as given.

The data points are written into the main program LEVDRV in a DATA statement. This approach was taken since there was not a great number of points to be fitted. An alternative where the number of data points is large, is to read the data in from a disk file or from the keyboard. It was thought the extra programming effort required to incorporate this feature would not give any significant improvement in the use of the program.

To use the program, the fitting function has to be defined in the appropriate subroutine and the data points inserted into the DATA statement. The suite of programs are then recompiled and linked as necessary. Putting the data points, the vector of initial values for the parameters and the function into the program makes execution of the program simple. The executable file is simply run, and the updated parameters are displayed on the monitor at the end of each iteration. Once a minimum has been found, execution ceases and the final list of parameters on screen are those that have been found to give the best fit. Also displayed are the uncertainties but these are meaningless since the sigma values are all set to one in the program. This means that all the data points are given equal weight during the fitting process.

```
C ****************************************
C * LEVENBERG-MARQUARDT PROGRAM TO FIND  *
C * THE PARAMETERS THAT GIVE THE BEST FIT*
C * OF A GIVEN FUNCTION TO A SET OF DATA *
C * POINTS.                              *
C * THE PROGRAM CONSISTS OF THIS MAIN    *
C * PROGRAM AND THE SUBROUTINES MRQMIN   *
C * MRQCOF, COVSRT,FUNCS AND GAUSSJ.     *
C ****************************************
C
 PROGRAM LEVDRV
C
 EXTERNAL FUNCS
C
 PARAMETER(NPT = 7,MA = 3)
C
 DIMENSION X(NPT),Y(NPT),SIG(NPT),A(MA),LISTA(MA),
&         COVAR(MA,MA),ALPHA(MA,MA),GUES(MA)
C
      DATA Y/116.,186.,236.,331.,447.,544.,625./
      DATA GUES/615.,1.,59./
      DATA X/-0.02,-0.01,0.0,0.01,0.02,0.03,0.05/
C
C     ***** SET SIGMA VALUES TO 1.0 *****
C
      DO 10 I=1,NPT
             SIG(I) = 1.0
10    CONTINUE
C
      MFIT = MA
C
      DO 20 I=1,MFIT
                LISTA(I) = I
20    CONTINUE
C
      ALAMDA = -1
      DO 30 I=1,MA
                A(I) = GUES(I)
30    CONTINUE
C
      CALL MRQMIN(X,Y,SIG,NPT,A,MA,LISTA,MFIT,COVAR,
&         ALPHA,MA,CHISQ,FUNCS,ALAMDA)
C
      K=1
      ITST=0
40    WRITE(*,'(/1X,A,I2,T18,A,F10.4,T43,A,E9.2)')
&     'ITERATION #',K,'CHI-SQUARED:',CHISQ,'ALAMDA',ALAMDA
      WRITE(*,'(1X,T5,A,T13,A,T21,A)')'A(1)','A(2)','A(3)'
      WRITE(*,'(1X,3F8.4)') (A(I),I=1,3)
      K=K+1
C
      OCHISQ=CHISQ
C
     CALL MRQMIN(X,Y,SIG,NPT,A,MA,LISTA,MFIT,COVAR,ALPHA,
&               MA,CHISQ,FUNCS,ALAMDA)
C
      IF (CHISQ.GT.OCHISQ) THEN
                ITST=0
```

```
      ELSE IF (ABS(OCHISQ-CHISQ).LT.0.1) THEN
                ITST=ITST+1
      ENDIF
      IF (ITST.LT.2) THEN
               GOTO 40
      ENDIF
      ALAMDA=0.0
C
      CALL MRQMIN(X,Y,SIG,NPT,A,MA,LISTA,MFIT,COVAR,ALPHA,
&                 MA,CHISQ,FUNCS,ALAMDA)
C
      WRITE(*,*) 'UNCERTAINTIES:'
      WRITE(*,'(1X,3F8.4/)') (SQRT(COVAR(I,I)),I=1,3)
      END
```

```
C ***************************************************
C * This subroutine MRQMIN does the actual work of    *
C * minimizing the least squares fit of the function  *
C * to the data points.                               *
C ***************************************************

SUBROUTINE MRQMIN(X,Y,SIG,NDATA,A,MA,LISTA,MFIT,
&     COVAR,ALPHA,NCA,CHISQ,FUNCS,ALAMDA)
      PARAMETER (MMAX=20)
      DIMENSION X(NDATA),Y(NDATA),SIG(NDATA),A(MA),LISTA(MA),
&               COVAR(NCA,NCA),ALPHA(NCA,NCA),ATRY(MMAX),
&               BETA(MMAX),DA(MMAX)
C
      IF(ALAMDA.LT.0.)THEN
        KK=MFIT+1
        DO 12 J=1,MA
          IHIT=0
          DO 11 K=1,MFIT
            IF(LISTA(K).EQ.J)IHIT=IHIT+1
11        CONTINUE
          IF (IHIT.EQ.0) THEN
            LISTA(KK)=J
            KK=KK+1
          ELSE IF (IHIT.GT.1) THEN
            PAUSE 'Improper permutation in LISTA'
          ENDIF
12      CONTINUE
        IF (KK.NE.(MA+1)) PAUSE 'Improper permutation in
&                                LISTA'
        ALAMDA=0.001
        CALL MRQCOF(X,Y,SIG,NDATA,A,MA,LISTA,MFIT,ALPHA,
&                   BETA,NCA,CHISQ,FUNCS)
C
        OCHISQ=CHISQ
        DO 13 J=1,MA
          ATRY(J)=A(J)
13      CONTINUE
      ENDIF
      DO 15 J=1,MFIT
        DO 14 K=1,MFIT
          COVAR(J,K)=ALPHA(J,K)
14      CONTINUE
        COVAR(J,J)=ALPHA(J,J)*(1.+ALAMDA)
        DA(J)=BETA(J)
15    CONTINUE
      CALL GAUSSJ(COVAR,MFIT,NCA,DA,1,1)
      IF(ALAMDA.EQ.0.)THEN
        CALL COVSRT(COVAR,NCA,MA,LISTA,MFIT)
        RETURN
      ENDIF
      DO 16 J=1,MFIT
        ATRY(LISTA(J))=A(LISTA(J))+DA(J)
16    CONTINUE
      CALL MRQCOF(X,Y,SIG,NDATA,ATRY,MA,LISTA,MFIT,
&                 COVAR,DA,NCA,CHISQ,FUNCS)
      IF(CHISQ.LT.OCHISQ)THEN
        ALAMDA=0.1*ALAMDA
        OCHISQ=CHISQ
```

```
        DO 18 J=1,MFIT
          DO 17 K=1,MFIT
            ALPHA(J,K)=COVAR(J,K)
17        CONTINUE
          BETA(J)=DA(J)
          A(LISTA(J))=ATRY(LISTA(J))
18      CONTINUE
      ELSE
        ALAMDA=10.*ALAMDA
        CHISQ=OCHISQ
      ENDIF
      RETURN
      END
```

```
C ***************************************************
C * This subroutine MRQCOF calculates the elements  *
C * the alpha matrix (Hessian) and the beta vector  *
C * that are used in the fitting process.           *
C ***************************************************

      SUBROUTINE MRQCOF(X,Y,SIG,NDATA,A,MA,LISTA,MFIT,ALPHA,
&                 BETA,NALP,CHISQ,FUNCS)
C
       PARAMETER (MMAX=20)
       DIMENSION X(NDATA),Y(NDATA),SIG(NDATA),
&                ALPHA(NALP,NALP),BETA(MA),DYDA(MMAX),
&                LISTA(MFIT),A(MA)
C
       DO 12 J=1,MFIT
         DO 11 K=1,J
           ALPHA(J,K)=0.
11       CONTINUE
         BETA(J)=0.
12     CONTINUE
       CHISQ=0.
       DO 15 I=1,NDATA
         CALL FUNCS(X(I),A,YMOD,DYDA,MA)
         SIG2I=1./(SIG(I)*SIG(I))
         DY=Y(I)-YMOD
         DO 14 J=1,MFIT
           WT=DYDA(LISTA(J))*SIG2I
           DO 13 K=1,J
             ALPHA(J,K)=ALPHA(J,K)+WT*DYDA(LISTA(K))
13         CONTINUE
           BETA(J)=BETA(J)+DY*WT
14       CONTINUE
         CHISQ=CHISQ+DY*DY*SIG2I
15     CONTINUE
       DO 17 J=2,MFIT
         DO 16 K=1,J-1
           ALPHA(K,J)=ALPHA(J,K)
16       CONTINUE
17     CONTINUE
       RETURN
       END
```

```
C ***********************************************
C * This subroutine is not really necessary, all *
C * it does is to rearrange the elements in the  *
C * covariance matrix COVAR.                     *
C ***********************************************

SUBROUTINE COVSRT(COVAR,NCVM,MA,LISTA,MFIT)
      DIMENSION COVAR(NCVM,NCVM),LISTA(MFIT)
      DO 12 J=1,MA-1
        DO 11 I=J+1,MA
          COVAR(I,J)=0.
11      CONTINUE
12    CONTINUE
      DO 14 I=1,MFIT-1
        DO 13 J=I+1,MFIT
          IF(LISTA(J).GT.LISTA(I)) THEN
            COVAR(LISTA(J),LISTA(I))=COVAR(I,J)
          ELSE
            COVAR(LISTA(I),LISTA(J))=COVAR(I,J)
          ENDIF
13      CONTINUE
14    CONTINUE
      SWAP=COVAR(1,1)
      DO 15 J=1,MA
        COVAR(1,J)=COVAR(J,J)
        COVAR(J,J)=0.
15    CONTINUE
      COVAR(LISTA(1),LISTA(1))=SWAP
      DO 16 J=2,MFIT
        COVAR(LISTA(J),LISTA(J))=COVAR(1,J)
16    CONTINUE
      DO 18 J=2,MA
        DO 17 I=1,J-1
          COVAR(I,J)=COVAR(J,I)
17      CONTINUE
18    CONTINUE
      RETURN
      END
```

```
C ************************************************
C * This subroutine is a GAUSS-JORDAN elimination *
C * routine that is used to solve the matrix      *
C * equations that arise from the fitting process.*
C ************************************************

SUBROUTINE GAUSSJ(A,N,NP,B,M,MP)
      PARAMETER (NMAX=50)
DIMENSION A(NP,NP),B(NP,NP),IPIV(NMAX),ROWINDX(NMAX),
&         COLINDX(NMAX)
      DO 11 J=1,N
        IPIV(J)=0
11    CONTINUE
      DO 22 I=1,N
        BIG=0.
        DO 13 J=1,N
          IF(IPIV(J).NE.1)THEN
            DO 12 K=1,N
              IF (IPIV(K).EQ.0) THEN
                IF (ABS(A(J,K)).GE.BIG)THEN
                  BIG=ABS(A(J,K))
                  IROW=J
                  ICOL=K
                ENDIF
              ELSE IF (IPIV(K).GT.1) THEN
                PAUSE 'Singular matrix'
              ENDIF
12          CONTINUE
          ENDIF
13      CONTINUE
        IPIV(ICOL)=IPIV(ICOL)+1
        IF (IROW.NE.ICOL) THEN
          DO 14 L=1,N
            DUM=A(IROW,L)
            A(IROW,L)=A(ICOL,L)
            A(ICOL,L)=DUM
14        CONTINUE
          DO 15 L=1,M
            DUM=B(IROW,L)
            B(IROW,L)=B(ICOL,L)
            B(ICOL,L)=DUM
15        CONTINUE
        ENDIF
        ROWINDX(I)=IROW
        COLINDX(I)=ICOL
      IF (A(ICOL,ICOL).EQ.0.) PAUSE 'Singular matrix.'
        PIVINV=1./A(ICOL,ICOL)
        A(ICOL,ICOL)=1.
        DO 16 L=1,N
          A(ICOL,L)=A(ICOL,L)*PIVINV
16      CONTINUE
        DO 17 L=1,M
          B(ICOL,L)=B(ICOL,L)*PIVINV
17      CONTINUE
        DO 21 LL=1,N
          IF(LL.NE.ICOL)THEN
            DUM=A(LL,ICOL)
            A(LL,ICOL)=0.
```

```
            DO 18 L=1,N
              A(LL,L)=A(LL,L)-A(ICOL,L)*DUM
18          CONTINUE
            DO 19 L=1,M
              B(LL,L)=B(LL,L)-B(ICOL,L)*DUM
19          CONTINUE
          ENDIF
21      CONTINUE
22    CONTINUE
      DO 24 L=N,1,-1
        IF(ROWINDX(L).NE.COLINDX(L))THEN
          DO 23 K=1,N
            DUM=A(K,ROWINDX(L))
            A(K,ROWINDX(L))=A(K,COLINDX(L))
            A(K,COLINDX(L))=DUM
23        CONTINUE
        ENDIF
24    CONTINUE
      RETURN
      END
```

```
C ***********************************************
C * This subroutine is where the function to be *
C * fitted to the data is defined.              *
C ***********************************************

      SUBROUTINE FUNCS(X,A,Y,DYDA,NA)
C
       DIMENSION A(NA),DYDA(NA)
C
       Y=0.
       ARG = EXP(-A(3)*X)
       Y = A(1)/(A(2)*ARG + 1.)
       DYDA(1) = 1.0/(A(2)*ARG + 1.)
       DYDA(2) = (-A(1)*ARG)/(A(2)*ARG +1.)**2
       DYDA(3) = (A(1)*A(2)*A(3)*ARG)/(A(2)*ARG + 1.)**2
       RETURN
       END
```